Photochemical Modeling of Ozone Pollution in the Paso del Norte Region

PREPARED FOR:

El Paso Metropolitan Planning Organization

El Paso, TX 79913

PREPARED BY:

Victor Valenzuela[1], Rosa Fitzgerald[2], Huiyan Yang[2]

George Pinal[3], Kelvin Ruey Long Cheu[3]

Wen-Whai Li[1,3,*]

[1]Environmental Science and Engineering Ph.D. Program

[2]Physics Department

[3]Department of Civil Engineering

The University of Texas at El Paso

El Paso, Texas 79968

January 23, 2013

[*]Corresponding author

TABLE OF CONTENTS

Acknowledgements

This study was supported by a grant from the Texas Commission on Environmental Quality (TCEQ) through the El Paso Metropolitan Planning Organization (MPO). This project would not have been possible without the support of many people. The authors thank Mr. Fernando Mercado and Dr. Bright Dornblaser of TCEQ for their valuable inputs and foresight, Mr. Sergio Rocha of the Center for Transportation Infrastructure Systems at UTEP for computer system and programming support; Dr. Alberto Correa of the UTEP Environmental Science and Engineering Program, Mr. Chris Emery and Dr. Uarporn Nopmongcol of Environ International Corporation for CAMx modeling support; Mr. Michael Medina, Ms. Christine Ponce-Diaz and Mr. Efren Meza of El Paso MPO for administrative support and project guidance.

The contents of this report are solely the responsibility of the authors and do not necessarily represent the official views of the MPO, TCEQ, or UTEP.

Abstract

This report documents a photochemical air quality modeling study conducted at the University of Texas at El Paso (UTEP) to evaluate ozone pollution in El Paso using the WRF meteorological and CAMx photochemical air quality models. The primary objective of the study was to develop a photochemical model appropriate for a Texas SIP revision for the Paso del Norte (PdN) region. The models performance was evaluated for the 2006 base case ozone episode between June 12 and June 21 and Sensitivity of the CAMx model to changes in area emissions in Cd. Juarez was addressed.

Meteorology for the PdN region was first simulated using 3 nested domains centered at El Paso with 36-, 12-, and 4-km resolution. The WRF results were reviewed based on the model's phenomenological and operational performance in the studied domains. The simulation was judged acceptable and the results for the 4-km domain were used in the base case ozone study. A series of CAMx simulations were conducted to investigate model performance for the 2006 base case ozone episode and sensitivity to selected changes in precursor emissions. The performance of two base case CAMx simulations, one with UTEP-defined meteorology and the other with TCEQ-defined meteorology, were judged acceptable.

Thirteen additional simulations were performed to evaluate the impacts of newly documented bridge emissions and various Cd. Juarez area source emissions on the PdN ozone levels. Addition of the bridge emissions to the PdN emissions inventory did not help in the prediction of ozone peak. Instead, peak ozone concentrations were under-predicted when compared to the simulation without adding the extra emissions from the bridge. The sensitivity of Cd. Juarez area emissions on the PdN ozone levels were evaluated by varying the VOC and NOx emission estimates in the reported Cd. Juarez area emissions. All sensitivity runs functioned within acceptable limits for the model performance evaluation and none of the runs displayed significant improvement in the model performance over the base case. An increase of 75% area source VOC emissions with or without concurrent increase in NOx emissions will bring the predicted peak ozone to be the same as the observed peak. Consequently, if the Cd. Juarez area source VOC emissions are reduced by 50% through some control strategies, one would be able to reduce the peak ozone by as much as 13%.

List of Figures

List of Tables

Chapter 1 Introduction

El Paso County was initially classified as an area in serious nonattainment of the 1-hour ozone National Ambient Air Quality Standard (NAAQS) of 0.12 ppm at the promulgation of the federal Clean Air Act amendments of 1990. Since then, ozone pollution in El Paso has been decreased (Li et al 2011a) and El Paso became attainment in 1997 when the 1-hour 0.12 ppm ozone standard was replaced by an 8-hour ozone NAAQS of 0.08 ppm. El Paso continues to maintain its attainment status even after the U.S. EPA established a more stringent 8-hour ozone standard of 0.075 ppm (73 FR 16436) in 2008. In 2011, the U.S. EPA announced its proposal to lower the primary 8-hour ozone standard to a range of 0.060 ppm to 0.070 ppm. This proposal was later rescinded by the EPA Administrator at the request of the President of the United State in 2012, based on the considerations of reducing regulatory burden and regulatory uncertainty during the period the country is recovering from an economic downturn. Nevertheless, scientific review of the effects of ozone on human health and the environment continues and "work is already underway to update a 2006 review of the science that will result in the reconsideration of the ozone standard in 2013" (White House 2011). It is anticipated that the current standard of 0.075 ppm will be replaced by a new standard between 60 and 70 ppb after 2013.

1.1 Background of the Project

In anticipation of a more stringent ozone standard, the 81st Texas Legislature in 2009 appropriated the Rider 8 program to assist those metropolitan areas that may become nonattainment should the ozone NAAQS be reduced to below 0.070 ppm in undertaking steps to attain the ozone NAAQS. Activities required by the Rider 8 program include identifying inventorying, monitoring and modeling of pollutant levels; and the identification, quantification, and implementation of appropriate pollution reduction controls. The El Paso Metropolitan Planning Organization (MPO) is tasked by the Texas Commission on Environmental Quality (TCEQ) under the Rider 8 program to implement the above-referenced activities. As part of the Rider 8 program, the University of Texas at El Paso (UTEP) is contracted by MPO to assist in implementing these activities in a two-phase approach. The first phase (Phase I) of tasks include

- Update the conceptual understanding of local ozone formation processes;
- Review emissions inventories and identify potential improvements;
- Analyze the adequacy of air quality monitoring in the area; and
- Identify controls for future in-depth study.

The recommendations identified from Phase I are used to implement the following tasks in the second phase (Phase II) of the study:

- Improve local ambient air monitoring networks;
- Improve emission inventories;
- Recommend and develop local air quality control strategies;
- Perform photochemical modeling of the identified ozone episode;
- Conduct sensitivity tests to the photochemical model to test results due to emission reduction measures;
- Improve public understanding of the ozone problem and motivate the public to voluntarily reduce its contribution to ozone pollution; and
- Involve local stakeholders in developing air quality planning strategies to gain broad support within the communities.

The tasks included in Phase I study have been completed and documented in three separate reports (Li et al 2011a, 2011b; Yang et al 2012). This report summarizes the tasks in Phase II study that are related to the setup, running, and evaluation of the meteorological and photochemical models.

1.2 Findings from the Ozone Conceptual Model

A conceptual model of ozone pollution in the PdN region was performed by UTEP (Li et al 2011a; Yang et al 2012). Major findings of the study are summarized below in accordance to the guidance set forth by the U.S. EPA (U.S. EPA 2005).

- Ozone nonattainment in El Paso is not a local issue. Transport ozone and emissions in the greater PdN region contribute to the ozone problem in El Paso.
- Previous modeling study suggested transport ozone aloft was high. It could be as high as 50-80 ppb ozone aloft during an ozone episode (Yocke 2000).
- Violations of the 75 ppb ozone NAAQS occurred at multiple monitoring locations throughout the region.
- Exceedance of the 75 ppb ozone NAAQS does not occur frequently in El Paso, decreasing from 13 to 4 a year between 2007 and 2010.
- Similar pattern of spatial distribution of the daily maximum 8-hour design values was observed in the PdN.
- Mesoscale wind patterns occurred frequently in the summer seasons.
- Emissions of VOCs and NOx in the region decreased in the past.
- Several categories of emissions had significant changes. On-road mobile emissions NOx and VOCs have been decreasing.

- Ozone design values have decreased at almost all sites since 2001.
- Ambient concentrations of ozone precursors and VOC species in general decreased in the past 10 years.

In particular, the conceptual model identified the ozone season and defined 2 ozone episodes for the PdN region as following:

- The ozone season in El Paso is defined as 4 months starting on June 1 and ending on Sep. 30, based on the ozone trend and exceedance analyses

- Two ozone episodes: a) June 13-22, 2006; and b) August 6-15, 2008 are identified for future air quality modeling analysis based on the criteria outlined by EPA.

Meteorological conditions for ozone episodes were identified as:

- Daily maximum 1-hour and 8-hour ozone concentrations were positively correlated to solar radiation, temperature, and afternoon mixing height, but negatively correlated to wind speed, humidity and morning mixing height.
- Daily maximum 8-hour average ozone concentrations exceeded 60 ppb only at temperatures above 75 ^{O}F and relative humidity less than 45% (82 ^{O}F and 45% for the 75 ppb standard).
- The surface meteorology indicated that high ozone concentrations were strongly associated with winds coming from the southeast octant whereas the mesoscale meteorology indicates that westerly winds could also be associated with high ozone concentrations.
- Four factors were identified by the principal component analysis. These four factors represent 1) atmospheric stability in terms of mixing height, solar radiation, temperature and humidity; 2) the effects of atmospheric winds in terms of wind speed and wind gust; 3) the ozone precursor NOx; and 4) the ozone formation accelerator TNMOCs.
- Adverse surface meteorology conditions in favor of ozone formation were identified below:
    - Low mixing height
    - High temperature
    - Low humidity
    - Low wind conditions
    - Prevailing east-west wind direction

1.3 Scope of Work

The University of Texas at El Paso (UTEP) was tasked by the MPO to assist in several photochemical modeling activities designed to advance the Texas State Implementation Plan (SIP), including setting up, running, and evaluating the performance of CAMx photochemical air quality model. UTEP has worked with Environ International Corporation to implement the following tasks:

1. Developing a photochemical modeling protocol appropriate for submittal as part of a Texas SIP revision based on a revised eight-hour ozone standard;
2. Improving and upgrading modeling emissions inventories for the 2008 baseline scenario of this ozone episode;
3. Investigating model performance of the 2006 base case ozone episode;
4. Investigating model sensitivity to broad changes in precursor emissions; and
5. Evaluation of potential local voluntary or mandatory control strategies.

1.4 Contents of the Report

This report documents the setup and results for a series of WRF meteorological and CAMx air quality simulations of the 2006 summer ozone episode for the PdN region. The project background and findings from the conceptual model are discussed in Chapter 1. The photochemical air quality modeling system is described in Chapter 2 with a brief description of the study area and components in the modeling system. UTEP's effort in providing an El Paso centered meteorology is discussed in Chapter 3. The meteorology obtained from the WRF concentric nested domains is presented and reviewed. Phenomenological and operational performance evaluation of the model outputs was conducted and the 4-km WRF meteorology was judged acceptable. Three sets of CAMx simulations were performed with UTEP 4-km meteorology or TCEQ's 4 km meteorology. Run 1 used El Paso centered nested domains for WRF and CAMx simulation. Runs 2a and 2b use TCEQ's 36-, 12-, and 4-km domains with TCEQ meteorology and UTEP meteorology, respectively. Sensitivity analysis of fugitive emissions on the PdN ozone levels was performed. Run 3a evaluated the impact of border crossing emissions on the PdN ozone levels whereas Runs 3.1 – 3.12 examined the impacts of Cd. Juarez area emissions on the PdN ozone levels. Two sets of emissions inventory files were used in the simulations due to the difference in modeling domains. Chapter 4 discussed the emissions inventories used in this project. Chapter 5 presents the results and performance evaluations for Runs 1, 2a, and 2b (Sections 5.1 and 5.2). Run 1 was judged unacceptable and both Run 2a and Run 2b were judged acceptable. Run 2a was selected to be the base case simulation and the basis for the 13 scenarios for sensitivity analysis. Section 5.3 presents and discusses the

results of the sensitivity analysis. Chapter 6 discusses the uncertainties that might have been introduced into the final ozone predictions and how they could or should have been reduced to improve the quality of the ozone predictions. A summary of the project is presented in Chapter 7.

Chapter 2 Summary of the Modeling Approach

A TCEQ-preferred photochemical air quality model, CAMx, was used in this study to evaluate ozone pollution and its sensitivities associated with changes in precursor emissions for the PdN region during the June 2006 ozone episode. The emissions inventory required for the analysis was obtained from the TCEQ Rider 8 emission inventory (TCEQ 2011) and the meteorology for the modeling period was developed by UTEP using the WRF model.

Three sets of modeling configurations were developed in this study for CAMx runs. UTEP configured the first set of CAMx simulation using concentric CAMx air quality and WRF meteorological domains centered at El Paso (discussed in Chapter 3) and EPA documented emissions inventory. In order to independently validate the results from the first simulation, UTEP contracted Environ to perform the second set of simulations which included 2 base case simulations: one with TCEQ 36/12/4 km grid and another with a single 4-km grid using UTEP's concentric 4-km WRF meteorology (Appendix A). Based on the results of the first 2 sets of simulations, a third set of configuration was conducted to evaluate the sensitivities of certain potential emissions inventory improvements on the region's ozone pollution (Section 5.3). This chapter describes the air quality model system and UTEP's first run configuration. Run configurations for the 2nd and 3rd sets of simulations are included in Appendix A.

2.1 Photochemical Modeling System

Photochemical simulations of ozone concentrations in the PdN were performed using the TCEQ-preferred air quality model CAMx (Version 5.4). The Comprehensive Air Quality Model with Extensions (CAMx) is an Eulerian photochemical dispersion model that allows for an integrated 'one-atmosphere' assessment of gaseous and particulate air pollution over scales ranging from sub-urban to continental (Environ 2009a). The CAMx modeling system, containing the core model of CAMx and a number of submodels, preprocessors, and postprocessors, is capable of simulating the emission, dispersion, chemical reaction, and removal of pollutants by dry/wet deposition in the troposphere by solving the pollutant (Eulerian) continuity equation for each chemical species on a nested three-dimensional grid. TCEQ and U.S. EPA rely on CAMx as the air quality model of choice for State Implementation Plan (SIP) demonstrations. CAMx Version 5.4 has been extensively utilized by TCEQ for simulations of baseline, basecase, and future-case ozone pollution in various cities in Texas. The use of this version maintains consistency with CAMx simulations for Houston, Dallas-Fort Worth, and San Antonio and other potential nonattainment regions of Texas (Environ 2009b). The following variables affect photochemical air quality (Environ, 2009a):

- Spatial (vertical and horizontal) and temporal distribution of anthropogenic and biogenic emissions;
- Chemical composition of the emitted emissions NOx, VOC, and $PM_{2.5}$;
- Spatial and temporal variations in wind fields;
- Dynamics of the boundary layer, including stability and mixing;
- Chemical reactions involving VOC, NOx, CO, and other important compounds;
- Diurnal variations of solar radiation and temperature;
- Loss of ozone and ozone precursors by dry deposition; and
- Ambient background concentrations of VOC, NOx, CO, and other pollutants within, immediately upwind of, and above the study region

A file needs to be developed for each of the above-mentioned variables for the CAMx simulation. Variables and output must be assessed early in the simulations to confirm the model does not generate spurious data.

2.2 CAMx Input Files and Run Configurations

Photochemical modeling with CAMx involves a process of integrating ambient air quality data, emissions inventories, meteorology, and other variables with the goal of obtaining results that correspond to ambient data observed at local air quality monitoring stations. The following databases require preprocessing to operate CAMx for the ozone modeling episodes selected for this study:

- Three-dimensional hourly meteorological data;
- Land-use distribution data;
- Three-dimensional hourly emissions data;
- Initial conditions and boundary conditions; and
- Photolysis rates inputs, including ultraviolet (UV) albedo, haze opacity, and total atmospheric ozone column fields.

2.2.1 Meteorological Inputs

The WRF meteorological outputs need to be processed by the WRFCAMx pre-processing program for CAMx to extract data from the hourly WRF outputs and create CAMx-ready meteorological input files. Simulations of the meteorology for the concentric domains are discussed in Chapter 3.

2.2.2 Emission Inputs

Emissions data was prepared for input into the CAMx model. Model-ready gridded emissions were processed from point, county-level surrogate area sources, and link-level emission inventories. TCEQ provided speciated emissions inventory data from local El Paso and Cd. Juárez point sources. Point, county-level area source, and link-level emissions were generated by the emission processor EPS3. The county-level area source emissions data were processed to more accurately spatially allocated emissions within the 4-km modeling grid. The emission inventories used are reviewed and discussed in Chapter 4.

2.2.3 Concentric CAMx Modeling Domains

The concentric CAMx modeling analysis was performed over a three-nested domain configuration with 36-, 12- and 4-km resolutions for coarse, middle and fine domains, respectively. All domains were centered at the city of El Paso, TX (31.70 N, 106.40 W). All three CAMx grids possessed identical 24 vertical layer structures spanning the entire troposphere and lower stratosphere up to a pressure altitude of 100 mb. Figure 2.1 shows the nested domain configuration used in the CAMx. The meteorological input was obtained from the non-hydrostatic WRF model (version 3.3) for every hour (Skamarock et al 2008). Table 2.1 shows the vertical layers configuration for CAMx and WRF. The WRF model was run with 35 sigma vertical levels.

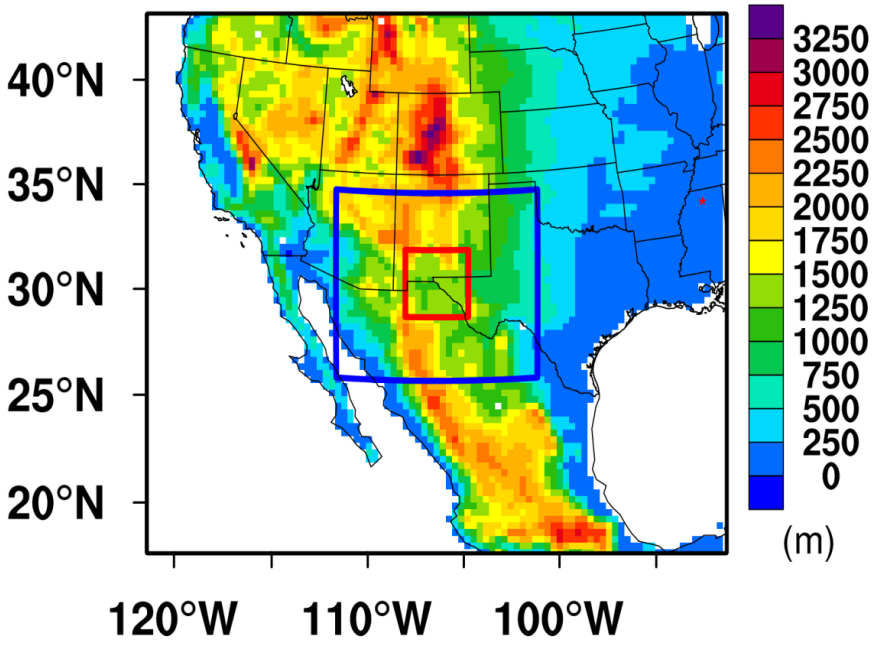

Figure 2.1 Configuration for the concentric nested CAMx domains (The three domains are in 36-, 12- and 4-km horizontal resolutions. Shaded contours are terrain height with unit of meters)

Table 2.1 Vertical layer definition for the WRF (34 layers) and CAMx (24 layers)

	WRF			CAMx	
Layer	Sigma	Height (m)	Layer	Sigma	Height (m)
34	0	19052	24	0	19052
33	0.013	17960			
32	0.026	17014	23	0.026	17014
31	0.04	16152			
30	0.055	15386	22	0.055	15386
29	0.07	14641			
28	0.088	13918	21	0.088	13918
27	0.106	13213			
26	0.127	12495	20	0.127	12495
25	0.15	11781			
24	0.175	11072	19	0.175	11072
23	0.202	10372			
22	0.231	9670	18	0.231	9670
21	0.263	8959			
20	0.298	8251	17	0.298	8251
19	0.335	7539			
18	0.376	6819	16	0.376	6819
17	0.42	6098			
16	0.468	5373	15	0.468	5373
15	0.52	4683			
14	0.571	4045	14	0.571	4045
13	0.622	3450	13	0.622	3450
12	0.672	2908	12	0.672	2908
11	0.719	2410	11	0.719	2410
10	0.765	1960	10	0.765	1960
9	0.807	1565	9	0.807	1565
8	0.845	1216	8	0.845	1216
7	0.88	919	7	0.88	919
6	0.909	675	6	0.909	675
5	0.934	476	5	0.934	476
4	0.954	319	4	0.954	319
3	0.97	196	3	0.97	196
2	0.983	99	2	0.983	99
1	0.993	29	1	0.993	29
0	1	0	0	1	0

2.2.4 Chemistry Treatments and Related Inputs for CAMx

The Gas-phase photochemistry was treated with the Carbon Bond 2005 mechanism (CB05; Yarwood et al., 2005) by UTEP. CAMx provides two options for the representation of the particle size distribution: a static two-mode coarse/fine (CF) scheme, and the multi-sectional CMU scheme, which treats the size evolution of each aerosol constituent among a number of fixed size sections. In this study, CF scheme was applied. Three options are available to solve the gas-phase chemistry in CAMx. The Euler-Backward Iterative (EBI) solver was selected for this study. With respect to vertical diffusion (mixing), the Asymmetric Convective Model Version 2 (ACM2; Pleim, 2007), which includes mixing between adjacent layers using K-theory and mixing between non-adjacent layers only for transfer from the surface to layers aloft during convective conditions, was selected. ACM2 includes the basic features of both local and the most important component of non-local exchange. The Piecewise Parabolic Method (PPM) method has been used to calculate horizontal advection (Colella and Woodward 1984). The updated Zhang scheme (Zhang et al., 2001, 2003) was applied for dry deposition. This method is a state-of-the-science algorithm that incorporates vegetation density effects via leaf area index (LAI). It possesses an updated representation of non-stomatal deposition pathways including a better snow cover treatment, and has been tested extensively through its use in daily air quality forecasting. The Zhang model uses 26 landuse categories. The TUV radiative transfer and photolysis model (Madronich 2002), developed at the National Center of Atmospheric Research (NCAR), was used as a preprocessor to provide the air quality model with a multi-dimensional lookup table of clear-sky photolysis rates by surface albedo, total ozone column, haze turbidity, altitude, and zenith angle. The approach uses a fast in-line version of TUV (Emery et al 2010) to calculate photolysis adjustment profiles through each cloudy grid column. One notices that a slightly improved version of the gas-phase photochemistry (CB06) was used by Environ for the base case CAMx simulations.

2.2.5 Initial and Boundary Conditions

The CAMx model was run for 10 consecutive days from 1200 UTC June 12, 2006 through 1200 UTC June 21, 2006. For the cold starting run (e.g., the first day of simulation), chemical initial and boundary conditions for the 36 km grid were obtained from idealized profile data of the CMAQ, Version 4.7, (Byun and Ching 1999) model package by using an interface program documented by ENVIRON (2012). This processor interpolates three-dimensional concentration fields horizontally and vertically to the CAMx initial and boundary grid definition. It then maps the predefined gas species in profile to the CB05 compounds required by CAMx. Initial and boundary conditions for each 12- and 4-km simulations were subsequently extracted from the CAMx 36 km simulation results on an hourly basis. For the warm starting run (e.g., cycle

running), the simulation results of the previous day were used to generate initial and boundary conditions.

Chapter 3 Meteorological Modeling

Meteorology plays a critical role in determining atmospheric ozone concentrations. It affects the background ozone transport from the stratosphere, air pollutant emission rates, the mixing and transport of emissions and their products, and chemical reaction rates along with dry and wet deposition. A good synoptic scale weather forecast is essential to accurately forecast tropospheric and surface ozone concentrations.

The meteorological model selected for our simulations was the Weather Research Forecast (WRF).

3.1 The Study Area

El Paso and the El Paso County, Texas, US locate in the westernmost corner of Texas. El Paso County stands on the Rio Grande (Río Bravo del Norte), neighboring the adjacent cities of Ciudad Juárez, Chihuahua, Mexico and Sunland Park, New Mexico. According to the 2010 census, the population of El Paso was approximately 800,647 with a density of 2,939 people per square mile (American FactFinder 2012).

3.1.1 Geographic location

El Paso city's elevation is 3,800 feet above sea level and covers a total area of 250.5 square miles. El Paso is located at 31°47’25”N 106°25’24”W (31.790208, -106.423242). It is the only major Texas City on Mountain Time. The rustic North Franklin Peak towers at 7,192 feet (2,192 m) above sea level and is the highest peak in the city. The peak can be observed from 60 miles (97 km) in all directions. In addition, the Franklin Mountains extend into El Paso from the north and nearly divide the city into two sections; the western half forms the beginnings of the Mesilla valley and the eastern slopes connect in the central business district at the south end of the mountain range. According to the United States Census Bureau, the city has a total area of 250.5 square miles (648.9 km²). Figure 3.1 shows the location of El Paso County and the border between the United States and Mexico.

3.1.2 Climate

El Paso Texas has a warm, arid climate with very hot summers and generally mild and dry winters (http://en.wikipedia.org/wiki/K%C3%B6ppen_climate_classification, Koppen climate classification). The temperature ranges have an average high of 55 F (13 °C) and an average low of 28 °F (−2 °C) in January to an average high of 97 °F (36 °C) in June and an average low of 68 °F (20 °C) in August. The city's record high is 114 °F (45.5 °C), and its record low is −8 °F (−22 °C).

The rainfall averages 8.74 inches (223 mm) per year, most of which occurs during the summer from July through September and is principally caused by monsoonal flow from the Gulf of California. During this period, winds originate more from the south to southeast and bring moisture from the Pacific Ocean, the Gulf of California, and the Gulf of Mexico into the region. El Paso, at 3,800 feet (1,200 m) elevation, is also exposed to snowy weather systems that have produced more than a foot of snow on many occasions. In 1980, three major snowstorms produced over a foot of snow; one in February, another in April and the last one in December, producing a white Christmas for the city. A major snowstorm in December 1987 accumulated over two feet (65 cm) of snow (NOAA 2012).

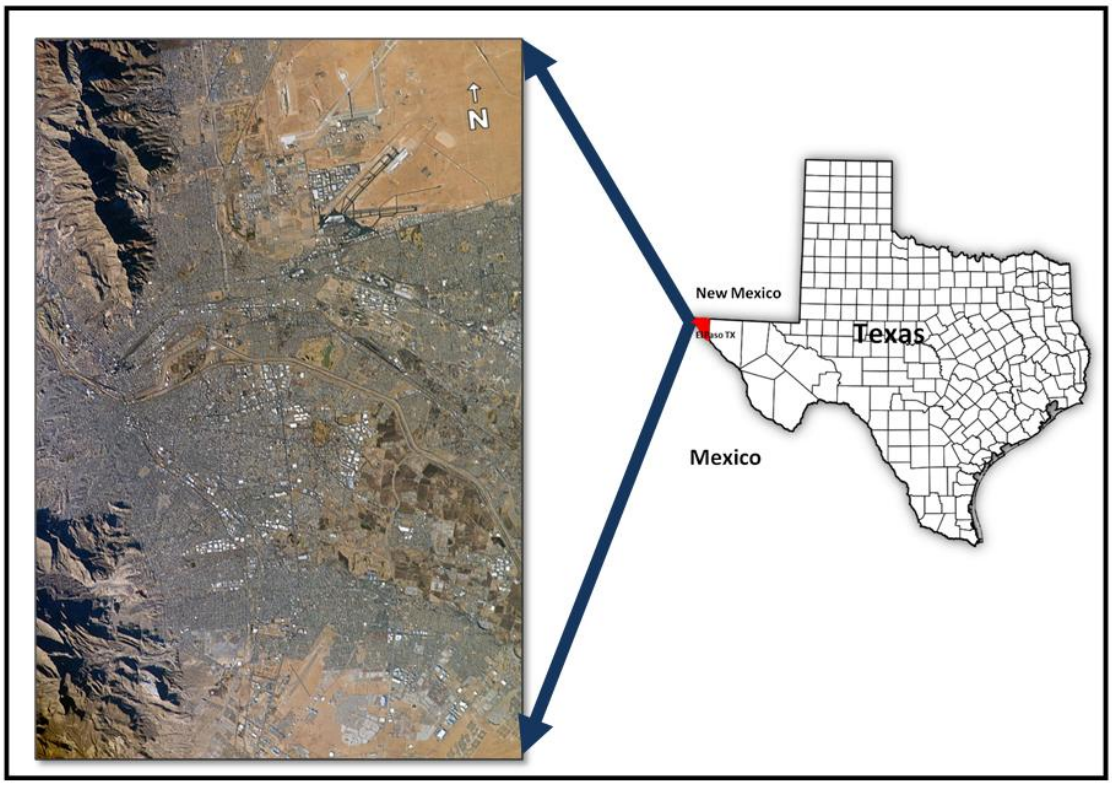

Figure 3.1 Map of the study area

3.2 The WRF Model

The WRF model is a limited–area, nonhydrostatic (with a hydrostatic option), primitive-equation mode (Skamarock et al 2001). Its vertical coordinate is a terrain-following hydrostatic pressure coordinate. The grid staggering is the Arakawa C-grid. The model uses the Runge-Kutta 2nd and 3rd order time integration schemes, and 2nd to 6th order advection schemes in both horizontal and vertical directions. It uses a time-split small step for acoustic and gravity-wave modes. The dynamics conserves scalar variables. The model is a collaborative product of many research institutes under the leadership of the National Center for Atmospheric Research (NCAR). The model has been fully validated and researched, detailed descriptions of the model and its applications can be found at the Mesoscale and Microscale Meteorology Division of NCAR website and in the literature (e.g., Michalakes et al 2001; Skamarock et al 2005).

The WRF model is a versatile weather forecasting model with a variety of capabilities including:

- Real-data and idealized simulations;
- Various lateral boundary condition options for real-data and idealized simulations;
- Full physics options;
- Positive-definite advection scheme;
- Non-hydrostatic and hydrostatic (runtime option);
- One-way, two-way nesting and moving nest;
- Three-dimensional analysis nudging; and
- Observation nudging.

A “warm run” with a spin up period of three days was performed using the WRF model over the Paso del Norte region to generate meteorology for use in the photochemical simulation of the 2006 June ozone episode.

3.2.1 Map Projection

The modeling domains are defined on Lambert Conformal Conic map projection the same as that defined by TCEQ:

First True Latitude: 33 ° N

Second True Latitude: 45 ° N.

Central Longitude (Gamma): 33 ° N

Projection Origin: (97°W, 40° N)

3.2.2 Nested three-grid system

Figure 3.2 shows the 36-, 12-, 4-km nested grid system used in this study that is centered at the city of El Paso. Initial and boundary conditions obtained from the NCEP Final Analysis (FNL) dataset with a 6-h interval were incorporated into the WRF model. FNL is a global dataset in the format of the grid with the resolution of 1×1°. This set of concentric, nested grid system is different from the one prescribed by TCEQ for their Rider 8 program application, which contains three nested domains centered at Dallas, Texas (Figure 3.3). The decision to use a nested grid system centered at El Paso was made on the basis of 2 considerations. First, although TCEQ generates 4-km domain centered at El Paso, the 12- and 36-km domains generated by TCEQ are still centered at Dallas. The El Paso 4-km domain is positioned in the close vicinity of the Texas 12-km domain. WRF model filters in a lot of information across the domain boundary, it is understood that errors may propagate into the smaller domain unevenly within the first few grid points. Nevertheless, the magnitude of the error caused by this effect is not well studied. Second, previous studies on the mesoscale and microscale meteorology at El Paso conducted by Fitzgerald and coworkers (Pearson and Fitzgerald 2001; Rivera et al 2009; Lu et al 2008, 2011; Becerra and Fitzgerald 2012) as well as other researchers (Brown et al 2001; Choi et al 2006; Lee and Fernando 2003) support the use of the concentric grid system. Effects due to the use of different domains in the WRF weather simulation on the spatial and temporal distributions of ozone prediction in the Paso del Norte region are discussed in Chapter 6. In addition, the use of El Paso-concentric domains in the WRF simulations creates unexpected complications in processing the emissions inventories data available from TCEQ, which is addressed in Chapter 4.

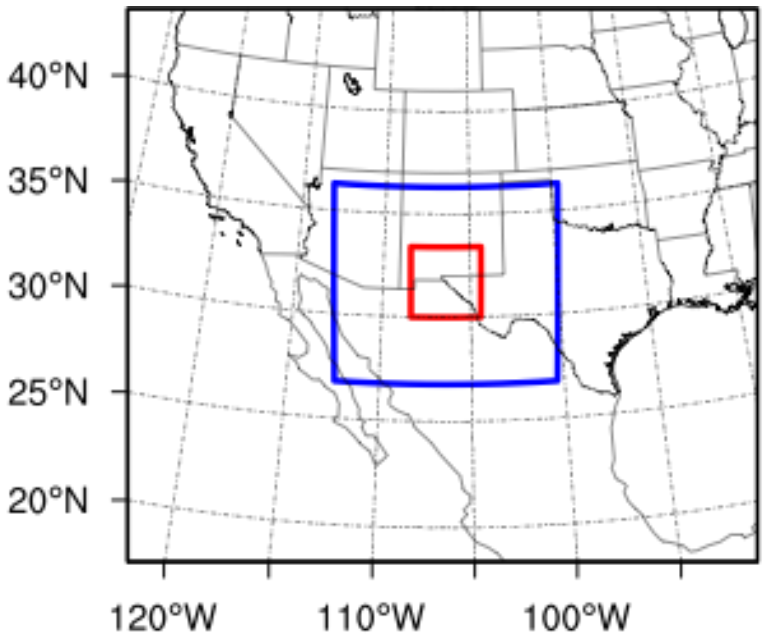

Figure 3.2 Nested three-grid system for WRF

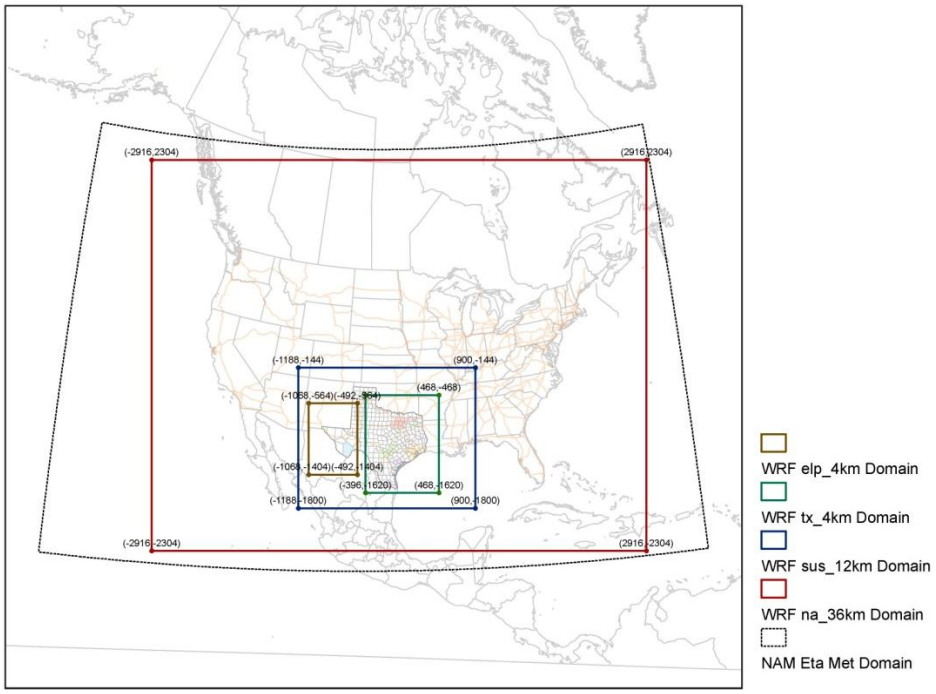

Figure 3.3 TCEQ Rider 8 ozone modeling domain

3.2.3 Vertical layers used

Thirty four sigma vertical levels were used to characterize the vertical domain of the nested grid system. Table 3.1 lists the altitude and thickness of each layer.

3.2.4 Landuse classification

The USGS 24-category, global coverage with the resolution of 1-degree land use data were used for landuse classification in the WRF modeling domains (Fitzgerald et al 2011). Figure 3.4 displays the vegetation in the modeling domains in color with a description of each category included.

3.2.5 Topography

The terrestrial inputs including terrain, landuse, soil type, annual deep soil temperature, monthly vegetation fraction, maximum snow albedo, monthly albedo, and slope data were provided from previous WRF simulations (Lu et al 2008). Figure 3.5 shows the topography of the model domains in color.

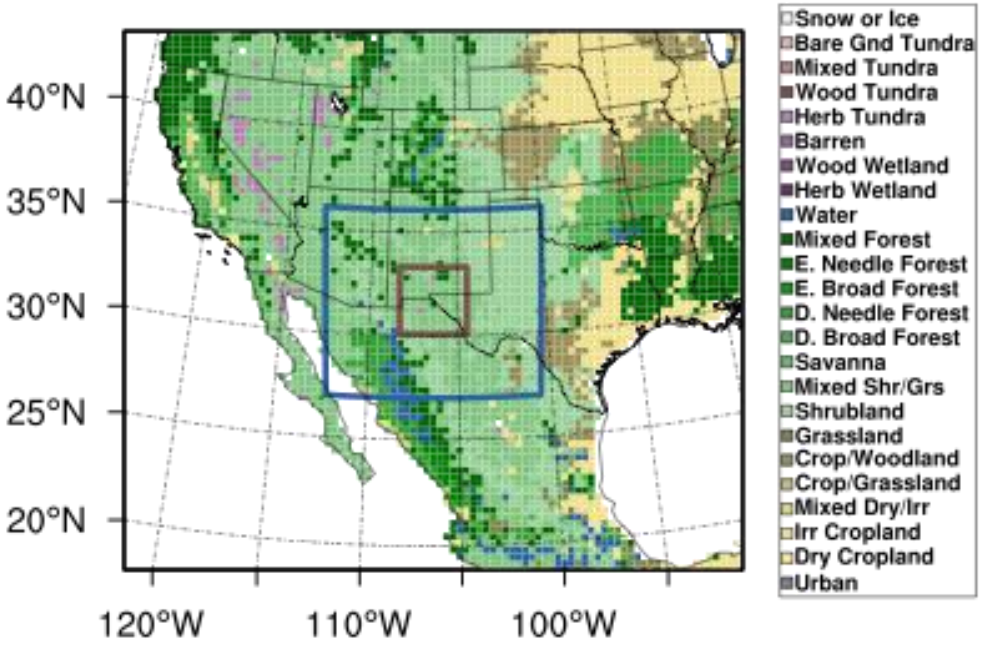

Figure 3.4 Land use classification for the modeling domains

Table 3.1 Vertical layer defined for the WRF model

Layer	Sigma	Height (m)
34	0	19052
33	0.013	17960
32	0.026	17014
31	0.04	16152
30	0.055	15386
29	0.07	14641
28	0.088	13918
27	0.106	13213
26	0.127	12495
25	0.15	11781
24	0.175	11072
23	0.202	10372
22	0.231	9670
21	0.263	8959
20	0.298	8251
19	0.335	7539
18	0.376	6819
17	0.42	6098
16	0.468	5373
15	0.52	4683
14	0.571	4045
13	0.622	3450
12	0.672	2908
11	0.719	2410
10	0.765	1960
9	0.807	1565
8	0.845	1216
7	0.88	919
6	0.909	675
5	0.934	476
4	0.954	319
3	0.97	196
2	0.983	99
1	0.993	29
0	1	0

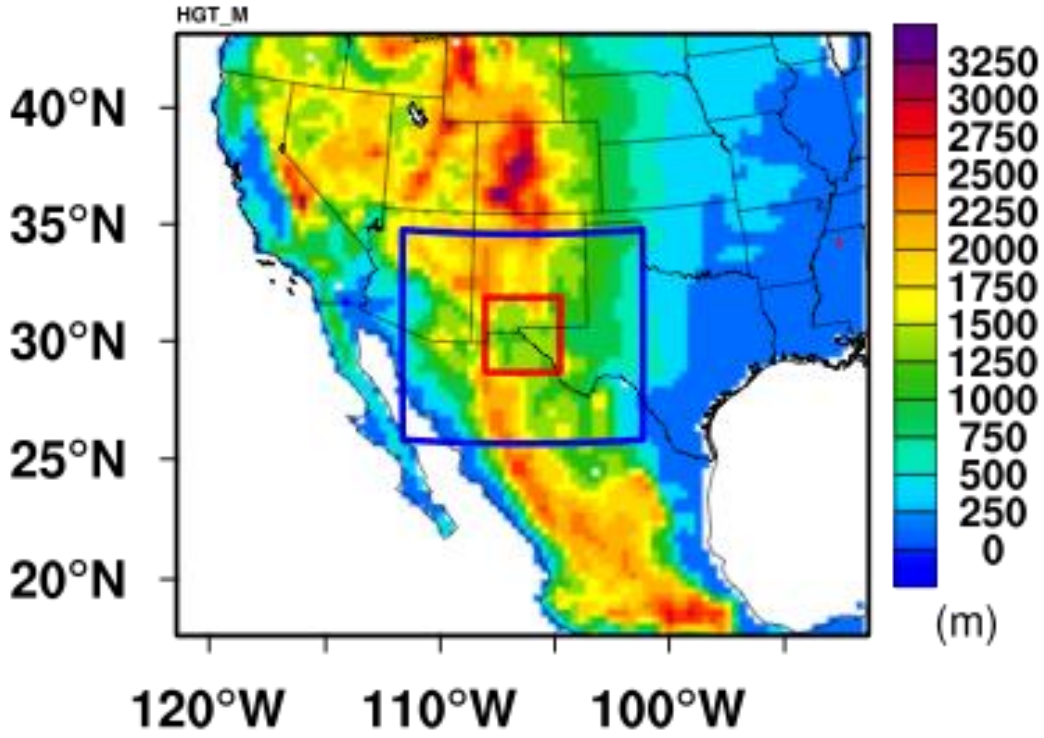

Figure 3.5 Graphic presentation of the topography in the modeling domain

3.2.6 Modeling Options

The WRF model is equipped with a suite of physics options that allow users to select critical features to be simulated. Determination of an optimal configuration of various physics options for a simulation is difficult to achieve and could be subjective due to the size of the region being evaluated, complexity of terrain, time periods evaluated, and numbers and locations of data available for performance evaluation. The configuration which results in predictions that provide the best statistical match with the observed data over the most cases, in general, is the one that should be chosen (U.S. EPA 2005). Needless to mention that other qualitative information available for consideration should also be taken into consideration.

Based on the review of previously conducted meteorological studies (Brown et al 2001; Choi et al 2006; Lee and Fernando 2003; MacDonald et al 2001) and numerous sensitivity analyses performed by Fitzgerald and colleagues (Pearson and Fitzgerald 2001; Lu et al 2008, 2011; Becerra and Fitzgerald 2012) for the region, the following WRF Physics Options were selected without repeating a series of sensitivity analyses:

- Microphysics option: WSM 3-class simple ice scheme

- Surface-layer option: Monin-Obukhov
- Land-surface option: thermal diffusion scheme
- PBL: YSU scheme
- Cumulus option: Grell-Devenyi ensemble scheme
- Four Dimensional Data Assimilation (FDDA): grid-nudging (analysis nudging)

3.2.7 Initial and boundary conditions

The data incorporated into the WRF model as initialization and lateral boundary conditions are obtained from NCEP Final Analysis (FNL) dataset with a 6-h interval. This is the global dataset in the format of the grid with the resolution of 1×1°.

3.3 Model Performance Evaluation

As recommended by the EPA, meteorological outputs to be used in the air quality model should be evaluated to ensure that good meteorological model performance will yield more confidence in predictions generated from the air quality model (U.S. EPA 2005). It is of paramount importance that the meteorological model outputs represent a reasonable approximation of the actual meteorology that occurred during the modeling period. Furthermore, it is of equally importance that the effects of the errors and biases in the meteorological model outputs on the subsequent air quality model predictions be quantified. While both operational evaluation and phenomenological assessment are critical in determining if the meteorological outputs produce high quality air quality predictions no benchmarks in the pass/fail mode have been given by EPA (U.S. EPA 2005).

We have relied on the modeling experience acquired and reported in the literature and selected the optimal physics options for the WRF simulations of the meteorology for the PdN region. Therefore, our performance evaluation focused on the performance of the model using the selected optimal physics options.

3.3.1 The June 13-22 2006 ozone episode

Based on the EPA-recommended four criteria for selecting ozone episodes, the conceptual model identified June 13-22, 2006 as the ozone episode for a base case air quality modeling assessment. During this ozone episode, the 8-hour ozone NAAQS was exceeded at multiple air monitoring stations in El Paso on June 18, a day designated as the ozone event day.

3.3.2 Phenomenological Evaluation

This episode was a classic set-up, showing a massive high pressure aloft overhead with subsidence causing warming and drying with maximum solar irradiance to produce ozone. The strong inversion trapped the pollutants with light, stagnant conditions observed in the middle of a string of 8 consecutive days, in particular on June 18, 2006. Temperatures were over 100 and peaked at 103 F. The synoptic weather events that took place were classical for large amounts of surface ozone produced in the heavily suppressed stagnant polluted air. The movement of the subtropical high pressure determined the direction and intensity of the annual monsoon season in the Borderland (June 15 - September 30).

The geopotential height at 500 mb is shown in Figure 3.6, which clearly shows the H5 subtropical high occurred to the south of El Paso at 22:00 UTC (or 15:00 MST) on June 18, 2006 that would have caused considerable subsidence (down vertical velocity). This type of subsidence in conjunction with clear skies, high maximum temperatures, and light low-level winds would create and trap high levels of ozone.

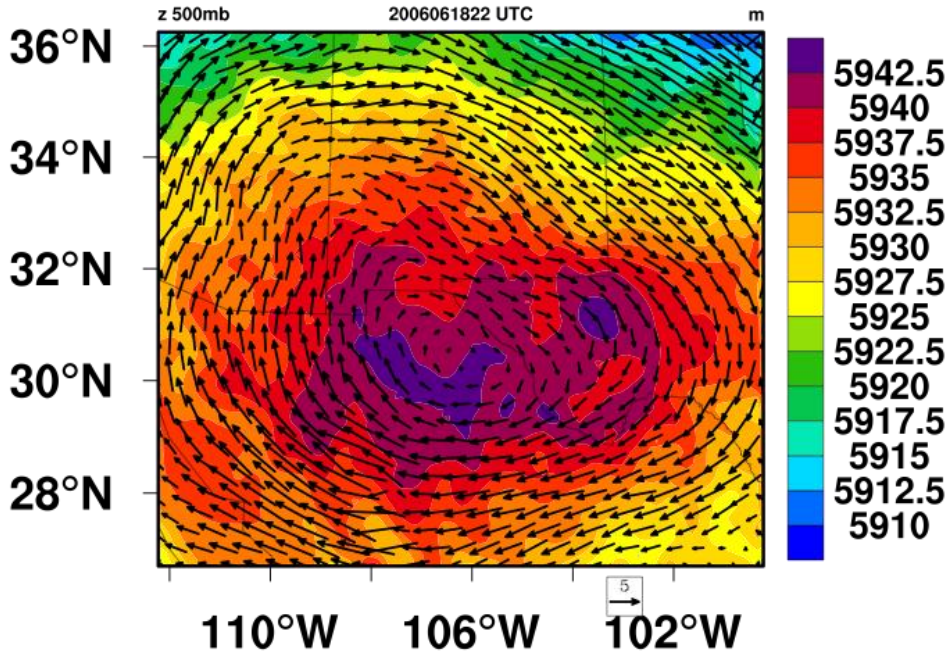

Figure 3.6 Geopotential height at Z =500 mb at 22:00 UTC on June 18, 2006, 12-km grid

Figure 3.7 depicts the geopotential height at a lower altitude of Z =850 mb at the same time on June 18th. The white regions shown in the graph correspond to mountainous areas. Indeed, as observed in Figure 3.8, high temperatures were observed in the Paso del Norte region on June 18, 2006, the day when ozone NAAQS was exceeded during this episode. The calm to low-wind conditions on June 18 were the apparent consequence of weak surface pressure gradients, which can be observed in Figure 3.9, the sea level pressure graph in the Paso del Norte region. In Figure 3.10, the low relative humidity pocket is seen to coincide with the center of the high pressure corresponding to subsiding air which is warmed dry adiabatically at 5.5 ^{o}F/1,000ft while the dew point decreases at 4 ^{o}F /1,000ft, therefore creating the minimal relative humidity pocket.

Figure 3.11 shows that the Planetary Boundary Layer (PBL) height was low in the PdN region on June 18, 2006, which was a contributing factor to the high ozone levels observed on that day. To illustrate such effect, the time-varying Planetary Boundary Layer (PBL) height for a high ozone day (June 18) is shown in Figure 3.12 for a comparison with that of a low ozone day (June 16th) in Figure 3.13. In Figure 3.12, the observed rise of the PBL corresponds nicely with the rises of the anticipated solar elevation angle and temperature during the day.

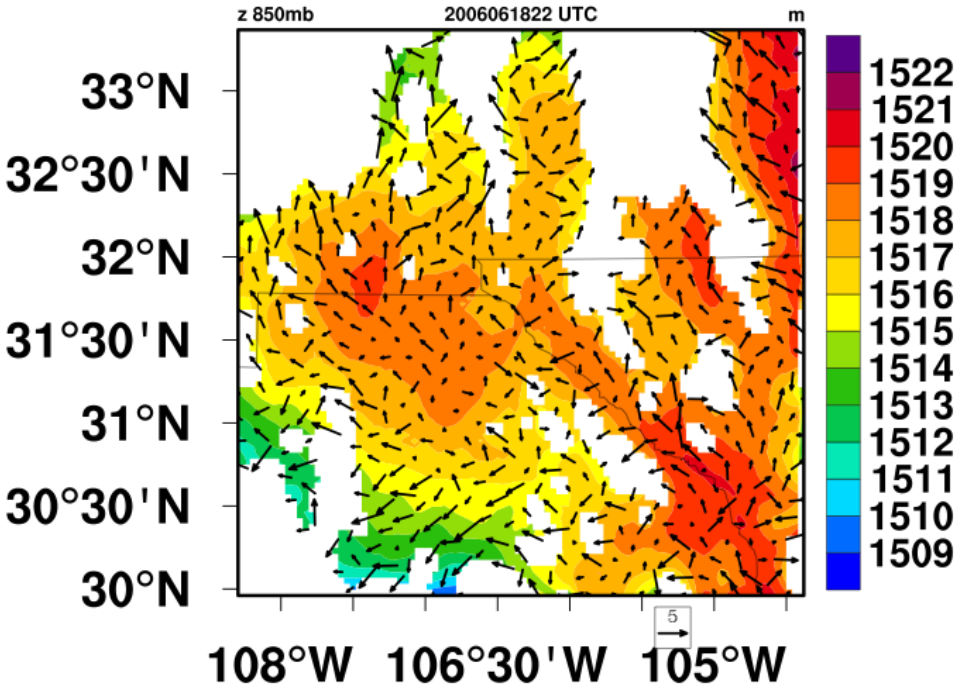

Figure3.7 Geopotential height at Z =850 mb at 22:00 UTC on June 18, 2006, 4-km resolution

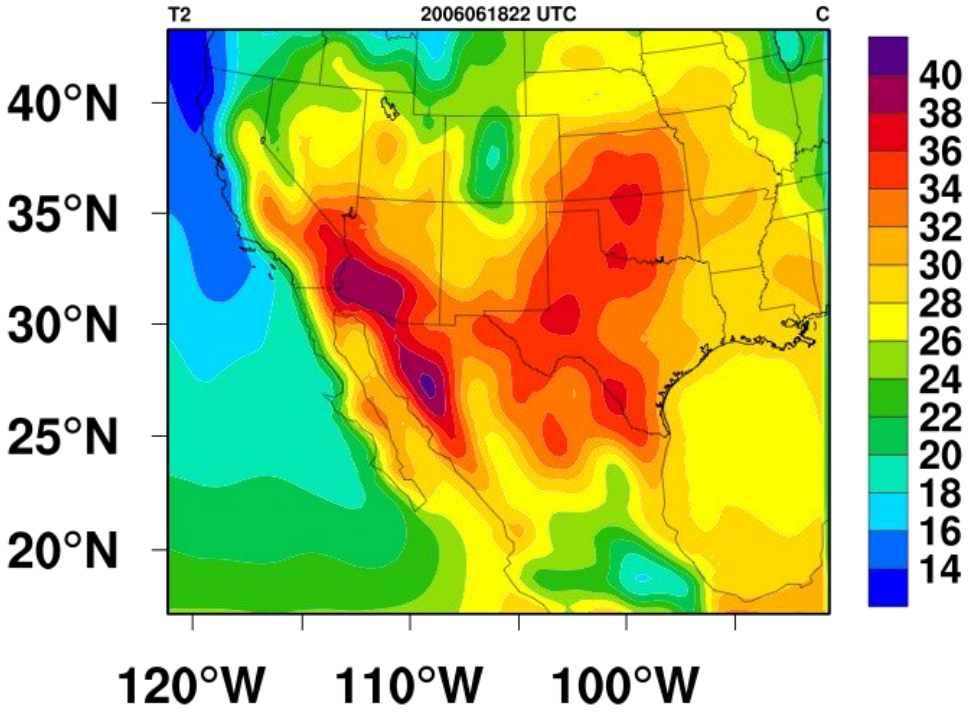

Figure 3.8 Surface temperature at 2m at 22:00 UTC on June 18, 2006, 36 km-resolution

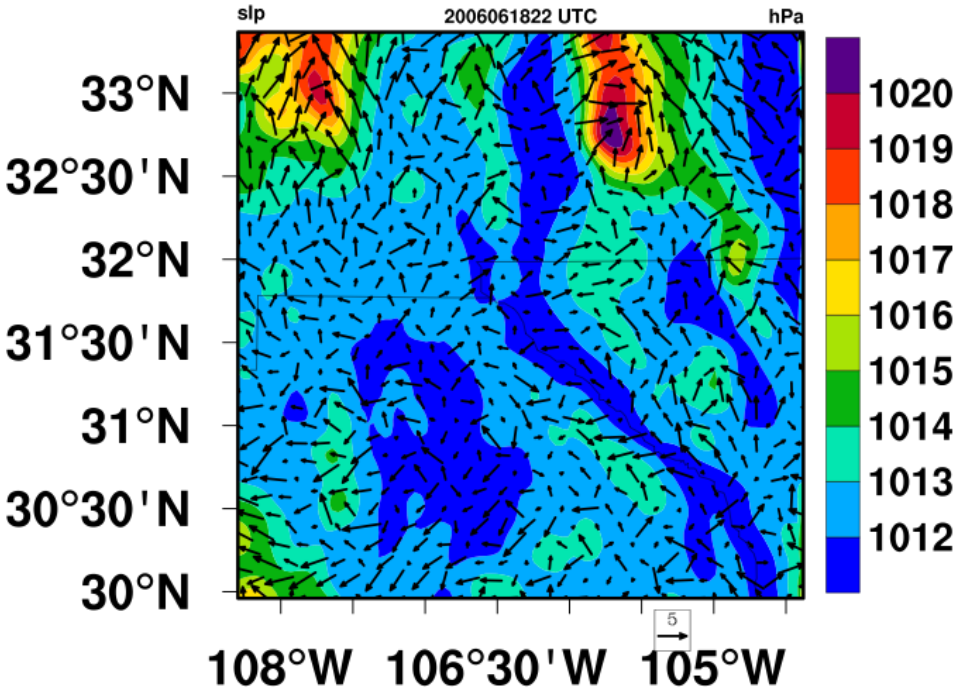

Figure 3.9 Sea-level pressure at 22:00 UTC on June 18, 2006, 4km resolution

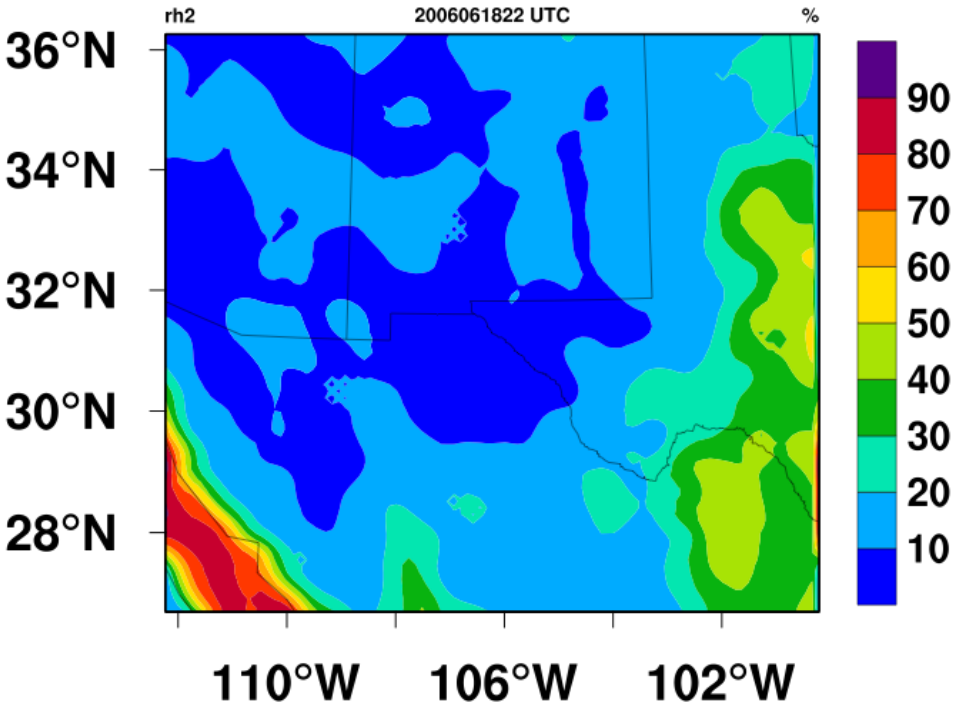

Figure 3.10 Relative Humidity at 2 m height, at 22 UTC, June 18, 2006, 12 km resolution

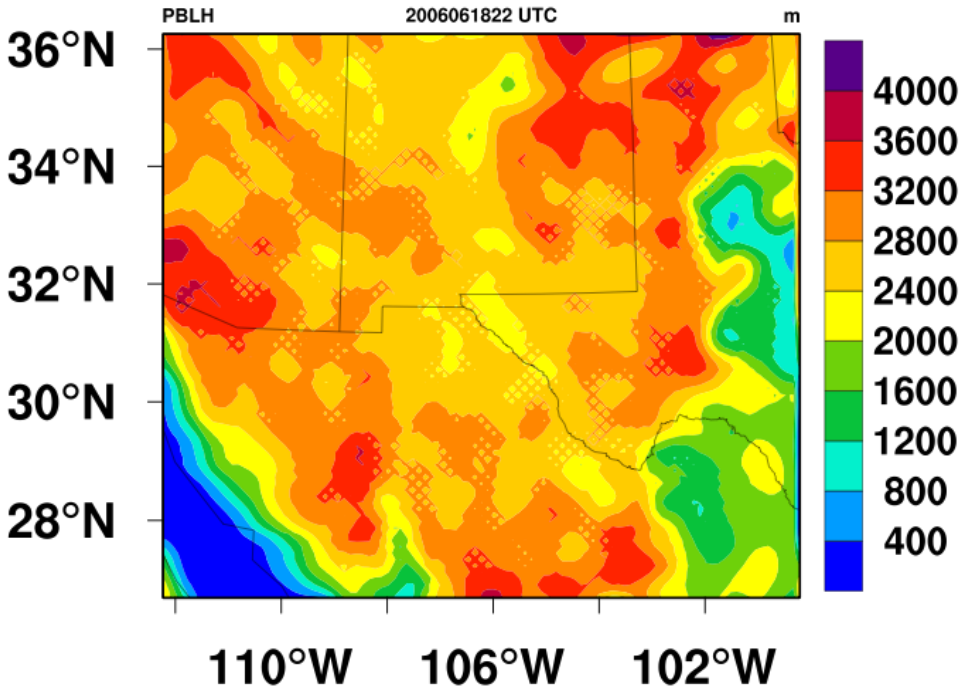

Figure 3.11 Planetary boundary layer (PBL) height at 22:00 UTC on June 18, 12 km resolution

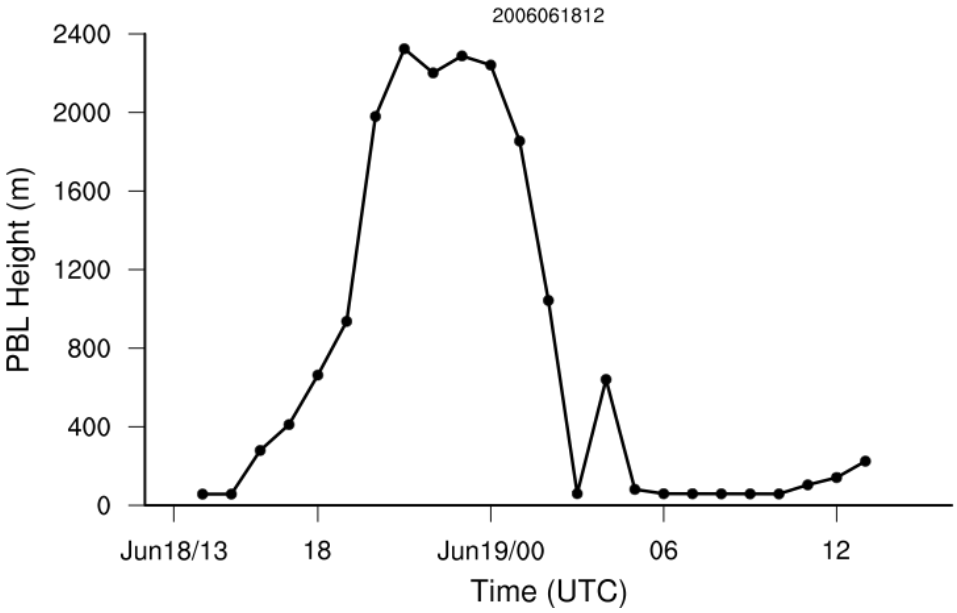

Figure 3.12 PBL height at C12 station, on June 18-19

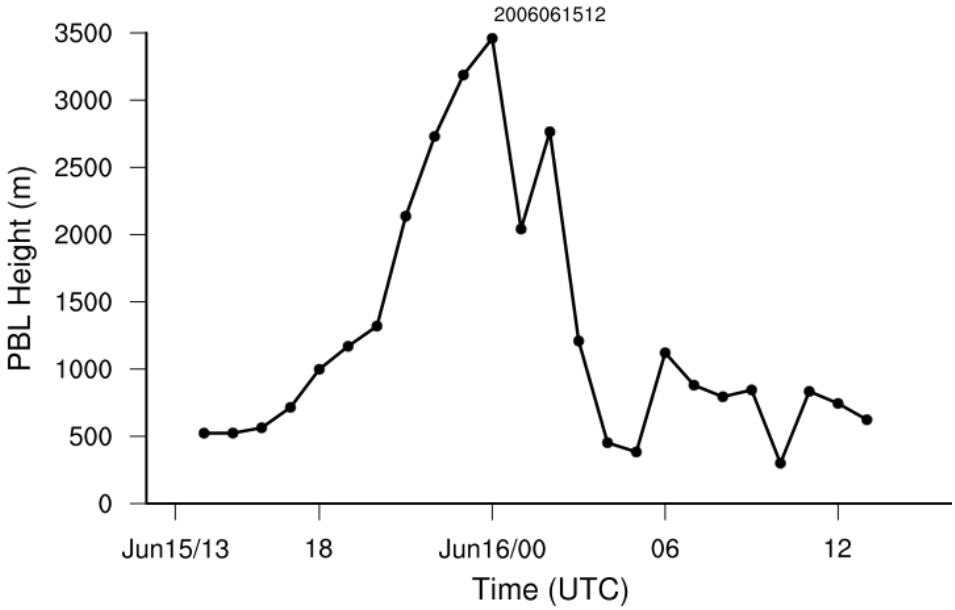

Figure 3.13 PBL height at CAMS 12 station on June 15-16

In summary, a close examination was conducted of the synoptic and local meteorology for the June 2006 ozone episode using the WRF model to determine how meteorological parameters

influence the formation, transport and dispersion of ozone in the PdN. The predominant synoptic feature of the ozone event day was the expansion, intensification, and slow progression of an upper-level ridge of high pressure. This kind of meteorological event is known to be associated with days of high ozone pollution. This meteorology is associated with highly stable atmospheres, strong temperature inversions with low mixing heights and therefore low mixing volumes. Under these conditions emissions lead to highly polluted conditions that are favorable to ozone formation. This type of synoptic event can best be illustrated by reviewing the characteristics of the 500-mb constant pressure pattern over the western USA and other associated sub-synoptic patterns (Figure 3.6). There is an evident anticyclone observed near the Paso del Norte region. This feature introduced aloft warming and increased atmospheric stability in the study area. At the lower level, weak surface pressure gradients were also found to be associated with these synoptic high pressure conditions (Figure 3.9) and, thus, with high ozone concentrations in the area. Fair weather with weak surface winds was observed and therefore, horizontal dispersion and dilution were relatively weak. Maximum surface temperatures were near 33 ^{o}C (Figure 3.8) around the region produced favorable conditions for the photochemical production of ozone from precursor emissions. Figure 3.10 shows surface relative humidity distribution from the 12 km domain. A dry area was found around the study region especially the southern El Paso-Juarez area. Lower relative humidity near the surface can be partly attributed to adiabatic heating due to small scale local downdrafts, which will lead to stronger temperature inversions. The resulting increase in atmospheric stability will suppress the vertical mixing process and cause lower level pollutants to be trapped near the ground.

Historically, maximum daytime mixing heights have often been considered to be proportional to the mixing volume. Figures 3.12 and 3.13 show the time series of PBL height on a high ozone day (June 18, 2006) and a day with lower ozone concentrations (June 16, 2006), respectively. The model provides very good simulations for diurnal variations of PBL height on both days. Our simulation findings are that low mixing heights play an important role in the high ozone concentrations observed in the Paso del Norte study area, as observed on June 18th, and this result is in agreement with the local experimental data. When the PBL mixing height is shallow, ozone and its precursors are confined to a smaller volume than with a deeper mixed layer. The reduced mixing volume tends to keep precursor emissions concentrated near the ground.

Separately, the HYSPLIT trajectory of the low level air into el Paso on June 18, shown in the conceptual model (Chapter 4, Li et al 2011a), depicted the parcels coming from the west (not the east as climatology would dictate). This can be explained by the 850 and 700 mb graphs shown below. Figure 3.14 shows the surface pressure field is flat, the 1,008 mb thermal low

over the southwest desert, and weak high pressure over El Paso. Figure 3.15, the 700 mb chart at 1200 UTC for June 18, 2006, shows a westerly weak trajectory from northwest Mexico to El Paso. In Figure 3.16, it is noticeable at 1200 UTC on June 18, 2006 the subsidence inversion of the subtropical ridge at 550 mb and the very strong inversion at 750-800 mb with easterlies and north northwest winds above trapping the pollution and taking a longer time for the inversion to burn off, thus giving a major pollution day with light winds at 10 kts or less. This experimental data confirms the results obtained in the WRF simulations.

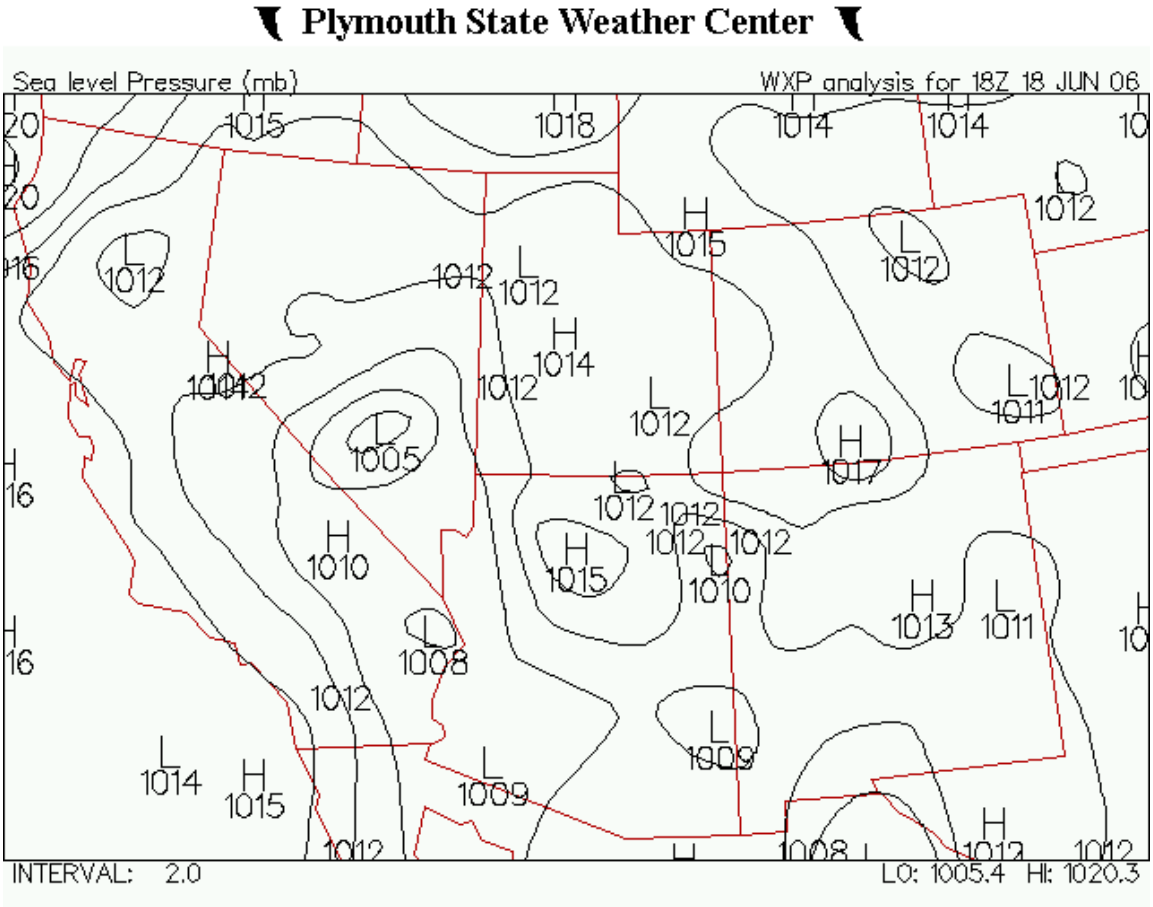

Figure 3.14 The mean sea level pressure on June 18, 2006 at 18:00 UTC

.

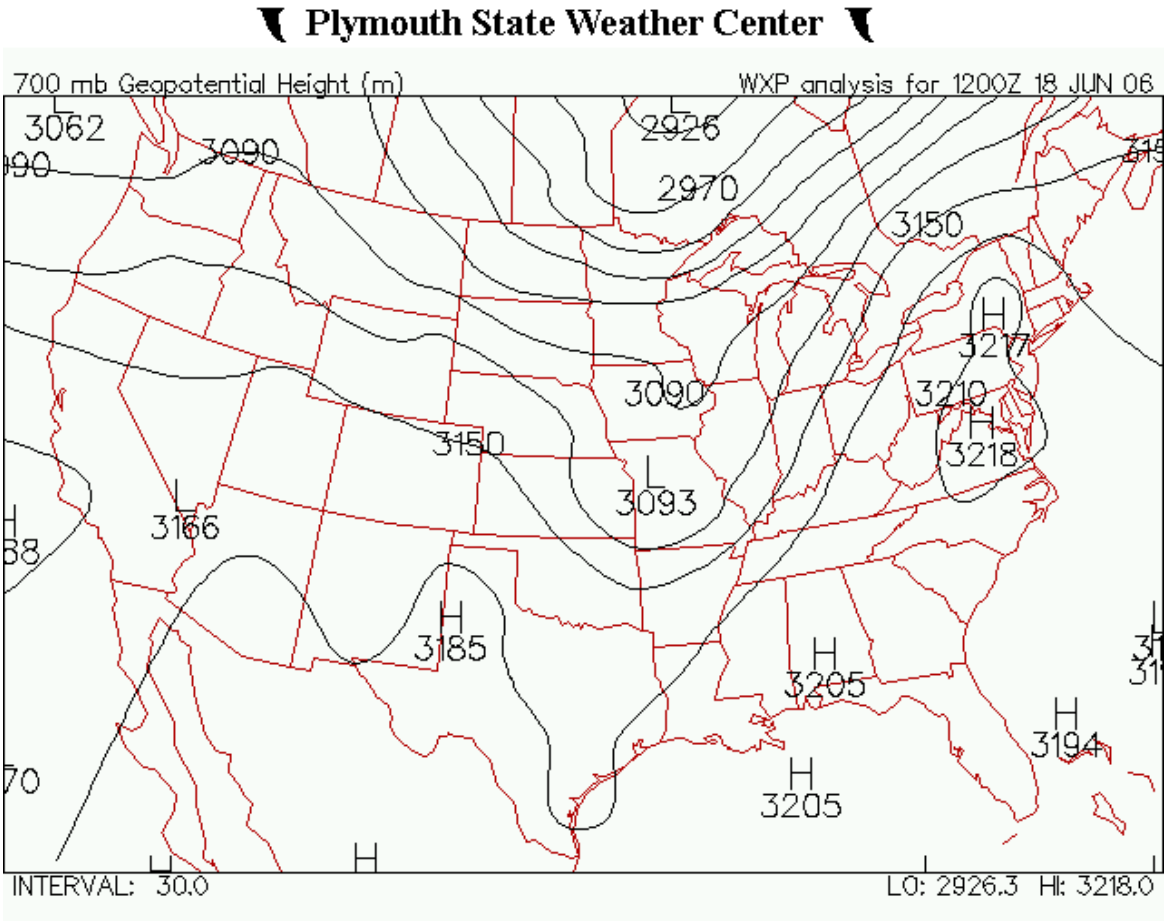

Figure 3.15 The 700 mb chart on June 18, 2006 at 12:00 UTC

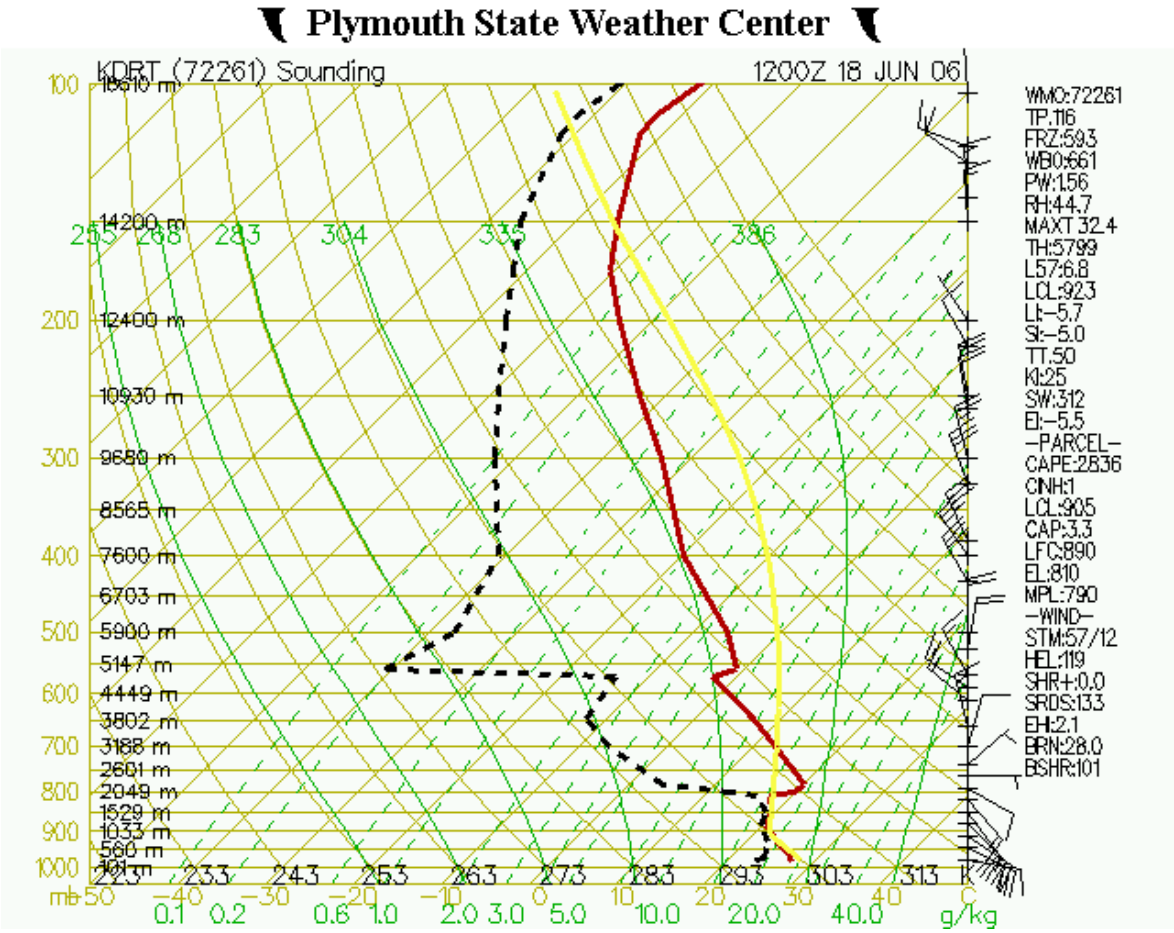

Figure 3.16 Soundings on June 18, 2006 at 12:00 UTC

3.3.3 Operational Evaluation

Operational evaluation of the model performance compares the model predictions and distributions of specific meteorological parameter to the observed values. As stated in the EPA guidelines (U.S. EPA 2005), comparisons of mean, mean bias, mean normalized bias, mean absolute error, mean absolute normalized error, root mean square error, and an index of agreement are desired for key meteorological parameters. In this section, we evaluate WRF model's performance by comparing meteorological variables simulated against corresponding data recorded by TCEQ at four CAMS locations. The four locations represent the stations in three different jurisdictions in the PdN that historically display high levels of ozone. The four stations are: CAMS 12, CAMS 41 (El Paso, TX), CAMS 6ZM (Dona County, NM), CAMS 663 (Cd. Juarez, Chihuahua, Mexico).

Three meteorological variables were selected: wind speed, temperature , and humidity for statistical evaluation between the WRF predictions and observed values at the four stations. Wind direction is considered an important parameter for performance evaluation. However, the finest grid resolution used in this study is 4-km and the surface wind direction is highly dependent on the local topography and surface obstructions. The comparison for this variable is invalidated due to insufficient spatial resolutions in local topography, land use, and other variables in the WRF model and, therefore, statistical evaluation for this variable is omitted. Table 3.2 lists the metrics used for the statistical comparisons of the three meteorological parameters, as recommended by the EPA (U.S. EPA 2005). In addition, a t-test with a null hypothesis of equal mean for the two distributions was performed between the simulated and observed data for each parameter evaluated. The statistics of the t-test are included in the comparison tables below.

Figures 3.17 through 3.19 display the time series plots of wind speed, temperature, and humidity, respectively, for the four CAMS stations during the ozone episode. Although the temporal trend of the simulated wind speed, in general, follows the observed value reasonable well in Figure 3.17 the WRF model tends to overpredict the wind speed during the days prior to the ozone event. Nevertheless, the low wind speed condition during the ozone event day of June 18 was captured by the WRF. The smallest 4-km grid used in this study is likely insufficient to capture the micro features of the local terrain and land use in the modeling domain. This deficiency can only be overcome by increasing the spatial resolutions of the topography and defining a smaller grid, 1-km or less, for the modeling domain. Figure 3.18 shows that the WRF performs well in simulating the less spatially dependent parameter of temperature with the current modeling scheme. The WRF systematically over-predicted the daytime humidity by as much as 100%, although the nighttime humidity was most of the time correctly simulated. Figures 3.20 through 3.22 present the correlations between the predicted and observed values for the three parameters whereas Tables 3.3 through 3.6 list the statistics of distributions for the three parameters evaluated for each of the four stations. It is encouraging to notice that all three parameters were well simulated during the high ozone day in Figures 3. 17 through 3.19.

It is observed that the WRF simulations are optimal. There is reasonable agreement between the WRF simulations and the observed data for the four representative CAMS in the PdN.

Table 3.2 Definition of model performance statistics

METRIC	ACRÓNYM	MATEMATICAL EXPRESION
t-test		
Mean observation	OBS	$OBS = \frac{1}{N}\sum_{1}^{N} Obs$
Mean Prediction	PRED	$Model = \frac{1}{N}\sum_{1}^{N} Model$
Ratio	Ratio	$Ratio = \frac{1}{N}\sum_{1}^{N} \frac{Pred_{x,t}^{i}}{Obs_{x,t}^{i}}$
Mean Bias	BIAS	$BIAS = \frac{1}{N}\sum_{1}^{N} (Model - Obs)$
Normalized Mean Bias (percent)	NMB	$NMB = \frac{\sum_{1}^{N} (Model - Obs)}{\sum_{1}^{N} (Obs)} \cdot 100\%$
Mean Fractional Bias (percent)	FBIAS	$FBIAS = \frac{2}{N}\sum_{1}^{N} \left(\frac{(Model - Obs)}{(Model + Obs)} \right) \cdot 100\%$
Mean Error	ERR	$ERR = \frac{1}{N}\sum_{1}^{N} \lvert Model - Obs \rvert$
Normalized Mean Error (percent)	NME	$NME = \frac{\sum_{1}^{N} \lvert Model - Obs \rvert}{\sum_{1}^{N} (Obs)} \cdot 100\%$
Mean Fractional Error (percent)	FERROR	$FERROR = \frac{2}{N}\sum_{1}^{N} \left(\frac{\lvert Model - Obs \rvert}{(Model + Obs)} \right) \cdot 100\%$
Root Mean Square Error	RMSE	$RMSE = \sqrt{\frac{1}{N}\sum_{i=1}^{N} P_i - O_i^{\,2}} = \sqrt{\frac{1}{N}\sum_{i=1}^{N} E_i^{\,2}} = \sqrt{BIAS^2 + STDE^2}$
Index of Agreement	IOA	$IOA = 1 - \frac{\sum_{i=1}^{N} P_i - O_i^{\,2}}{\sum_{i=1}^{N} \lvert P_i - \bar{P} \rvert + \lvert O_i - \bar{O} \rvert^{\,2}}$
Correlation Coefficient	CORRCOEFF	$CORRCOEFF = \frac{\sum_{1}^{N} (Model - \overline{Model})(Obs - \overline{Obs})}{\sqrt{\sum_{1}^{N} (Model - \overline{Model})^2 \sum_{1}^{N} (Obs - \overline{Obs})^2}}$

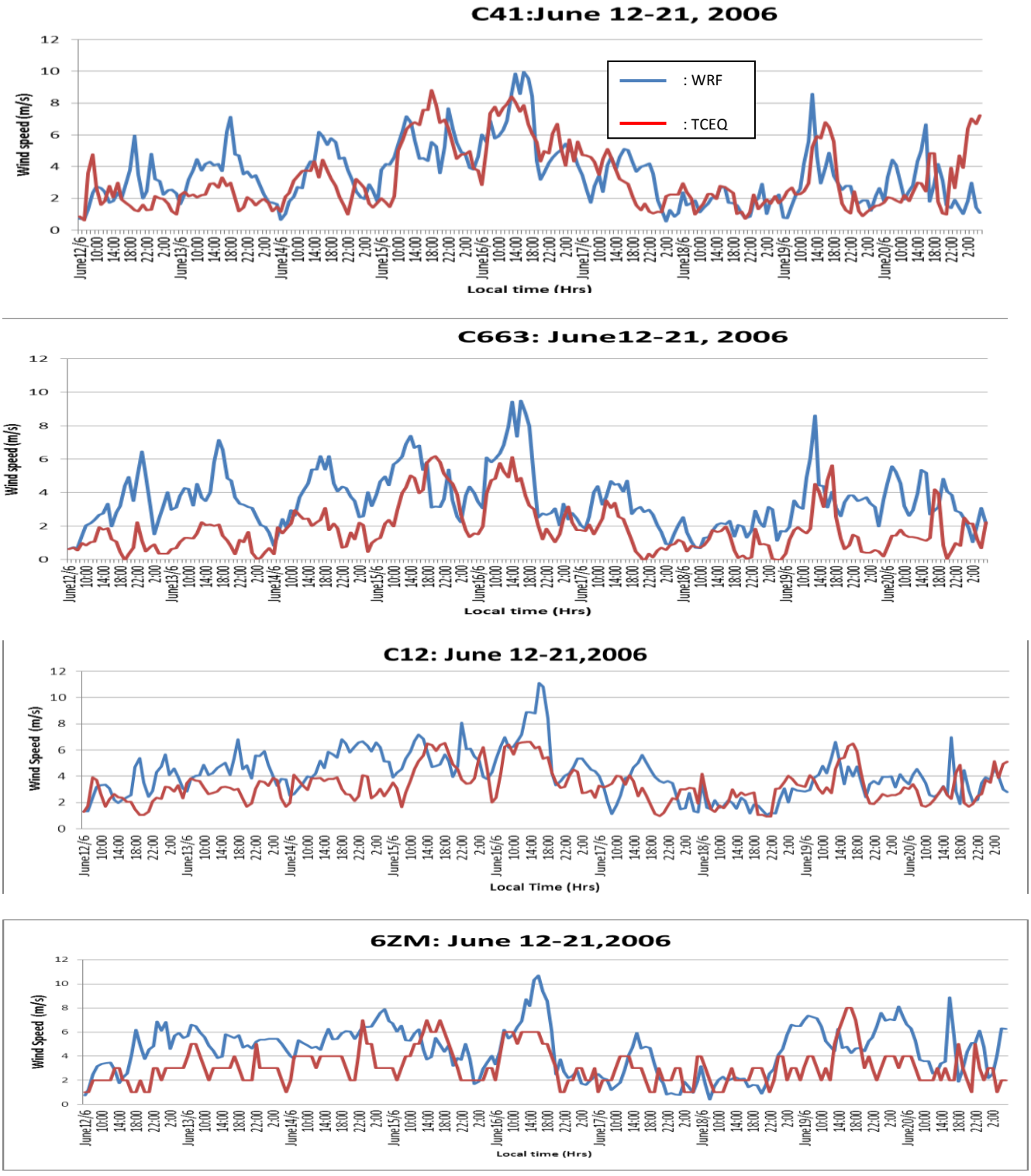

Figure 3.17 Time series plots of surface wind speed at 4 ACAMS stations

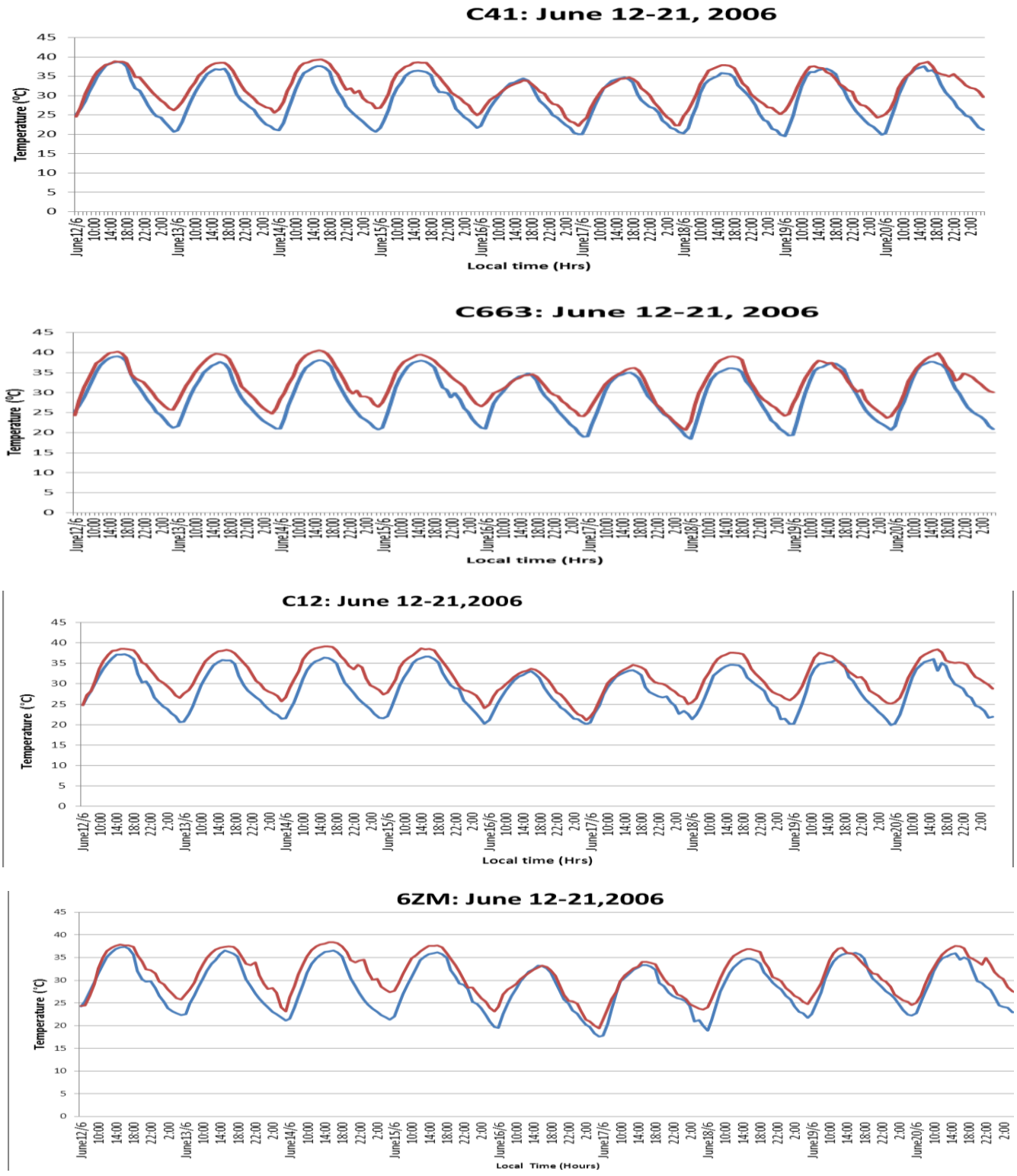

Figure 3.18 Time series plots of ambient temperature at 4 ACAMS stations

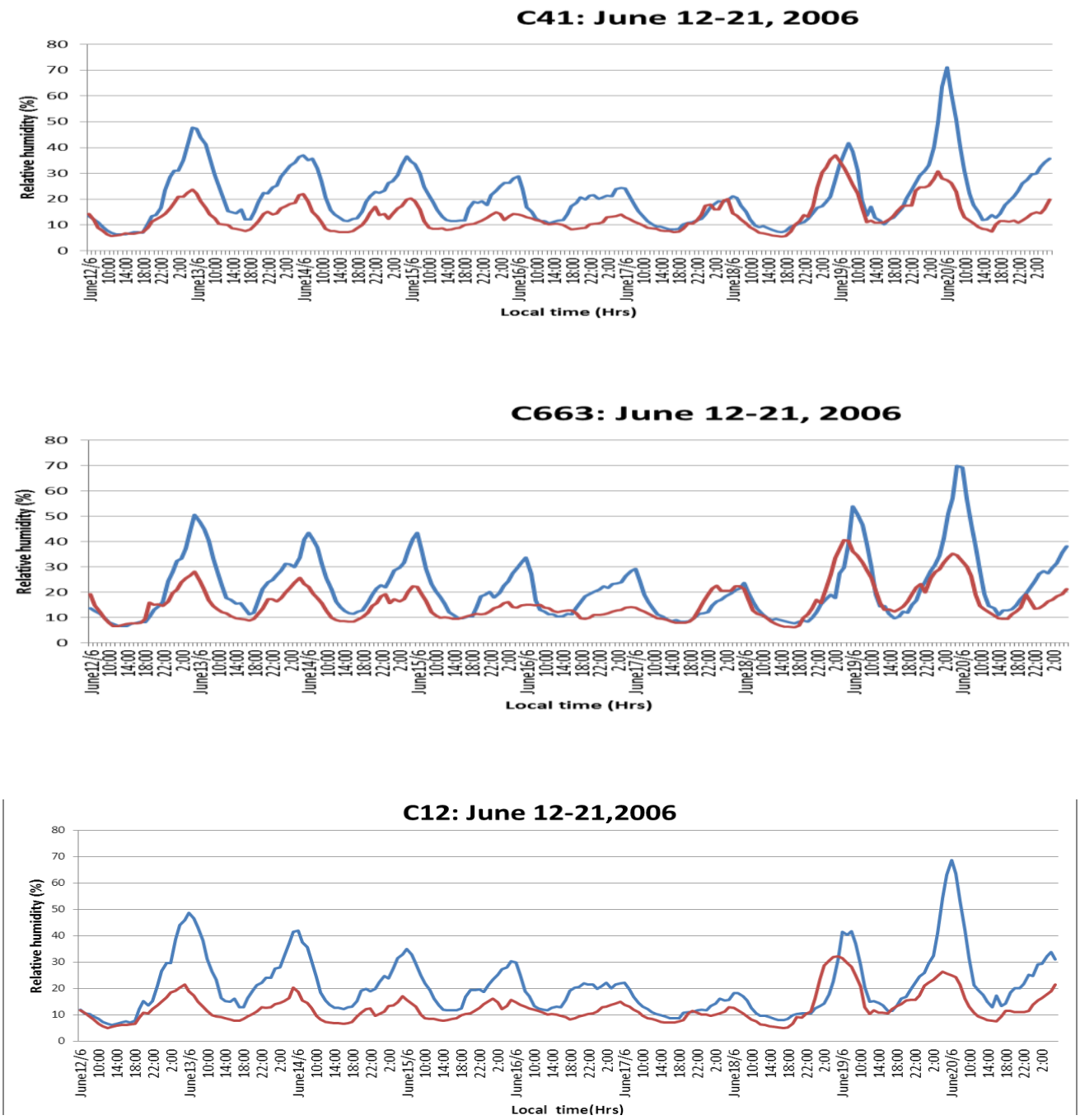

Figure 3.19 Time series plots of atmospheric humidity at 4 ACAMS stations

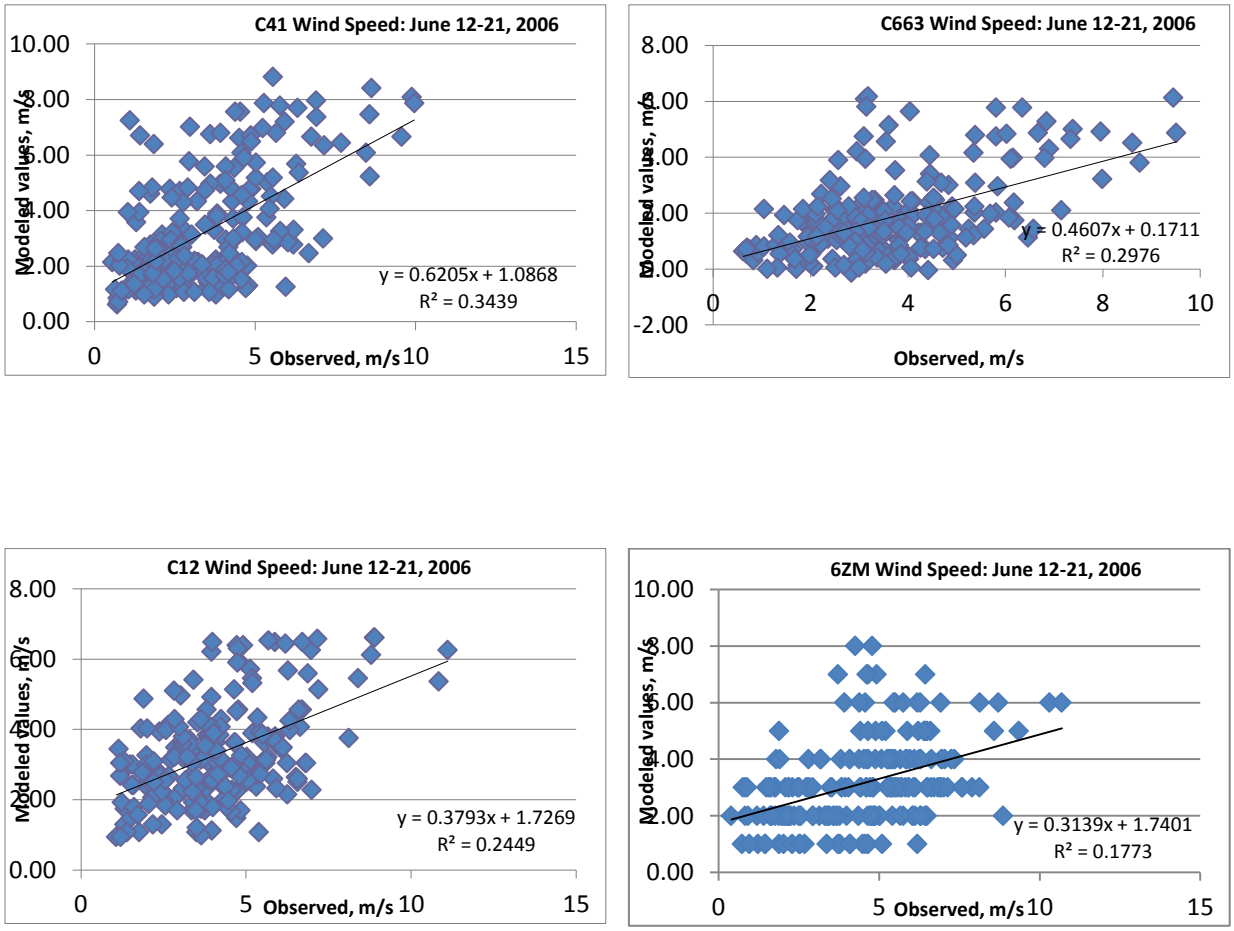

Figure 3.20 Correlation between the predicted and observed wind speed at four CAMS stations

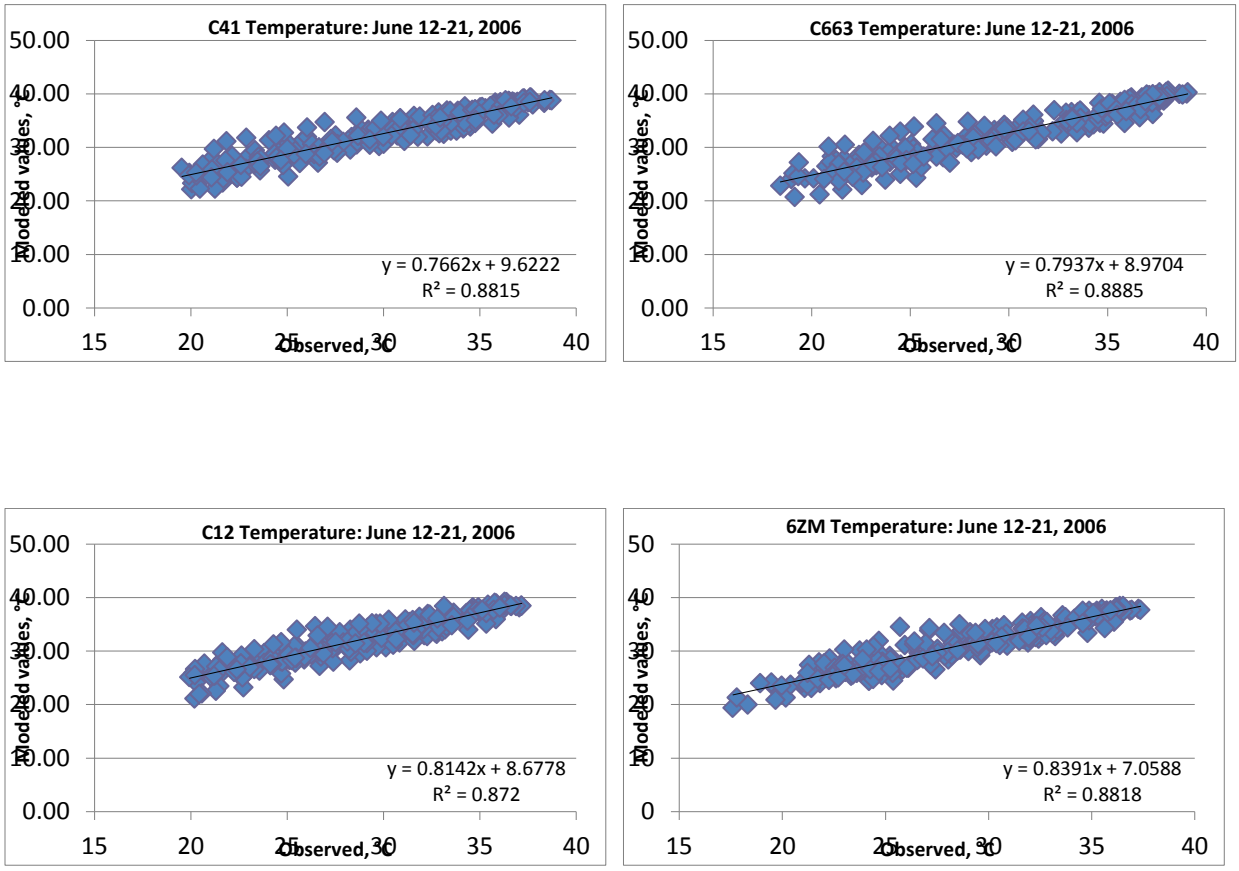

Figure 3.21 Correlation between the predicted and observed temperature at four CAMS stations

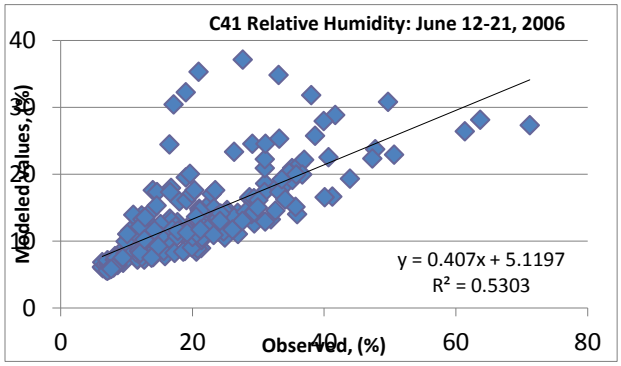

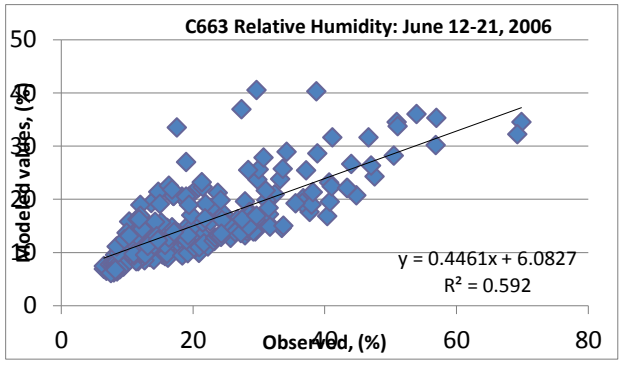

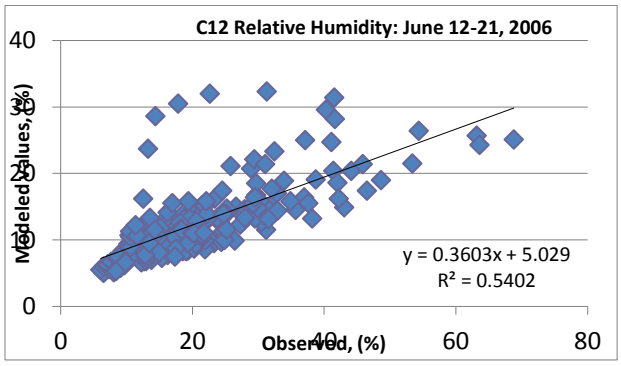

Figure 3.22 Correlation between the predicted and observed humidity for four CAMS stations (Data for CAMS 6ZM was not available for the studied period)

Table 3.3 Model performance statistics for Station CAMS 41

Metirc Acronym	Station ID: CAMS 41		
	WS	Temperature	Relative Humidity
t-test	t = 0.7689 df =1065.1810 p-value = 0.4421 alternative hypothesis: true difference in means is not equal to 0. 95 percent confidence interval: -1.16792 2.6730	t = 5.7115 df =413.3740 p-value = 2.143e-08 alternative hypothesis: true difference in means is not equal to 0. 95 percent confidence interval: 1.8341 3.7591	t = 1.0821 df =592.6300 p-value = 0.2796 alternative hypothesis: true difference in means is not equal to 0. 95 percent confidence interval: -1.0453 3.6104
OBS	3.2549	31.9861	13.658
PRED	3.4943	29.1896	20.6584
Ratio	0.0050	0.0042	0.0071
BIAS	0.2394	-2.7965	7.130
NMB	7.3552	-8.7429	52.7007
FBIAS	9.3204	-9.9607	37.0399
ERR	1.3943	2.8735	7.8538
NME	42.8370	8.9835	58.0528
FERROR	44.1659	10.1894	40.4172
RMSE	24.3989	3.4575	24.3334
IOA	0.7961	0.8898	0.6456
COR. COE.	0.5864	0.9389	0.7282

Table 3.4 Model performance statistics for Station CAMS 663

Metirc Acronym	Station ID: CAMS 663		
	WS	Temperature	Relative Humidity
t-test	t = -11.4741 df =418.3010 p-value <2.2e-16 alternative hypothesis: true difference in means is not equal to 0. 95 percent confidence interval: -2.0561 -1.4566	t = 5.5735 df =417.893 p-value =4.484e-08 alternative hypothesis: true difference in means is not equal to 0. 95 percent confidence interval: 1.8792 3.9269	t =-6.0412 df =344.855 p-value =3.963e-09 alternative hypothesis: true difference in means is not equal to 0. 95 percent confidence interval: -7.7065 -3.9209
OBS	1.8174	32.3163	15.6625
PRED	3.5730	29.4133	21.4762
Ratio	0.0091	0.0042	0.0063
BIAS	1.7556	-2.9031	5.8137
NMB	96.6022	-8.9832	37.1186
FBIAS	74.5855	-10.2412	25.1739
ERR	1.9541	2.9613	7.3019
NME	107.5234	9.1635	46.6200
FERROR	80.2491	10.4178	34.1423
RMSE	2.3252	3.5467	9.9981
IOA	0.5938	0.8974	0.7374
COR. COE.	0.5455	0.9425	0.7694

Table 3.5 Model performance statistics for Station CAMS 12

Metirc Acronym	Station ID: CAMS 12		
	WS	Temperature	Relative Humidity
t-test	t =-5.5521 df =402.793 p-value = 5.131e-08 alternative hypothesis: true difference in means is not equal to 0. 95 percent confidence interval: -1.1357 -0.5418	t = -9.6515 df =312.6990 p-value = 2.2e-16 alternative hypothesis: true difference in means is not equal to 0. 95 percent confidence interval: -9.6515 -6.5524	t =-9.6515 df =312.699 p-value =2.2e-16 alternative hypothesis: true difference in means is not equal to 0. 95 percent confidence interval: -9.9081 -6.5524
OBS	3.2948	31.9925	12.4977
PRED	4.1333	28.6354	20.7280
Ratio	0.0058	0.0041	0.0077
BIAS	0.8385	-3.3572	8.2303
NMB	25.4501	-10.4936	65.8544
FBIAS	20.4694	-11.6674	44.4599
ERR	1.4292	3.3641	8.7255
NME	43.3778	10.5152	69.8166
FERROR	39.1211	11.6885	46.8413
RMSE	1.8068	3.8208	11.5431
IOA	0.6536	0.8537	0.5978
COR. COE.	0.4949	0.9338	0.735

Table 3.6 Model performance statistics for Station CAMS 6ZM

Metirc Acronym	Station ID: CAMS 6ZM		
	WS	Temperature	Relative Humidity
t-test	t =-7.909 df =397.532 p-value=2.593e-14 alternative hypothesis: true difference in means is not equal to 0. 95 percent confidence interval: -1.6834 -1.0131	t = 5.2452 df =425.07 p-value=2.468e-07 alternative hypothesis: true difference in means is not equal to 0. 95 percent confidence interval: 1.5409 28.7301	NA
OBS	3.1528	31.1653	NA
PRED	4.5011	28.7300	NA
Ratio	0.0066	0.0043	NA
BIAS	1.3483	-2.4352	NA
NMB	42.7651	-7.8139	NA
FBIAS	31.6890	-8.6473	NA
ERR	1.9228	2.4942	NA
NME	60.9883	8.0032	NA
FERROR	51.4201	8.8364	NA
RMSE	2.3547	3.0400	NA
IOA	0.5665	0.9077	NA
COR. COE.	0.4211	0.9390	NA

Chapter 4 Development of Model-ready Emissions

Model-ready emission files are available from the TECQ Rider 8 program for the Dallas centered 36- and 12-km domains as well as the 4-km domain for El Paso. As stated in Chapter 2, the concentric nested domains centered at El Paso in the first set of CAMx modeling analysis was selected for the first set of CAMx modeling analysis. This decision created serious technical difficulties in generating emission files for the base year emissions using the EPS3 processor. In addition, emissions from Mexico were unavailable for use in processing the base year emissions. It was then decided to prepare the emission files using available dataset from EPA and TCEQ, although UTEP has since updated the 4-km emission files using EPS3.

The Sparse Matrix Operator Kernel Emissions(SMOKE), version 2.7, emission model (Houyoux et al 2000) was used in conjunction with the readily available National Emissions Inventory (NEI) dataset to generate the necessary emission files for the first set of CAMx runs. SMOKE was used to convert the source-level emissions (county total emissions) reported on a yearly basis to spatially resolved, hourly emissions, with detailed speciation information. It produces the basic model-ready emission files including gases and particulate matter emissions from point, area, non-road, on-road, and biogenic sources.

This section describes the model and dataset used in generating the emission files for the concentric domains. Development of model-ready emission files from TCEQ Rider 8 program for the 2nd set of base year CAMx modeling and the 3rd set of sensitivity analysis is provided by Environ and included in Section 2 of Appendix A.

4.1 The Sparse Matrix Operator Kernel Emissions (SMOKE) Model System

The Sparse Matrix Operator Kernel Emissions (SMOKE) modeling system is a set of programs that is used by the U.S. EPA, Regional Planning Organizations (RPOs), and State environmental agencies to prepare emissions inventory data for input to an air quality model such as CMAQ and CAMx. SMOKE integrates annual or daily county-level emissions inventories with source-based temporal, spatial, and chemical allocation profiles to create hourly emissions fluxes on a predefined model grid. For elevated sources that require allocation of the emissions to the vertical model layers, SMOKE integrates meteorology data to derive dynamic vertical profiles.

In addition to its capacity to simulate emissions from stationary area, stationary point, and non-road mobile sectors, SMOKE is also instrumented with the Biogenic Emissions Inventory System, version 3 (BEIS3) for estimating biogenic emissions fluxes and both MOBILE6 and the Motor Vehicle Emission Simulator (MOVES) 2010 model for estimating on-road mobile

emissions fluxes from county-level vehicle activity data. SMOKE can additionally be used to calculate future-year emissions estimates, if the user provides data about how the emissions will change in the future.

SMOKE uses C-Shell scripts as user interfaces to set configuration options and call executables. SMOKE is designed with flexible QA capabilities to generate standard and custom reports for checking the emissions modeling process. After modeling all of the emissions source categories individually, SMOKE creates two files per day for input into CMAQ or CAMx: (1) an elevated point source file for large stationary sources, and (2) a merged gridded source file of low-level point, mobile, non-road, area, and biogenic emissions. The efficient processing of SMOKE makes it an appropriate choice for handling the large processing needs of regional and seasonal emissions processing, as described in more detail by Houyoux et al. (1996, 2000).

Figure 4.1 gives a simplified flow chart of SMOKE processing. The processing begins with importing inventory files and finishes at merging of matrixes to produce the speciated, gridded, and hourly emission files for air quality modeling.

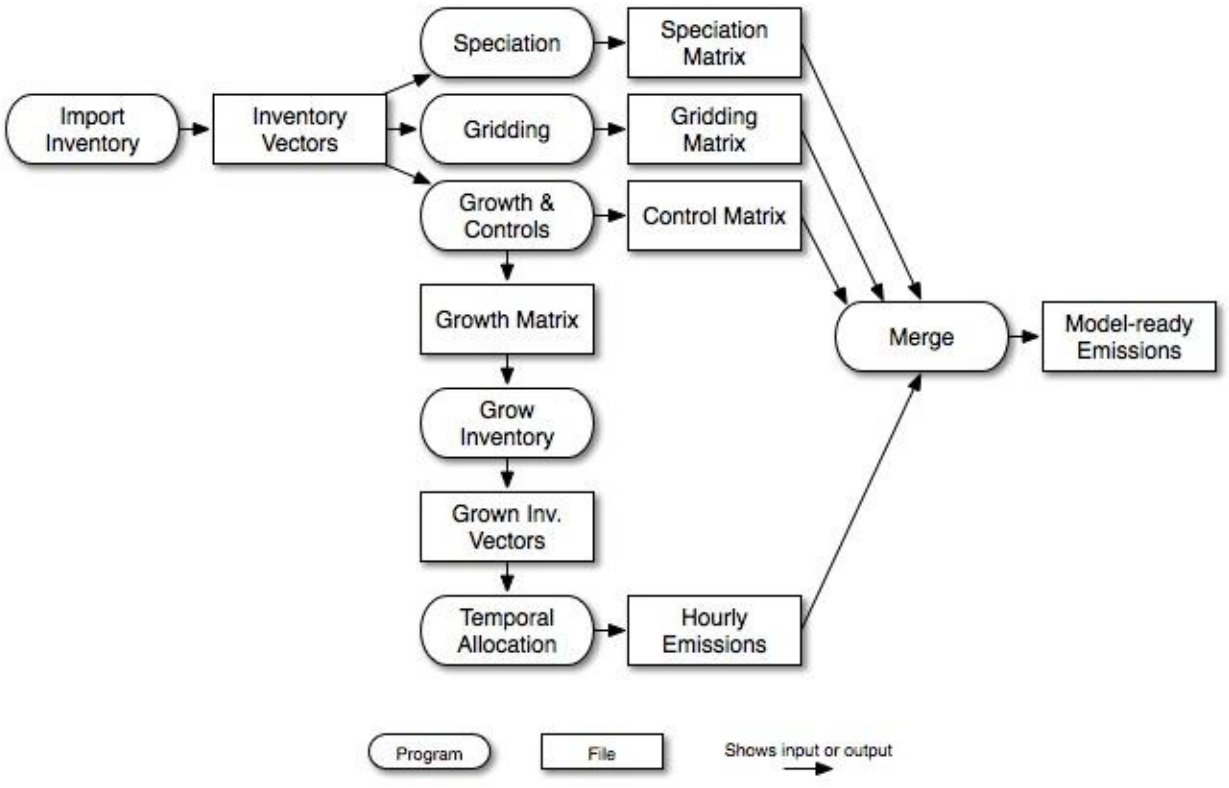

Figure 4.1 SMOKE Modeling System

4.2 The Emission Inputs

SMOKE primarily uses two types of input file formats: ASCII files and I/O API files. Input files are files that are read by at least one core SMOKE program, but are not written by a core program. SMOKE uses strict rules that define the format and content of the input files. These rules are explicitly laid out in the SMOKE User's Manual. All data input to SMOKE must be either formatted to one of the prescribed input file types or converted to an intermediate form, such as a gridded I/O API inventory file, before it can be input to SMOKE.

In general SMOKE requires an emissions inventory, temporal allocation, spatial allocation, and chemical allocation data to prepare emissions estimates for an air quality model. For some source categories, such as on-road mobile and stationary point sources, SMOKE also requires meteorology data to calculate emissions. SMOKE calculates biogenic emissions estimates with gridded land use, vegetative emissions factors, and meteorology data. Further details about the SMOKE input requirements are available at CMAS website (www.cmascenter.org).

EPA processes the National Emissions Inventory (NEI) in SMOKE. Through the Emissions Modeling Clearinghouse (EMCH, www.epa.gov/ttn/chief/emch/index.html), EPA distribute SMOKE formatted input inventories based on the latest versions of its NEI databases. In addition to the emissions data, this site is also used to document and distribute the Agency's latest versions of the ancillary files used to support the temporal, spatial, speciation, and projection of these emissions.

4.2.1 Biogenic Emissions

Biogenic emissions were used In the CAMx modeling. However, since biogenic emissions are not archived in NEI, and they are dependent on landuse characteristics, we used the Biogenic Emission Inventory System (BEIS, version 3) for computation of hour-specific, meteorology-based biogenic emissions from vegetation and soils. This program is included in SMOKE.

4.2.2 Meteorology

The meteorological parameters including temperature, wind, pressure, and humidity from WRF outputs were also ingested in the SMOKE model to produce emission flux.

4.2.3 Other Related Emissions

The national emissions inventory is a composite of inventories for different source categories: point, nonpoint, mobile, and biogenic and is an input used in the SMOKE program. However, it should be noted that the National Emissions Inventory (NEI) used for the SMOKE runs is the NEI 2001, which represents archived old data and it is not an updated emissions inventory.

In addition, the regular emission inventory data used in this study for Cd. Juarez emissions is EPA's NEI99 (final version 2), available from ftp://ftp.epa.gov/EmisInventory. Since the modeling domain includes both USA and Mexico, the latest released Mexico emission dataset (Mexico NEI99, http://www.epa.gov/ttn/chief/net/mexico.html), which includes six northern border states of Mexico, has also been obtained as the supplementation for NEI99.

Chapter 5 Evaluation of the CAMx Performance

CAMx was applied to simulate the ozone levels during June 2006 ozone episode, June 12-21. Three sets of simulations were conducted:

Set 1: Concentric grid system centered at El Paso and NEI emission inventory dataset

Set 2: TCEQ Rider 8 nested grid system with Rider 8 emission inventory dataset

Run 2a: TCEQ 36, 12, and 4-km CAMx grids with 4 km meteorology interpolated from TCEQ 12-km WRF outputs

Run 2b: TCEQ 36, 12, and 4-km CAMx grids with 4 km meteorology from UTEP concentric 4-km WRF outputs.

Set 3: Sensitivity Analysis based on Run 2a

Run 3a: with new bridge emission

Runs 3.1 - 3.12: with controlled area emissions from Cd. Juarez

Sets 1 and 3 were conducted by UTEP and Set 2 was contracted to Environ for independent evaluation. Performance of Set 1 was judged unacceptable and a decision was made to seek opinions from the initial program developer (Environ). The results of both runs for Set #2 were judged satisfactory and a sensitivity analysis was followed by UTEP using the model setup for Run 2a. Further discussion on the performance of different simulation configurations is included in Chapter 6.

5.1 CAMx Run Set 1: Concentric grid

Figure 5.1 shows the average ozone levels for a representative non-ozone day, June 15, 2006, whereas Figure 5.2 shows the levels for a high ozone day on June 18, 2006. The model was able to pick up the increase of ozone levels in the modeling domain from a low ozone day to a high ozone day. Although this run could capture the general temporal ozone trend in the modeling domains, it, however, could not reasonably predict the magnitudes and locations at critical receptor locations in the modeling domains.

A brief statistical performance evaluation on the 1-hour predictions was conducted over 3 CAMS sites (CAMS 12, 41, and 663) using the statistics metrics described in Table 2.1. These 3 stations were selected for the following reasons: 1) C663 is the CAMS observing the daily

maximum 1-hour ozone across the PdN region; 2) CAMS 12 at UTEP is the site in El Paso observing the most exceedances on the US side of the border; and 3) CAMS 41, equipped with an Auto-GC for hourly TNMHC concentration measurements, constantly observes high ozone and is exposed to the possible transport ozone from Cd. Jaurez. Figure 5.3 shows the time series plots of the 1-hour ozone predictions at the three CAMS locations in comparison to the observed values reported by TCEQ. A regression analysis was conducted between the predicted and observed values and the results are shown in Figure 5.4. Although the CAMx simulations follow the weekly cycle of ozone concentrations, major discrepancies are observed between the CAMx model simulations and the corresponding TCEQ observed data for these selected monitoring stations. Set 1 run significantly under-predicted the ozone levels in the modeling domain by as much as 100% with only poor and moderate correlations (R^2 = 0.13 to 0.28). Further evaluation of this set of simulation was deemed unnecessary.

Although the agreement between the meteorological observations and WRF simulations of temperature, relative humidity, and wind speed using concentric domains was deemed acceptable during the study period (particularly on the high ozone day) in Chapter 3, the CAMx simulations using the same domains and NIE emission inventory did not produce satisfactory results. The dated emissions inventory and low resolutions of landuse, topography, and other modeling parameters in the model may have been the major causes for the poor performance of this set of CAMx simulation. However, the results exhibited a strong negative bias. Therefore, scaling factors, such as EPA's "relative reduction factors" could perhaps be used to scale the model's ozone estimates, if necessary, in order to correlate the results well to the observed local ozone values.

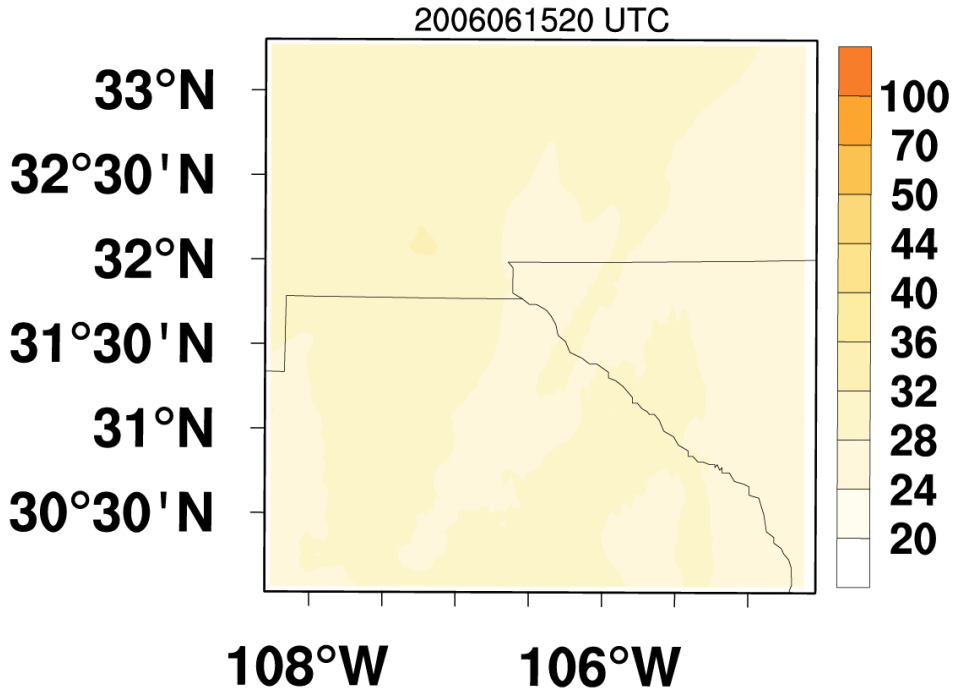

Figure 5.1 Ozone concentrations values on June 15, 2006 at 20:00 UTC

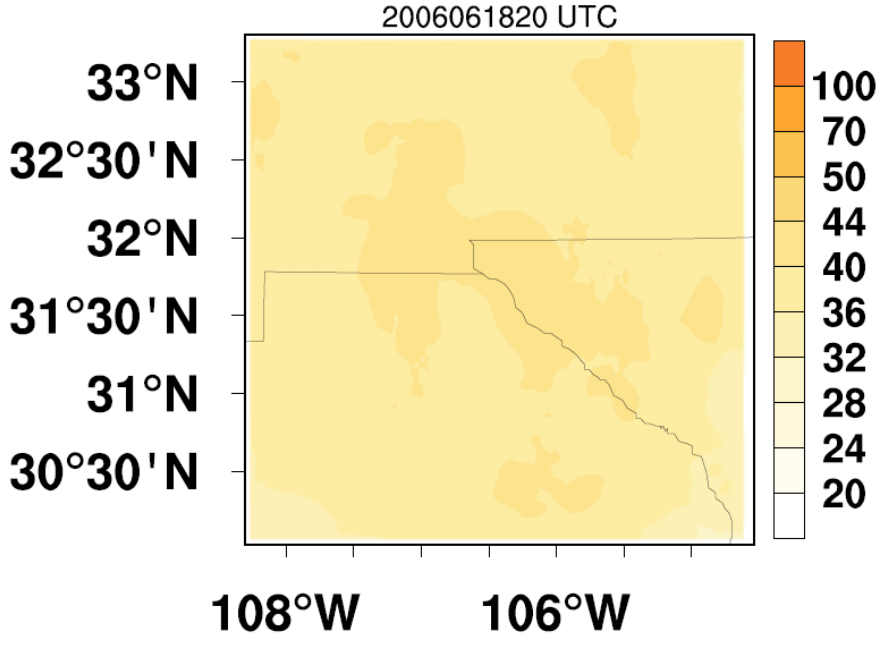

Figure 5.2 Ozone concentration values on June 18, 2006 at 20:00 UTC.

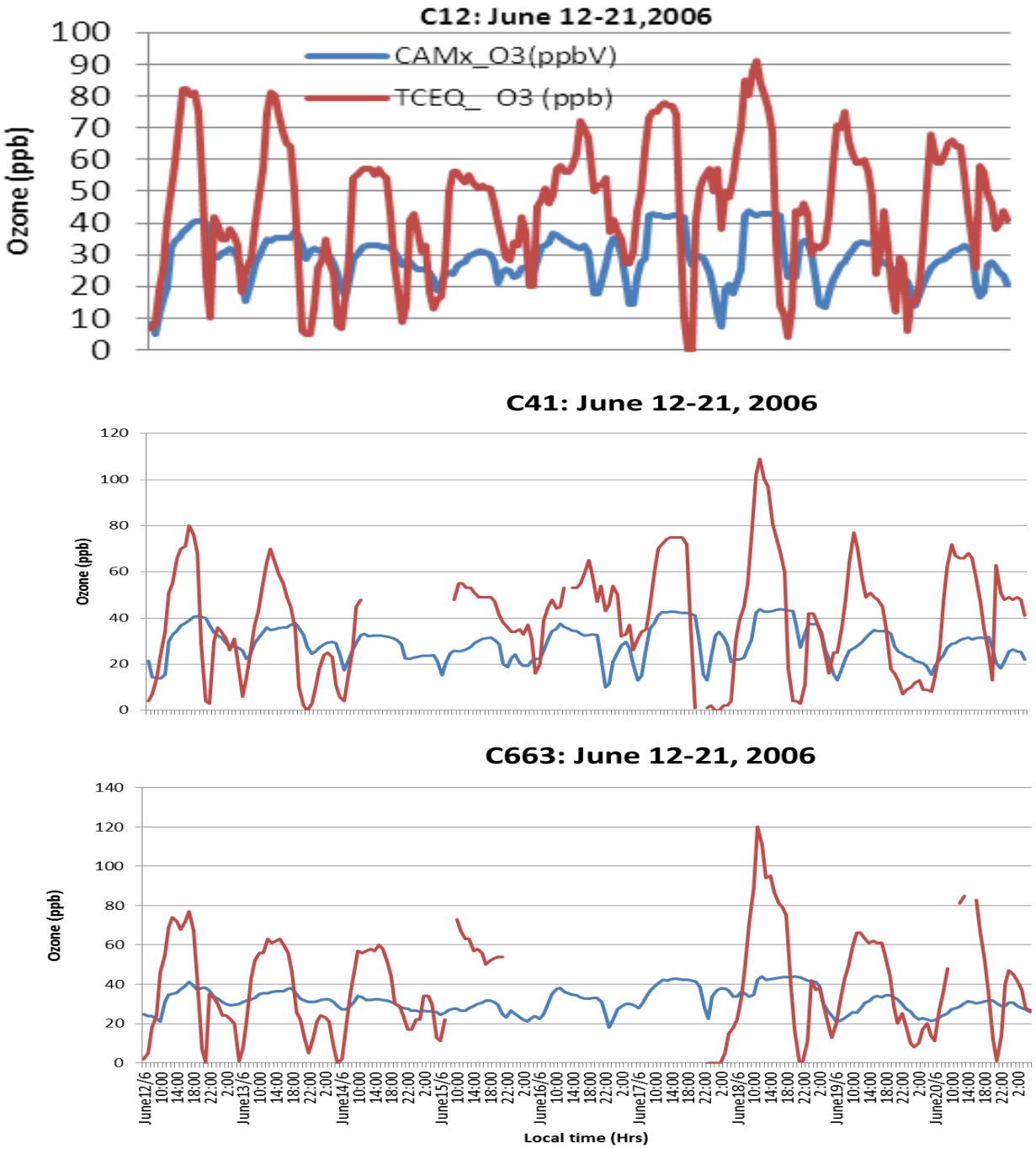

Figure 5.3 Time series plots of surface ozone concentration at 3 CAMS stations

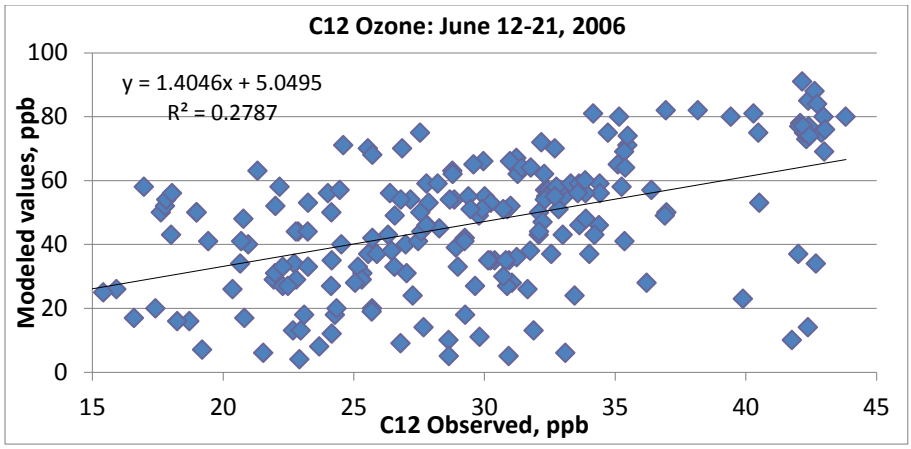

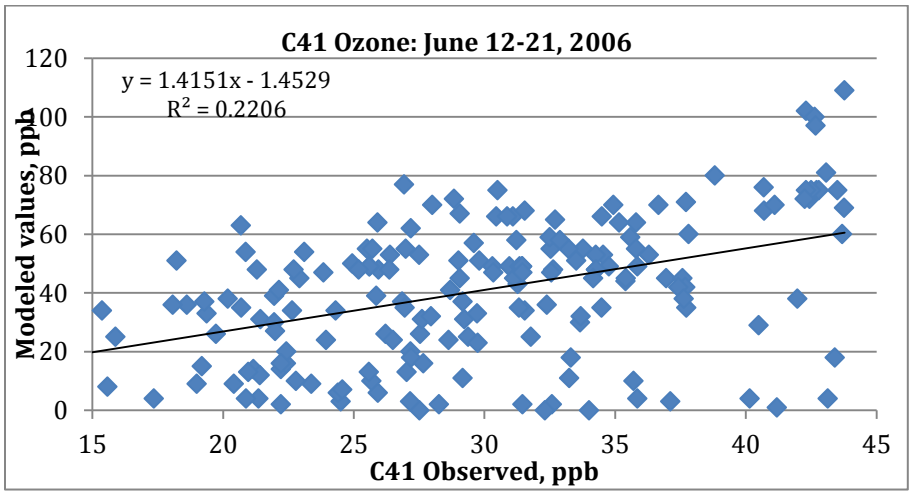

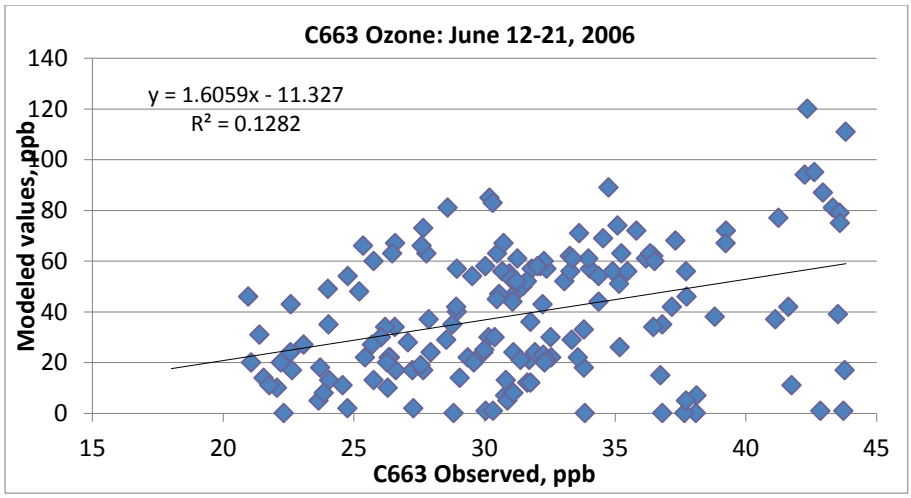

Figure 5.4 Correlation between the predicted and observed ozone levels at four CAMS stations

Table 5.1 Model performance statistics for Set 1 simulation

Metric	CAMS ID		
Acronym	CAMS 12	CAMS 41	CAMS 663
t-test	t = 6.2492 df =229.568 p-value =1.986e-09 alternative hypothesis: true difference in means is not equal to 0. 95 percent confidence interval: 7.6911 14.7746	t = 5.9454 df =231.3540 p-value =1.009e-08 alternative hypothesis: true difference in means is not equal to 0. 95 percent confidence interval: 7.1720 14.2817	t = 3.7719 df =175.875 p-value = 0.0002 alternative hypothesis: true difference in means is not equal to 0. 95 percent confidence interval: 3.7182 11.8790
OBS	45.5093	40.0680	39.3665
PRED	28.8039	29.0290	31.6242
Ratio	0.0030	0.0040	0.0050
BIAS	28.8039	-6.4020	2.2816
NMB	63.8839	-18.0790	7.7758
FBIAS	83.8807	14.8070	53.1851
ERR	45.5093	23.4950	31.5484
NME	100.0000	58.6390	80.1403
FERROR	117.2045	88.9080	130.4115
RMSE	23.4765	25.7723	25.3123
IOA	0.5199	0.5070	0.4129
COR.	0.5279	0.4700	.3581

5.2 CAMx Run Set 2: TCEQ Dallas centered CAMx grid with TCEQ 4-km meteorology

ENVIRON performed two CAMx base case simulations of June 12-21, 2006 employing alternative approaches in defining 4 km grid meteorology. Both simulations used the 4 km El

Paso/Juarez emission inputs (Appendix A). Run 2a used the TCEQ 36/12 km grids together with the 4 km grid in 2-way nested mode, where meteorology on the 4 km grid was internally interpolated by CAMx from the 12 km meteorology. Run 2b used the single 4-km grid alone using meteorological data from UTEP's WRF outputs. Boundary conditions for the 4 km grid were extracted from CAMx runs on the 36/12 km grid in a manner referred to as 1-way nesting. This was necessary to appropriately accommodate the potentially different meteorology and different vertical grid structures between the 4 km (UTEP) and 12 km (TCEQ) meteorological data. Results from both runs were compared to evaluate differences arising from the use of different meteorology and grid structures. The comparisons are presented using spatial concentration maps and model performance statistics.

5.2.1 Emissions and Modeling Parameters

All emission data files were downloaded from TCEQ's FTP site for Rider 8 program. Specific files for the emissions are listed in Appendix A. Mexican emissions were obtained from the recent Western Regional Air Partnership (WARP) modeling inventories for 2008 compiled for the Westjump project. This 2008 emission inventory for Mexico was used "as is" for 2006 in this study without back casting to 2006. EPS3 was used to process criteria pollutant emissions using CB6 chemical mechanism. EPS3 generated model-ready hourly low-level point, area, non-road mobile, and on-road mobile emissions on the El Paso 4 km grid system for a representative weekday, Friday, Saturday and Sunday. Biogenic emissions were developed separately using the MEGAN model, which estimated hourly emission rates on 4 km grid for each day of the June 2006 modeling episode. Details of how the emissions were processed and the modeling inputs are summarized in Appendix A.

5.2.2 Operational Performance of Runs 2a and 2b

5.2.2.1 Ozone

Time series plots of the CAMx ozone simulations in comparison with the observed levels at each of the 13 CAMS sites are shown in Appendix A. Model performance was also evaluated for 8-hour and 1-hour ozone data observed at these 13 sites. The locations and monitored parameters are listed in Table 5.2. Figure 5.5 compares the daily statistics of three values: the highest observed 8-hour ozone among all sites in the El Paso/Juarez area (in beige), the co-located daily maximum 8-hour ozone from Run 2a (in yellow and indicated as FE36124k by Environ), and Run 2b (in blue and indicated as 4kUTEPmet by Environ). Both runs under-estimated the peak observation on two dates (June 13 and June 18) when at least one site exceeded 75 ppb, although Run 2b successfully predicted an exceedance on the 18th of June.

Figure 5.6a shows the average paired peak accuracy by comparing the highest observed 1-hour ozone value from each of the thirteen monitors to their co-located peaks predicted by Run 2a and Run 2b. Both simulations tended to under-predict ozone level with the worst accuracy close to 30% on June 16. Run 2b (4kUTEPmet) performed better on June 18 (highest observed 8-hour ozone date) compared to the Run 2a (FE36124k); however, its accuracy was worse on seven out of ten dates modeled. Figures 5.6b and 5.6c show the statistics of normalized bias and normalized error, respectively, using all hours of data at all sites. Pairings when the observed 1-hour ozone was less than 40 ppb were excluded. The model performance goals for normalized bias and error of ±15% and 35%, respectively, are indicated in the figures. The biases show under prediction of ozone on all dates for both simulations. Run 2b simulation met the normalized bias goal on the two ozone exceedance dates and the bias was better than the Run 2a on nine out of ten dates modeled. Both simulations satisfied the ±35% error performance goal on all dates. The errors are similar in magnitude to bias indicating that underestimation trends are consistent in time and space.

Table 5.2 Station IDs and monitored parameters in the Paso del Norte region (Table 2.1 of the Conceptual Model)

List of Paso del Norte CAMS and Monitored Parameters												
Station ID	Site Name	City, State	O3	NO	NO2	NOx	CO	WS	WD	UV	SLR	Data Range
C12	UTEP	El Paso, TX	✓	✓	✓	✓	✓	✓	✓	✓	✓	1999-2010
C37	Ascarate	El Paso, TX	✓	✓	✓	✓	✓	✓	✓			2000-2010
C41	Chamizal	El Paso, TX	✓	✓	✓	✓	✓	✓	✓			2000-2010
C49	Socorro	El Paso, TX	✓	✓	✓	✓	✓	✓	✓			2000-2010
C72	Skyline	El Paso, TX	✓	✓	✓	✓	✓	✓	✓			2000-2010
C414	Ivanhoe	El Paso, TX	✓				✓	✓	✓			2002-2010
C661	Advanced	Juarez, Chih	✓				✓	✓	✓			2003-2010
C662	20-20 Club	Juarez, Chih	✓				✓	✓	✓			2003-2010
C663	SEC	Juarez, Chih	✓				✓	✓	✓			2003-2010
6CM	Anthony	Anthony, NM						✓	✓			2006-2010
6O	La Union	La Union, NM						✓	✓		✓	2004-2010
6ZK	Chaparral	Chaparral, NM	✓					✓	✓		✓	2001-2010
6ZG	SPCY	Sunland Park, NM	✓					✓	✓		✓	2001-2010
6ZM	Desert View	Sunland Park, NM	✓	✓	✓	✓		✓	✓		✓	2001-2010
6ZN	Santa Teresa	Santa Teresa, NM	✓	✓	✓	✓		✓	✓		✓	2001-2010

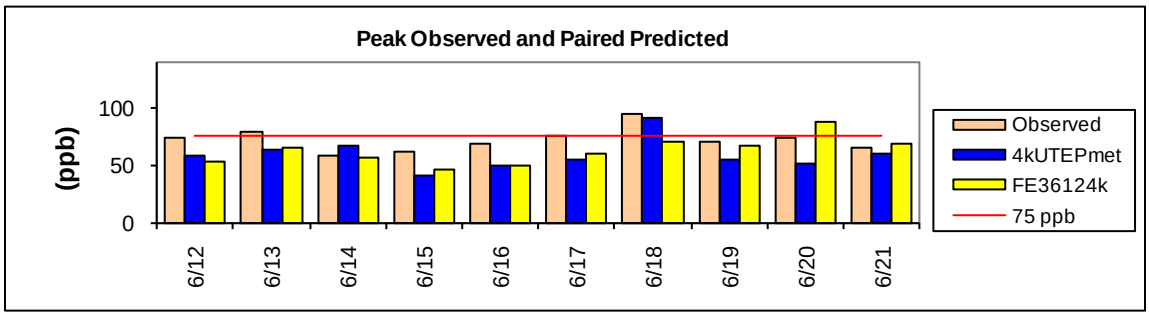

Figure 5.5 Peak observed and paired predicted 8-hour ozone (Figure 4-2 of Appendix A)

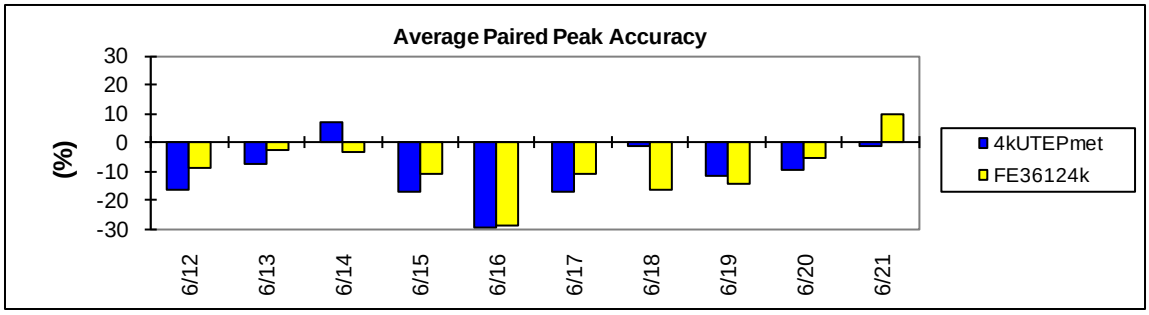

(a)

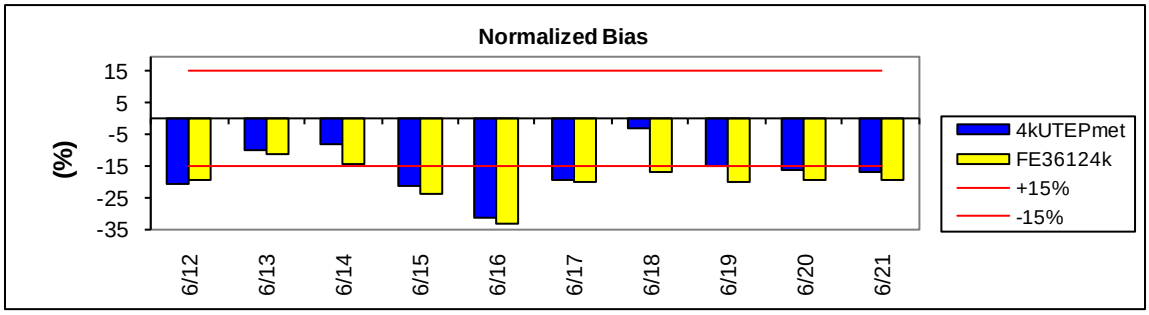

(b)

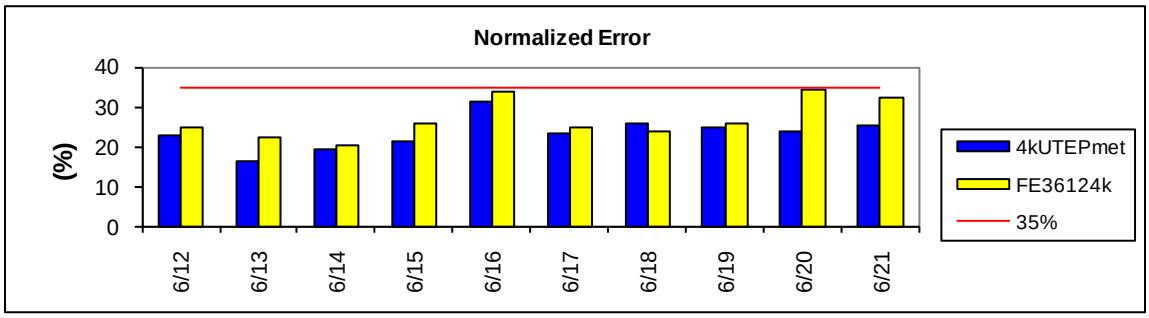

(c)

Figure 5.6 Model performance statistics for 1-hour ozone (Figure 4-3 of Appendix A)

Diurnal variability of the 1-hour ozone was examined for Run 2a (Appendix B and Appendix C). Figure 5.7 illustrates the diurnal variability in 1-hour ozone by comparing the observed and predicted diurnal hourly values on June 18. Predicted hourly ozone is presented as dotted lines, and observed hourly ozone is presented as solid lines. The H_2O_2/HNO_3 ratio is presented as a dashed line. The difference between the occurrence of the observed and predicted peaks is indicted as PEAK TIME BIAS (PTB), which is 4 hours for Run 2a. Comparisons were made at

three stations (CAMS 12, 41, and 663). Reasons for the selection are given in Section 5.1. The diurnal ozone formation graphic includes the H_2O_2:HNO_3 ratio which helps in determining whether ozone formation conditions are NOx- or VOC-limited. A ratio $\geq$0.35 indicates NOx-limited conditions while a ratio <0.35 indicates VOC-limited conditions (ENVIRON, 2011).

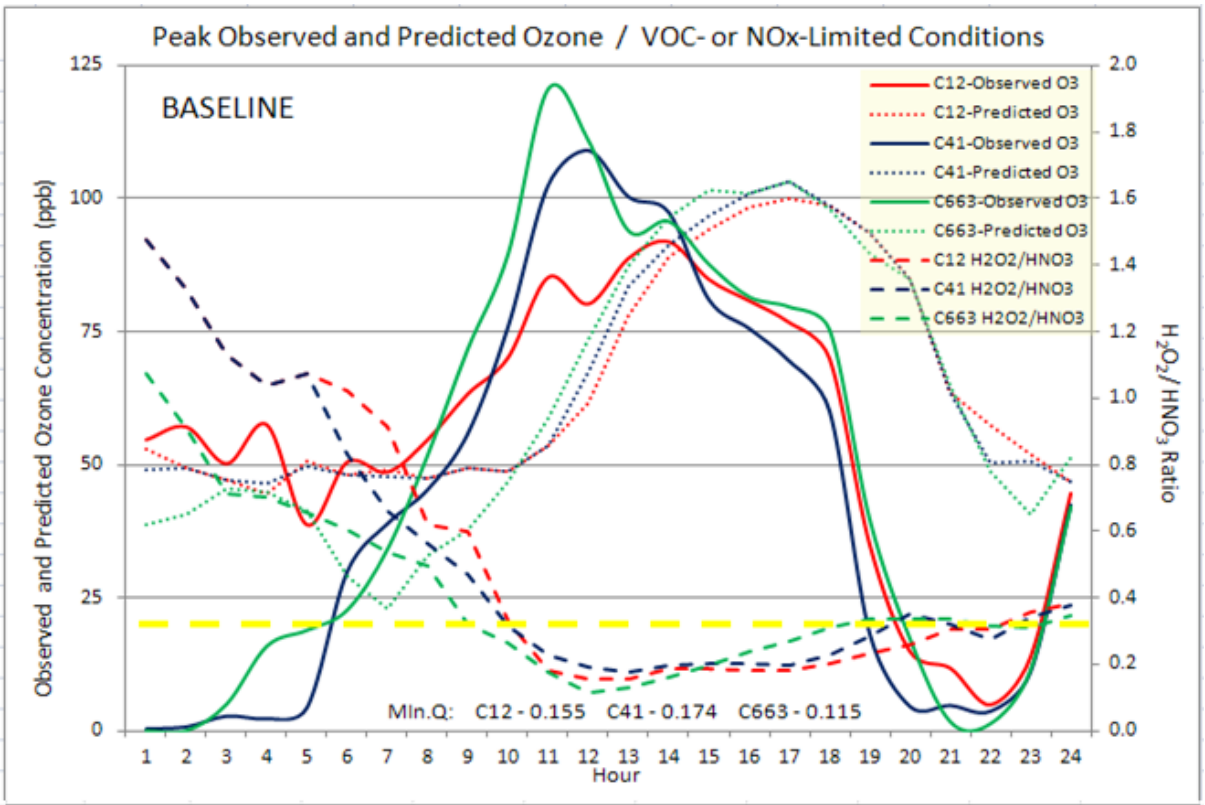

NOx	---	PeakObs	PeakPred	PairPred	UPPA	APPA	EPPA	PTB	NB	NE
VOC	---	120.7	103.3	99.3	-14.4	-1.5	12.2	4	-3.3	25.6

Figure 5.7 Diurnal Predicted and Observed 1-Hour Ozone (ppb) /H_2O_2/HNO_3 Ratios – Run 2a

Figure 5.8 illustrates the diurnal variability in daily 8-hour ozone by comparing the observed and predicted ozone concentrations on June 18. The H_2O_2/HNO_3 ratio is presented as dashed lines for reference. A red line of 75ppb is plotted in the graph to represent the 8-hour ozone NAAQS. PTB is slightly improved to 3 hours compared to 1-hour ozone for 8-hour ozone. CAMx under-predicts the peak ozone (93 ppb) and the PAIRED PREDICTED (92.1 ppb) 8-hour average ozone concentration while NB (3.9%) and NE (23.7%) are within acceptable model performance parameters.

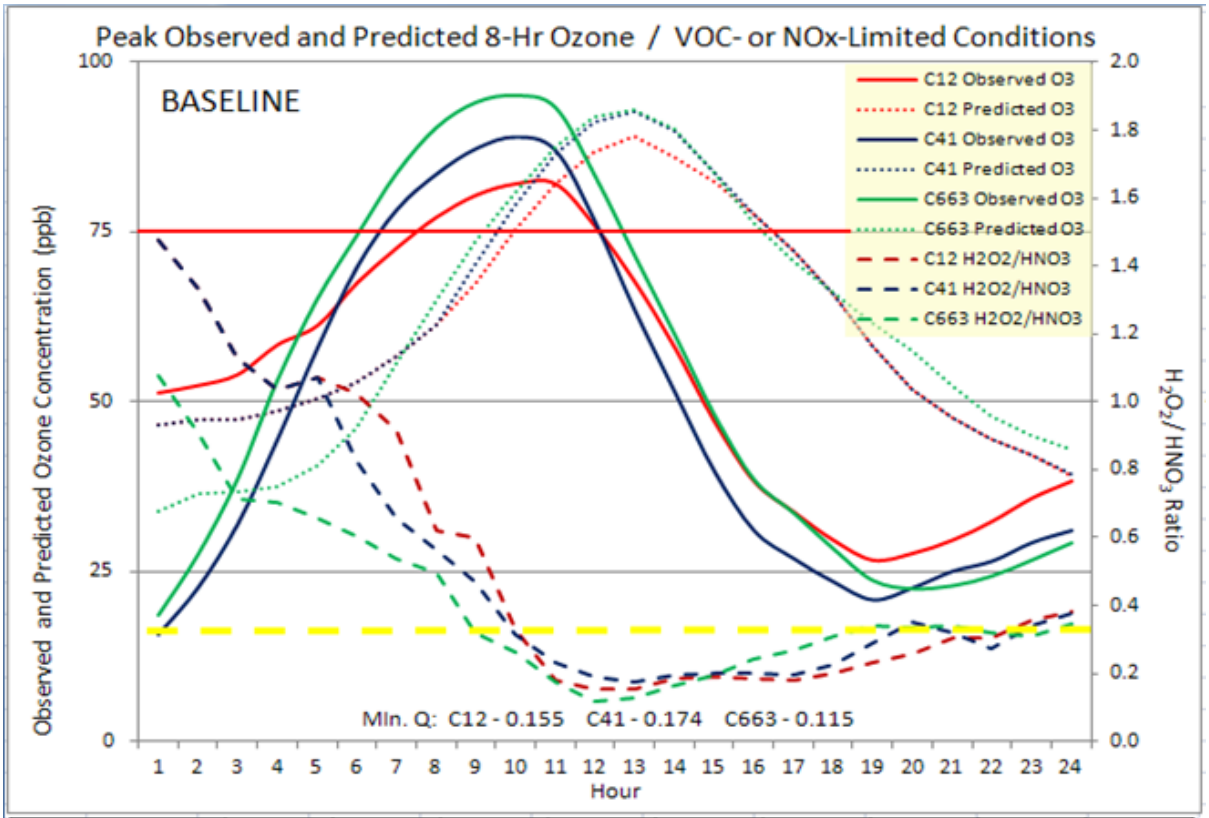

BASELINE	PeakObs	PeakPred	PairPred	UPPA	APPA	EPPA	PTB	NB	NE
	95.1	93	92.1	-2.1	2.5	9	3	3.9	23.7

Figure 5.8 Diurnal Predicted and Observed 8-Hour Ozone (ppb) /H_2O_2/HNO_3 Ratios – Run 2a

5.2.2.2 NOx

Similar performance evaluation of the model predictions was conducted for paried 1-hour NOx data at the seven CAMS sites with available NOx measurements (see Table 5.2). Daily statistics are presented in Figure 5.9. Both CAMx runs under estimated the peak observation on all dates except June 20 in Run 2a, as seen in the top panel of Figure 4-5 in Appendix A. The highest observed NOx was 462 ppb and both simulations failed to capture this extremely high NOx event at CAMS 41 during the afternoon (12:00 to 16:00 CST) on June 18 (Figure 4-6 of Appendix A). Ozone was titrated to below 20 ppb during this high NOx event and both simulations reproduced the strong ozone titration that was observed (Figure 4-4 of Appendix A) even though they under-predicted the observed NOx. Time series of NOx (Figure 4-6 of Appendix A) reveal an event with very high NOx on the afternoon of June 18. Even though both CAMx

simulations tended to over-predict NOx on average, they generally could not replicate events with very high NOx that occurred at multiple monitors and on multiple days during the episode.

The average paired peak accuracy (Top panel of Figure 5.9) compares the highest observed 1-hour NOx from each of the seven monitors with their co-located peaks predicted by Run 2a and Run 2b. The NOx average paired peak is less accurate than ozone because NOx is more influenced by local scale features. Days were evenly split between over- and under-prediction of peak NOx for the flexi-nested simulation whereas the 1-way nested simulation under-predicted peak NOx on 7 of 10 days.

The last two statistics compare the normalized bias and error using all hours and sites. Pairings when the observed 1-hour NOx was less than 2 ppb were excluded. There are no model performance goals for NOx. Both simulations over predicted NOx on all dates except June 16 in the flexi-nested simulation. The biases were comparable between the two simulations on high NOx dates (June 17 and 18). Performance was poorest on June 21, the last day of the episode. The CAMx 1-way nested simulation performed better than the flexi-nested simulation on half of the dates modeled. The largest discrepancy between the two simulations occurred on June 20 when the bias of the flexi-nested simulation was four times higher than the 1-way nested simulation.

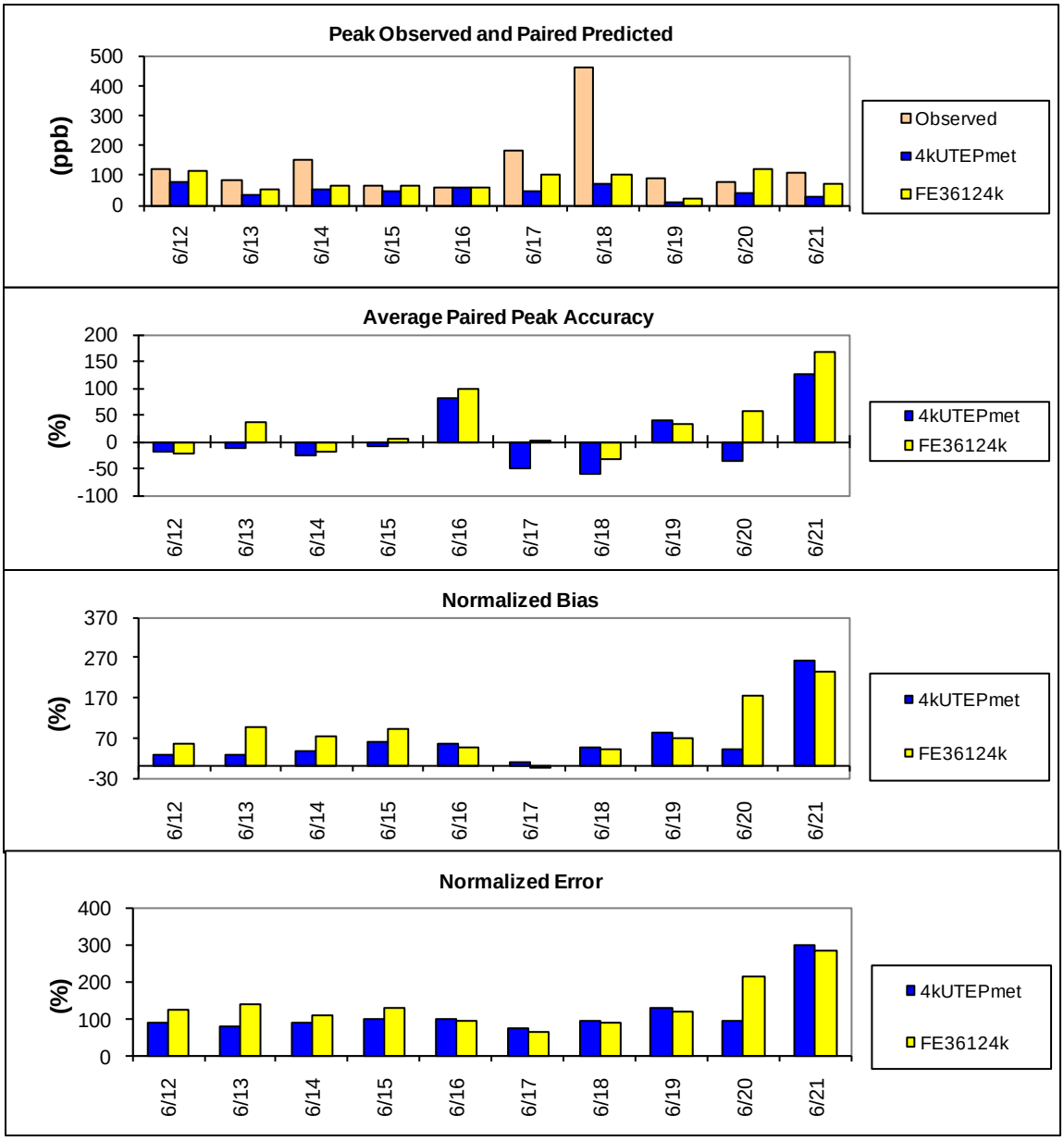

Figure 5.9 Model performance statistics for 1-hour NOx (Figure 4-5 of Appendix)

5.2.3 Phenomenological Evaluation

Figure 5.10 shows the ozone maps of the daily maximum 8-hour ozone for each date for both Run 2a (right panels) and Run 2b (left panels). The domain peak location is different on most dates. Animations of hourly ozone and wind vectors for June 12 reveal that the different ozone peak locations result from differences in modeled wind directions. At CAMS 12, the

observed daily maximum 8-hour ozone was 82 ppb on June 18. Run 2b predicted 8-hour ozone in agreement with the observations at CAMS 12 while Run 2a predicted an 8-hour ozone in the 60s (Figure 4-4 of Appendix A) with a domain peak of 73 ppb nearby (Figure 4-7 of Appendix A).

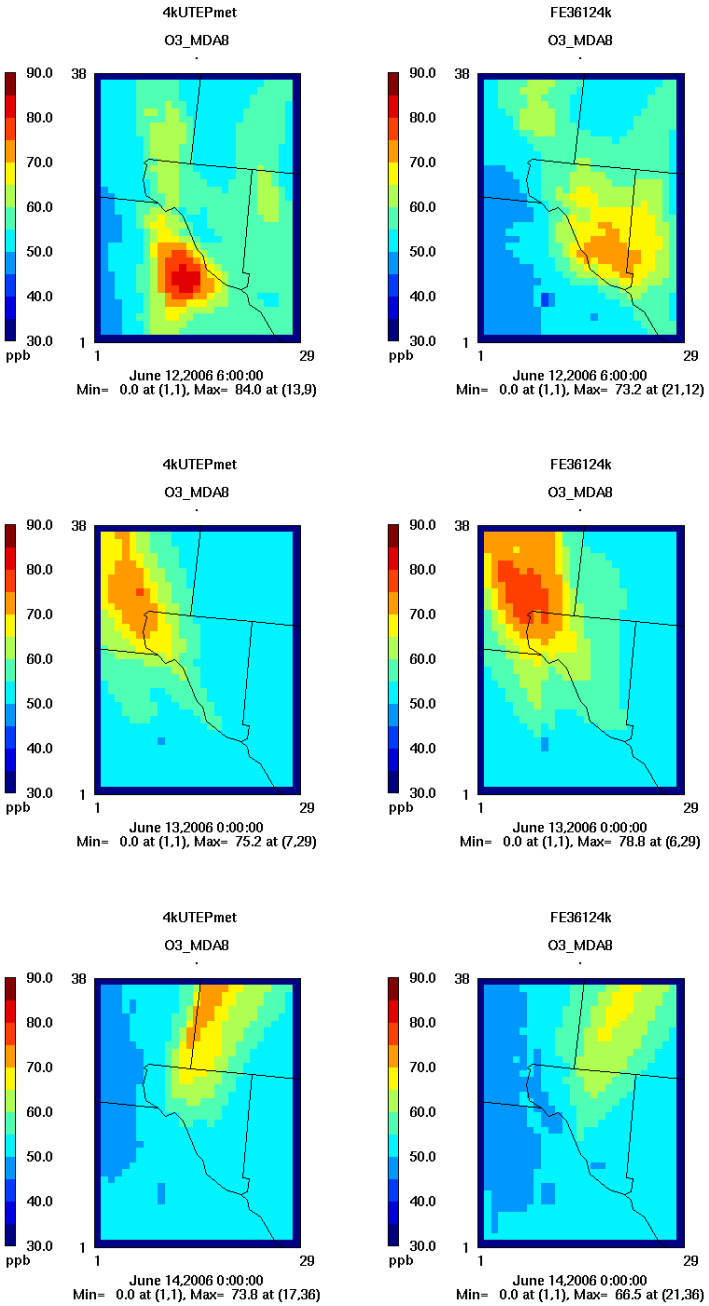

Figure 5.10 Ozone maps showing daily maximum 8-hour ozone concentrations predicted by Run 2b (left panel) and Run 2a (right panel) during June 12-21, 2006.

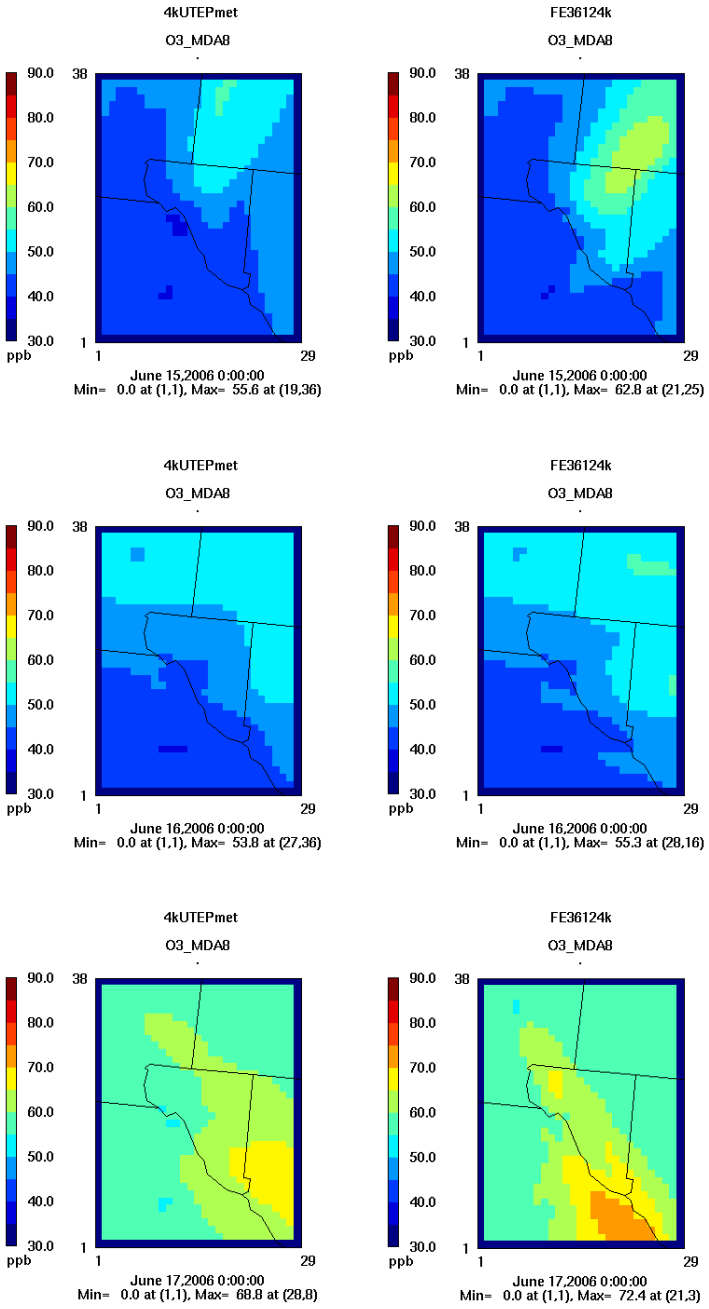

Figure 5.10 Ozone maps showing daily maximum 8-hour ozone concentrations predicted by Run 2b (left panel) and Run 2a (right panel) during June 12-21, 2006

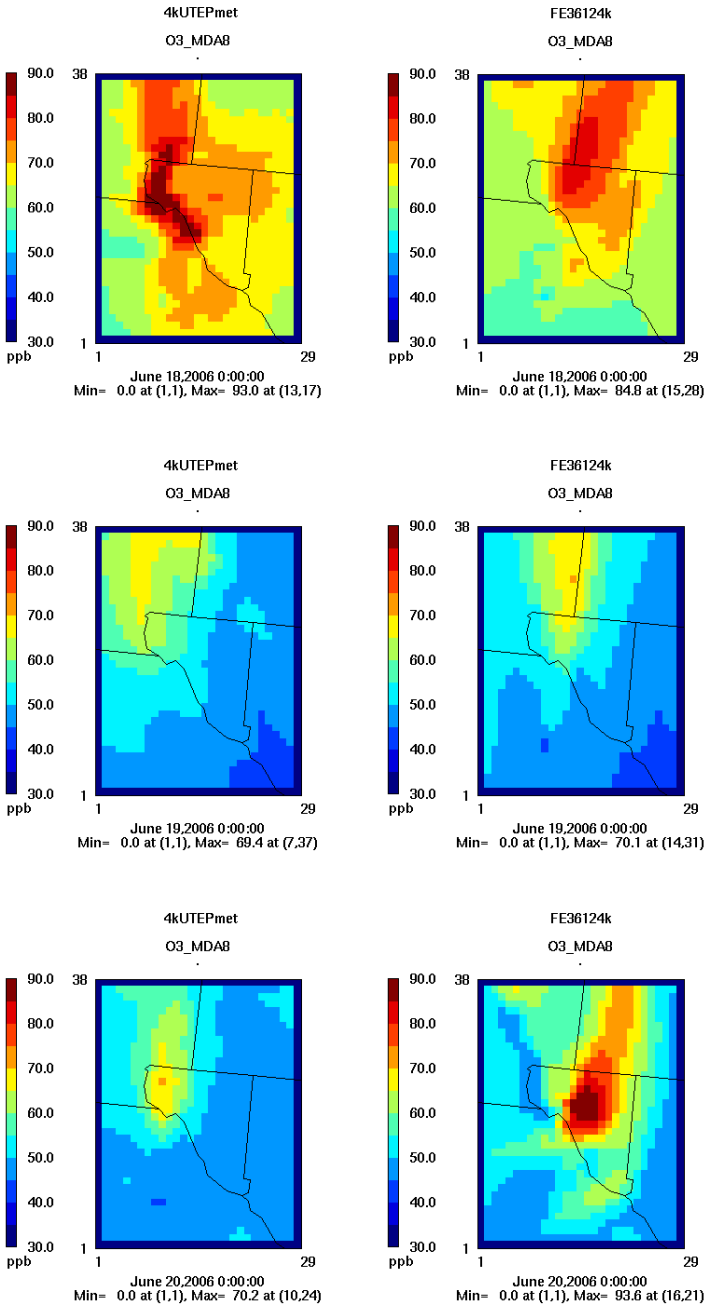

Figure 5.10 Ozone maps showing daily maximum 8-hour ozone concentrations predicted by Run 2b (left panel) and Run 2a (right panel) during June 12-21, 2006

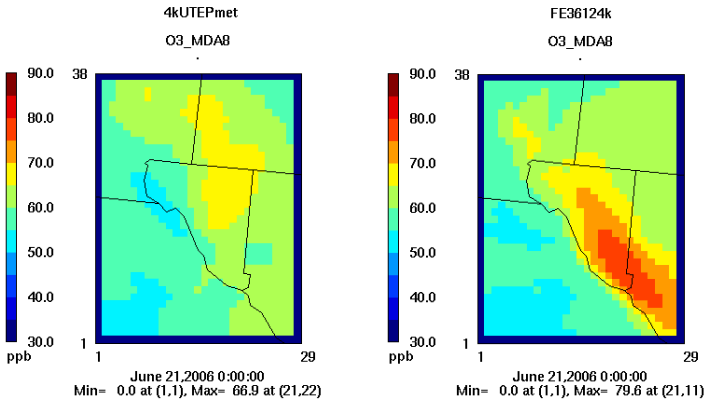

Figure 5.10 Ozone maps showing daily maximum 8-hour ozone concentrations predicted by Run 2b (left panel) and Run 2a (right panel) during June 12-21, 2006

Since the emissions inventory and modeling options were kept the same for both runs, the difference can only be attributed to the difference in meteorology used in both runs. It is interesting to notice that Run 2a was unable to capture any high ozone day in Cd. Juarez (all right panels in Figure 5.8) although high ozone levels were observed at the two Cd. Juarez CAMS sites with an exceedance day (June 18) registered at CAMS 663. Run 2a also missed high ozone levels observed along the U.S.-Mexico border and downtown areas of both El Paso and Cd. Juarez. This is particularly obvious in the June 18 ozone maps. As a matter of fact, all right panels in Figure 5.8 show high ozone levels on the east side of Franklin Mountains and far northeast of El Paso, except on June 13. Of particular interest are the ozone maps for the high ozone day on June 18. On this day, high ozone was observed at Sunland Park, NM and far northeast of El Paso, where the two locations were identified in the conceptual model for future monitoring.

Spatial plots of the daily maximum 1-hour NOx for each date were prepared by Environ in Appendix A. Both runs agree well on the domain peak location.

5.3 CAMx Run Set 3: Sensitivity Analysis

Based on the results and performance evaluations of the CAMx simulations conducted by UTEP and Environ, Run 2a was selected as the base case for the 2006 ozone episode. Sensitivity analysis was subsequently performed to incorporate the improvements made in the emissions inventory (Li et al 2011b; Yang et al 2012) and the sensitivity of Cd. Juarez area emissions on ozone pollution in the PdN. Run 3a represents a CAMx simulation using the setup of Run 2a by

adding the recently processed emission estimates for the port of entry into the emission inventory. Runs 3.1- 3.12 were conducted to evaluate the potential benefit in ozone reduction resulting from reductions in area emissions from Cd. Juarez.

5.3.1 Bridge emissions from the Port of Entry

Five sources were identified in the Emission Inventory Improvement Plan (Li et al 2011b). Emission estimates for these sources were provided in a separate report (Yang et al 2012). These emissions were not accounted for in the archived TCEQ emission inventories for the region and it was suggested that inclusion of these emissions in the region's photochemical air quality modeling study will help improve understanding of the nature of ozone pollution in the region and subsequently reduce the uncertainties in the diagnosis of high ozone episodes in the PdN.

Among the five sources, light duty and heavy duty vehicles at the El Paso-Juarez international ports of entry (POEs) were found to emit a significant amount of pollutants while waiting to cross the border. NOx emissions at the POEs were found to be significant, adding ~5.5% of the total onroad NOx emissions in El Paso to the atmosphere. VOC emissions at the POEs were also found to be significant, releasing another ~2.0 % of the total onroad VOC emissions in El Paso to the atmosphere (Yang et al 2012). As a result, a CAMx sensitivity run (Run 3a) was conducted to evaluate the impact of the additional bridge emissions on the PdN ozone level.

The bridge emissions quantified for emission modeling (Yang et al 2012) were processed in EPS3 and merged with other emissions on the El Paso 4 km domain. The CAMx model-ready emission files are available at UTEP and can be downloaded upon the approval of MPO. The bridge emissions used developed for this simulation shown in Table 5.3 (Table 7, Yang et al 2012). Only NOx, VOC and CO emissions were processed and the emissions were applied at the Bridge of the America (BOTA), which may only represent a fraction of the total emissions from all ports of entry in El Paso. Hourly and daily profiles used in CAMx modeling were taken from the EIIP report (Yang et al 2012) and displayed in Figures 5.11 through 5.14.

Table 5.3 June 2006 daily emissions at POEs in El Paso (tons/day)

	BOTA		(PdN)		Zaragoza		Total
	passenge	commercia	passenge	commercia	passenge	Commercia	
NOx	0.56	0.40	0.23	0.00	0.22	0.47	**1.89**
VOC	0.41	0.07	0.17	0.00	0.16	0.08	**0.89**
CO	3.63	0.52	1.48	0.00	1.42	0.60	**7.66**
SO2	0.012	0.002	0.005	0.00	0.005	0.002	**0.03**
PM2.5	0.011	0.021	0.005	0.00	0.004	0.024	**0.07**
PM10	0.025	0.027	0.010	0.00	0.010	0.031	**0.10**

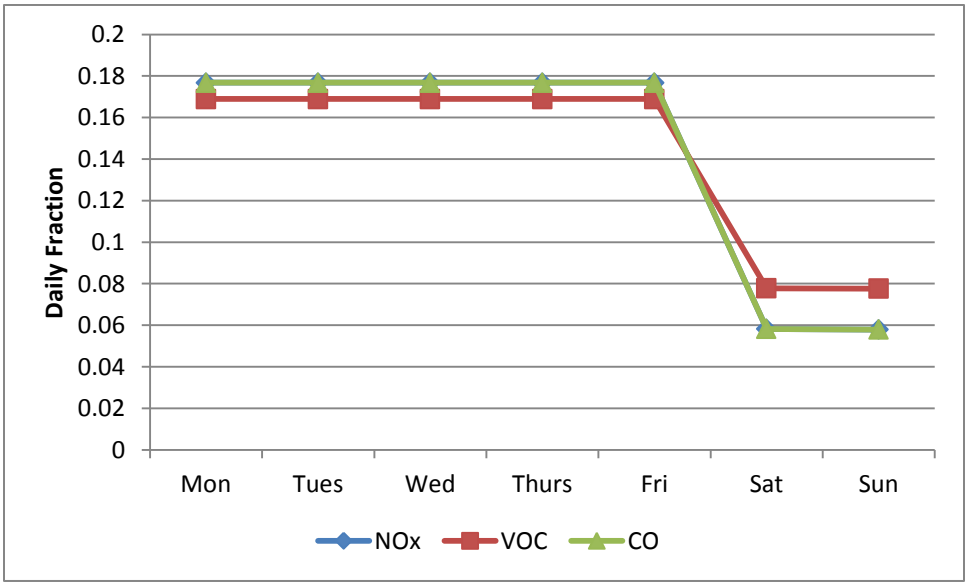

Figure 5.11 Daily profiles of POE emissions

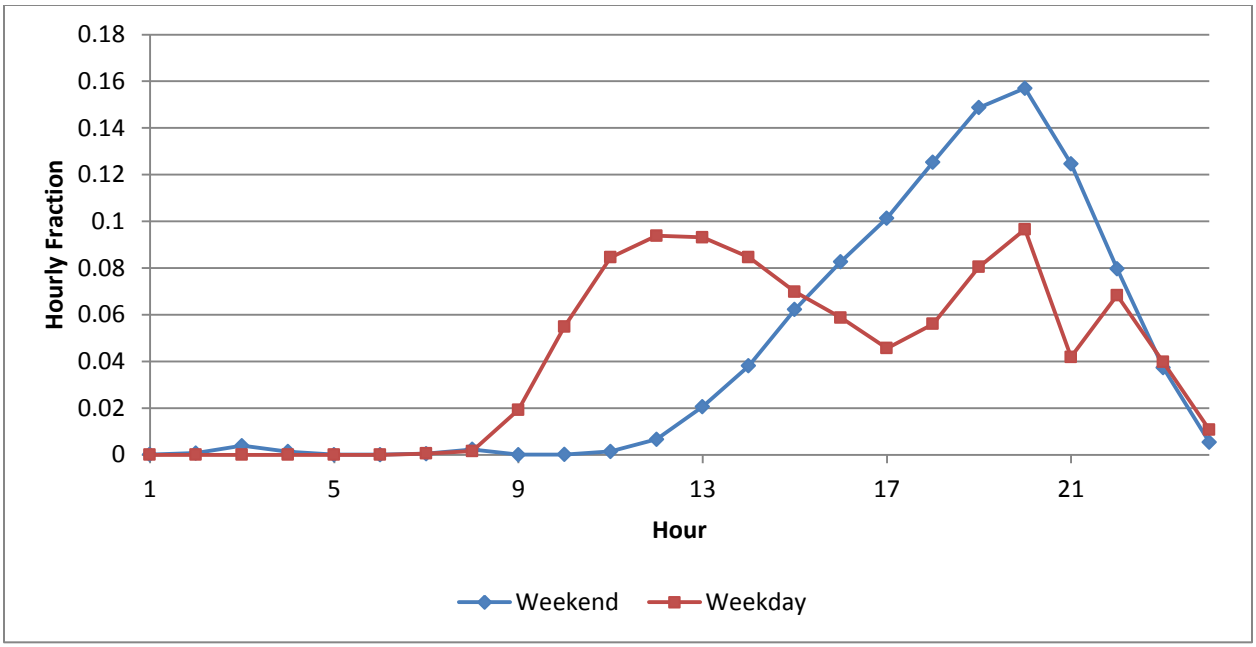

Figure 5.12 Hourly profiles of POE NOx emissions

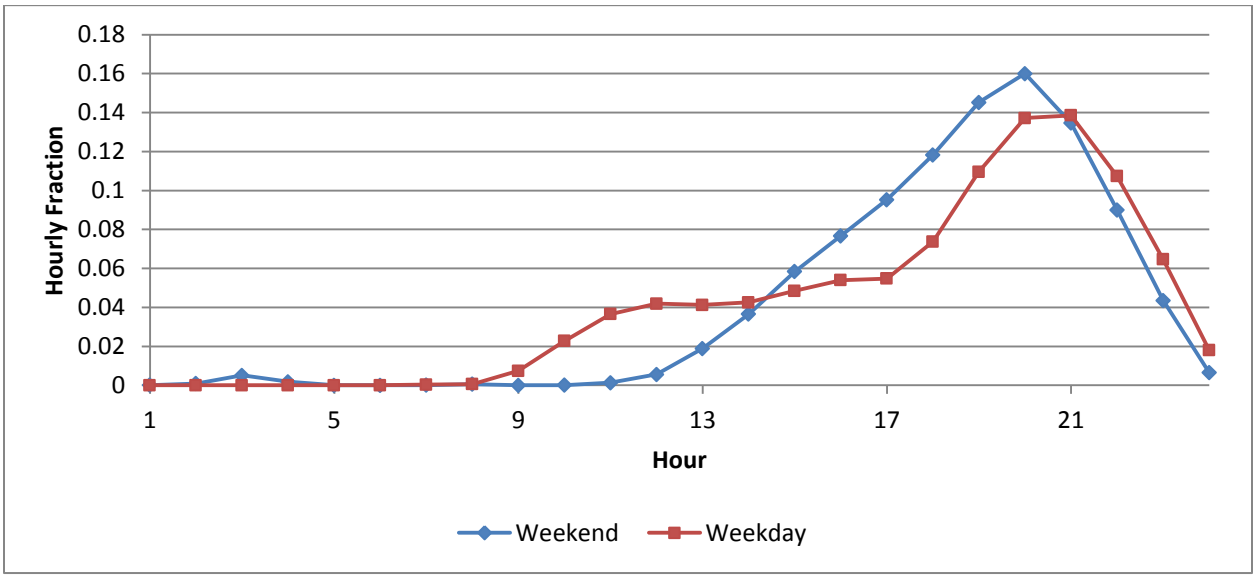

Figure 5.13 Hourly profiles of POE VOC emissions

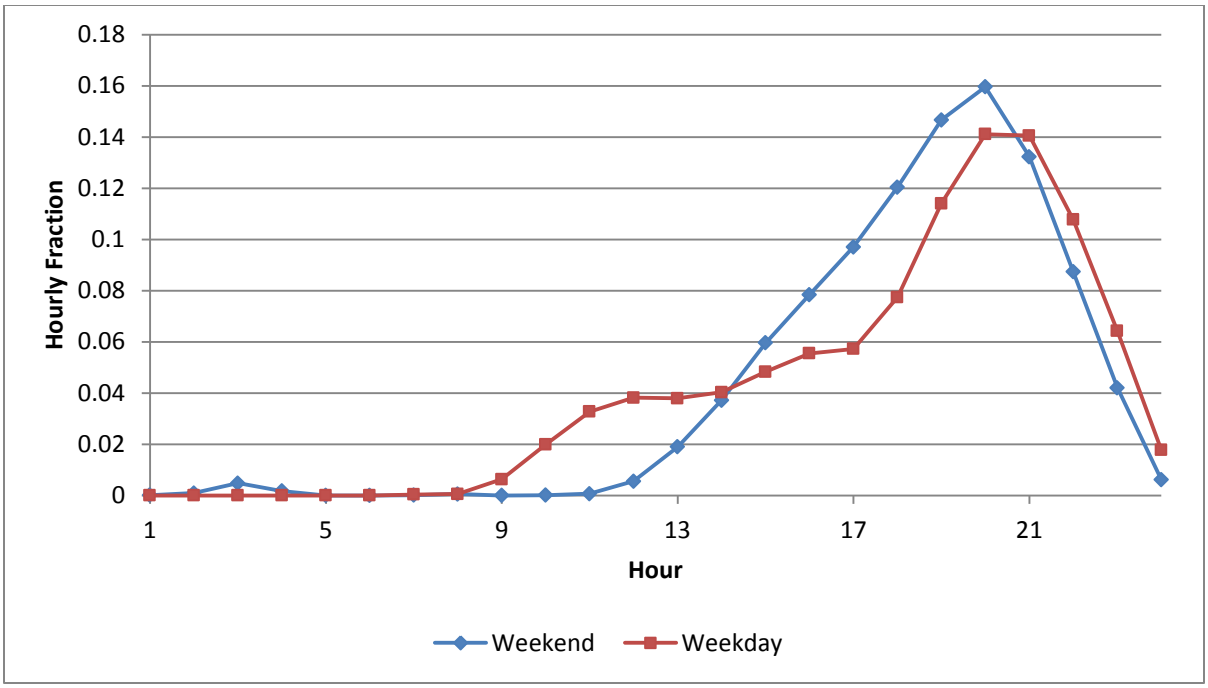

Figure 1.14 Hourly profiles of POE CO emissions

The updated emissions were run in CAMx for June 12-21, 2006. Figure 5.15 contains the ozone maps showing daily maximum 8-hour ozone concentrations predicted by Run 3a: a) with NOx, VOC, and CO emissions from the BOTA; b) without the bridge emissions; c) difference due to the contribution from the emissions from the BOTA on the high ozone day of June 18, 2006. One notices that the difference in ozone concentrations is calculated as Difference = Ozone (without bridge emissions) – Ozone (with bridge emissions). Figure 5.15b is the same as the one in Run 2a for June 18. A quick inspection of the results revealed that the peak ozone concentrations were not improved with the added bridge emissions. Instead, ozone concentrations are actually reduced a little when compared with the simulation without adding the extra emissions from the BOTA.

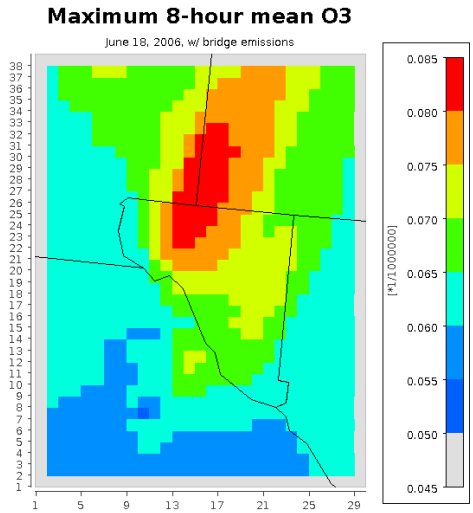

a) with bridge emissions

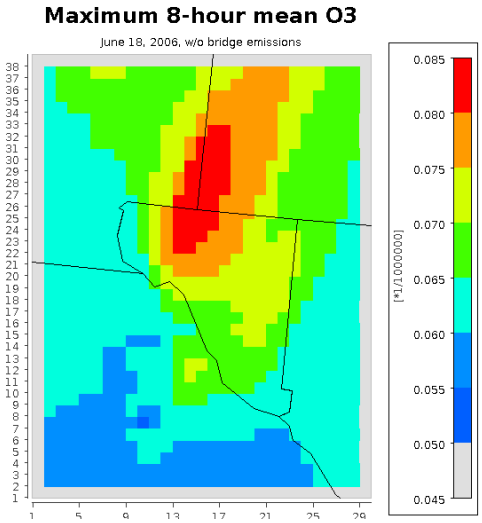

b) without bridge emissions

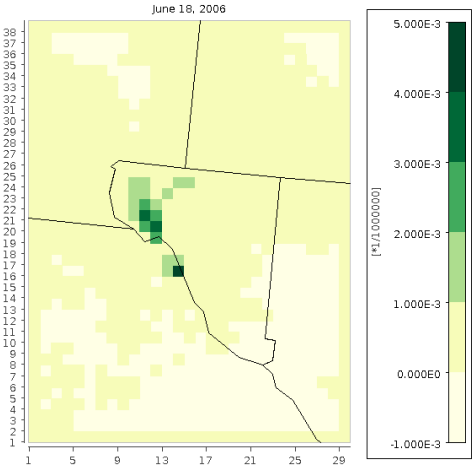

b) difference = b – a

Figure 5.15 Ozone maps showing daily maximum 8-hour ozone concentrations predicted by Run 3a: a) with bridge emissions; b) without bridge emissions; c) difference between b and a on June 18, 2006

5.3.2 Reduction in Cd. Juarez Area Emissions

Fugitive emissions of ozone precursors, particularly VOCs, from the area sources in Cd. Juarez have been identified as one of the major contributors to the PdN's ozone pollution. Information on the fugitive area source emissions, such as VOC emissions from the gasoline fueling stations and /or from automotive paint and body shops, is incomplete and unreliable. Operations of these area sources are well distributed in the city and relatively proportional to the population distribution/landuse in the city. The uncertainty in the emission estimates could propagate into the CAMx ozone predictions and reduce the accuracy of the model predictions. It is therefore desirable to examine the impact of reduction/increase in the Juarez area emissions on the PdN ozone levels by conducting CAMx simulations in conjunction with a series of combinations of reduction/increase in ozone precursor emissions. The goals of this evaluation are: 1) to determine the uncertainty of area emissions of VOCs and NOx in Cd Juarez on ozone peak and spatial distribution in the PdN; and 2) to provide a basis for consideration of future control strategies in terms of how much reduction in ozone level could be achieved if effort is put in to reduce a fraction of area VOC and/or NOx emissions.

CAMx simulations were performed for 12 scenarios which modified Cd. Juárez area source VOC and / or NOx emissions from the base case (Run 2a). Model performance was evaluated for daily maximum 1-hour and 8-hour ozone. Comparisons were made of the PREDICTED ozone concentrations vs. ozone concentrations OBSERVED at the regional CAMS across the modeled domain for the whole modeling period (June 12-21). Only 1 CAMS, C662, was not included in this assessment due to the current limitations in the OBSCAT, which is one of the CAMx post-processing tools.

All scenarios were also compared to the base case CAMx run for the high ozone event day (June 18, 2006). Each of the 12 simulations produced a set of results for assessing potential air quality improvement strategies based on modifications to NOx or VOC emissions. The statistical tools available in the CAMx modeling system were used to determine if the emissions modifications fall within acceptable parameters regarding model performance. This performance evaluation was made to three CAMS (CAMS 12, 41, and 663) in the PdN. On 18 June, CAMS 663 observed the highest 8-hour ozone concentration among the 8 CAMS observing an exceedance of the 8-hour ozone NAAQS. CAMS 663 also observed the highest 8-hour ozone concentrations in the PdN region during 2006, 99 ppb on 26 August, 2006 as indicated in Table 5.4 below. On the US side of the border, CAMS 12 at UTEP tends to observe the highest ozone concentrations and multiple exceedances during the year. CAMS 41 is the only Auto-GC station in PdN and is another location on the border observing high ozone level.

5.3.2.1 Model Performance Goals

Each simulation must generate results that are within acceptable parameters for Normalized Bias (NB) and Normalized Error (NE) as air quality models in order to be acceptable for NAAQS modeling purposes (EPA, 2007). NB and NE are important statistics in assessing the accuracy of the model to predict ambient ozone. Model performance goals for NB and NE are $\pm$15% and $\leq$35% respectively. Positive NB indicates over-prediction of ozone and negative NB indicates under-prediction of ozone. NE and NB are based on all predicted and observed values in the modeling simulation for the entire 4 km domain. Equation 5.1 is applied to calculate NE, and Equation 5.2 is applied to calculate NB.

	Acceptable Parameters	
$NME = \frac{\sum_{1}^{N} \lvert Model - Obs \rvert}{\sum_{1}^{N} (Obs)} \cdot 100\%$	NE $\leq$ 35%	Equation 5.1
$NMB = \frac{\sum_{1}^{N} (Model - Obs)}{\sum_{1}^{N} (Obs)} \cdot 100\%$	-15% $\leq$ NB $\geq$ +15%	Equation 5.2

5.3.2.2. Model run and performance definitions

Table 5.4 presents model performance results and statistics for 1-hour ozone. PEAK OBSERVED (PeakObs) and PREDICTED PEAK (PredPeak) ozone plus the suite of statistics generated by CAMx are identified. The maximum PeakObs on 6/18 was 120.7 ppb. The 12 runs (Runs 3b.1 – 3b.12) are identified as RUN1 through RUN12 in the second row of the table whereas BASELINE has the same run configuration as Run 2a in Chapter 5 of this report. Emission variations in VOC and NOx for each run are shown in the last 2 rows of the table.

The differences between each RUN the BASELINE are summarized in the 3 rows between 2 bold lines in Table 5.4. Abbreviations in Table 5.4 are explained below:

- PredPeak | BL-PredPeak indicates the difference between the PredPeak for the specific RUN and BASELINE PredPeak.

- PairPred | BL PairPred indicates the difference between the PAIRED PREDICTED PEAK value and the BASELINE PAIRED PREDICTED PEAK. The PairPred Peak represents the peak value predicted by CAMx that is paired to the specific CAMS observed value. CAMx generates a PredPeak value for each grid cell for each time-step and interpolates a predicted ozone concentration at the CAMS within the grid cell taking into consideration the concurrent time-step ozone values at the adjacent cells for the purposes of interpolating an ozone concentration value at the specific CAMS.

- PredPeak | PeakObs indicates the difference between the PREDICTED PEAK and the PEAK OBSERVED value for each RUN. The PeakObs value does not change given this is the peak 1-hour ozone concentration on 6/18. This variable helps determine the model performance by indicating the variation between predicted and observed peaks and the impact on ozone concentrations due to emissions modifications.

Table 5.4 Results and statistics for 1-hour ozone simulations

Date ID		BASELINE	1201-0000	1201-0900	1201-1100	1201-1300	1201-2100	1201-2300	1202-1000	1202-1300	1202-1500	1202-1800	1202-2330	1203-0200
RUN ID			1	2	3	4	5	6	7	8	9	10	11	12
Model Output and Statistics	Cell	13,18	13,18	13,17	11,26	13,17	13,18	13,18	13,18	13,17	13,17	11,26	13,17	11,26
	PredPeak	103.3	102.1	102.4	91.7	113.9	113.0	92.7	100.1	102.3	119.7	86.8	118.8	87.8
	PeakObs	120.7	120.7	120.7	120.7	120.7	120.7	120.7	120.7	120.7	120.7	120.7	120.7	120.7
	PairPred	99.3	89.1	98.4	86.7	107.8	108.7	89.1	95.2	97.6	112.1	80.1	113.6	83.3
	UPPA	-14.4	-23.2	-15.1	-24	-5.6	-6.4	-23.2	-17.1	-15.3	-0.9	-28.1	-1.6	-27.2
	APPA	-1.5	-8.7	-2.1	-10	4.8	5.2	-8.7	-3.6	-2.7	7.8	-14.6	8.6	-12.8
	EPPA	12.2	14.4	11.9	15.3	13.1	13.2	14.4	13.3	11.9	15.2	17.2	15.2	16
	PTB	4	4	3	4	3	4	4	4	3	3	4	4	4
	NB	-3.3	-6.7	-2.1	-8.7	1.2	0.1	-6.7	-6.3	-1.8	3.1	-11.5	1.8	-8.7
	NE	25.6	23.2	24.2	24.2	27.1	28.1	23.2	26.3	23.3	27.8	23.9	29.5	22.4
	NOx		↑ 50%	↓ 50%			↑ 50%	↓ 50%	↑ 75%	↓ 75%			↑ 75%	↓ 75%
	VOC				↓ 50%	↑ 50%	↑ 50%	↓ 50%			↑ 75%	↓ 75%	↑ 75%	↓ 75%
Difference between Peaks (%)	PredPeak | BL-PredPeak		-1.1	-0.8	-11.2	10.3	9.4	-10.3	-3.1	-1.0	15.8	-16.0	15.0	-15.0
	PairPred | BL-PairPred		-10.3	-0.9	-12.7	8.6	9.5	-10.3	-4.1	-1.7	12.9	-19.3	14.4	-16.1
	PredPeak | Peak Obs		-15.4	-15.1	-24.0	-5.6	-6.4	-23.2	-17.1	-15.3	-0.9	-28.1	-1.6	-27.2
Difference between Peaks(ppb)	PredPeak | BL-PredPeak		-1.2	-0.9	-11.6	10.6	9.7	-10.6	-3.2	-1.0	16.4	-16.5	15.5	-15.5
	PairPred | BL-PairPred		-10.2	-0.9	-12.6	8.5	9.4	-10.2	-4.1	-1.7	12.8	-19.2	14.3	-16.0
	PredPeak | Peak Obs		-18.6	-18.3	-29.0	-6.8	-7.7	-28.0	-20.6	-18.4	-1.0	-34.0	-1.9	-32.9

5.3.2.3 Model Performance Summary for 1-Hour Ozone

Comparing each RUN to BASELINE data in Table 5.4 indicates that modifying VOC emissions generated the greatest variability in 1-hour ozone (RUN 3, 4, 9, and 10). Modifications to NOx generated minimal variability in 1-hour ozone. Comparing PredPeak | BL-PredPeak indicates that increasing only NOx by 50% (RUN 1) or 75% (RUN7) results in reduced 1-hour ozone by 1.1 ppb and 3.1 ppb respectively. Reducing only NOx by 50% (RUN2) or 75% (RUN8) reduced 1-

hour ozone 0.8 ppb and 1.1 ppb respectively. NOx tends to titrate ozone albeit minimally as compared to the BASELINE results.

Increasing only VOC by 50% or 75% resulted in improved bias by 2% compared to BASELINE. Increasing or decreasing both VOC and NOx combined did not produce results significantly different from VOC-only modifications. Modifications to NOx emissions, at existing concentrations, are insignificant contributors to improvements or further degradation of air quality. These results indicate that the PdN region ozone formation conditions are VOC-limited as will be discussed for each RUN in the following section.

Figure 5.16 presents the PAIRED PREDICTED PEAK for 1-hour ozone CAMx simulation RUNS. The yellow bar at the base of the graph represents results identified as BASELINE. The PAIRED PREDICTED PEAK for 1-hour compares ozone concentrations observed at the CAMS to a concentration predicted by CAMx. Figure 5.17 presents the PREDICTED PEAK 1-hour ozone concentrations for all runs. The value of each bar in Figure 5.17 represents the maximum ozone concentration within any particular grid cell in the modeling domain regardless of location within the cell for the specific run evaluated. As can be observed in either Figure 5.16 or Figure 5.17, the greatest variability in 1-hour ozone concentrations occurs when VOC emissions are modified.

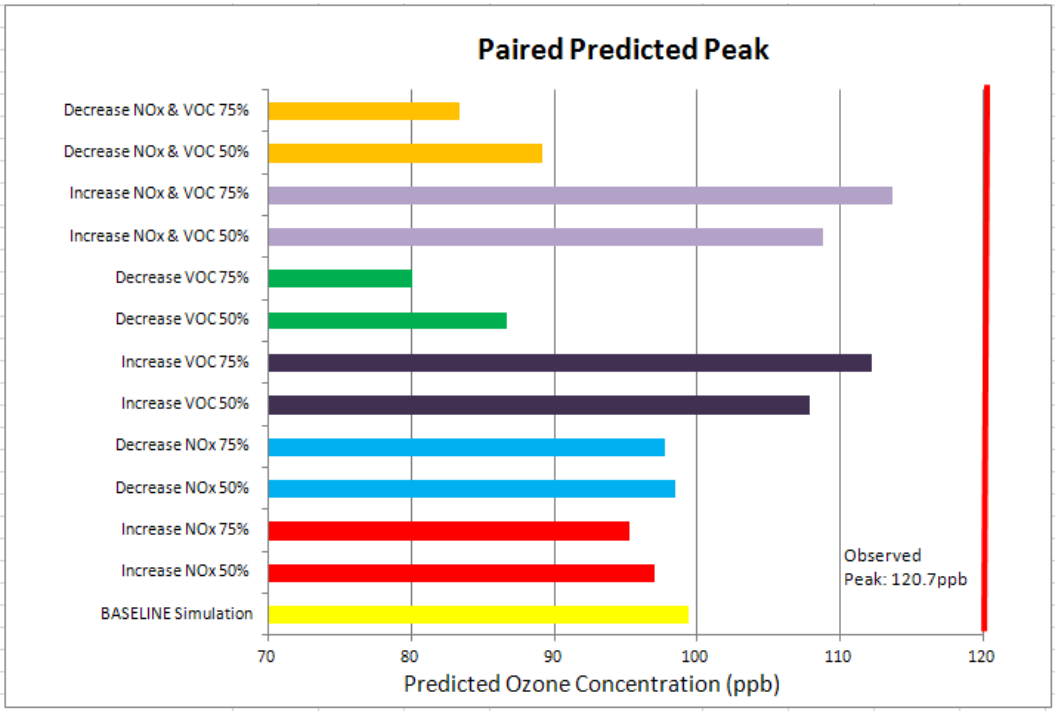

Figure 5.16 Paired predicted peak for CAMx simulations and 1-hour ozone

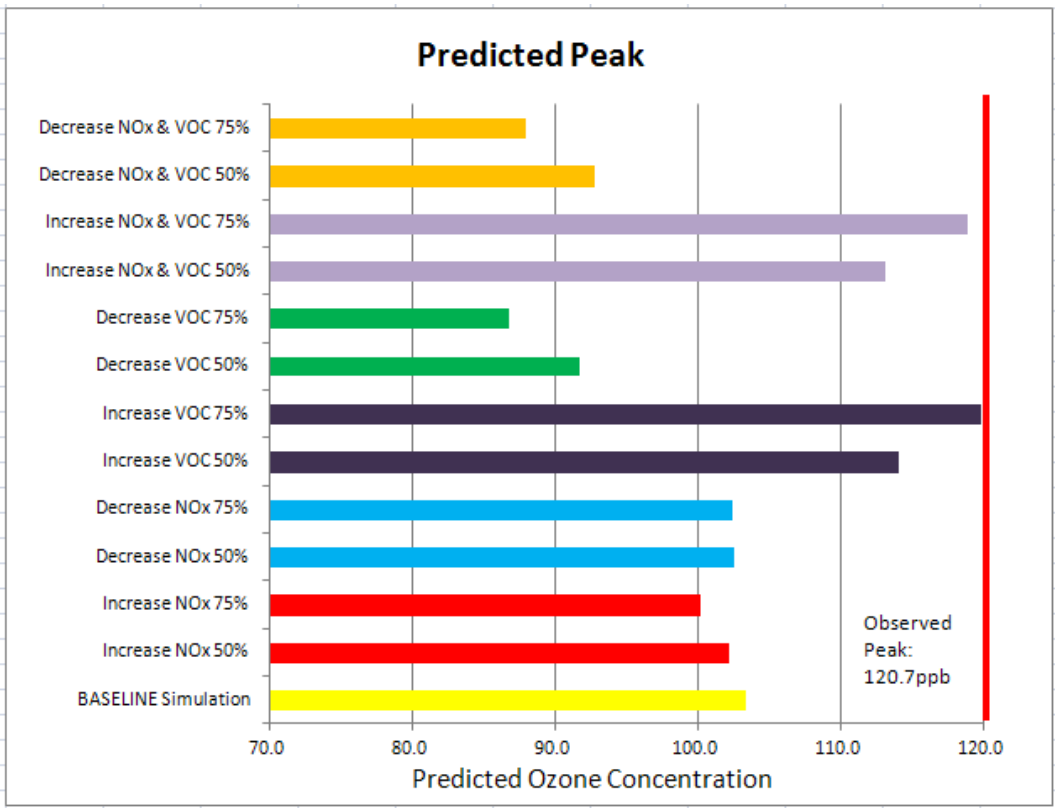

Figure 5.17 PREDICTED PEAK for CAMx simulations and 1-hour ozone

While all simulations consistently under-predict the PEAK OBSERVED 1-hour ozone concentrations, modifying VOC emissions tends to generate predicted 1-hour ozone peaks closer to the PEAK OBSERVED concentration. Increasing or decreasing combined NOx and VOC emissions vary little from modifications to VOC emissions alone.

5.3.2.4 Results and Statistics for 8-Hour Ozone

Table 5.5 presents the results and statistics for 8-hour ozone simulations for June 18. PEAK OBSERVED and PREDICTED PEAK ozone plus the suite of statistics generated by CAMx are also indicated. 8-hour ozone results varied significantly from 1-hour ozone results. The maximum 8-hour PEAK OBSERVATION on 6/18 was 95.1 ppb. Comparing each RUN to the BASELINE data indicate that modifying VOC emissions generates the greatest variability in 8--hour ozone concentrations. Model performance statistics presented in Table 5.5 are generated by comparing 8-hour predicted averages to 8-hour average observed ozone.

Table 5.5 Results and statistics for 8-hour ozone simulations

Date ID		BASELINE	1201-0000	1201-0900	1201-1100	1201-1300	1201-2100	1201-2300	1202-1000	1202-1300	1202-1500	1202-1800	1202-2330	1203-0200
RUN ID			1	2	3	4	5	6	7	8	9	10	11	12
Model Output and Statistics	Cell	13,18	13,18	13,17	11,27	13,17	13,18	13,18	14,17	13,17	13,17	11,27	13,17	11,27
	PeakObs	95.1	95.1	95.1	95.1	95.1	95.1	95	95.1	95.1	95.1	95.1	95.1	95.1
	PredPeak	93	90.11	94.05	83.22	102.9	101.8	84.49	89	93.28	107.1	80.51	106.3	80.71
	PairPred	92.1	83.6	92.6	80.3	100.5	100	83.6	88.3	86.9	103.7	73.8	104.1	78.8
	UPPA	-2.1	-11.1	-1	-12.4	8.3	7.1	-11.1	-5.2	-7	12.7	-15.3	11.9	-15.1
	APPA	2.5	-3.9	3	-5.9	9	8.5	-3.9	0.6	-0.7	11.6	-10.5	11.7	-7.6
	EPPA	9	8.3	9.5	8.9	14.3	13.7	8.3	8.5	8.5	16.6	12.1	16.4	9.5
	PTB	3	3	3	3	3	3	3	3	3	3	3	3	3
	NB	3.9	0.4	5.4	-1.8	8.8	7.4	0.4	1.8	0.6	10.8	-4.8	9.2	-1.6
	NE	23.7	22.1	22.4	23	24.4	25.4	22.1	24.3	24.5	24.8	22.8	26.5	21.5
	NOx		↑ 50%	↓ 50%			↑ 50%	↓ 50%	↑ 75%	↓ 75%			↑ 75%	↓ 75%
	VOC				↓ 50%	↑ 50%	↑ 50%	↓ 50%			↑ 75%	↓ 75%	↑ 75%	↓ 75%
Difference between Peaks (%)	PredPeak | BL-PredPeak		-3.1	1.1	-10.5	10.6	9.4	-9.2	-4.3	0.3	15.1	-13.4	14.3	-13.2
	PairPred | BL-PairPred		-9.2	0.5	-12.8	9.1	8.6	-9.2	-4.1	-5.6	12.6	-19.9	13.0	-14.4
	PredPeak | Peak Obs		-5.2	-1.1	-12.5	8.1	7.0	-11.1	-6.4	-1.9	12.6	-15.3	11.8	-15.1
Difference between Peaks(ppb)	PredPeak | BL-PredPeak		-2.9	1.1	-9.8	9.8	8.8	-8.5	-4.0	0.3	14.1	-12.5	13.3	-12.3
	PairPred | BL-PairPred		-8.5	0.5	-11.8	8.4	7.9	-8.5	-3.8	-5.2	11.6	-18.3	12.0	-13.3
	PredPeak | Peak Obs		-5.0	-1.1	-11.9	7.8	6.7	-10.5	-6.1	-1.8	12.0	-14.6	11.2	-14.4

Modifications to NOx generated minimal variability in 8-hour ozone. NE and NB improved by 1.6% and 0.7% when NOx emissions increase or decrease by 50% respectively when compared to the BASELINE. The variability in 8-hour ozone was sufficient to qualify modifications to NOx emissions as a potential air quality control strategy if only a 1 or 2 ppb reduction in ozone is required to attain a modified 8-hour ozone NAAQS. As reported earlier, El Paso's design value in 2011 was 71 ppb. Reducing the NAAQS to a hypothetical concentration of 70 ppb, for example, would cause El Paso to be designated nonattainment of the new NAAQS. As reported by ENVIRON (Appendix A), elevated NOx concentrations in the PdN ambient air tends to titrate ozone albeit minimally.

Increasing only VOC by 50% or 75% produced results which did not significantly change the NE or NB. Increasing or decreasing both VOC and NOx combined did not produce results which significantly differ from modification on RUNs with only VOC modifications. This indicates that modifications to NOx emissions, at existing concentrations, are insignificant contributors to improvements or further degradation of air quality when coupled with modification to VOC. It should be noted that Cd. Juarez comprises 83.4% of regional area source NOx emissions (20.1 TPD vs. 3.35 TPD for El Paso). Juarez area sources comprise roughly 33% of all Cd. Juarez NOx emissions considering only the modeled emissions inventory. As has been indicated, the regional modeled EI requires substantial modifications insofar as point source NOx emissions are concerned.

It should also be noted that NE for all simulations was ≤35% which is within acceptable parameters. NB for all simulations was between ±15% which is also within acceptable parameters. A discussion on the specific runs is provided in the following section. Figure 5.18 presents the PAIRED PREDICTED PEAK for CAMx simulations and 8-hour ozone. The yellow bar at the base of the graph represents BASELINE results. The greatest variability in 8-hour ozone concentrations occurs when VOC emissions increase or decrease. Figure 5.19 illustrates the PEAK PREDICTED 8-hour ozone concentration generated by the CAMx simulations. Most of the simulations under-predict 8-hour ozone. Results indicate the model over-predicts the PEAK OBSERVED 8-hour ozone concentration in simulations where VOC emissions were increased either 50% or 75% either alone or in combination with concurrent increases in NOx. Of note are increases in NOx tend to reduce 8-hour ozone compared to BASELINE results due to the ability of NOx to titrate ozone. Decreases in NOx did very little to change 8-hour ozone concentrations. The greatest decreases in 8-hour ozone occurred when both NOx and VOC were reduced 50% and 75%.

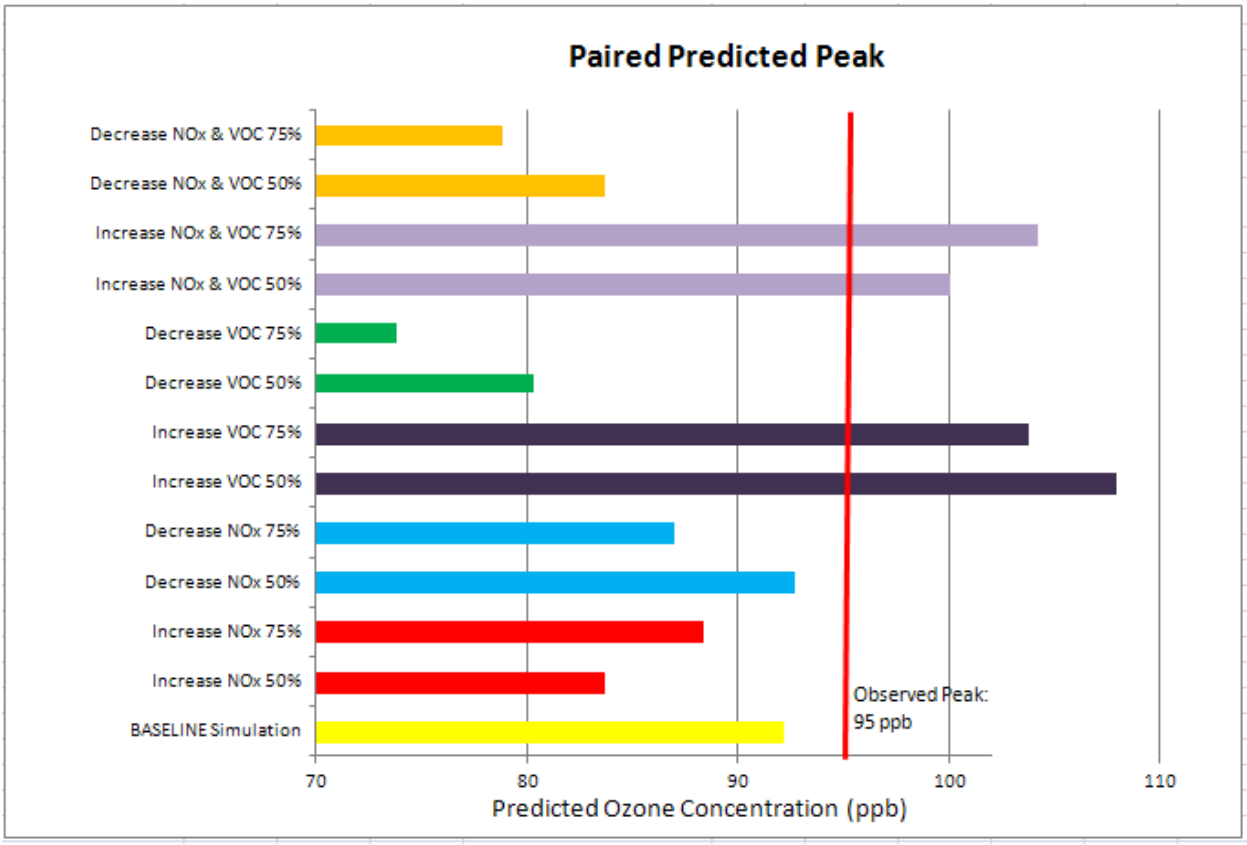

Figure 5.18 Paired predicted peaks for CAMx simulations and 8-hour ozone

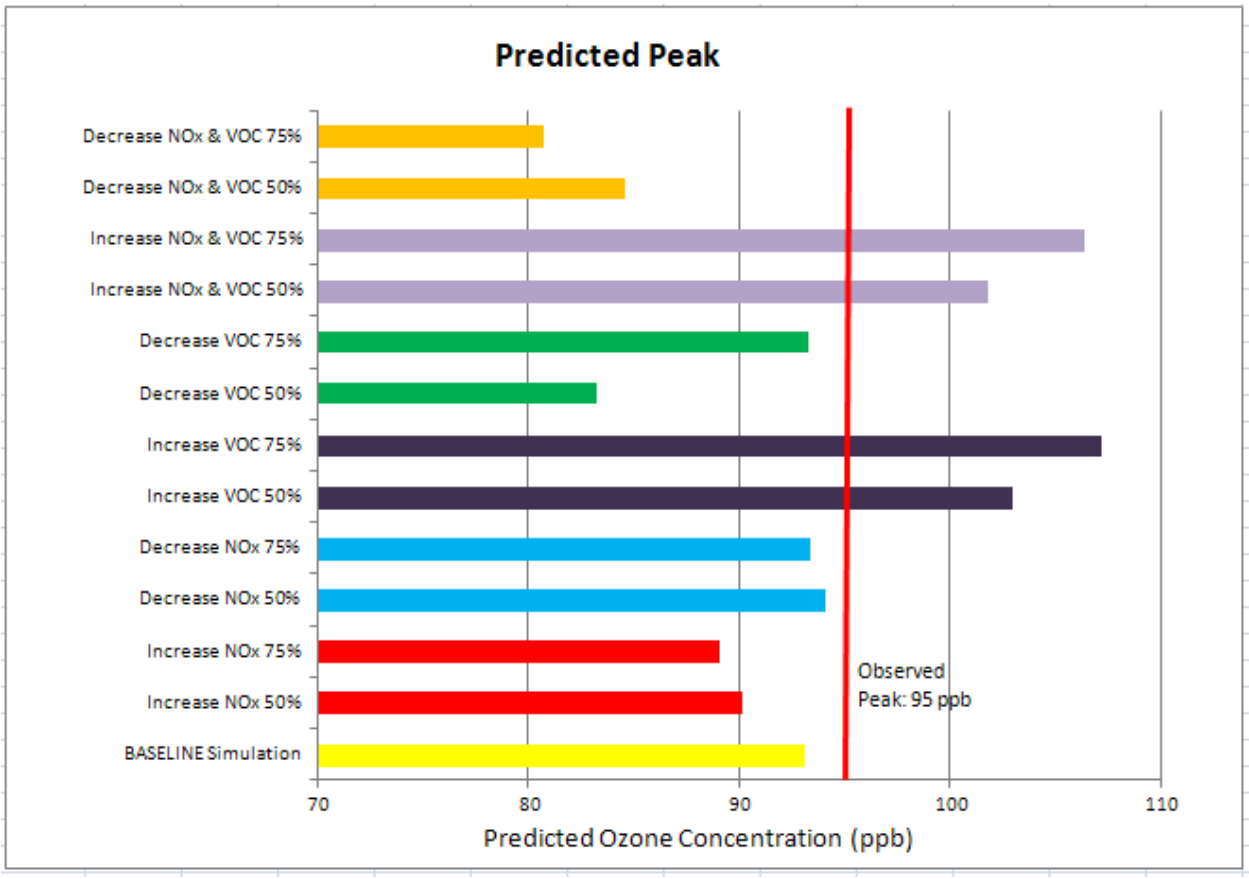

Figure 5.19 PREDICTED PEAK for CAMx simulations and 1-hour ozone

5.3.2.5 Performance Evaluation for Individual Simulation

Model performance was evaluated for 1-hour and 8-hour ozone concentrations only at the regional CAMS which were included in the modeling simulation. This section addresses the diurnal formation and destruction of ozone on 6/18 which is the day of the ozone exceedance.

Each RUN including the BASELINE provides model performance data and the model's ability to predict ozone within acceptable parameters. The BASELINE model performance was discussed in Appendix A and presented in Figures 5.7 and 5.8 in this chapter. Model performance statistics for all RUNs are compared to the BASELINE. As indicated in the previous section the model should obtain NE $\leq$35% and NB $\pm$15%. Table 5.4 and Table 5.5 show that the performance of each run is reasonably acceptable. Varying NOx and VOC either improved or

diminished model performance, but NE and NB were within acceptable modeling performance parameters on all simulations.

Figure 5.20 presents the model performance statistics for selected runs. Complete statistics for all runs are included in Appendix C. The bar graphs in the first panel of Figure 5.20 indicate the PEAK OBSERVED (in green) and PAIRED PREDICTED (in red) ozone concentrations. The maximum observed 8-hour ozone concentrations are plotted along with co-located daily maximum 8-hour ozone among all sites. The following statistics are measures of model performance (ENVIRON, 2011):

- Average paired peak accuracy (APPA).
- Normalized Error (NE)
- Normalized Bias (NB)

APPA compares the PEAK OBSERVED 1-hour or 8-hour ozone concentration from each regional CAMS included in the simulation with the co-located PEAK PREDICTED value. The following formula is applied to calculate APPA:

$$APPA = \frac{Cp\ \ x,t\ - Co(x,t)}{Co(x,t)}\ 100\% \qquad \text{Equation 5.3}$$

APPA quantifies the difference between the magnitude of the peak 1-hour or 8-hour ozone concentrations observed at a monitoring station (C_o) and the PEAK PREDICTED ozone concentrations $C_{p,}$ at the same space and time (x,t). Model estimates and observations are thus "paired in space and time." The paired peak estimation accuracy is a stringent model evaluation measure. It quantifies the model's ability to reproduce, at the same time and location, the highest observed ozone concentrations during the simulation. APPA does not have specifications regarding acceptable limits. NE reflects the scatter of the entire dataset generated by CAMx during the simulation for all sites and observations. The goal is to minimize NE to $\leq$35%. NB represents the ability of the model to over-predict or under-predict ozone concentrations.

Figure 5.20a depicts daily BASELINE model statistics, the highest 8-hour ozone PEAK OBSERVED among all sites in the PdN region, and the co-located daily PAIRED PREDICTED PEAK. As stated by Environ in Section 5.2, the baseline model under-predicts 1-hour ozone on 9 of 10 simulation-days. Model performance was good on 6/18, the ozone exceedance day. The positive APPA on 6/14 indicates several other CAMS over-predicted maximum 1-hour ozone. The very low APPA (-29.8%) on 6/16 is validated by the very low NB and NE (-31.2% & -31.5% respectively) indicating a very strong under-prediction. On 6/18 the model performed very well regarding NB & NE notwithstanding under-prediction of the maximum peak. The APPA on 6/18

was very good at -1.5% indicating minimal under-prediction of ozone concentrations. Similar statistics were observed for all runs and the results are described in Appendix C. Figure 5.20b presents the performance statistics for RUN4. RUN4 examines the impact on regional ozone resulting from a systematic increase of 50% VOC emissions in the Cd. Juárez area. The model under-predicts 1-hour ozone on 9 of 10 days. On 6/18 the model moderately over-predicts OBSERVED ozone as indicated by NB (1.2%). The simulation failed NB on 4 of 10 days where NB was <-15%. The PREDICTED PEAK on 6/18 for 1-hour ozone was 113.9 ppb indicating good model response to increased VOC emissions. The PAIRED PREDICTED PEAK which occurred at C663 was 107.8 ppb. An increase of 50% in area source VOC emissions increased the PREDICTED PEAK 1-hour ozone ~114 ppb or ~10.6%. The increase in 10 ppb greater than BASELINE continues to be less than 10 ppb below the PEAK OBSERVED. PTB improves (3 hours) compared to the BASELINE (4 hours). NE is reduced by 1.5 percentage points. Overall the model performance improves slightly from the BASELINE case with no significance.

Diurnal PREDICTED and OBSERVED 1-hour ozone and H_2O_2/HNO_3 ratios were evaluated. Figure 5.21 presents diurnal the results for all modeling runs. Figure 5.22 presents the same ratios for the 8-hour values. Similar plots for the BASELINE run are presented in Figures5.7 and 5.8, respectively. The H_2O_2/HNO_3 ratio is presented as dashed lines and provides a general reference. A red line is set at 75ppb indicating the 8-hour ozone NAAQS.

In general, the diurnal H_2O_2/HNO_3 ratio indicates NOx-limiting conditions exist during the early morning hours. As photochemistry increases and HNO_3 production accelerates a VOC-limiting condition develops for the duration of the elevated ozone event on 6/18. The shift from NOx-limited to VOC-limited conditions occurs at 0900hrs however given the PTB of ~4 hours it is possible the VOC-limited condition developed 4-hours earlier.

In summary, CAMx simulations were performed for 12 modifications on the Cd. Juarez area VOC and NOx emissions. All the simulations functioned within acceptable limits for NE and NB on 6/18, the ozone event day in the PdN. Area sources in Cd. Juarez apparently make small contribution to the ozone levels in the PdN.

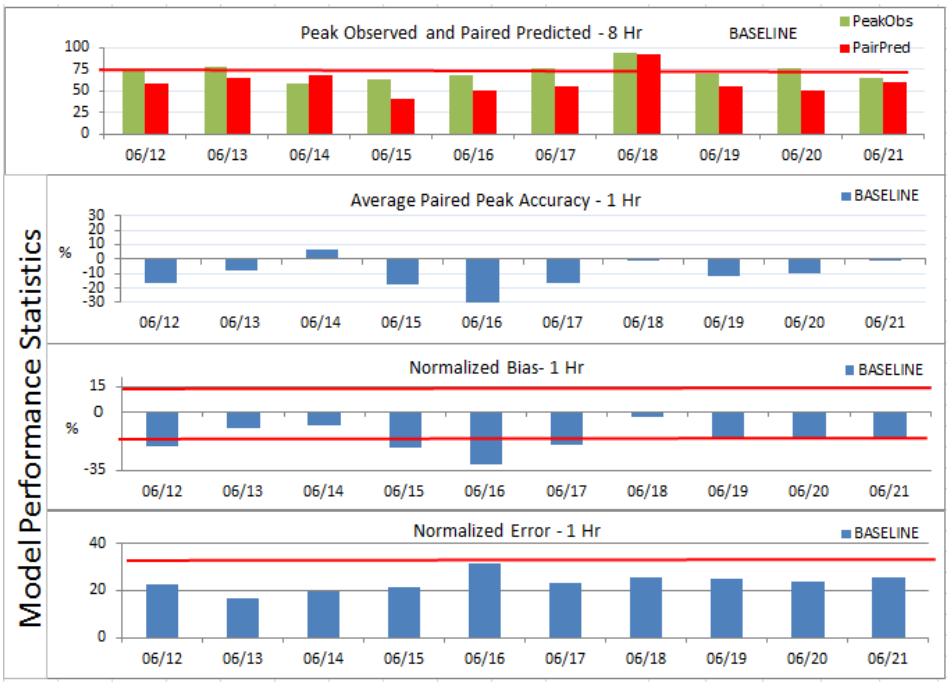

a) Base Case

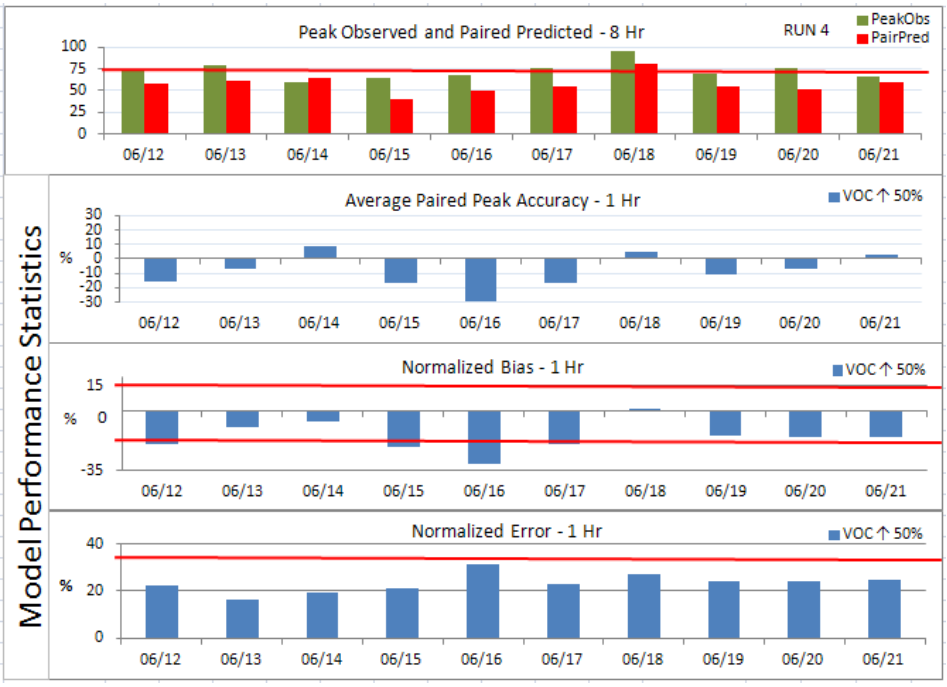

b) Run 4

Figure 5.20 Model performance statistics for selected runs

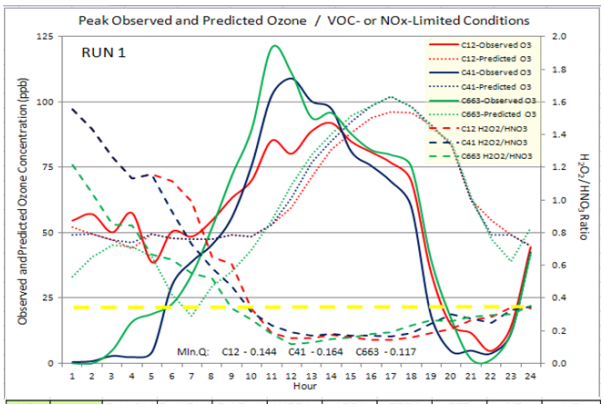

NOx	↑ 50%	PeakObs	PeakPred	PairPred	UPPA	APPA	EPPA	PTB	NB	NE
VOC	---	120.7	102.1	96.9	-15.4	-2.6	12.6	4	-5.2	26.2
BASECASE			103.3	99.3	-14.4	-1.5	12.2	4	-3.3	25.6

RUN 1

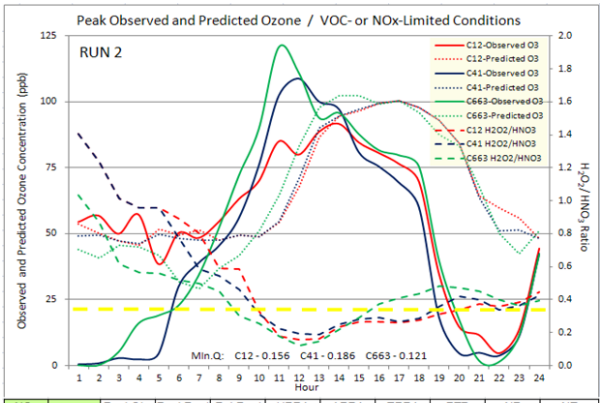

NOx	↓ 50%	PeakObs	PeakPred	PairPred	UPPA	APPA	EPPA	PTB	NB	NE
VOC	---	120.7	102.4	98.4	-15.1	-2.1	11.9	3	-2.1	24.2
BASECASE			103.3	99.3	-14.4	-1.5	12.2	4	-3.3	25.6

Run 2

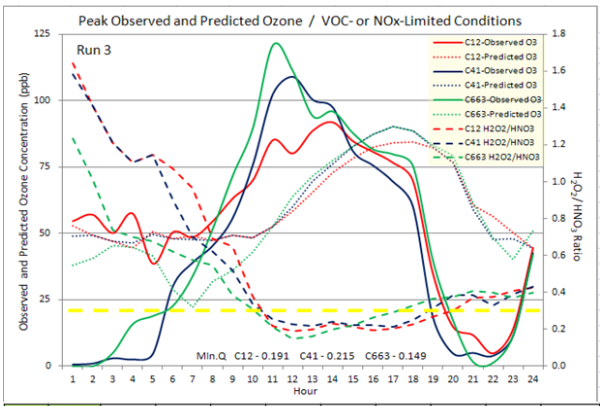

NOx	---	PeakObs	PeakPred	PairPred	UPPA	APPA	EPPA	PTB	NB	NE
VOC	↓ 50%	120.7	91.7	86.7	-24	-10	15.3	4	-8.7	24.2
BASECASE			103.3	99.3	-14.4	-1.5	12.2	4	-3.3	25.6

RUN 3

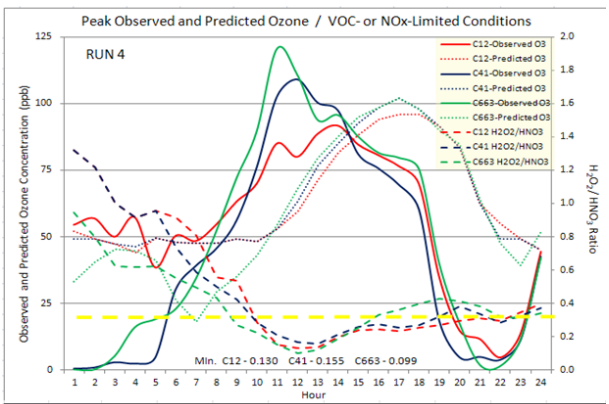

NOx	---	PeakObs	PeakPred	PairPred	UPPA	APPA	EPPA	PTB	NB	NE
VOC	↑ 50%	120.7	113.93	107.8	-5.6	4.8	13.1	3	1.2	27.1
BASECASE			103.3	99.3	-14.4	-1.5	12.2	4	-3.3	25.6

Run 4

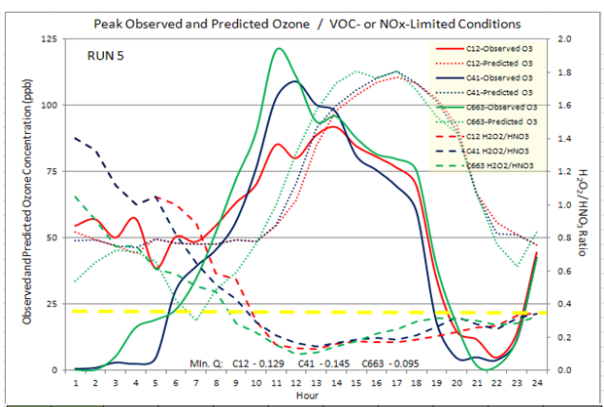

NOx	↑ 50%	PeakObs	PeakPred	PairPred	UPPA	APPA	EPPA	PTB	NB	NE
VOC	↑ 50%	120.7	113.0	108.7	-6.4	5.2	13.2	4	0.1	28.1
BASECASE			103.3	99.3	-14.4	-1.5	12.2	4	-3.3	25.6

RUN 5

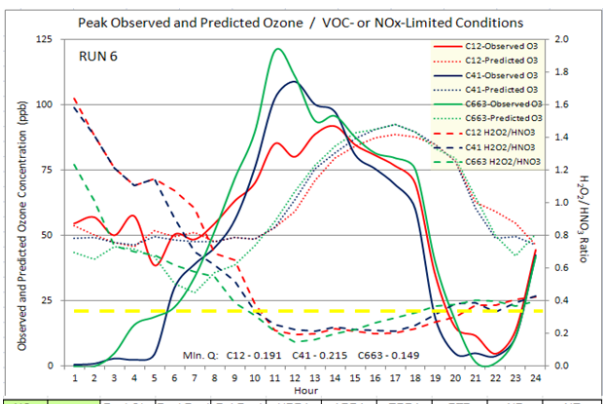

NOx	↓ 50%	PeakObs	PeakPred	PairPred	UPPA	APPA	EPPA	PTB	NB	NE
VOC	↓ 50%	120.7	92.7	89.1	-23.2	-8.7	14.4	4	-6.7	23.2
BASECASE			103.3	99.3	-14.4	-1.5	12.2	4	-3.3	25.6

Run 6

Figure 5.21 Diurnal predicted and observed 1-hour ozone (ppb) / H_2O_2/HNO_3 ratios

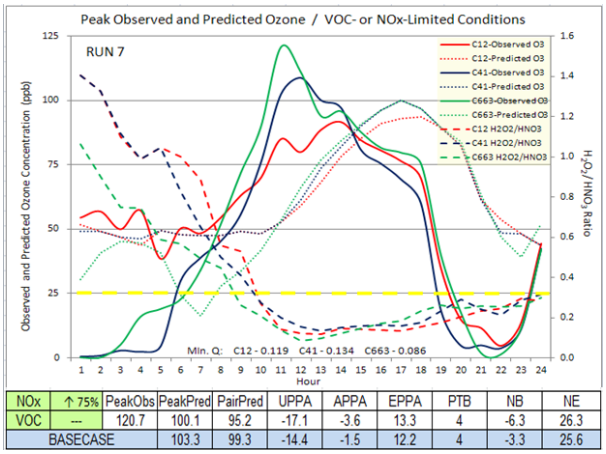

NOx	↑ 75%	PeakObs	PeakPred	PairPred	UPPA	APPA	EPPA	PTB	NB	NE
VOC	---	120.7	100.1	95.2	-17.1	-3.6	13.3	4	-6.3	26.3
BASECASE			103.3	99.3	-14.4	-1.5	12.2	4	-3.3	25.6

RUN 7

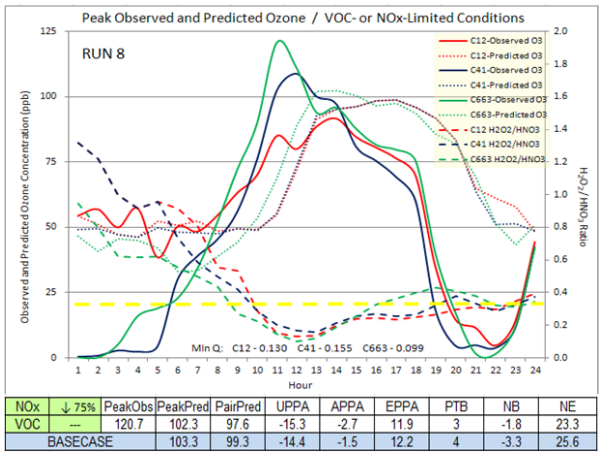

NOx	↓ 75%	PeakObs	PeakPred	PairPred	UPPA	APPA	EPPA	PTB	NB	NE
VOC	---	120.7	102.3	97.6	-15.3	-2.7	11.9	3	-1.8	23.3
BASECASE			103.3	99.3	-14.4	-1.5	12.2	4	-3.3	25.6

Run 8

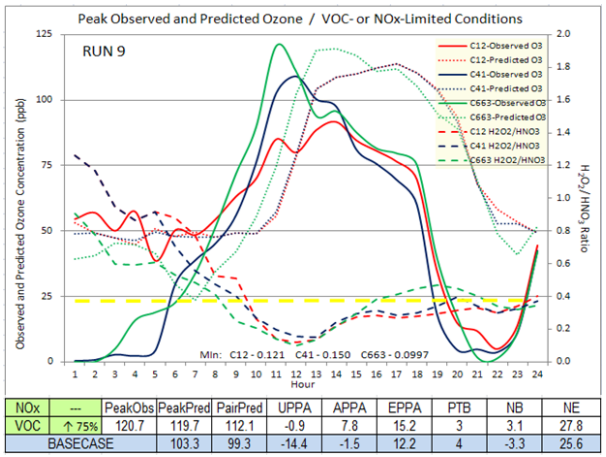

NOx	---	PeakObs	PeakPred	PairPred	UPPA	APPA	EPPA	PTB	NB	NE
VOC	↑ 75%	120.7	119.7	112.1	-0.9	7.8	15.2	3	3.1	27.8
BASECASE			103.3	99.3	-14.4	-1.5	12.2	4	-3.3	25.6

RUN 9

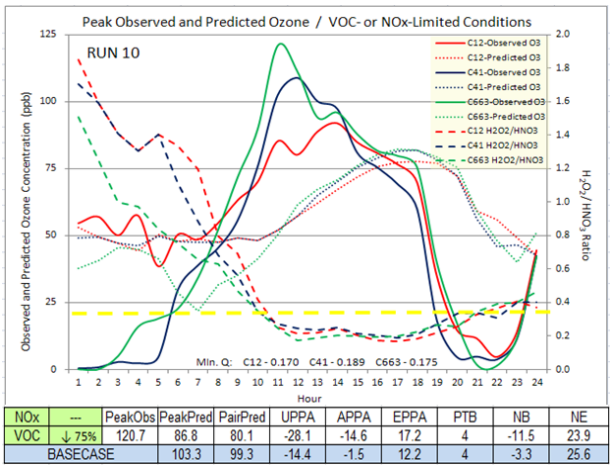

NOx	---	PeakObs	PeakPred	PairPred	UPPA	APPA	EPPA	PTB	NB	NE
VOC	↓ 75%	120.7	86.8	80.1	-28.1	-14.6	17.2	4	-11.5	23.9
BASECASE			103.3	99.3	-14.4	-1.5	12.2	4	-3.3	25.6

Run 10

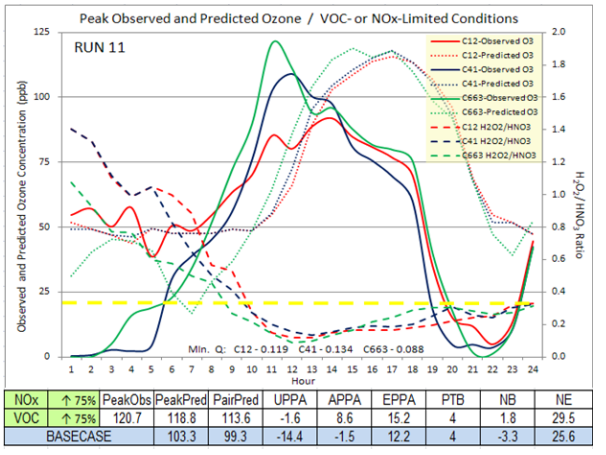

NOx	↑ 75%	PeakObs	PeakPred	PairPred	UPPA	APPA	EPPA	PTB	NB	NE
VOC	↑ 75%	120.7	118.8	113.6	-1.6	8.6	15.2	4	1.8	29.5
BASECASE			103.3	99.3	-14.4	-1.5	12.2	4	-3.3	25.6

RUN 11

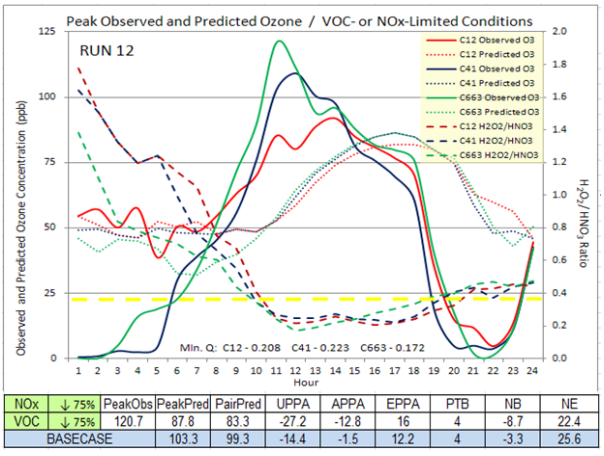

NOx	↓ 75%	PeakObs	PeakPred	PairPred	UPPA	APPA	EPPA	PTB	NB	NE
VOC	↓ 75%	120.7	87.8	83.3	-27.2	-12.8	16	4	-8.7	22.4
BASECASE			103.3	99.3	-14.4	-1.5	12.2	4	-3.3	25.6

Run 12

Figure 5.21 Diurnal predicted and observed 1-hour ozone (ppb) / H_2O_2/HNO_3 ratios (Continued)

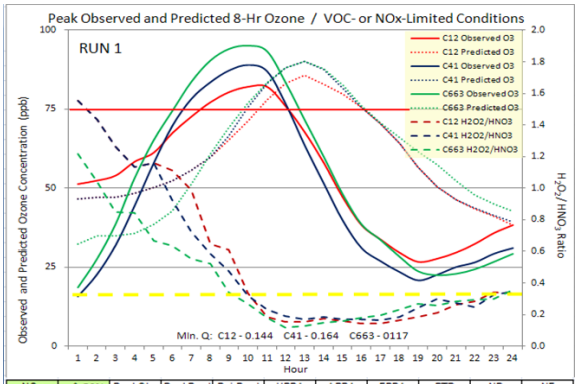

NOx	↑ 50%	PeakObs	PeakPred	PairPred	UPPA	APPA	EPPA	PTB	NB	NE
VOC	--	95.1	90.11	83.6	-11.1	-3.9	8.3	3	0.4	22.1
BASELINE			93	92.1	-2.1	2.5	9	3	3.9	23.7

RUN 1

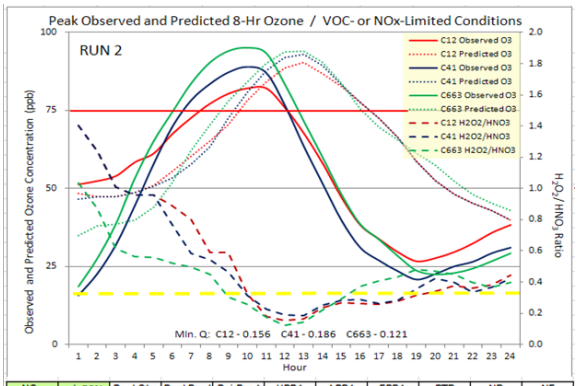

NOx	↓ 50%	PeakObs	PeakPred	PairPred	UPPA	APPA	EPPA	PTB	NB	NE
VOC	--	95.1	94.05	92.6	-1	3	9.5	3	5.4	22.4
BASELINE			93	92.1	-2.1	2.5	9	3	3.9	23.7

Run 8

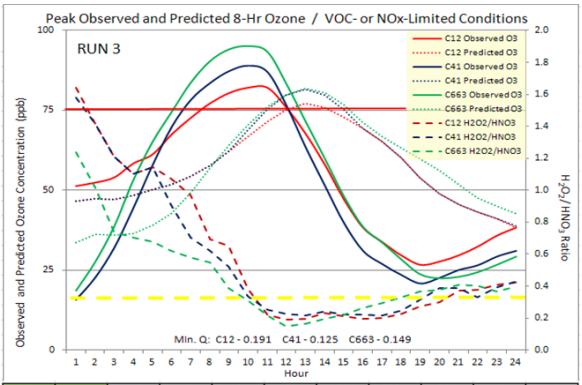

NOx	--	PeakObs	PeakPred	PairPred	UPPA	APPA	EPPA	PTB	NB	NE
VOC	↓ 50%	95.1	83.22	80.3	-12.4	-5.9	8.9	3	-1.8	23
BASELINE			93	92.1	-2.1	2.5	9	3	3.9	23.7

RUN 3

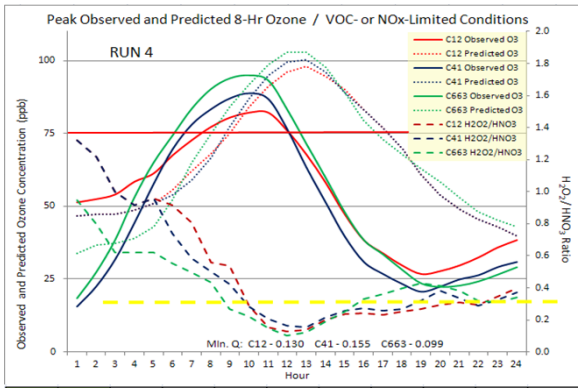

NOx	--	PeakObs	PeakPred	PairPred	UPPA	APPA	EPPA	PTB	NB	NE
VOC	↑ 50%	95.1	102.85	100.5	8.3	9	14.3	3	8.8	24.4
BASELINE			93	92.1	-2.1	2.5	9	3	3.9	23.7

Run 4

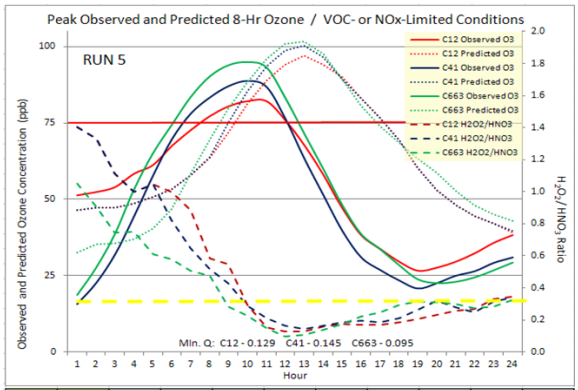

NOx	↑ 50%	PeakObs	PeakPred	PairPred	UPPA	APPA	EPPA	PTB	NB	NE
VOC	↑ 50%	95.1	101.76	100	7.1	8.5	13.7	3	7.4	25.4
BASELINE			93	92.1	-2.1	2.5	9	3	3.9	23.7

RUN 5

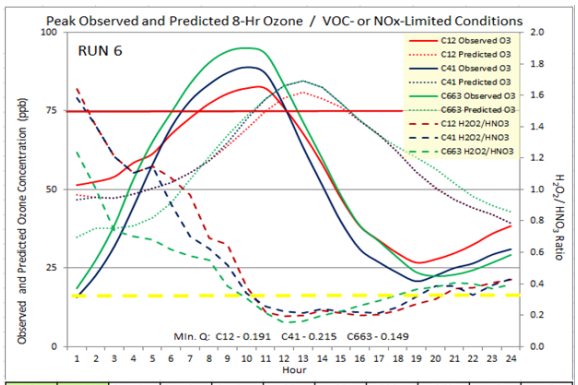

NOx	↓ 50%	PeakObs	PeakPred	PairPred	UPPA	APPA	EPPA	PTB	NB	NE
VOC	↓ 50%	95	84.49	83.6	-11.1	-3.9	8.3	3	0.4	22.1
BASELINE			93	92.1	-2.1	2.5	9	3	3.9	23.7

Run 6

Figure 5.22 Diurnal predicted and observed 8-hour ozone (ppb) / H_2O_2/HNO_3 ratios

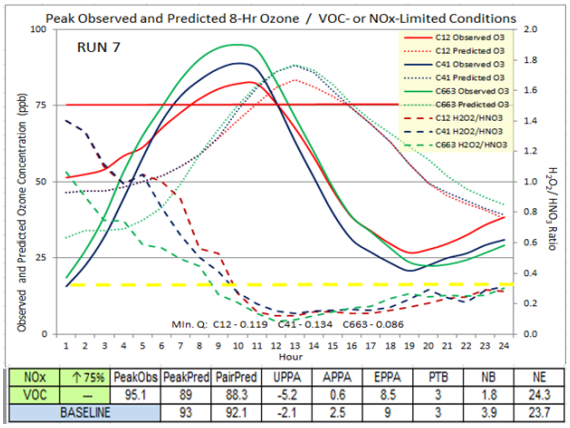

NOx	↑75%	PeakObs	PeakPred	PairPred	UPPA	APPA	EPPA	PTB	NB	NE
VOC	--	95.1	89	88.3	-5.2	0.6	8.5	3	1.8	24.3
BASELINE			93	92.1	-2.1	2.5	9	3	3.9	23.7

RUN 7

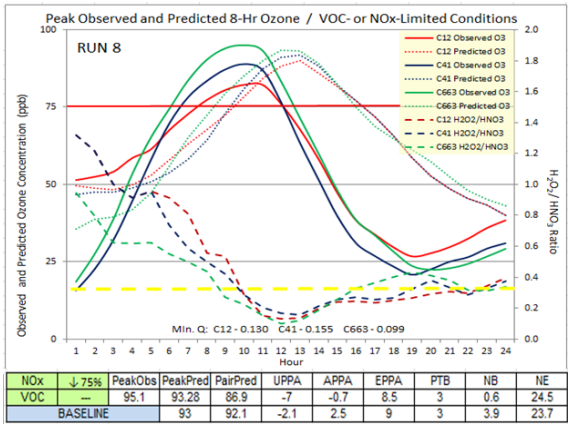

NOx	↓75%	PeakObs	PeakPred	PairPred	UPPA	APPA	EPPA	PTB	NB	NE
VOC	--	95.1	93.28	86.9	-7	-0.7	8.5	3	0.6	24.5
BASELINE			93	92.1	-2.1	2.5	9	3	3.9	23.7

Run 8

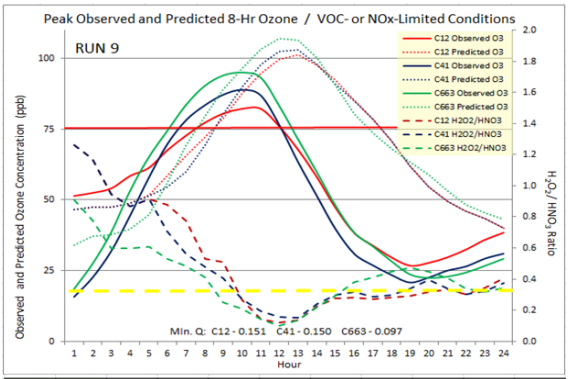

NOx	--	PeakObs	PeakPred	PairPred	UPPA	APPA	EPPA	PTB	NB	NE
VOC	↑75%	95.1	107.08	103.7	12.7	11.6	16.6	3	10.8	24.8
BASELINE			93	92.1	-2.1	2.5	9	3	3.9	23.7

RUN 9

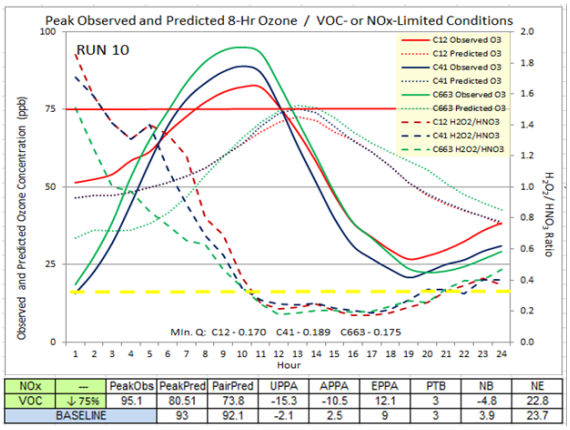

NOx	--	PeakObs	PeakPred	PairPred	UPPA	APPA	EPPA	PTB	NB	NE
VOC	↓75%	95.1	80.51	73.8	-15.3	-10.5	12.1	3	-4.8	22.8
BASELINE			93	92.1	-2.1	2.5	9	3	3.9	23.7

Run 10

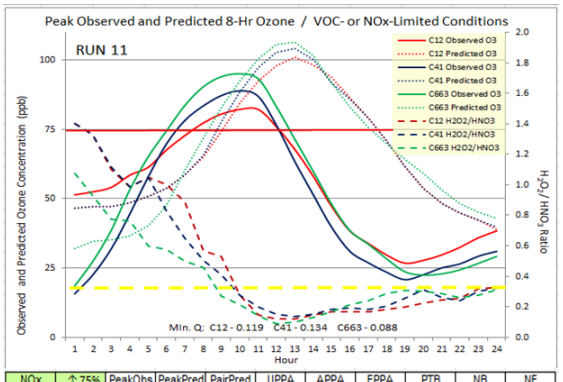

NOx	↑75%	PeakObs	PeakPred	PairPred	UPPA	APPA	EPPA	PTB	NB	NE
VOC	↑75%	95.1	106.31	104.1	11.9	11.7	16.4	3	9.2	26.5
BASELINE			93	92.1	-2.1	2.5	9	3	3.9	23.7

RUN 11

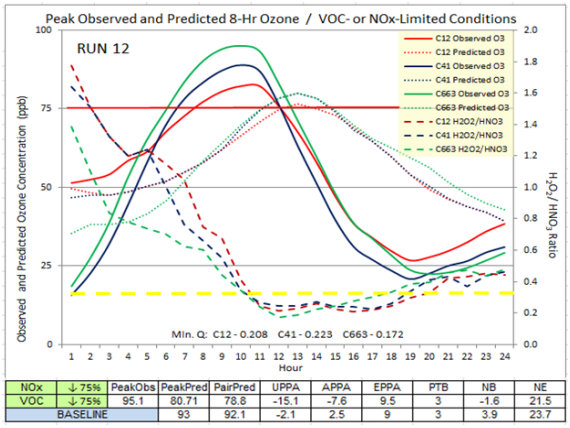

NOx	↓75%	PeakObs	PeakPred	PairPred	UPPA	APPA	EPPA	PTB	NB	NE
VOC	↓75%	95.1	80.71	78.8	-15.1	-7.6	9.5	3	-1.6	21.5
BASELINE			93	92.1	-2.1	2.5	9	3	3.9	23.7

Run 12

Figure 5.22 Diurnal predicted and observed 8-hour ozone (ppb) / H_2O_2/HNO_3 ratios (Continued)

Chapter 6 Discussion

The complexity in meteorology, topography, and emissions inventory for the PdN region makes numerical simulation of air pollution challenging, notwithstanding the uncertainties involved in the already complicate and convolutional photochemical air quality models. This chapter discusses the uncertainties that might have been introduced into the final ozone predictions and how they could or should have been reduced to improve the quality of the ozone predictions.

6.1 Meteorology Modeling

Meteorology is pivotal to the success of photochemical air quality modeling. The existing meteorological files available for the Rider 8 program were developed for a nested 36- and 12-km domains centered at Dallas, Texas, where the western boundary of the 12-km domain is immediately adjacent to the 4-km El Paso domain. Although the 4-km domain is centered at El Paso, the initial and boundary conditions filtering from the larger domains into the 4-km domain might have been heavily influenced by the mesoscale meteorology of east Texas and, to certain extent, east continent of the U.S. The effect may be subtle to notice in the WRF outputs, but could be pronounced in the CAMx model and generate systematically biased ozone predictions in the 4-km domain. This may help explain why the CAMx model with TCEQ's 4-km meteorology was unable to capture any high ozone day in Cd. Juarez (right panels in Figure 5.8) and missed high ozone levels observed along the U.S.-Mexico border and downtown areas of both El Paso and Cd. Juarez.

While using El Paso centered domains makes sense for both meteorology and air quality modeling, initial and boundary conditions for the concentric domains were not quite accessible for this study. Much of the concentric domains information was obtained from the NCEP Final Analysis (FNL) dataset with a 6-h interval. FNL is a global dataset in the format of the grid with the resolution of 1×1°. This set of nested grid system is different from the one prescribed by TCEQ for the Rider 8 program application. The resolutions for many input parameters such as vertical layers, landuse, and topography were not as fine as expected resulting in compromise of the resolutions at the local scales. For instance, inconsistency exists in the domain size and vertical layers for the UTEP WRF, TCEQ WRF, and CAMx simulations.

6.1.1 Structure of the vertical layers

The inconsistency in the vertical layers between TCEQ WRF and UTEP WRF is seen in the 2nd and 3rd columns of Table 6.1. The UTEP WRF vertical layer thickness is much larger beginning at layer 3 and increases substantially as altitude above ground increases. Contrarily, the TCEQ WRF vertical layer thickness is fairly consistent from layer 3 up to layer 10 and between layers

11 and 14. It may be beneficial to develop a new WRF vertical layer structure for the PdN region that is consistent with the TCEQ WRF vertical structures. This inconsistency in the selection of vertical layers made it extremely difficult to map the UTEP WRF outputs directly onto the TCEQ layer structure. As a result, two different sets of vertical layers were used in the CAMx simulations. Effects due to the use of different domains in the WRF weather simulation on the spatial and temporal distributions of ozone prediction in the Paso del Norte region remain unresolved. In addition, the use of El Paso-centered domains in the WRF simulations creates unexpected complications in processing the emissions inventories data available from TCEQ. Further evaluation may be needed.

6.1.2 4-km domain

Figure 6.1 illustrates the 4 km domain established for the PdN in Runs 2 and 3. Care should be taken to not confuse the dashed grid lines on Figure 6.1 with the bold oblique rectangle which represents the 4 km domain. The dashed grid lines are artifacts obtained from the TCEQ website where the image was obtained. The PdN domain encompasses El Paso and Hudspeth Counties in Texas, Doña Ana and Otero Counties in New Mexico, and the Municipality of Juárez, Chihuahua, Mexico. The 4-km domain definition was recommended by the TCEQ. Dimension and extent of the 4 km domain was established to include all potential source areas in the PdN area that contribute emissions to the airshed.

The CAMx 4-km domain consists of a grid system with 1,102 cells and encompasses 4,408 km^2. Figure 6.2 presents the grid cell configuration for the 4-km domain over census tracts of the PdN community. Each grid cell is enumerated beginning with the bottom left grid cell which is identified as (1, 1). Numbering follows a Cartesian coordinate system for rows in the *u* (east-west) direction and columns in the *v* (north-south) direction. The purpose of presenting census tracts instead of a centerline street map is that CAMx applies surrogate data to allocate pollutants across a modeling domain. Each grid cell is allocated a percentage of total population within the MSA. For example, area sources such as residential fuel consumption are calculated according to population as are emissions from dry cleaners or gasoline stations. This method of applying population spatial surrogates simplifies allocating emissions across the modeling domain, yet it contributes to modeling error.

On the contrary, the 4-km domains initially used in the WRF and CAMx for Run 1 spanned a wider area of 150,544 km^2 with 9,409 (97 by 97) grid cells (Figure 3.2). The initial 36- and 12-km domains used in WRF and Run 1 were also larger than that used in Runs 2 and 3. The 36-km domain for Run 1 has 97x85 cells and the 12-km domain has 103x91 cells. Selections of these large domains increased the computational time and resulted in difficulties using the already available TCEQ emissions inventories for the Rider 8 program.

Table 6.1 TCEQ CAMx vertical layer structure

TCEQ WRF Layer	TCEQ Layer Top (m AGL)	UTEP Layer Top (m AGL)	TCEQ CAMx Layer		UTEP CAMx Layer	
			ID	Thickness (m)	ID	Thickness(m)
38	15179.1		28	3082.5		
37						
36	12096.6		27	2930		
35						
34		19052			22	
33		17960				
32	9166.6	17014	26	2205.7		
31		16152			21	
30		15386				3605
29	6960.9	14641	25	1125		
28		13918				
27	5835.9	13213	24	937.9	20	2841
26		12495				
25	4898	11781	23	791.6		
24		11072			19	
23	4106.4	10372	22	733		2121
22		9670			18	
21	3373.5	8959	21	347.2	17	
20	3026.3	8251	20	335.9	16	1432
19	2690.4	7539	19	324.3	15	
18	2366.1	6819	18	262.8	14	721
17	2103.3	6098	17	256.2	13	725
16	1847.2	5373	16	249.9	12	690
15	1597.3	4683	15	243.9	11	638
14	1353.4	4045	14	143.6	10	595
13	1209.8	3450	13	141.6	9	542
12	1068.2	2908	12	139.7	8	498
11	928.5	2410	11	137.8	7	450
10	790.6	1960	10	90.9	6	395
9	699.7	1565	9	90.1	5	349
8	609.7	1216	8	89.3	4	297
7	520.3	919	7	88.5	3	244
6	431.8	675	6	87.8	2	199
5	344	476	5	87.1	1	157
4	256.9	319	4	86.3		123
3	170.6	196	3	85.6		97
2	85	99	2	51		70
1	33.9	29	1	33.9		29

Figure 6.1 PdN 4-km CAMx domain

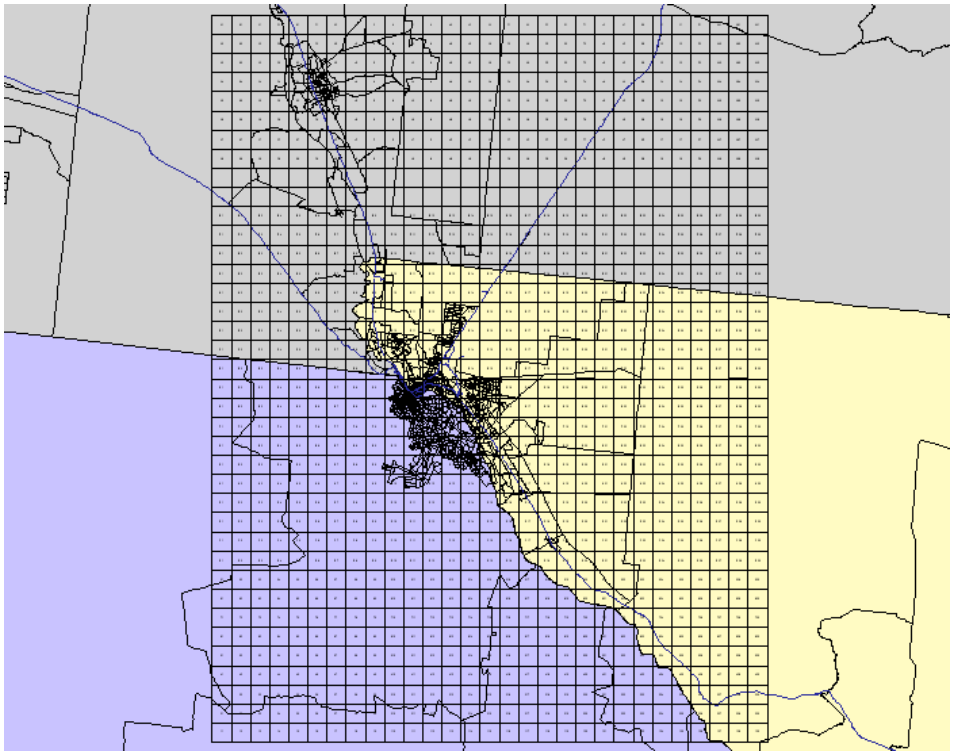

Figure 6.2 Grid cells of the 4-km CAMx domain

6.1.3 Atmospheric mixing height

The atmospheric mixing height is another parameter that could introduce significant errors in the predicted ozone values. The atmospheric mixing height defines the depth from the ground in the atmosphere in which rigorous mixing and transport of pollutants would take place. This information is transferred from the meteorological model simulation to the air quality model. This height is heavily dependent on the local meteorology and terrain topography. The topography in the PdN is considered extremely complex and could complicate the formation of the mixing height. In addition, it is known that a boundary layer parameterization scheme selected on the basis of best performance in the meteorological model may not be the ideal parameterization scheme for best performance in an air quality model. A smoothed mixing layer for WRF may help improve the ozone predictions in CAMx. It is also desirable to define a finer domain with 1-km grid resolution to capture the features of the terrain and other parameters in the WRF and CAMs simulations.

6.2 Emissions Inventory

An emissions inventory (EI) is a summary of air pollutants generated by multiple sources. As the term indicates, an inventory is an accounting of air pollution emissions from the four major source categories consisting of area, onroad mobile, nonroad mobile, and point. UTEP and MPO developed an emissions inventory implementation plan (EIIP) for the PdN (Li et al 2011b) and quantified the emissions of those recommended sources for improvement in the EI (Yang et al 2012). The documented EI for the PdN are summarized in Tables 6.2 through 6.5. Table 6.2 shows the EI used in the 1996 PdN ozone study whereas Tables 6.3, 6.4, and 6.5 list the reported EI in the PdN for El Paso, TX, Donna County, NM, and Cd. Juarez, Chihuahua, respectively. Overall, emissions of ozone precursors decreased in the PdN and area sources contribute about half of the total VOC emissions.

It should be noted that the EI used in the CAMx simulations are not necessarily based on the EI reported in the EIIP. The EI reported in the EIIP are taken from either the official EI used by TCEQ for air quality planning purposes or data available in the public domain. TCEQ provided the EI for the baseline CAMx modeling. The 36- and 12-km modeling inputs and raw inventory data files for the CAMx baseline runs (Run 2a and 2b) are provided on the TCEQ's Rider 8 modeling website (http://www.tceq.texas.gov/airquality/airmod/rider8). The Rider 8 emissions data files for 2006 and EPS3 ancillary files for all anthropogenic source categories were downloaded from TCEQ's FTP site (described in Appendix A). Mexico emissions inventories

were not available on the TCEQ's FTP site. They were obtained from the recent Western Regional Air Partnership (WRAP) modeling inventories compiled for the WestJump project. These emissions inventories for Mexico were interpolated to the year 2008 and used "as is" for this modeling without back casting them to 2006 (Appendix A). The discrepancy between that reported by the EIIP and used in the CAMx simulations could be substantial in certain source categories and jurisdictions.

Table 6.2 Emission estimates for the PdN in 1996 (Robert et al 1997)

Source Category	VOC tpy	NO_x tpy	CO tpy
El Paso County, TX			
Area Sources	14,965	12,045	50,005
Point Sources	6,935	29,930	15,330
Mobile Sources	9,855	14,235	101,835
Biogenic Sources	3,285	1,095	--
County Total	35,040	57,305	167,170
Hudspeth County, TX			
Area Sources	183	73	438
Point Sources	3,285	0	0
Mobile Sources	110	183	1,095
Biogenic Sources	5,110	1,825	--
County Total	5,402	2,081	548
Dona Ana County, NM			
Area Sources	5,110	3,650	13,870
Point Sources	0	1,825	183
Mobile Sources	5,110	2,555	53,290
Biogenic Sources	6,205	2,190	--
County Total	16,425	10,220	67,525
Otero County, NM			
Area Sources	3,285	1,460	10,585
Point Sources	292	37	3,650
Mobile Sources	2,190	2,555	21,900
Biogenic Sources	23,725	1,460	--
County Total	29,492	5,512	36,135
Ciudad Juarez, MX			
Area Sources	16,790	1,095	6,570
Point Sources	1,825	15,695	4,380
Mobile Sources	57,305	25,185	483,260
Biogenic Sources	12,045	4,380	--
County Total	87,965	46,355	494,210

Table 6.3 The 1996 and 2008 emissions inventories for Ciudad Juárez

	VOC (tpy)			**NOx** (tpy)		
Ciudad Juarez, MX	1996	2008	Change	1996	2008	Change
Area Sources	16,790	24,895	48%	1,095	1,080	-1%
Point Sources	1,825	--		15,695	--	
Mobile Sources*	57,305	8,151	-86%	25,185	12,564	-50%
Biogenic Sources	12,045	3,035	-75%	4,380	1,720	-61%
County Total	87,965	36,081	-59%	46,355	15,364	-67%

* Includes both on-road and non-road emission estimates

Table 6.4 Emission inventories for El Paso

	VOC (TPY)			NOx (TPY)		
El Paso	2002	2005	2008	2002	2005	2008
onroad	6,868	5,563	4,475	16,600	14,352	10,159
area	7,887	8,308	9,513	1,198	1,221	1,240
nonroad	1,712	1,547	1,377	2,897	2,875	2,382
point	780	961	1056	3695	3397	4687
Total	17,247	16,379	16,421	24,390	21,845	18,468

Table 6.5 Total emissions of CO, VOC, and NOx for Doña Ana, NM

Baseline Year	**CO** (tpy)	**NOx** (tpy)	**VOC** (tpy)
1996*	67,525	10,220	16,425
2002	65,238	10,991	8,507
2005	54,079	9,635	7,320
2008	49,188	8,501	7,359

* from (Haste et al, 1998)

Emission inventories tend to be inaccurate. Perhaps this is due to the degree of estimation and surrogacy applied to developing the EI. Area source EIs tend to have a high level of estimation due to the large number of emissions sources and the method of allocating emissions across the population or other methods of applying activity data. This matter must be taken into consideration when applying an estimated emissions inventory to a photochemical model.

6.2.1 Emissions Inventories for CAMx

TCEQ developed an ozone season EI from which the modeled EI is prepared. The term "typical ozone season day" refers to activities that occur during the three-month period at which the highest ozone exceedances occur, averaged on a daily basis. For example, if during the summer weekdays (Monday – Friday, June – August) of any particular year a manufacturing process produces 12,000 tons of material, and this period includes 13 weeks, 5 operating days per week, then the average or "typical" ozone season day activity would be: 12,000/(13 x 5) = 185 tons/day. This value would then be multiplied by the emission factor, control factor, and rule effectiveness factor, if applicable, to calculate the typical ozone season day emissions. The Texas Air Emissions Repository (TexAER) which contains emissions inventories for Texas provides a simple proportion applied by TCEQ for determining ozone season emissions. Ozone season emissions were 28.8% of annual emissions. Based on this ratio, the daily emissions are developed.

The model-ready emissions for a representative weekday, Friday, Saturday and Sunday, as developed by Environ in Appendix A, are summarized in Table 6.6. These emissions were the bases for the BASELINE and all sensitivity CAMx runs.

Table 6.6 Emissions summary (tons/day) for the 4 km grid

Source Category	Weekday	Friday	Saturday	Sunday
NOX (tpd)				
Area	24.3	24.3	22.4	21.1
Nonroad	33.5	33.5	21.4	19.7
Onroad	92.3	95.6	75.9	67.5
Point	43.7	42.6	41.9	42.3
Biogenic	2.8	2.0	2.2	2.6
VOC (tpd)				
Area	250.3	250.3	235.8	226.4
Nonroad	10.4	10.4	13.8	11.9
Onroad	50.6	52.5	43.9	41.2
Point	11.0	10.9	10.9	11.0
Biogenic	244.0	182.0	199.7	230.4
CO (tpd)				
Area	84.0	84.0	68.5	53.4
Nonroad	107.9	107.9	132.3	112.1
Onroad	445.0	465.0	382.8	350.1
Point	13.0	12.7	12.7	12.9
Biogenic	28.1	21.2	23.8	27.4

NOx and VOC are the two pollutants of primary interest for this study since they play a major role in the ozone chemistry. The breakdown of the daily averages of 542 TPD of VOC and 154 TPD of NOx emissions for the 4-km domain are shown in Figure 6.3. The green bar in both the VOC and NOx charts identifies the area source emissions for each pollutant. The area source VOC and NOx emissions from Cd. Juárez account to approximately ½ of the non-biogenic VOC emissions. They are selected for a series of simulations to assess the sensitivity of Juarez area emissions on the PdN ozone levels. The uncertainties and inaccuracies involved in the development of these Cd. Juárez area source NOx and VOC emissions, relative to the well regulated, documented El Paso and New Mexico area source emissions, are the basis for the sensitivity analysis. The results of the sensitivity analysis are further discussed in Section 6.2.3.

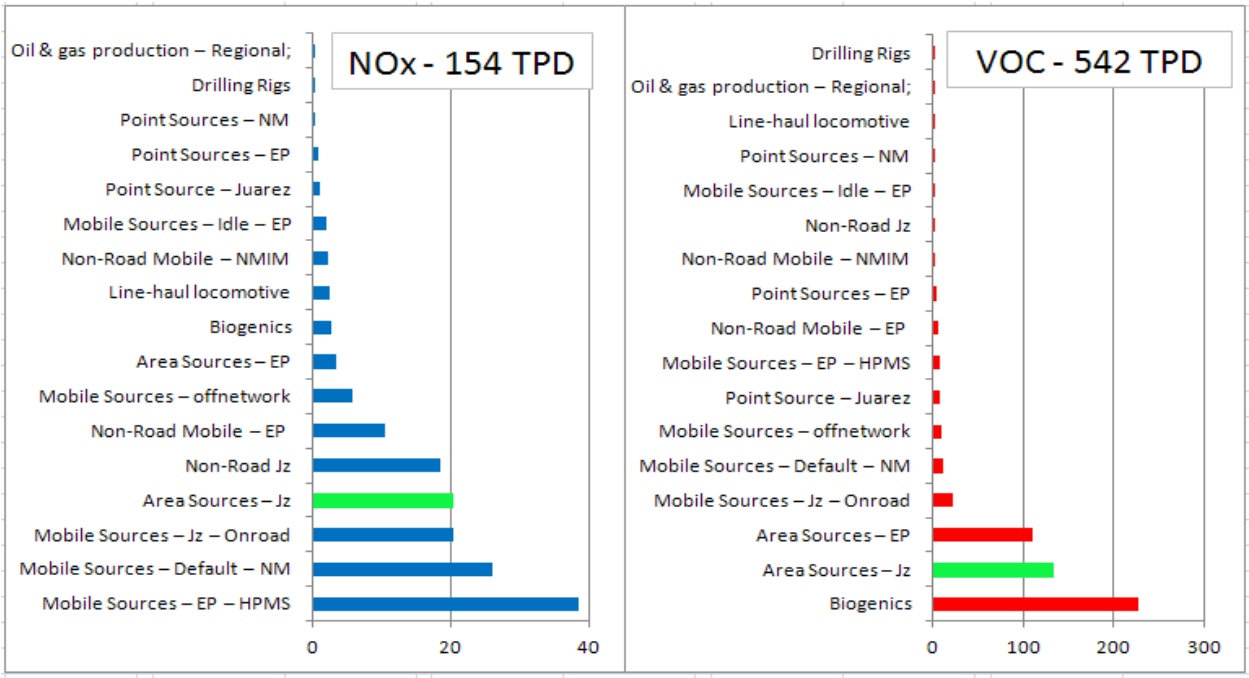

Figure 6.3 Total emissions processed by CAMx (in TPD)

Table 6.7 presents daily modeled VOC and NOx emissions obtained from the CAMx ARGV file for regional source categories for the BASELINE (Run 2a) simulation. Of note in the datasets are the low point source NOx emissions, as compared to the point source NOx emissions in Table 6.6. Only 1.9 TPD of NOx are indicated for the regional emissions compared to 43.7 TPD of NOx emissions for Weekdays in Table 6.6. This discrepancy is not explained, and it needs to be investigated.

Figure 6.4 identifies modeled VOC emissions by source category. The modeled VOC EI indicates area sources and biogenics emissions comprise 242.5 TPD (45%) and 227 TPD (42%) of total emissions respectively. Biogenic VOC contributions in the PdN region consist primarily of

monoterpenes which have low reactivity insofar as participation in tropospheric photochemical reactions is concerned. Figure 6.5 presents the daily modeled NOx emissions which are processed for use in the CAMx BASELINE simulation. Onroad and nonroad mobile sources emissions comprise 60% and 22% respectively of total NOx emissions.

Table 6.7 Daily modeled VOC and NOx emissions for regional source categories

Source Category	Weekday	Saturday	Sunday
NOx (TPD)			
Area	23.4	21.8	20.7
Nonroad	33.5	21.4	19.7
Onroad	92.3	75.9	67.5
Point	1.9	1.6	1.3
Biogenics	2.8	2.2	2.6
VOC (TPD)			
Area	242.5	230.2	223.2
Nonroad	10.4	13.8	11.9
Onroad	50.6	43.9	41.2
Point	11.8	9.6	7.2
Biogenics	226.9	199.7	230.4

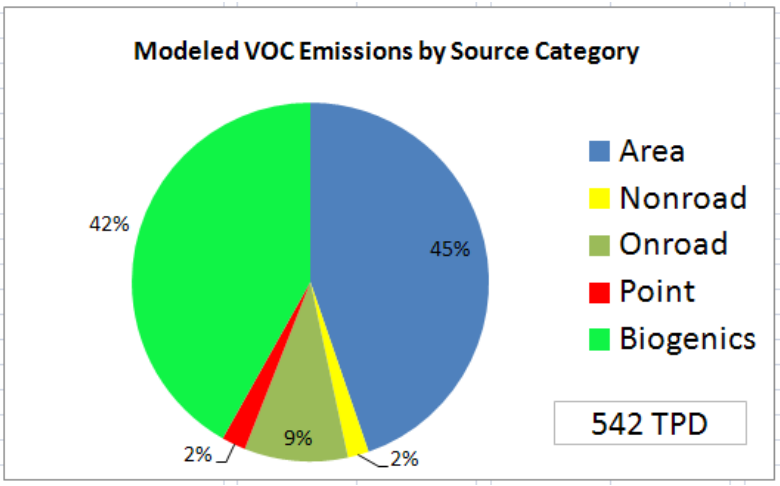

Figure 6.4 Modeled VOC emissions in TPD processed for CAMx

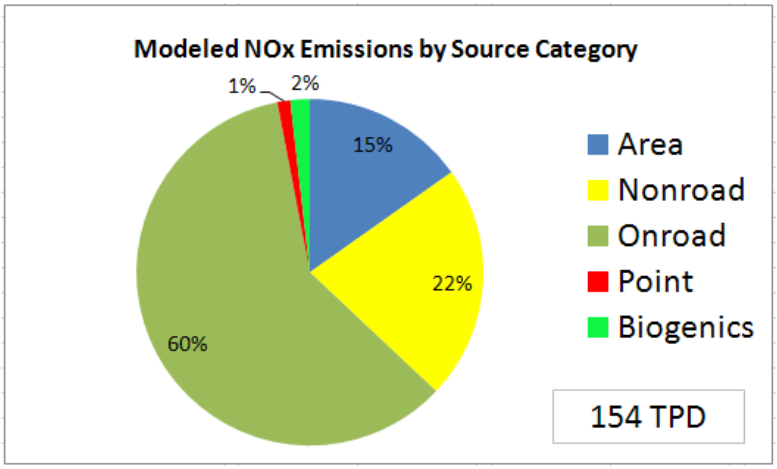

Figure 6.5 Modeled NOx emissions in TPD for CAMx BASELINE simulation

Table 6.8 identifies modeled VOC and NO emissions by source category and jurisdiction. Of note regarding inputs entering the CAMx simulations are the very low point source NOx emissions in both U.S. (indicated as EP in the table) and Mexico (indicated as Jz in the table). A total point source NOx emissions of 1.9 TPD for a community (El Paso and Cd. Juarez) of 2.6 million inhabitants is likely inaccurate. Given biogenic emissions are ubiquitous throughout the airshed, the total biogenics amount (226.9 TPD) was split between the 2 communities. Future modeling endeavors should consider establishing single regional emissions datasets for each source category.

Table 6.8 Modeled VOC and NOx emissions by source category and jurisdiction (TPD)

	EP NOx	EP VOC
Area	3.3514	110.049
Nonroad	12.9113	6.0629
Onroad	66.4417	18.6152
Point	0.964	3.9927
Biogenics	1.38245	113.4382
TOTALS	85.05085	252.158
	Jz NOx	Jz VOC
Area	20.0853	132.4435
Nonroad	18.5067	1.7355
Onroad	20.2795	22.2122
Point	0.8963	7.808
Biogenics	1.38245	113.4382
TOTALS	61.15025	277.6374

6.2.1.1 Emissions from El Paso and south-central New Mexico

The U.S. emissions listed in Table 6.8 include VOC and NOx emissions not only from El Paso but also from south-central New Mexico (SC-NM) which consists of Doña Ana and Otero Counties.

Figures 6.6 and 6.7 provide the U.S. VOC and NOx emissions, respectively, by source category. Given Doña Ana County (DAC) accounts for the majority of emissions due to both population and industrial activity, the SC-NM region is henceforth identified as DAC in the figures. Approximately 252 TPD of VOC are generated in the U.S. portion of the airshed, which is ~25 TPD fewer emissions than Cd. Juárez (the Mexican Portion of the airshed). Solvent utilization is the highest source of VOC emission from area sources. Mobile sources account for 9% of total emissions with modeled point source VOC emissions accounting for only 2% of total modeled VOC emissions.

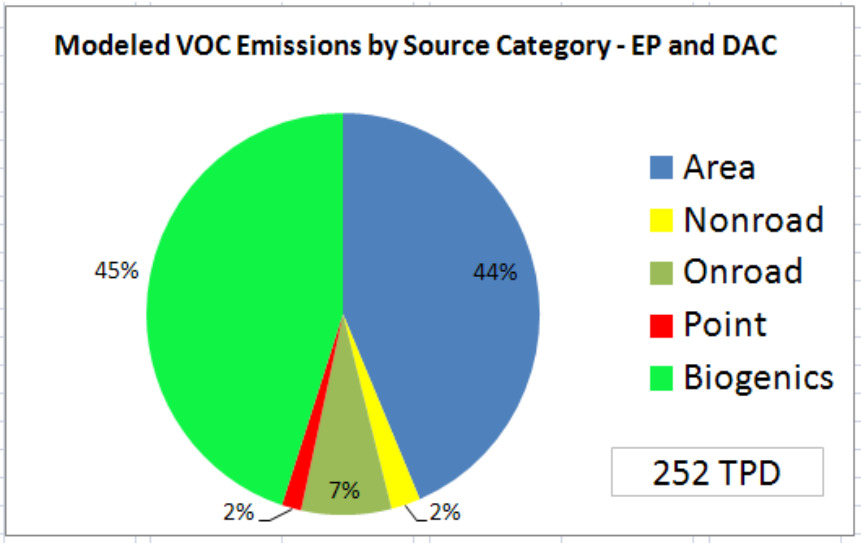

Figure 6.6 Modeled VOC emissions by source category – EP and DAC

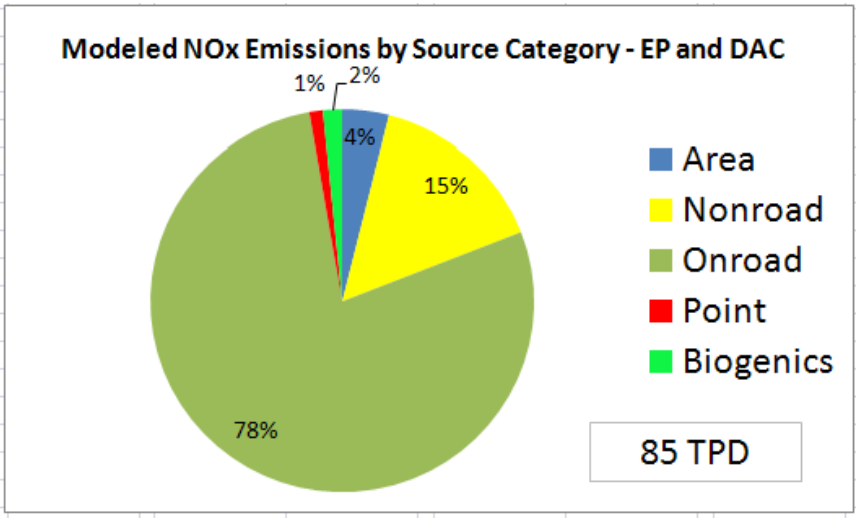

Figure 6.7 Modeled NOx emissions by source category - EP & DAC

6.2.1.2 Emissions from Cd. Juarez

Figure 6.8 identifies modeled VOC emissions by source category in Cd. Juárez. Area sources comprise 132 TPD (48%) of VOC emissions modeled by the CAMx simulation. Biogenic emissions comprise 113 TPD (41%) of VOC emissions generated in Cd. Juárez that are modeled by CAMx. Considering the very low reactivity of biogenic emissions, one may stipulate that if just the VOCs from anthropogenic sources were considered by the simulation then area sources comprise almost 90% of all VOC emissions generated in Cd. Juárez. Table 6.8 indicates 7.8 TPD of VOC point sources emitted from Cd. Juárez. Examination of the point source dataset which is processed by EPS3 indicated the PEMEX terminal in Cd. Juárez provided the bulk of these emissions.

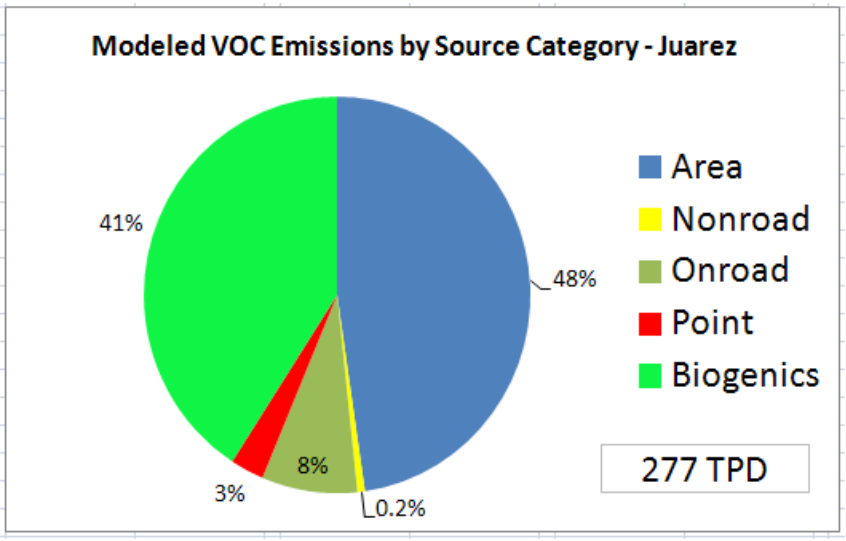

Figure 6.8 Modeled VOC emissions by source category for Cd. Juárez

Figure 6.9 presents the modeled NOx emissions for Cd. Juárez. Mobile sources constitute ~66% of NOx emission totaling 28 TPD for the BASELINE simulation. Biogenic NOx is generated by soil nitrification which occurs below the soil surface and is emitted into the atmosphere. The total emitted volume of this pollutant is minimal. It should be noted that the 2 Electric Generating stations in Juárez were listed as emitting minimal VOC's notwithstanding the electric generating facilities (EGF) are fired by #6 diesel fuel (bunker oil), have no emissions control equipment, and utilize no stacks.

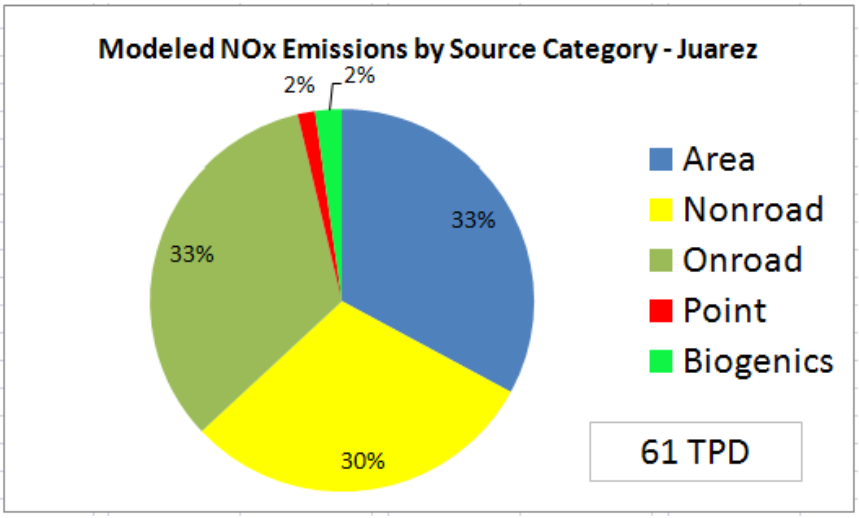

Figure 6.9 Modeled NOx emissions by source category for Cd. Juárez

Table 6.9 specifies the daily modeled NOx and VOC emissions in TPD for the BASELINE simulation. Of note are the modifications in daily emissions based on Weekday, Friday, Saturday, and Sunday simulation days. The ozone event occurred on Sunday, 18 June as indicated in Table 11.5.

Table 6.9 BASELINE daily modeled emissions in the PdN (TPD)

Date		NOX	VOC
12-Jun-06	Monday	153.9	559.4
13-Jun-06	Tuesday	153.9	558.3
14-Jun-06	Wednesday	154.0	553.5
15-Jun-06	Weekday	154.0	542.2
16-Jun-06	Friday	156.5	499.3
17-Jun-06	Saturday	123.0	497.2
18-Jun-06	Sunday	111.8	514.1
19-Jun-06	Monday	153.9	520.0
20-Jun-06	Tuesday	154.0	501.4
21-Jun-06	Wednesday	154.0	519.0

6.2.2 Cd. Juarez Area Emissions

Area sources are those air pollution sources considered too small and too numerous to be handled individually as point source emissions. Area sources are primarily subdivided into two groups characterized by the emission mechanism: 1) evaporative emissions, and 2) fuel combustion emissions. Sources of evaporative losses include gasoline service stations, solvent use, such as dry cleaning, degreasing, surface coating operations, automotive paint shops, architectural coatings, and leaking underground storage tanks. Fuel combustion sources include stationary source fuel combustion in residences, industrial processes, commercial operations, forest fires, structural fires, and solid waste disposal by burning.

Previous reports on Cd. Juárez area source emissions inventories indicate the EI for this city are inaccurate (Emery 2000) or emissions required substantial modification (Nagaraj 2002). Sullivan (2012) provided an EI with a 2008 base year. Many small industrial and traditional area source categories were not included in the 2008 Juarez area emissions inventory either because they were considered insignificant sources or because data collection was judged unfeasible (Li et al 2011b).

In 2002, total VOC emissions for Ciudad Juárez were reported at 14,500 TPY with most (87%) contributed to area sources as opposed to small-sources (13%). The total NO_x emissions were estimated at 1,428 TPY with only 1% contributed by small sources. The most dominant small source of VOC emissions was Water Treatment at an estimate of 1,353 TPY, whereas the most dominant area source was residential fuel combustion with an estimated value of 6,629 TPY. Consumer Solvents (4787 TPY) and Brick Kilns (372 TPY) also contributed a significant amount (36%) of VOC emissions. The most dominant area source category of NO_x emissions was also residential fuel combustion with an estimate of 973 TPY (Table 6-10).

Table **Error! No text of specified style in document.**.10 Emission estimates for the 2002 Ciudad Juárez

	Small Source			Area Source	
	NOx	VOC		NOx	VOC
Source Category	tpy	tpy	**Source Category**	tpy	tpy
Asphalt	9.5	4.9	Brick Kilns	28.5	371.5
Concrete			Open Burning	34.5	43.6
Foundries	0.2	0.1	Fertilizers		
Woodworking			Pesticides		3.4
Wastewater Treatment	0.4	1352.9	Agricultural Burning		14
Quarries			Agricultural Tilling		
Landfill			Feedlots and Dairies		
Autobody Refinishing		3.2	Livestock		
Drycleaners		33.4	Structural Fires	0.1	0.3
Bakeries		1.3	Wind Erosion		
Gas/Diesel Marketing		198.1	Fuel Combustion –		
LPG Marketing		237.5	Commercial and Institutional	252.8	7.9
Restaurants	0.4	0.5	Fuel Combustion –		
Street Vendors	0.3	1	Residential	973.1	6629.3
Ice Plants			Construction		
Graphic Arts		1.4	Consumer Solvents		4781.6
Grain Mills			Border Crossings	128.2	814.6
Sub-Total	11	1834	**Sub-Total**	1417	12666

The total VOC emissions reported for 2002 (area and small source categories) were 14% higher than the area source emissions reported for Ciudad Juárez in 1996. Conversely, the total NO_x emissions reported for 2002 (area and small source categories) were 30% lower than the area source emissions reported for Ciudad Juárez in 1996 (Haste et al 1998). These relative changes coincide with the suggested overestimation of NOx and/or underestimation of VOC emissions for Ciudad Juárez identified during the top-down evaluation of the 1996 emission inventory (Roberts et al 1997; Funk et al 2001).

The 2008 EI for Cd. Juárez was developed by Eastern Research Group (ERG). It was based on surrogate data which grows the 1999 national emissions inventory (NEI). ERG also prepared the 1999 NEI for EPA. Figure 6.10 illustrates the 2008 area source EI for Juárez. The 2008 EI reported an increase of 48% for VOC area source emissions and almost the same for NO_x from 2002 (Li et al 2011b). The most dominant VOC and NO_x area source categories were industrial residual fuel combustion (59%) and solvent use – degreasing (36%), respectively.

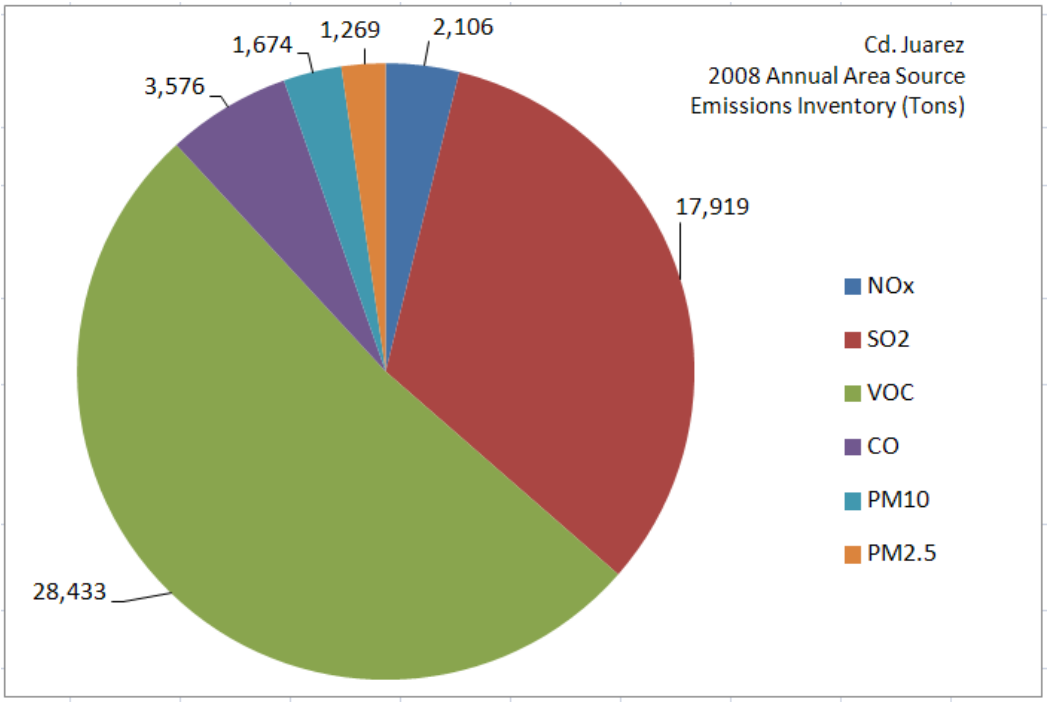

Figure 6.10 2008 Cd. Juárez annual area source emissions inventory (TPY)

In summary, area source emissions from Cd. Juarez have not been accurately reported. Fugitive emissions from the brick kilns scattering throughout the community continue to be poorly studied. VOC emissions from the gasoline fueling stations and automotive paint and body shops have been identified as two other major contributors to the PdN's ozone pollution. These unresolved area emissions in Cd. Juarez continue to limit the accuracy of any EIs. However, the area sources are likely to be well distributed in the city regardless the magnitudes of the emissions. It is thus decided to conduct a sensitivity study to understand the impacts of the inaccuracy in the area source emissions estimates on the PdN ozone.

6.2.3 Biogenic Emissions

The magnitude and spatial distribution of the biogenic emissions for the PdN are not well studied. VOC emissions from biogenic sources represent ~50% of the total VOC emissions in the CAMx simulations of 2006 ozone episode (Table 6.6), compared to ~29% in 1996 (Table 6.2). The total amount of biogenic emissions grew from ~138 TPD in 1996 to ~240 TPD in 2006. In the meantime, biogenic emissions decreased in Cd. Juarez from 12,045 TPY to 3035 TPY (Table 6.3). Approximately 47% of biogenic emissions were distributed to south central New Mexico in 1996. Although biogenic compounds in general have low reactivity in ozone chemistry, more accurate estimates for the biogenic emissions in the PdN are needed.

6.3 Sensitivity Analysis on the Cd. Juarez Area Emissions

The sensitivity analysis was performed based on the concerns of the significant amount of VOC emissions and the inaccuracies in the VOC and NOx emission estimates. Table 6.11 is a matrix of modifications applied to Cd. Juárez area source emissions data for the sensitivity analysis. The results of the 12 distinct simulations were compared to the BASELINE simulation in Section 5.3. From this perspective one may identify potential air quality control strategies (PAQCS) that could be recommended. For each RUN identified in Table 6.11, an arrow pointing up indicates emissions increase. An arrow pointing down indicates emissions decrease. The number which follows indicates if BASELINE emissions for the specific pollutant are modified by 50% or 75% in the specified direction.

Table 6.11 Matrix of area source emissions modifications for CAMx simulations

	1	2	3	4	5	6	7	8	9	10	11	12
NOx	↑ 50%	↓ 50%			↑ 50%	↓ 50%	↑ 75%	↓ 75%			↑ 75%	↓ 75%
VOC			↓ 50%	↑ 50%	↑ 50%	↓ 50%			↑ 75%	↓ 75%	↑ 75%	↓ 75%

Figure 6.12 provides a better resolution format for viewing the emissions simulated during each of the 12 sensitivity analysis RUNS. It shows that El Paso area source emissions remain unchanged while the Juárez area source emissions for the 2 pollutants increase or decrease based on the scenario specifications.

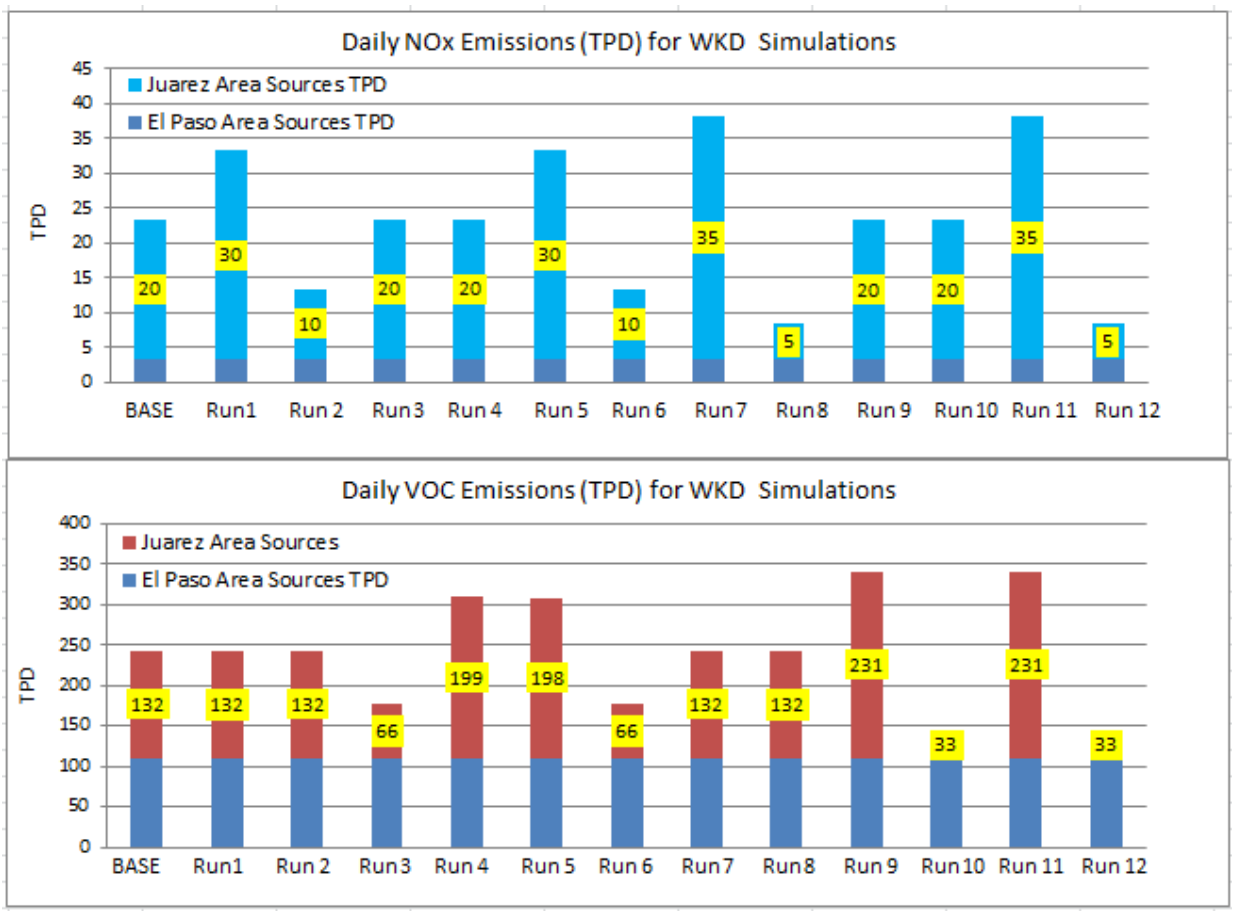

Figure 6.11 Total daily weekday NOx and VOC area emissions used in the sensitivity analysis

As stated in Section 5.3, all sensitivity runs functioned within acceptable limits for the model performance evaluation. None of the runs displayed significant improvement in the model performance over the BASELINE run. An increase of 75% area source VOC emissions with or without concurrent increase in NOx emissions will bring the predicted peak ozone to be the same as the observed peak (Run 7 Figure 5.17). Variation in 50 or 75% of NOx area emissions represent only a small fraction of NOx changes in the PdN (5% and 8%, respectively, from Table 6.6) which may not be sufficient to make visible changes in the ozone predictions. On the other hand, if one reduces the Juarez area source VOC emissions by 50% through some control strategies, one would be able to reduce the peak ozone by as much as 13%.

Chapter 7 Summary

This report documents the results obtained by the University of Texas at El Paso (UTEP) for the El Paso Metropolitan Planning Organization (MPO), under a grant provided by the Texas Commission on Environmental Quality (TCEQ) for the Rider 8 program, using WRF meteorological and CAMx photochemical air quality models. The primary objective for the study was to develop a photochemical modeling protocol appropriate for a Texas SIP revision for the Paso del Norte (PdN) region. The model performance was evaluated for the 2006 base case ozone episode between June 12 and June 21. During the course of the study, Environ International Corporation was contracted to perform a portion of the CAMx simulations.

Meteorology for the PdN region was first simulated using 3 nested domains centered at El Paso and with 36-, 12-, and 4-km resolution. The results were reviewed based on the model's phenomenological and operational performance in the studied domains. The simulation was judged acceptable and the results for the 4-km domain were used in the base case ozone study.

A series of CAMx simulations were conducted to investigate the model performance of the 2006 base case ozone episode and sensitivity to selected changes in precursor emissions. The impacts of potential local voluntary or mandatory control strategies on the PdN ozone levels were implicitly reviewed in the sensitivity analysis. CAMx simulation was first performed on the UTEP concentric domains. Unfortunately, the corresponding 2006 emissions inventory for the concentric domains were not available in time for CAMx modeling and the default NEI 1999 emissions inventory was used instead in the first CAMx simulation (Run 1). Performance of this run was judged unacceptable based on the performance evaluation conducted. Two additional runs for the base case episode were performed independently by Environ.

ENVIRON performed two CAMx base case simulations (Run 2a and Run 2b) employing alternative approaches in defining 4 km grid meteorology. Both simulations used identical 4 km El Paso/Juarez emission inputs. Run 1a used the TCEQ defined 36- and 12-km grids together with the 4-km grid in 2-way nested mode, where meteorology on the 4 km grid was internally interpolated by CAMx from the 12 km meteorology (called flexi-nesting). Run 2b was conducted for the single 4-km grid alone using UTEP 4-km meteorology. Boundary conditions for the 4-km grid were extracted from CAMx runs on the 36/12 km grid in a manner referred to as 1-way nesting. This was necessary to most appropriately accommodate the potentially different meteorology and different vertical grid structures between the 4 km (UTEP) and 12 km (TCEQ) meteorological data. Emissions data files for 2006 and EPS3 ancillary files for all anthropogenic source categories were downloaded from TCEQ's FTP site. The recent Western Regional Air Partnership (WRAP) modeling inventories of 2008 compiled for the WestJump project were used "as is" for 2006 in this study.

Both Run 2a and 2b satisfied the 35% error performance goal for ozone on all dates. The errors are similar in magnitude to bias indicating that underestimation trends are consistent in time and space. Both simulations tended to over-predict NOx on average but under-predicted events with very high NOx that occurred throughout the episode. Consequently, it is difficult to reach conclusions about the overall accuracy of the NOx emission inventory used for the CAMx modeling. Review of the spatial distributions of ozone and NOx reveals that ozone under prediction is related to the NOx over prediction. Potential causes include overestimated NOx emissions or under estimated dispersion of NOx emissions (e.g., because of under estimated vertical dilution). Under estimated VOC emissions also could be a contributing factor to under estimated peak ozone concentrations. Sensitivity tests with alternative meteorology or modified vertical diffusivity fields (Kv) should be conducted.

Run 2a was selected as the preferred 2006 base case simulation for sensitivity analysis. Twelve CAMx simulations (Runs 3.1 – 3.12) were performed to evaluate the impacts of varies Cd. Juarez area source emissions on the PdN ozone levels. The 12 runs were performed based on the concerns of the significant amount of VOC emissions and the inaccuracies in the VOC and NOx emission estimates in the reported Cs. Juarez area emissions. The matrix of modifications applied to Cd. Juárez area source emissions data for the sensitivity analysis are listed below:

	1	2	3	4	5	6	7	8	9	10	11	12
NOx	↑ 50%	↓ 50%			↑ 50%	↓ 50%	↑ 75%	↓ 75%			↑ 75%	↓ 75%
VOC			↓ 50%	↑ 50%	↑ 50%	↓ 50%			↑ 75%	↓ 75%	↑ 75%	↓ 75%

An arrow pointing up in the matrix indicates emissions increase. An arrow pointing down indicates emissions decrease. The number which follows indicates if BASELINE emissions for the specific pollutant are modified by 50% or 75% in the specified direction.

All sensitivity runs functioned within acceptable limits for the model performance evaluation. None of the runs displayed significant improvement in the model performance over the BASELINE run. An increase of 75% area source VOC emissions with or without concurrent increase in NOx emissions will bring the predicted peak ozone to be the same as the observed peak (Run 7 Figure 5.17). Variation in 50 or 75% of NOx area emissions represent only a small fraction of NOx changes in the PdN (5% and 8%, respectively, from Table 6.6) which may not be sufficient to make visible changes in the ozone predictions. On the other hand, if one reduces the Juarez area source VOC emissions by 50% through some control strategies, one would be able to reduce the peak ozone by as much as 13%.

References

American FactFinder. Factfinder2.census.gov, 2012. http://factfinder2.census.gov/faces/nav/jsf/pages/index.xhtml, (Retrieved 2012-05-21)

Becerra F and Fitzgerald R, 2012. The Influence of Photolysis Rate Constants in Ozone Production for the Paso del Norte Region, Joint Spring 2012 Meeting of the Texas Sections of the APS and AAPT and Zone 13 of the SPS, Volume 57, Number 2, San Antonio, TX, March 22-24, 2012.

Brown M, Muller C, Wang G, Costigan K, 2001. Meteorological simulations of boundary-layer structure during the 1996 Paso del Norte Ozone Study, the Science *of The Total Environment*, *276:111-133.*

Byun DW, Ching JKS, 1999. Science algorithms of the EPA Models-3 Community Multiscale Air Quality Model (CMAQ) modeling system. EPA/600/R-99/030, US Environmental Protection Agency, Office of Research and Development, Washington, DC.

Choi Y, Hyde P, Fernando H, 2006. Modeling of episodic particulate matter events using a 3-D air quality model with fine grid: Applications to a pair of cities in the US/Mexico border, Atmospheric Environment, 40(27):5181–5201

Colella P, and Woodward PR, 1984. The Piecewise Parabolic Method (PPM) for Gas-dynamical Simulations. J. Comp. Phys., 54: 174-201.

Emery CA, Yocke MA, Yarbrough JW, Paramo-Figuero VH, 2000. CAMx modeling of ozone and carbon monoxide in the Paso del Norte airshed, Paper 1097, in Proceedings of the Ninety-Third Annual Conference of Air & Waste Management Association. Pittsburgh, PA, June 18-22, 2000.

Emery C, Jung J, Johnson J, Yarwood G, Madronich S, Grell G, 2010. Improving the Characterization of Clouds and their Impact on Photolysis Rates within the CAMx Photochemical Grid Model. Prepared for the Texas Commission on Environmental Quality, Austin, TX. Prepared by ENVIRON International Corporation, Novato, CA (August 27, 2010).

Environ Corporation. 2009a. User's Guide: Environmental Processor System, Version 3, ENVIRON International Corporation, Novato, CA.

Environ Corporation, 2009b. Application of CAMx for the Austin / San Antonio Joint Meteorological Model Refinement Project.

Environ Corporation. 2011. User's Guide: Comprehensive Air quality Model with extensions (CAMx), version 5.40. Prepared by ENVIRON International Corporation, Novato, CA.

Environ Corporation, 2012. CAMX Support Software. http://www.camx.com/download/support-software.aspx.

Funk TH, Chinkin LR, Roberts PT, Seager M, Mulligan S, Paramo VH, Yarbrough J, 2001. Compilation and evaluation of a Paso del Norte emission inventory. The Science of the Total Environment, 276:135-151.

Haste TL, Kumar N, Chinkin LR, Roberts PT, 1998. Compilation and evaluation of a gridded emission inventory for the El Paso del Norte area. Sonoma Technology, Petaluma CA. Final Report: STI-998110-1828-FR.

Houyoux MR, Vukovich JM, Coats CJ Jr, Wheeler NM, Kasibhatla PS, 2000. Emission inventory development and processing for the Seasonal Model for Regional Air Quality (SMRAQ) project, J. Geophys. Res., 105(D7): 9079-9090.

Houyoux MR, Coats CJ Jr, Eyth A, Lo S, 1996. Emissions modeling for SMRAQ: A seasonal and regional example using SMOKE, paper presented at Computing in Environmental Resource Management, Air and Waste Manage. Assoc., Research Triangle Park, N. C., Dec. 2-4, 1996.

Lee, SM and Fernando HJS. 2003. Chapter II: Planetary Boundary Layer Structure of the Paso del Norte Airshed: A Numerical Study, in *The U.S. – Mexican Border Environment: Air Quality Issues along the U.S.-Mexico Border,* ed. A. Sweedler, San Diego State University Press, San Diego, CA. SCERP Monograph Series 6: 59-80.

Li W-W, Fitzgerald R, Yang HL, Yang HY, Olvera H, Cheu KRL, 2011a. Conceptual Model for Ozone Reduction in El Paso, Texas. Submitted to the El Paso MPO, Dept. of Civil Engineering, the University of Texas at El Paso. El Paso, TX, 272 pages.

Li WW, Yang HY, Olvera H, Cheu KRL, Fitzgerald R, Yang HL, 2011b. Emission Inventory Review and Improvement Plan. Submitted to the El Paso MPO, Dept. of Civil Engineering, the University of Texas at El Paso. El Paso, TX, 79 pages.

Lu D, Reddy R, Fitzgerald R, Stockwell W, Williams Q, Tchounwou P, 2008. Sensitivity Modeling Study for an Ozone Occurrence during the 1996 Paso Del Norte Ozone Campaign, International Journal of Environmental Research and Public Health, 5:181-203.

Lu D, Reddy RS, Fitzgerald R, Stockwell WR, Williams QL,Tchounwou PB, 2011. Multiscale comparison of air quality modeling for an ozone occurence during the 1996 Paso Del Norte Ozone Campaign, WIT Transactions on Biomedicines and Health, 15:47-58, 2011.

MacDonald PC, Roberts PT, Main HH, Dye TS, Coe DL, Yarbrough J, 2001. The 1996 Paso del Norte Ozone Study: analysis of meteorological and air quality data that influence local ozone concentrations. The Science of the Total Environment, 276:93-109.

Madronich, S. 2002. The Tropospheric Visible Ultra-violet (TUV) model web page. National Center for Atmospheric Research, Boulder, CO.

Michalakes J, Chen S, Dudhia J, Hart L, Klemp J, Middlecoff J, Skamarock W, 2001. *Development of a Next Generation Regional Weather Research and Forecast Model. Developments in Teracomputing: Proceedings of the Ninth ECMWF Workshop on the Use of High Performance Computing in Meteorology*. Eds. Walter Zwieflhofer and Norbert Kreitz. World Scientific, Singapore. pp. 269-276.

Nagaraj A, 2002. Sensitivity analysis of ozone predictions in Paso del Norte airshed, M.S. Thesis, the University of Texas at El Paso, TA.4998.N343, 2002.

National Oceanic and Atmospheric Administration (NOAA), 2012. Climatography of the United States No. 20: El Paso Intl AP, TX 1971–2000. 2012. http://en.wikipedia.org/wiki/K%C3%B6ppen_climate_classification

Pearson R and Fitzgerald R, 2001. Application of a Wind Model for the El Paso-Juarez Airshed, J. of Air & Waste Manage. Asso., 5(5):669-680.

Pleim J, 2007. A combined local and nonlocal closure model for the atmospheric boundary layer. Part I: Model description and testing. J. Appl. Met. and Clim., 46:1383-1395.

Rivera N, Gill T, Gebhart K, Hand J, Bleiweiss M, Fitzgerald R, 2009. Wind modeling of Chihuahuan Desert dust outbreaks, Atmos. Environment, 43(2):347-354.

Roberts PT, MacDonald CP, Main HH, Dye TS, Coe DL, Haste TL, 1997. Analysis of meteorological and air quality data for the 1996 Paso del Norte Ozone Study, Final report prepared for the U.S. Environmental Protection Agency, Region 6; Dallas, TX, USA, by Sonoma Technology, Inc. Santa Rosa, CA. September 1997. Under subcontract to Science Applications International Corporation Mclean, VA, STI-997330-1754-FR.

Skamarock W C, Klemp JB, Dudhia J, 2001. Prototypes for the WRF (Weather Research and Forecasting) model. Reprints, Ninth Conf. on Meso-scale Processes, Fort Lauderdale, FL, Amer. Meteor. Soc., J11-J15, 2001.

Skamarock WC, Klemp JB, Dudhia J, Gill DO, Barker DM, Wang W, Powers JG, 2005. A Description of the Advanced Research WRF Version 2, NCAR TECHNICAL NOTE, NCAR/TN–

468+STR, Mesoscale and Microscale Meteorology Division, National Center for Atmospheric Research, Boulder, Colorado, USA.

Skamarock WC, Klemp JB, Dudhia J, Gill DO, Barker DM, Duda MG, Huang XY, Wang W, Powers JG, 2008. A description of the advanced research WRF Version 3. National Center for Atmospheric Research (NCAR), Boulder, CO (NCAR/TN 475 þ STR; June 2008).

Texas Commission on Environmental Quality (TCEQ), 2011. TexAER, http://www.tceq.texas.gov/airquality/areasource/TexAER.html.

Texas Commission on Environmental Quality, 2012. Emission Inventory Guidelines. RG-360A/11. Revised February 2012.

U.S. Environmental Protection Agency (U.S. EPA), 2005. Guidance on the Use of Models and Other Analyses in Attainment Demonstrations for the 8-hour Ozone NAAQS. EPA-454/R-05-002, U.S. Environmental Protection Agency, Office of Air Quality Planning and Standards, Emissions, Monitoring, and Analysis Division, Air Quality Modeling Group, Research Triangle Park, NC, October 2005.

U.S. Environmental Protection Agency (U.S. EPA), 2007, Guidance on the Use of Models and Other Analyses for Demonstrating Attainment of Air Quality Goals for Ozone, PM2.5, and Regional Haze. EPA-454/B-07-002, U.S. Environmental Protection Agency, Office of Air Quality Planning and Standards, Research Triangle Park, NC, April 2007.

White House, 2011. Statement by the President on the Ozone National Ambient Air Quality Standards, September 2, 2011.

Yang HY, Cheu KRL, Montoya T, Fitzgerald R, Li W-W, 2012. Quantification of Selected Sources for Emission Inventory Improvement in El Paso, Texas. Submitted to the El Paso MPO, Dept. of Civil Engineering, the University of Texas at El Paso. El Paso, TX, 56 pages.

Yarwood G, Rao ST, Yocke M, Whitten GZ, 2005. Updates to the Carbon Bond chemical mechanism: CB05. Final Report prepared for US Environmental Protection Agency, Research Triangle Park, NC.

Yocke M, Emery C, Jimenez M, Tran C, Evans R, Capuano M, Atchison K, 2000. Evaluation of ambient ozone and carbon monoxide concentrations resulting from automotive fuel changes in the Paso del Norte Airshed, Environ International Corporation. December, 2000.

Zhang L, Gong S, Padro J, Barrie L, 2001. A size-segregated particle dry deposition scheme for an atmospheric aerosol module. Atmos. Environ., 35:549-560.

Zhang L, Brook JR, Vet R, 2003. A revised parameterization for gaseous dry deposition in air-quality models. Atmos. Chem. Phys., 3:2067–2082.

Appendix A

Base Case CAMx Modeling

(Submitted by Environ)

Final Report
CAMx 4-km Modeling of El Paso/Juarez

Prepared for:
Dr. Wen-Whai Li
Department of Civil Engineering
The University of Texas at El Paso
500 W University Ave.
El Paso, Texas 79968

Prepared by:
ENVIRON International Corporation
773 San Marin Drive, Suite 2115
Novato, California, 94945
www.environcorp.com
P-415-899-0700
F-415-899-0707

August 31, 2012

Project Number 0630047A

ENVIRON

CONTENTS

Tables

Figures

1.0 INTRODUCTION

ENVIRON assisted the University of Texas at El Paso (UTEP) in conducting photochemical ozone modeling of the El Paso/Juarez area. The model employed in this study was the Comprehensive Air quality Model with extensions (CAMx; ENVIRON, 2011). The study used existing datasets prepared by the Texas Commission on Environmental Quality (TCEQ) and UTEP. ENVIRON enhanced the current TCEQ Rider 8 June 2006 CAMx modeling dataset, which consists of a national grid with 36 km resolution and a south-central US grid with 12 km resolution, by adding a 4 km resolution grid specifically covering El Paso/Juarez. ENVIRON developed 4 km modeling inputs including anthropogenic and biogenic emissions, meteorology, initial/boundary conditions, and other data.

ENVIRON performed two CAMx base case simulations of June 12-21, 2006 employing alternative approaches in defining 4 km grid meteorology. Both simulations used the 4 km El Paso/Juarez emission inputs. The first CAMx simulation ran the TCEQ 36/12 km grids together with the 4 km grid in 2-way nested mode, where meteorology on the 4 km grid was internally interpolated by CAMx from the 12 km meteorology. The second CAMx simulation was run for the single 4 km grid alone using meteorological data from UTEP's application of the Weather and Research Forecasting (WRF) model. Boundary conditions for the 4 km grid were extracted from CAMx runs on the 36/12 km grid in a manner referred to as 1-way nesting. This was necessary to most appropriately accommodate the potentially different meteorology and different vertical grid structures between the 4 km (UTEP) and 12 km (TCEQ) meteorological data.

The CAMx 1-way nested and the 2-way flexi-nested 4 km grid results were compared to evaluate differences arising from the use of different meteorology and grid structures. The comparisons are presented using spatial concentration maps and model performance statistics.

1.1 Modeling Database

Most information supporting the modeling was based on TCEQ's Rider 8 Near Non-Attainment Area modeling database. The 36 km and 12 km modeling inputs and raw inventory data files for the June 2006 episode are provided on the TCEQ's Rider 8 modeling website (http://www.tceq.texas.gov/airquality/airmod/rider8). The 4 km WRF data covering El Paso/Juarez were provided by UTEP on their FTP site.

1.2 Modeling Domain

Model simulations used the TCEQ 36 km US domain with nested 12 km and 4 km domains, as shown in Figure 1-1. The map projection is Lambert Conic Conformal as defined in the TCEQ's Rider 8 database.

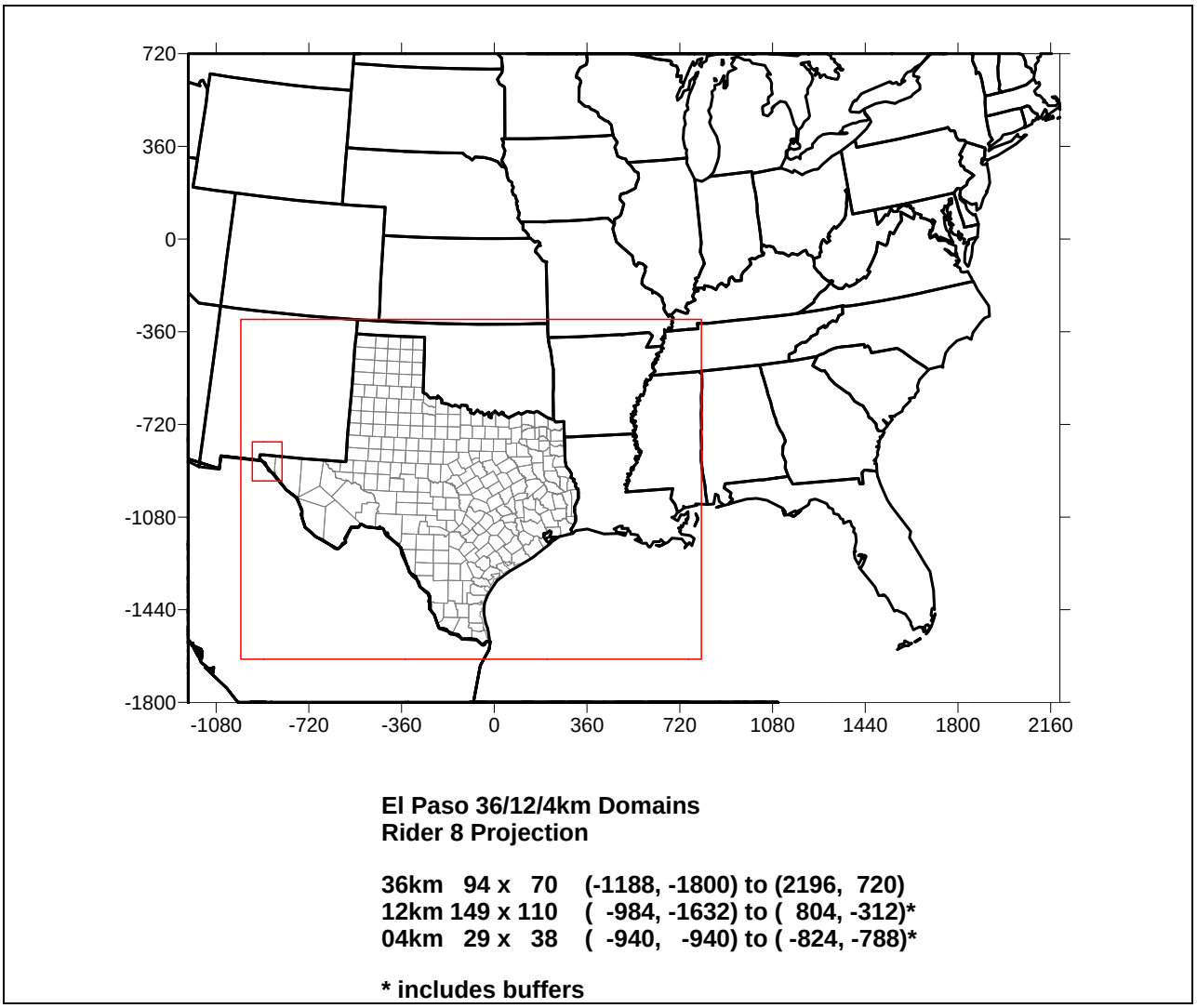

Figure 1-1. UTEP CAMx Modeling Domains

1.3 Modeling Episode

The CAMx 2-way nested simulation was run for the June 9-21, 2006 modeling episode, using June 9-11 as a spin-up period. Both 2-way and 1-way simulations introduced the 4 km domain at 6:00 AM CST on June 12, which was the first hour of UTEP's WRF meteorology.

1.4 Report Organization

This report documents the approach to develop modeling inputs, and presents CAMx simulation results focusing in the El Paso area. Section 2 describes emission processing and provides a summary of emissions for the 4 km domain. Section 3 presents development of ancillary CAMx inputs such as meteorology and boundary conditions. Comparisons of the two CAMx simulations are presented in Section 4.

2.0 DEVELOPMENT OF MODEL-READY EMISSIONS

Anthropogenic emissions were processed using the Emissions Processing System version 3 (EPS3) to generate CAMx model-ready emissions at 4 km grid resolution. The TCEQ's Rider 8 emission inventory formed the framework of modeling emissions. The emissions were generated for a modeling episode in June 2006 (June 12-21) that are day-specific, gridded, speciated and temporally (hourly) allocated. The model-ready emissions for the 36 km and 12 km grids were obtained from the Rider 8 modeling emissions previously prepared by TCEQ. The CAMx elevated point source file uses stack coordinates for spatial allocation and therefore is not grid resolution dependent. Hence the 36 km domain elevated point source file from the Rider 8 database was used directly in this modeling as it contains all elevated point sources for El Paso/Juarez as determined by TCEQ.

2.1 Emissions Processing by Source Category

2.1.1 TCEQ's Rider 8 and other Emissions Database

The Rider 8 emissions data files for 2006 and EPS3 ancillary files for all anthropogenic source categories were downloaded from TCEQ's FTP site.

Stationary (i.e. point and area), off-road and non-road source inventories were obtained from ftp://amdaftp.tceq.texas.gov/pub/Rider8/ei/basecase/.

On-road mobile emission inventories for regions inside Texas were obtained from ftp://amdaftp.tceq.texas.gov/pub/Mobile_EI/Statewide/eps3/2006/mvs/.

Inventories for regions outside Texas were obtained from ftp://amdaftp.tceq.texas.gov/pub/Mobile_EI/USA/mvs/2006/.

Mexico emissions inventories were not available on the TCEQ's FTP site. They were obtained from the recent Western Regional Air Partnership (WRAP) modeling inventories compiled for the WestJump project. These emissions inventories for Mexico were interpolated to the year 2008 and used "as is" for this modeling without back casting them to 2006.

2.1.2 Overview of EPS3 Emissions Processing

EPS3 was set up to process criteria pollutant emissions using the Carbon Bond version 6 (CB6) chemical mechanism. Total un-speciated NOx emissions were allocated to NO and NO_2 components. Emission estimates for total VOC were converted to the more detailed chemical speciation used by the CB6 chemical mechanism in CAMx.

Emissions for the following model species were generated:

Criteria Pollutants	CB6 species
Nitrogen oxides (NOx)	nitric oxide (NO)
	nitrogen dioxide (NO2)
Volatile organic compounds (VOC)	paraffins (PAR)
	olefins (OLE, IOLE)
	ethene (ETH)
	ethane (ETHA)
	toluene (TOL)
	xylene (XYL)
	isoprene (ISOP)
	terpene (TERP)
	formaldehyde (FORM)
	higher aldehydes (ALD2, ALDX)
	acetylene (ETHY)
	propane (PRPA)
	benzene (BENZ)
	acetone (ACET)
	other ketones (KET)
Carbon monoxide (CO):	CO

EPS3 generated model-ready hourly low-level point, area, non-road mobile, and on-road mobile emissions on the El Paso 4 km grid system for a representative weekday, Friday, Saturday and Sunday. Biogenic emissions were developed separately using the MEGAN model, which estimated hourly emission rates on 4 km grid for each day of the June 2006 modeling episode.

Standard quality assurance/quality control (QA/QC) steps were conducted during all facets of the emissions processing. These steps followed the approach recommended in EPA modeling guidance (EPA, 2007). EPS3 log and message files were reviewed during processing for consistency and reasonableness. All error records reported during processing were reviewed and resolved. Summary tables were generated to compare input inventory totals against output model-ready totals by day, criteria pollutant, and county/state to ensure there was no spurious loss or gain of emissions mass. Spatial distribution plots were reviewed to assure reasonable coverage. The remainder of this sub-section details the emissions processing by source category.

2.1.2.1 Area Source Emissions

This category comprises stationary sources that are not identified as individual points and are distributed over a large spatial extent (i.e. county). For regions outside of Texas, annual area source emission inventories from the 2002 NEI were used as the starting point and adjusted using EGAS for growth to 2006. For regions inside of Texas, 2008 average daily area source

inventory was used and adjusted to 2006. The 2005 TexAER oil and gas production emissions estimated for average summer day were also included in the processing.

The CB6 VOC speciation profiles and profiles assignments to Source Classification Codes (SCC) were obtained from the TCEQ's Rider 8 modeling platform. Annual or average daily emissions were temporally allocated to hourly emissions using monthly, weekly and diurnal profiles obtained from the Rider 8 modeling platform. The gridding surrogates for the 4 km grid were generated using the EPA's surrogate tool (http://www.epa.gov/ttnchie1/emch/spatial/spatialsurrogate.html).

The EPA has provided GIS shapefiles to use with Surrogate Tool for developing spatial surrogates (ftp://ftp.epa.gov/EmisInventory/emiss_shp2003/). The spatial surrogate assignments to SCC were obtained from the Rider 8 modeling platform. The oil and gas production emissions were spatially allocated using "Rural Land" surrogate due to unavailability of O&G activity data.

2.1.2.2 Non-road Source Emissions

For regions outside of Texas, nonroad emission inventory for 2006 from the EPA NMIM model was used. For regions inside Texas, nonroad emission inventory, developed using Texas specific nonroad model (TexN), was used. The drill rigs emissions were also included in the processing.

EPS3 processing and ancillary files for speciation, temporal and spatial allocation were obtained from the same sources as area source category.

2.1.2.3 Off-road Source Emissions

The off-road emissions were developed for line haul locomotives for regions inside of Texas. There are no shipping or switcher locomotive emissions inside Texas region of the 4km domain. The link-based line haul locomotive emissions were obtained from the Rider 8 inventory and processed using link based (LBASE) module in EPS.

EPS3 processing and ancillary files for speciation and temporal allocation were obtained from the same sources as area source category.

2.1.2.4 On-road Source Emissions

For regions outside of Texas, MOVES default on-road emissions inventories obtained from the TCEQ's FTP site mentioned above were used. For regions inside of Texas, on-road emission inventories derived from traffic data collected by TxDOT for the Highway Performance Monitoring System (HPMS) were used. These emissions were processed as three separate processing streams: HPMS-based, truck idling and off-network for two Texas counties in the 4 km grid.

On-road emissions were processed for a representative weekday, Friday, Saturday and Sunday using temporal profiles and assignments from the Rider 8. On-road emissions were spatially allocated using 4 km resolution using gridding surrogates available in the Rider 8 database.

2.1.2.5 Low-level Point Source Emissions

In the Rider 8 modeling for point sources, TCEQ used a plume height cutoff of 30 m to discriminate elevated and low-level point for non-EGU sources. All the EGU sources from the Acid Rain Database were processed using plume height cutoff of 0.1 m to force all of these sources to be elevated. Low-level point emissions are gridded and depend on the modeling grid. Non-EGU sources were processed using the plume height cutoff of 30 m to generate low-level point emissions for the 4 km grid.

EPS3 speciation and temporal profiles needed for processing were obtained from the Rider 8.

2.1.2.6 Mexico Emissions

As mentioned above, emissions inventories for Mexico were obtained from the recent WRAP RPO modeling inventories compilation. Annual emissions for area, non-road and on-road source categories were obtained in the SMOKE format and reformatted for EPS3. In the Rider 8 modeling, point sources for Mexico were processed using plume height cutoff of 1 m. All the point sources in the 4 km grid were in the elevated point source file.

The speciation profiles and their SCC assignments were obtained from the Rider 8. Temporal profiles and their SCC assignments were obtained from the NEI2005 modeling platform. These files were available in SMOKE format from the EPA FTP site and were reformatted for EPS3. On-road emissions were spatially allocated using 4 km gridding surrogate available in the Rider 8. Area and non-road source emissions were spatially allocated using population surrogates. The population surrogates available from the EPA smear emissions over the Juarez municipality. New population spatial surrogates were developed using population data by census track block. These data were obtained from the Juarez Municipal Institute for Planning and Research (IMIP).

2.1.2.7 Biogenic Emissions

Biogenic emissions for the El Paso 4 km grid were estimated using the Model of Emissions of Gases and Aerosols from Nature (MEGAN). MEGAN was developed by the Biological-Atmospheric Interactions (BAI) group of the Atmospheric Chemistry Division (ACD) at the National Center for Atmospheric Research (NCAR)[1]. MEGAN estimates net emission of gases and aerosols from terrestrial ecosystems into the atmosphere (Guenther et al., 2006; Sakulyanontvittaya, et al., 2008) driven by land cover, weather, and atmospheric chemical composition. MEGAN is a global model with a base resolution of approximately 1 km.

ENVIRON implemented several improvements and modifications to the standard version of MEGAN:

- Biogenic emissions depend upon temperature and solar radiation input data. Previous versions of MEGAN obtained these data strictly from MM5 simulation output. ENVIRON

[1] http://bai.acd.ucar.edu/Megan/

added options to allow input of solar radiation from satellite data and temperature from interpolated observations or from models other than MM5.

- ArcGIS can be used to develop more flexible definitions of output emission grids.
- MEGAN can output emissions in CAMx format as well as CMAQ format.

Input data requirements for the MEGAN biogenic model are described below.

2.1.2.7.1 MEGAN Driving Variable Database (MDVD)

Biogenic emissions depend upon landuse/landcover input data. MEGAN landcover variables include total Leaf Area Index (LAI), tree fraction and plant species composition. These variables are determined primarily from satellite observations, such as ~1 km^2 Moderate Resolution Imaging Spectroradiometer (MODIS) and 30 m resolution LANDSAT data. Ground surveys of plant species distributions also are incorporated into the MEGAN landcover data. MEGAN driving variables include weather data, LAI, plant functional type (PFT) cover and emission factors for specific chemical compounds that depend on plant species composition. PFT cover is defined for 5 types: broad leaf trees, needle leaf trees, shrub/brush, cropland and herbaceous. All of these variables are available at various temporal scales and are provided in a geo-referenced gridded database in several formats (e.g., NetCDF, ESRI GRID). The MEGAN database has global coverage at 30 sec (~ 1 km) spatial resolution.

2.1.2.7.2 PFT Distributions

Each MEGAN grid cell location has an estimate of the fraction of the cell covered by each of 5 PFTs (broadleaf trees, needleleaf trees, shrub/brushland, cropland and other herbaceous) with the remainder of the cell considered barren with no vegetation. The PFT version 2.0 database (PFTv2.0; Guenther et al. 2006) was derived from three satellite databases with some adjustments in the U.S. using the USFS Forest Inventory Analysis (FIA) data. The satellite databases include the following:

- 500 m resolution global tree cover and ground vegetation cover based on MODIS data (Hansen et al. 2003)
- 1 km resolution database of broadleaf vs. needleaf tree fraction based on AVHRR data (DeFries et al. 2000)
- 1 km resolution database of landcover based on AVHRR data (Hansen et al. 2000)

The Hansen et al. (2003) database provides an estimate of the fraction of each grid cell covered by trees and the fraction covered by other vegetation. The DeFries et al. (2000) data were used to divide trees into broadleaf and needleleaf fractions. The Hansen et al. (2000) landcover database was combined with a simple scheme to divide non-tree vegetation into shrub, grass and crop fractions. The global coverage of these data provides a convenient approach for characterizing the entire earth system and these estimates provide reasonable results when averaged over large scales. However, Guenther et al. (2006) demonstrated that there are large uncertainties in the PFTv2.0 estimates on local scales and showed that emission estimates

varied considerably for alternative landcover databases. The PFT version 2.1 (PFTv2.1) database characterizes PFT distributions on at global 1 km spatial resolution.

2.1.2.7.3 SCT Distribution (ECMAP)

A chemical species-specific emission factor distribution requires accurate estimates of plant species distributions. This should be accomplished using a landcover database with sufficient detail for representing a relatively constant species composition type (SCT). The MEGAN version 2.0 SCT database (SCTv2.0) is described by Guenther et al. (2006).

2.1.2.7.4 Meteorological Data

There are three options to provide temperature and solar radiation (PAR) data to MEGAN, which are generated by the TPAR2IOAPI pre-processor. For this study, the emission estimates used temperature data from CAMx-ready meteorological files (developed from WRF output) and solar radiation derived from GOES satellite data (http://www.atmos.umd.edu/~srb/gcip/).

2.2 EMISSIONS SUMMARY

A summary of model-ready emissions for a representative weekday, Friday, Saturday and Sunday is presented in Table 2-1.

Figures 2-1 through 2-3 show NOx, VOC and CO emission density plots for a representative weekday, Friday, Saturday and Sunday during the modeling episode. Biogenic emissions for the El Paso 4 km grid are shown in Figure 2-4 for dates matching Figures 2-1 through 2-3 (biogenic emissions are date-specific because of meteorological differences). The sum of VOC emissions over the 4 km domain is comparable for biogenic and area sources. Anthropogenic emissions are concentrated in the populated areas of El Paso/Juarez and Las Cruces and along major highways. Biogenic VOC emissions occur along the course of the Rio Grande from Las Cruces to the southeast of El Paso.

Table 2-2 summarizes emissions over a sub-domain of 13×12 4 km grid cells covering the El Paso/Juarez urban area and shows that biogenic emissions are less than area sources within the urban area. Biogenic emissions are concentrated along the Rio Grande because of water availability and the area is agricultural including vegetables, animal feed and Pecan orchards. Pecan trees emit relatively little isoprene whereas cottonwoods, which are native to El Paso, are high isoprene emitters. There are areas of biogenic VOC in the upper elevations in New Mexico and west Texas as well. The distribution of biogenic VOC emissions from MEGAN shown in Figure 2-4 agrees well with a satellite photo of the region (Figure 2-5).

Table 2-1. Emissions summary (tons/day) for the 4 km grid.

Source Category	Weekday	Friday	Saturday	Sunday
NOX (tpd)				
Area	24.3	24.3	22.4	21.1
Nonroad	33.5	33.5	21.4	19.7
Onroad	92.3	95.6	75.9	67.5
Point	43.7	42.6	41.9	42.3
Biogenic	2.8	2.0	2.2	2.6
VOC (tpd)				
Area	250.3	250.3	235.8	226.4
Nonroad	10.4	10.4	13.8	11.9
Onroad	50.6	52.5	43.9	41.2
Point	11.0	10.9	10.9	11.0
Biogenic	244.0	182.0	199.7	230.4
CO (tpd)				
Area	84.0	84.0	68.5	53.4
Nonroad	107.9	107.9	132.3	112.1
Onroad	445.0	465.0	382.8	350.1
Point	13.0	12.7	12.7	12.9
Biogenic	28.1	21.2	23.8	27.4

Table 2-2. Emissions summary (tons/day) for the El Paso/Juarez urban area.

Source Category	Weekday	Friday	Saturday	Sunday
NOX (tpd)				
Area	22.6	22.6	21.1	20.0
Nonroad	26.1	26.1	15.5	14.2
Onroad	49.8	52.1	39.2	32.9
Point	11.4	10.8	10.2	10.1
Biogenic	0.4	0.3	0.3	0.3
VOC (tpd)				
Area	236.2	236.2	224.6	217.9
Nonroad	6.9	6.9	8.1	6.7
Onroad	28.7	29.8	24.6	22.8
Point	7.6	7.6	7.6	7.6
Biogenic	32.9	24.9	26.3	29.6
CO (tpd)				
Area	69.5	69.5	59.8	50.5
Nonroad	77.4	77.4	92.7	77.8
Onroad	267.1	281.2	227.8	203.4
Point	3.9	3.8	3.8	3.8
Biogenic	3.8	2.9	3.2	3.6

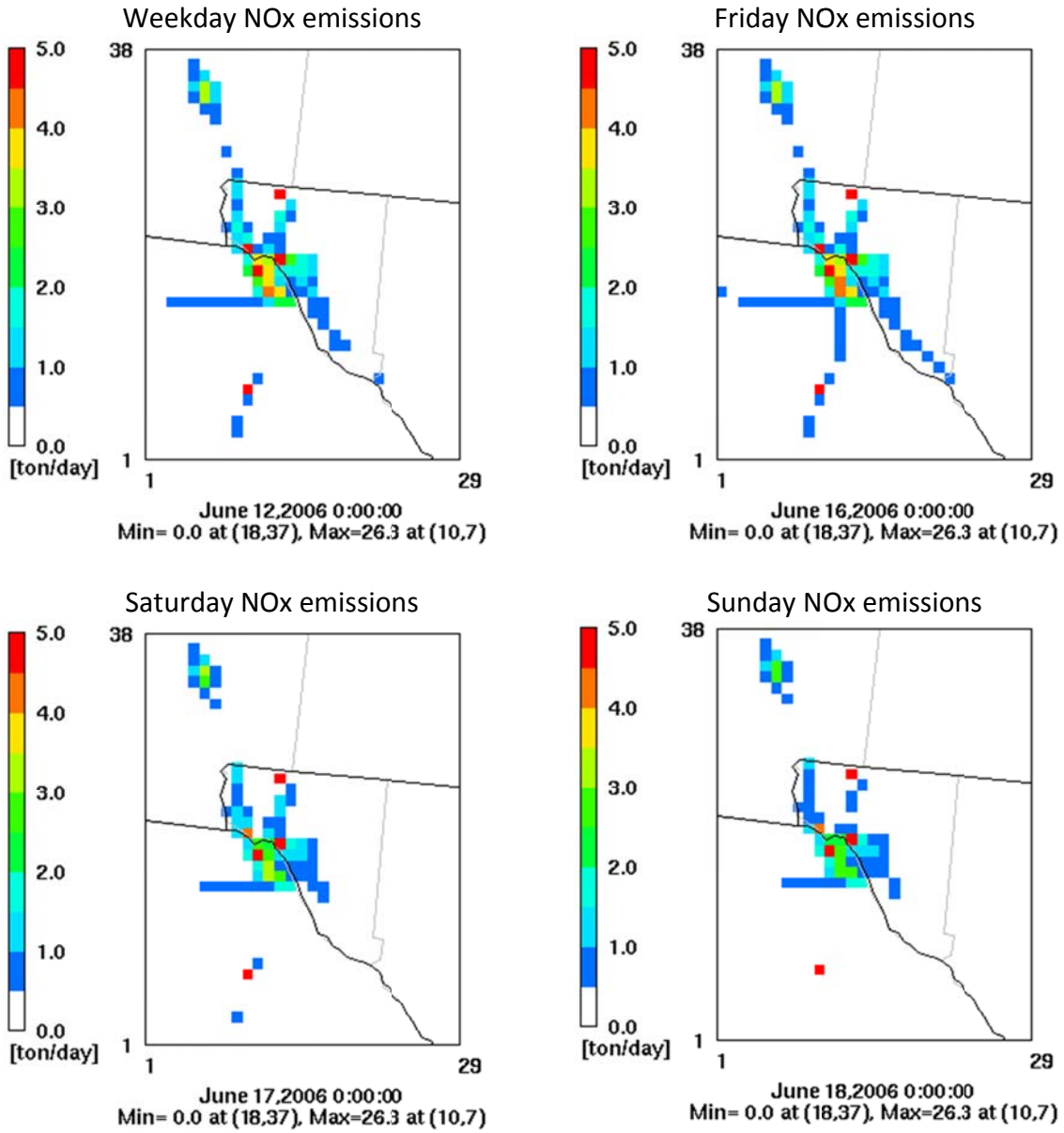

Figure 2-1. NOx emissions (tons/day) for a typical weekday, Friday, Saturday and Sunday for the 4 km domain.

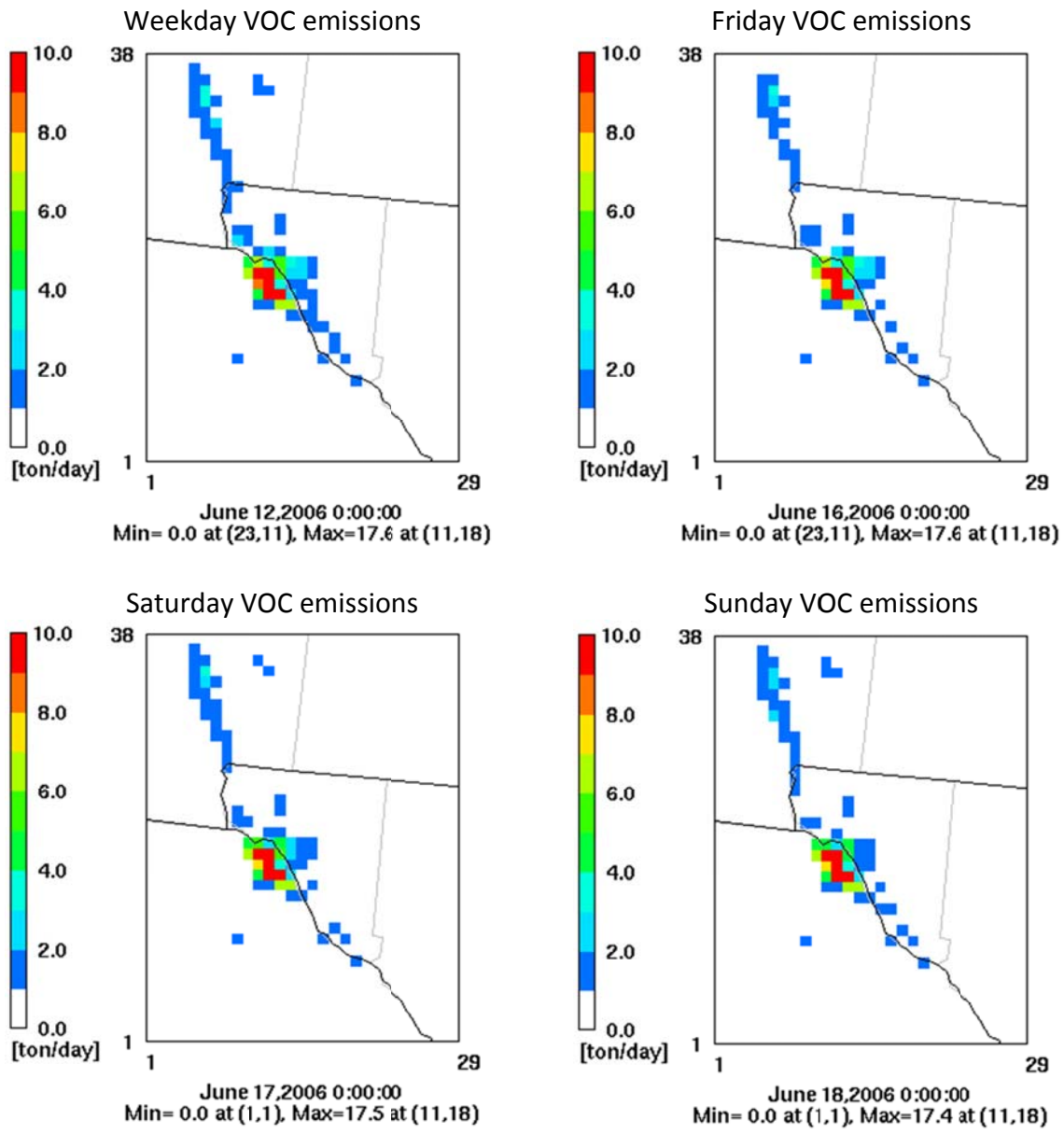

Figure 2-2. VOC emissions (tons/day) for a typical weekday, Friday, Saturday and Sunday for the 4 km domain.

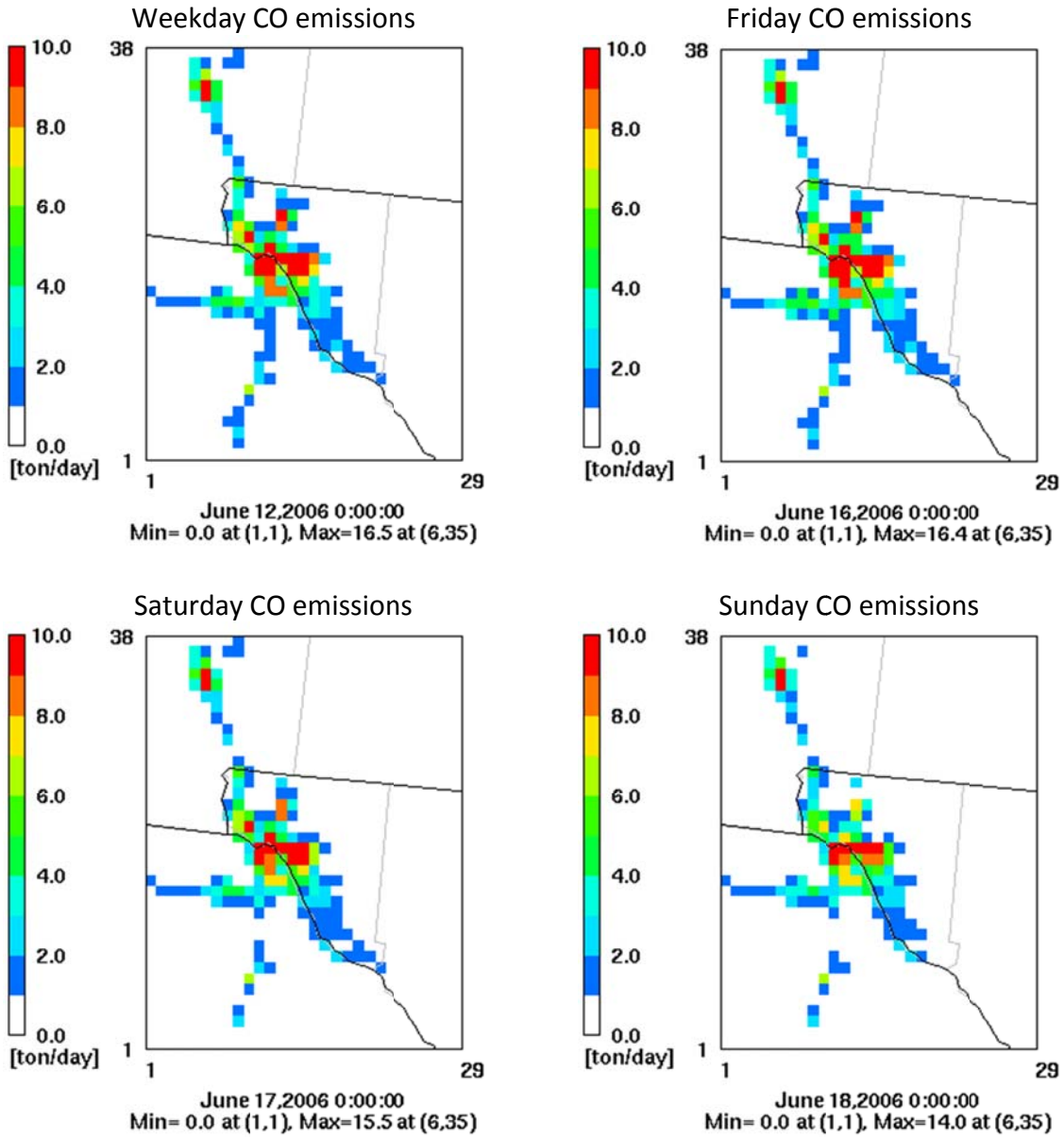

Figure 2-3. CO emissions (tons/day) for a typical weekday, Friday, Saturday and Sunday for the 4 km domain. Emission differences result from variations in human activities.

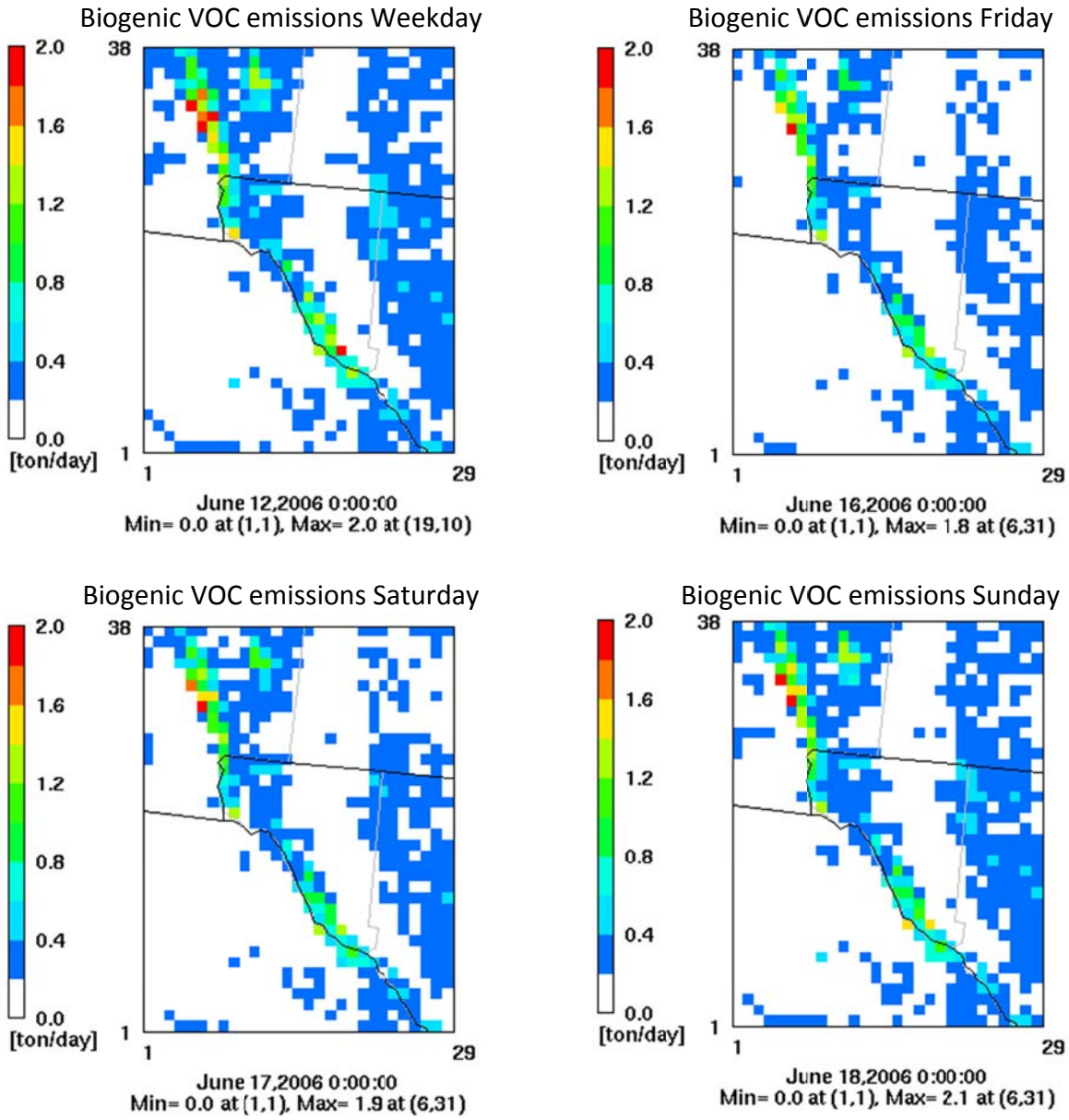

Figure 2-4. Biogenic VOC emissions (tons/day) for a representative weekday, Friday, Saturday and Sunday for the 4 km domain. Emission differences result from variations in temperature and sunlight.

Figure 2-5. Satellite image El Paso and nearby areas.

3.0 MODELING INPUTS AND CAMX SIMULATIONS

3.1 Modeling Inputs

3.1.1 4 km Meteorology

WRF 4 km outputs covering El Paso/Juarez were provided from June 12, 2006 at 12 PM UTC (6 AM CST) to June 22, 2006 at 12 UTC. The WRF domain contained 97x97 grid cells with 34 vertical layers in a Lambert Conformal Projection (LCP) with a center at 31.7°N/106.4°W and true latitudes at 33°N and 45°N.

An interface program (WRFCAMx version 3.3) was used to convert the WRF output to CAMx-ready meteorological input files. The program re-projected the variables to match the TCEQ LCP projection (center at 97°W/40°N, true latitudes at 33°N and 45°N) and applied time shifting to output hourly data from midnight to midnight in CST (except June 12, which started at 6 AM CST). WRFCAMx was configured to output the 22 vertical layers shown in the layer mapping table on the right side of in Figure 3-1. Variables in multiple WRF vertical layers are aggregated into single CAMx layers using a density weighting method. The left side of the figure shows the height profile of the TCEQ layer structure. It was not possible to map the WRF outputs from UTEP directly onto the TCEQ layer structure.

WRFCAMx outputs six meteorological files for each date:

- Height/pressure
- Wind
- Temperature
- Vertical diffusivity
- Moisture
- Cloud/rain

A landuse file is also output, but is not used because it only contains the dominant landuse category in each grid cell (as output by WRF). A better alternative is to create landuse files based on GIS, which can specify the fractional land cover of each landuse category within each grid cell. The vertical diffusivity (Kv) computation in WRFCAMx has several options. Since WRF was configured with the Mellor Yamada Janjic (MYJ) turbulent kinetic energy (TKE) boundary layer option, the Kv method chosen in WRFCAMx was MYJ with a standard minimum Kv set to 0.1 m^2/s.

TCEQ Domains			
Corresponding WRF Layer	Layer Top (m AGL)	CAMx Layer	Thickness (m)
38	15179.1	28	3082.5
36	12096.6	27	2930
32	9166.6	26	2205.7
29	6960.9	25	1125
27	5835.9	24	937.9
25	4898	23	791.6
23	4106.4	22	733
21	3373.5	21	347.2
20	3026.3	20	335.9
19	2690.4	19	324.3
18	2366.1	18	262.8
17	2103.3	17	256.2
16	1847.2	16	249.9
15	1597.3	15	243.9
14	1353.4	14	143.6
13	1209.8	13	141.6
12	1068.2	12	139.7
11	928.5	11	137.8
10	790.6	10	90.9
9	699.7	9	90.1
8	609.7	8	89.3
7	520.3	7	88.5
6	431.8	6	87.8
5	344	5	87.1
4	256.9	4	86.3
3	170.6	3	85.6
2	85	2	51
1	33.9	1	33.9

UTEP Domain			
UTEP WRF Layer	Layer Top (m AGL)	CAMx Layer	Thickness (m)
34	19052		
33	17960		
32	17014		
31	16152		
30	15386	22	3605
29	14641		
28	13918		
27	13213	21	2841
26	12495		
25	11781		
24	11072		
23	10372	20	2121
22	9670		
21	8959		
20	8251	19	1432
19	7539		
18	6819	18	721
17	6098	17	725
16	5373	16	690
15	4683	15	638
14	4045	14	595
13	3450	13	542
12	2908	12	498
11	2410	11	450
10	1960	10	395
9	1565	9	349
8	1216	8	297
7	919	7	244
6	675	6	199
5	476	5	157
4	319	4	123
3	196	3	97
2	99	2	70
1	29	1	29

Figure 3-1. CAMx vertical layer structure used by TCEQ (left) and for El Paso (right).

An additional program is often applied to adjust Kv fields to enhance low-level mixing, which is usually important in urban areas during stable nighttime periods. The program (KVPATCH) was developed by ENVIRON under sponsorship of the TCEQ. The Kv fields were enhanced for all model layers within the lowest 200 m.

3.1.2 Landuse

In the CAMx model, surface land cover distributions are specified through a binary input file that contains time-invariant fields of landuse fractions and leaf area index (LAI) in each grid cell. For the Zhang dry deposition scheme, the fractional distributions of 26 landuse categories are required for each grid cell. These are used to define surface characterization for dry deposition calculations and to set default surface roughness lengths. These landuse categories are described in Table 3-1 and are specific to the Zhang dry deposition scheme. Landuse/landcover (LULC) databases, including leaf area index, used in the development of the CAMx surface files are described below.

Table 3-1. CAMx landuse categories for the Zhang dry deposition scheme.

Category Number	Land Cover Category
1	Water
2	Ice
3	Inland Lake
4	Evergreen Needleleaf Trees
5	Evergreen Broadleaf Trees
6	Deciduous Needleleaf Trees
7	Deciduous Broadleaf Trees
8	Tropical Broadleaf Trees
9	Drought Deciduous Trees
10	Evergreen Broadleaf Shrubs
11	Deciduous Shrubs
12	Thorn Shrubs
13	Short Grass and Forbs
14	Long Grass
15	Crops
16	Rice
17	Sugar
18	Maize
19	Cotton
20	Irrigated Crops
21	Urban
22	Tundra
23	Swamp
24	Desert
25	Mixed Wood Forests
26	Transitional Forest

3.1.2.1 LULC

The North America Land Cover (NALC) database for the year 2000 (Latifovic, et al. 2002) was developed jointly by the Natural Resources Canada - Canada Centre for Remote Sensing, and the USGS EROS Data Center as part of the larger Global Land Cover 2000 project implemented by the Global Vegetation Monitoring Unit, Joint Research Center (JRC) of the European Commission. The North American database was compiled using satellite data during the 2000 growing season at a spatial resolution of 1 km.

The data are available as GIS raster datasets for each continent, in a geodetic coordinate system and can be obtained from the project website at http://edc2.usgs.gov/glcc/nadoc2_0.php. The land use classification scheme includes 29 separate categories as presented in Table 3-2.

Table 3-2. NALC classification.

Code	Description
1	Tropical or Sub-tropical Broadleaved Evergreen Forest - Closed Canopy
2	Tropical or Sub-tropical Broadleaved Deciduous Forest - Closed Canopy
3	Temperate or Sub-polar Broadleaved Deciduous Forest - Closed Canopy
4	Temperate or Sub-polar Needleleaved Evergreen Forest - Closed Canopy
5	Temperate or Sub-polar Needleleaved Evergreen Forest - Open Canopy
6	Temperate or Sub-polar Needleleaved Mixed Forest - Closed Canopy
7	Temperate or Sub-polar Mixed Broadleaved or Needleleaved Forest - Closed Canopy
8	Temperate or Sub-polar Mixed Broaddleleaved or Needleleaved Forest - Open Canopy
9	Temperate or Subpolar Broadleaved Evergreen Shrubland - Closed Canopy
10	Temperate or Subpolar Broadleaved Deciduous Shrubland - Open Canopy
11	Temperate or Subpolar Needleleaved Evergreen Shrubland - Open Canopy
12	Temperate or Sub-polar Mixed Broadleaved and Needleleaved Dwarf-Shrubland - Open Canopy
13	Temperate or Subpolar Grassland
14	Temperate or Subpolar Grassland with a Sparse Tree Layer
15	Temperate or Subpolar Grassland with a Sparse Shrub Layer
16	Polar Grassland with a Sparse Shrub Layer
17	Polar Grassland with a Dwarf-Sparse Shrub Layer
18	Cropland
19	Cropland and Shrubland/woodland
20	Subpolar Needleleaved Evergreen Forest Open Canopy - lichen understory
21	Unconsolidated Material Sparse Vegetation (old burnt or other disturbance)
22	Urban and Built-up
23	Consolidated Rock Sparse Vegetation
24	Water bodies
25	Burnt area (resent burnt area)
26	Snow and Ice
27	Wetlands
28	Herbaceous Wetlands
29	Tropical or Sub-tropical Broadleaved Evergreen Forest - Open Canopy

The land use classes available in the source GIS database needs to be cross referenced to those required for the Zhang dry deposition schemes used by the CAMx air quality model. Tables 3-3 present the cross references currently used for the Zhang schemes.

Table 3-3. LULC mapping between the NALC database and the 26 categories for the Zhang dry deposition scheme.

NALC-CODE	CAMx-CODE	Description
1	8	Tropical or Sub-tropical Broadleaved Evergreen Forest - Closed Canopy
2	8	Tropical or Sub-tropical Broadleaved Deciduous Forest - Closed Canopy
3	7	Temperate or Sub-polar Broadleaved Deciduous Forest - Closed Canopy
4	4	Temperate or Sub-polar Needleleaved Evergreen Forest - Closed Canopy
5	4	Temperate or Sub-polar Needleleaved Evergreen Forest - Open Canopy
6	25	Temperate or Sub-polar Needleleaved Mixed Forest - Closed Canopy
7	25	Temperate or Sub-polar Mixed Broadleaved or Needleleaved Forest - Closed Canopy
8	25	Temperate or Sub-polar Mixed Broaddleleaved or Needleleaved Forest - Open Canopy
9	10	Temperate or Subpolar Broadleaved Evergreen Shrubland - Closed Canopy
10	11	Temperate or Subpolar Broadleaved Deciduous Shrubland - Open Canopy
11	10	Temperate or Subpolar Needleleaved Evergreen Shrubland - Open Canopy
12	10	Temperate or Sub-polar Mixed Broadleaved and Needleleaved Dwarf-Shrubland - Open Canopy
13	14	Temperate or Subpolar Grassland
14	14	Temperate or Subpolar Grassland with a Sparse Tree Layer
15	13	Temperate or Subpolar Grassland with a Sparse Shrub Layer
16	22	Polar Grassland with a Sparse Shrub Layer
17	22	Polar Grassland with a Dwarf-Sparse Shrub Layer
18	15	Cropland
19	15	Cropland and Shrubland/woodland
20	4	Subpolar Needleleaved Evergreen Forest Open Canopy - lichen understory
21	13	Unconsolidated Material Sparse Vegetation (old burnt or other disturbance)
22	21	Urban and Built-up
23	24	Consolidated Rock Sparse Vegetation
24	1	Water bodies
25	24	Burnt area (resent burnt area)
26	2	Snow and Ice
27	23	Wetlands
28	23	Herbaceous Wetlands
29	10	Tropical or Sub-tropical Broadleaved Evergreen Forest - Open Canopy

3.1.2.2 Leaf Area Index

LAI data are an optional input for use with the Zhang dry deposition scheme in CAMx. We used the updated databases for the Model of Emissions of Gases and Aerosols from Nature (MEGAN) biogenic emissions model, developed by NCAR, to specify gridded LAI. The data are provided as un-projected global 30 arc second (~1 km horizontal resolution) GIS raster datasets. LAI is

defined as the ratio of total upper leaf surface area of vegetation divided by the surface area of the land on which the vegetation grows. The LAI data available with the MEGAN databases represent average values over each raster, in units of m^2/m^2 and are available as monthly averaged datasets for calendar year 2001. The LAI data can be obtained as ArcGIS raster GRID files from http://acd.ucar.edu/~guenther/MEGAN/MEGAN.htm.

3.1.2.3 Processing Procedures

A suite of GIS and Perl-based processors were used to prepare landcover and LAI input datasets for CAMx. Arc Macro Language (AML) scripts were used to process the raster-based and vector-based GIS data and to export ASCII datasets for subsequent processing with Perl scripts and FORTRAN programs. User-defined options are used to specify various parameters including the definition of output modeling domains, map projection parameters, and input LULC databases and the MEGAN LAI data. The CAMx landuse file was prepared for the 4 km grid.

3.1.3 Albedo-Haze-Ozone

The AHOMAP program is used to create a text file containing surface UV albedo, total atmospheric haze turbidity, and total atmospheric ozone column data (the AHO file). These parameters are used in the calculation of photolysis rates for the simulation period. The program reads in CAMx landuse files for all domains to be modeled and a global ozone column dataset, which can be downloaded for each episode date from http://ozoneaq.gsfc.nasa.gov/OMIOzone.md. The program is set up to read ozone column datasets with 1 degree resolution.

The top of the output file lists 5 categorical values for albedo, 3 for haze, and 5 for ozone. Each grid cell is assigned a bin number associated with these categorical values. Haze is assumed to have a uniform field (i.e., all grid cells are assigned a bin number of 2 for haze). Bin values are assigned to each grid cell in all domains for albedo; for haze and ozone, only data for the coarse grid are output and CAMx internally interpolates these values to each nested grid.

The TCEQ prepared AHO files daily for their 36/12/4 km domain runs. To preserve the same categorical values for the UTEP runs, which share the same 36 and 12 km domains as TCEQ, a modified version of AHOMAP was developed. For the El Paso/Juarez 2-way nested 36/12/4 km domain, the modified program reads the header of the TCEQ AHO file to obtain the categorical values before assigning a bin to each grid cell. Ozone column bins were copied from TCEQ since both share the same coarse grid; this ensures that the ozone column field would be identical to TCEQ's.

For the 1-way nested 4 km El Paso/Juarez domain, AHOMAP was modified again. The categorical values were copied from the TCEQ AHO file, just like when processing the 36/12/4 AHO file. For ozone, each 36 km grid cell in the TCEQ file that contained the El Paso 4 km domain was expanded into 81 (9x9) 4 km cells, all which were assigned the same bin number as the 36 km grid cell. Bins for the buffer cells were then added to match their neighboring grid cell. Specific albedo fields were developed according the 4 km CAMx landuse file.

3.1.4 TUV

The TUV program reads the categorical values in each AHO file and creates a lookup table listing the photolysis rates for each combination of the categorical values of albedo, haze, and ozone column at various solar angles and heights above the ground. Since the categorical values in the AHO files were copied from TCEQ, the photolysis rates for the El Paso/Juarez 2-way 36/12/4 km and 1-way 4 km domains did not change. Therefore, the TCEQ photolysis rate files could be used for the UTEP runs.

3.1.5 Initial and boundary conditions

In each CAMx run, boundary conditions are needed for the coarsest grid. Since the 36/12/4 km domain shares the same coarse grid as TCEQ's, the TCEQ initial and boundary condition files were used directly.

In the 1-way 4 km domain run, the initial and boundary condition files were generated by extracting concentrations from the 12 km grid results developed from the 36/12/4 km run. Typically, this is accomplished with the BNDEXTR program. However, since the vertical layer structure of the UTEP 4 km domain differs from the TCEQ vertical structure, vertical interpolation had to be added to the BNDEXTR program. The vertical interpolation to the TCEQ vertical structure weighted concentrations based on the thickness of all UTEP layers within each TCEQ layer. The program output a binary file of hourly lateral boundary conditions for each date and a three-dimensional initial conditions file at 6 AM on June 12.

3.2 CAMx Simulations

Air quality modeling for the El Paso/Juarez area employed CAMx version 5.40 (ENVIRON, 2011) to simulate physical and chemical processes governing the formation and transport of ozone with Carbon Bond 6 (CB6) gas phase chemistry. The nested 36/12/4 km modeling domains are shown in Figure 1-1. ENVIRON ran CAMx for the June 2006 episode using 36 km and 12 km Rider 8 modeling inputs provided by the TCEQ. The 4 km inputs were described previously. The model was run with the same user-selected options as the TCEQ Rider 8 modeling except that the plume-in-grid (PiG) submodel was turned off.

ENVIRON performed two CAMx base case simulations with alternative approaches for 4 km grid meteorology, while both simulations used the same 4 km emissions as described in Section 2:

- The first CAMx simulation used the TCEQ 36/12 km modeling datasets and "flexi-nested" (i.e., internally interpolated) meteorology to the 4 km grid. CAMx was run on all grids simultaneously (2-way nested) for the June 9-22, 2006 modeling episode. This simulation is referred to as the "**FE36124k**" run.
- The second CAMx simulation was run on the single 4 km grid but with the 4 km UTEP meteorology and boundary conditions extracted from the previous 12 km output. This simulation is referred to as the "**4kUTEPmet**" run.

CAMx was run in the CST time zone consistent with the TCEQ Rider 8 simulation. A 36/12 km nested run was starting at 00:00 AM on June 9, and the 2-way nested 4 km grid was introduced at 6:00 AM on June 12; the nested 36/12/4 run continued through midnight on June 21. To be consistent, the CAMx 1-way 4 km single grid run started at 6:00 AM on June 12 using initial conditions as described in Section 3.1.5, and ran through midnight on June 21.

4.0 MODEL PERFORMANCE COMPARISON

This section documents results from comparing the CAMx 1-way and flexi-nested 4 km grid simulations to evaluate differences arising from the use of different meteorology and grid structures. The comparisons are presented using spatial concentration maps. A model performance evaluation against available hourly ozone and NOx measurements at sites throughout the El Paso/Juarez area was also conducted for both simulations.

4.1 Approach

4.1.1 Observational Data

There are 13 ozone monitoring sites and 7 NOx monitoring sites in the El Paso/Juarez area (Table 4-1, Figure 4-1). Predicted ozone and NOx were compared to the observed values at these monitoring sites.

Table 4-1. Ozone and NOx monitoring sites in the El Paso/Juarez area.

Site ID	CAMS ID	Site Name	City, State	Monitored Parameters		Location			
				O_3	NOx	Latitude (deg)	Longitude (deg)	LCPX (m)	LCPY (m)
TC12	C12	UTEP	El Paso, TX	✓	✓	31.7683	-106.5013	-898.604	-865.303
TC37	C37	Ascarate	El Paso, TX	✓	✓	31.7467	-106.4028	-889.572	-868.661
TC41	C41	Chamizal	El Paso, TX	✓	✓	31.7657	-106.4552	-894.296	-866.045
TC49	C49	Socorro	El Paso, TX	✓	✓	31.6622	-106.3031	-881.141	-879.005
TC72	C72	Skyline	El Paso, TX	✓	✓	31.8939	-106.4258	-890.047	-852.124
C414	C414	Ivanhoe	El Paso, TX	✓		31.7864	-106.3242	-881.708	-865.032
C661	C661	Advanced	Juarez, Chih	✓		31.6897	-106.4597	-895.600	-874.423
C663	C663	SEC	Juarez, Chih	✓		31.7122	-106.3953	-889.262	-872.561
LAUN	6O	La Union	LaUnion, NM	✓		31.9183	-106.6331	-909.253	-847.365
CHPR	6ZK	Chaparral	Chaparral, NM	✓		32.0410	-106.4092	-886.788	-835.992
SPCY	6ZG	SPCY	Sunland Park, NM	✓		31.7972	-106.5567	-903.491	-861.550
DSVW	6ZM	Desert View	Sunland Park, NM	✓	✓	31.7962	-106.5839	-906.066	-861.389
STTS	6ZH	Santa Teresa	Santa Teresa, NM	✓	✓	31.7877	-106.6829	-915.487	-861.338

4.1.2 Post-processing Tools

This section describes several post processing utilities for CAMx, mainly for the purposes of statistical and graphical model performance evaluation. Most of these programs are packaged as part of the CAMxPOST system of post processors which is available from the CAMx website. The CAMxPOST system is used to combine observations and predictions, calculate statistics, and plot time series. The order in which the programs are described below are generally the order in which they are run.

Figure 4-1. Ozone and NOx monitoring sites in the El Paso/Juarez area within the CAMx 4 km grid.

4.1.2.1 CAMxTRCT

CAMxTRCT extracts two-dimensional concentration fields for one chemical species (e.g., ozone or NOx) from the raw grid-specific CAMx output average files. The CAMxTRCT output format is identical to the raw CAMx output format.

4.1.2.2 AVGCAT

AVGCAT concatenates several individual (e.g., daily) CAMx or CAMxTRCT files together into a single file. AVGCAT assumes that all files to be concatenated contain the same grid configuration, and the same number and order of chemical species. Generally, CAMx is run for individual days of a multi-day simulation episode. The main purpose for AVGCAT is to provide continuous hourly model output data in a single file to simplify the process of calculating running n-hour averages (e.g., 8, 24, etc.) over multi-day simulations.

4.1.2.3 OBSCAT

OBSCAT concatenates several text-formatted observation data files together into a single file. The program only operates on files formatted for the CAMxPOST system of post processors. OBSCAT assumes that all input observation files contain identical numbers of hour records (e.g., 24 hours per site) and identical lists of monitoring sites.

Generally, separate observation files are developed for the CAMx post processing system for each day of a multi-day simulation episode. However, the system will also work for a single observation file covering the entire episode. The main purpose for OBSCAT is to provide continuous hourly measurement data in a single file to simplify the process of calculating running n-hour averages (e.g., 8, 24, etc.) over multi-day simulations. The output of OBSCAT could also be used for all subsequent operations of the CAMx post processing system.

4.1.2.4 CAMXPOST

CAMxPOST is the central program in the CAMx post processing system to prepare files for statistical evaluation and/or to generate 8- or 24-hour mean predicted concentration fields. The program provides the following capabilities:

- Generates a running n-hourly file in CAMx format
- Generates a maximum n-hourly file in CAMx format
- Pairs predictions and observations and generates a text file of running n-hourly prediction-observations for further processing of statistics and plotting of time-series (also provides the minimum and maximum predicted concentrations within a nine-cell area around each monitoring location if only one scenario is selected).
- Generates a text file of maximum observations at each site

CAMxPOST processes only the surface layer (layer 1) from the input file, and operates on only one chemical species.

4.1.2.5 CAMXSTAT

CAMxSTAT reads an n-hourly prediction/observation paired file generated by CAMxPOST and calculates the following statistics:

1) Unpaired (time and space) peak prediction accuracy
2) Space-paired, time-unpaired peak prediction accuracy by site
3) Space-paired, time-unpaired peak bias and error over all sites
4) Space-paired, time-unpaired bias and error in peak timing
5) Space-paired, time-paired peak bias and error over all sites
6) Mean prediction
7) Mean observation
8) Difference and normalized difference in mean prediction and mean observation
9) Absolute, normalized, and fractional bias
10) Absolute, normalized, and fractional error
11) Root mean square error

These statistics are written to a text report file. CAMxSTAT operates on the entire contents of the input prediction/observation paired file, whether it spans a single day or several, whether 1-hourly or some other averaging period. Therefore, the user should ensure that the prediction/observation pairing file supplied to CAMxSTAT reflects the desired period. Statistics generated under items (2)-(5) and (9)-(11) are calculated only for prediction-observation pairings in which the observation is above some lower threshold. For example, 8-hour ozone statistics are calculated for observations above 40 ppb.

4.1.2.6 EXTSTAT

EXTSTAT is a small program that pulls important statistics from a series of report files generated by CAMxSTAT so that they may be more easily imported into a spreadsheet for producing graphical summaries. The statistics that are pulled are:

- Unpaired peak prediction accuracy (UPPA)
- Bias in paired peak accuracy among all valid sites (APPA)
- Error in paired peak accuracy among all valid sites (EPPA)
- Bias in peak timing (PTB)
- Overall normalized bias (NB)
- Overall normalized error (NE)

4.1.2.7 COMBINE

COMBINE2 prepares data contained in prediction/observation paired files for plotting in Excel spreadsheets. The key process of COMBINE2 is just to reformat the paired files into comma-

delimited records to ease the parsing of data as it is read by the Excel. However, COMBINE2 performs some other important functions, including:

- Concatenates individual paired files (e.g., daily) into a single file.
- Combines paired data from up to 3 different model runs into a single file, ordered into separate columns.
- Allows the user to split the resulting output file into multiple files each containing a sub-set of monitoring sites. This is necessary since Excel graphics are memory-intensive, and memory limits are easily exceeded for paired files with many sites (~50) over many days (~10).

This program assumes that all input paired files contain an identical number of hour records and an identical list of stations. Since CAMxPOST generates paired files containing only one chemical species, COMBINE2 must see that the same species is on all paired files to be combined.

4.2 Model Performance Evaluation

4.2.1 Ozone

Model performance was evaluated for 8-hour and 1-hour ozone at thirteen monitors throughout the El Paso/Juarez area. Daily statistics displayed in the form of bar charts are presented in Figure 4-2 and Figure 4-3. Figure 4-2 compares three values: the highest observed 8-hour ozone among all sites in the El Paso/Juarez area and the co-located daily maximum 8-hour ozone from two CAMx simulations. Both CAMx simulations under estimated the peak observation on two dates (June 13 and June 18) when at least one site exceeded 75 ppb.

The average paired peak accuracy compares the highest observed 1-hour ozone from each of the thirteen monitors with their co-located predicted peaks. When co-located, both simulations tended to under predict ozone with the worst accuracy close to -30% on June 16. The CAMx 1-way nested simulation (4kUTEPmet) performed better on June 18 (highest observed 8-hour ozone date) compared to the flexi-nested simulation (FE36124k); however, its accuracy was worse on seven out of ten dates modeled.

The last two statistics compare the normalized bias and error using all hours and sites. Pairings when the observed 1-hour ozone was less than 40 ppb were excluded. The model performance goals for normalized bias and error are ±15% and 35%, respectively. The biases show under prediction of ozone on all dates for both simulations. The CAMx 1-way nesting simulation met the normalized bias goal on the two ozone exceedance dates and the bias was better than the flexi-nested simulation on nine out of ten dates modeled. Both simulations satisfied the ±35% error performance goal on all dates. The errors are similar in magnitude to bias indicating that underestimation trends are consistent in time and space.

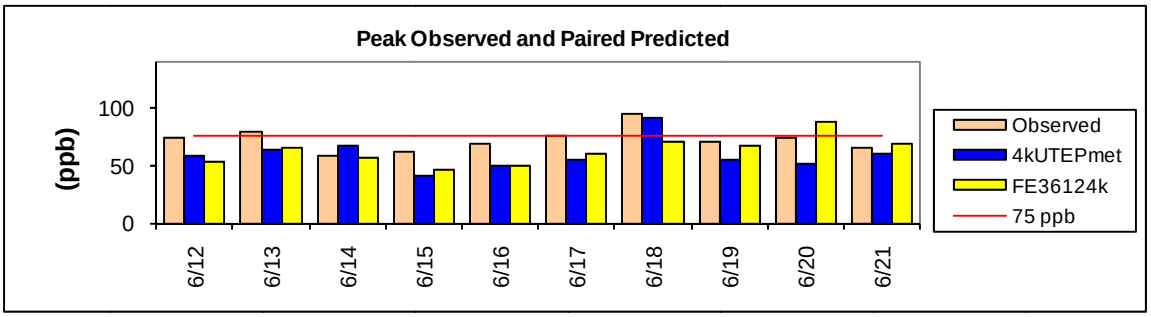

Figure 4-2. Peak observed and paired predicted 8-hour ozone.

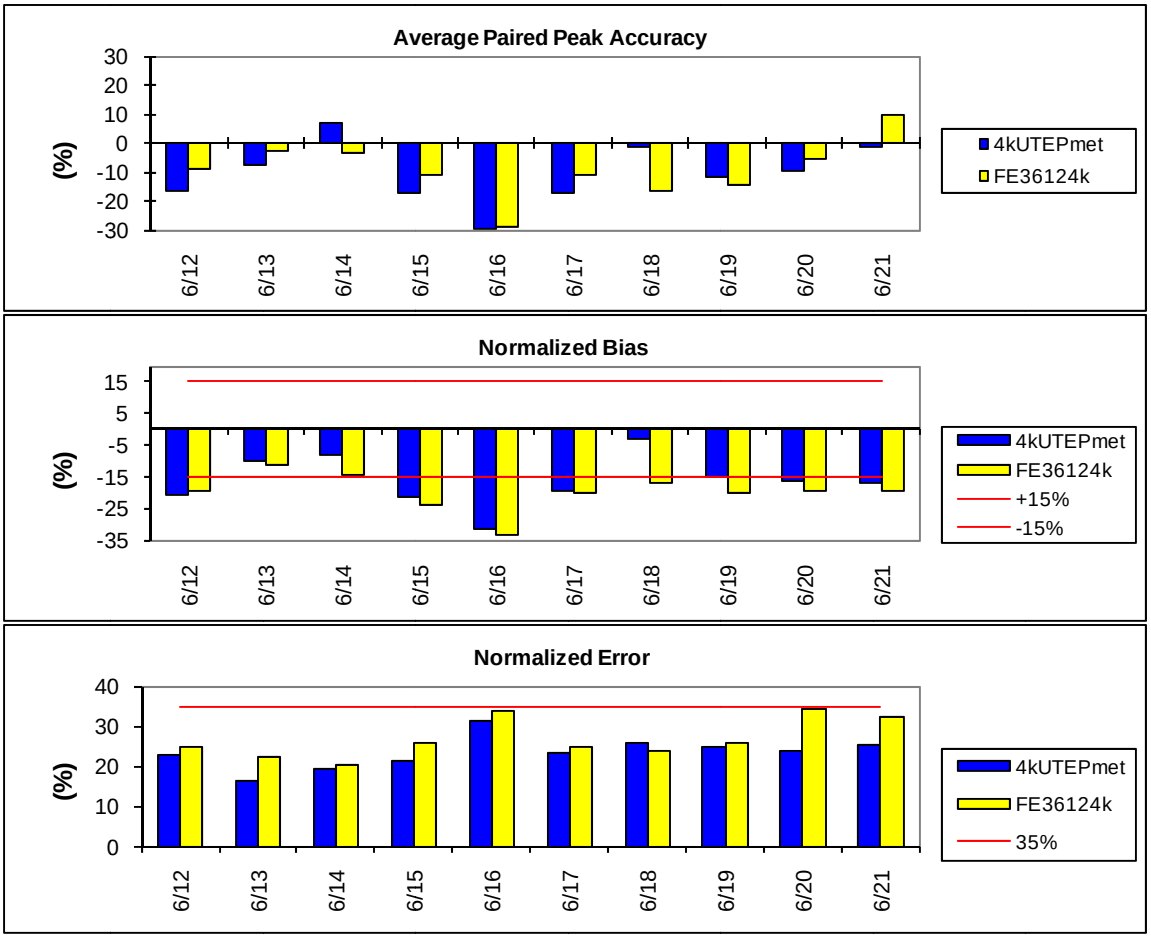

Figure 4-3. Model performance statistics for 1-hour ozone.

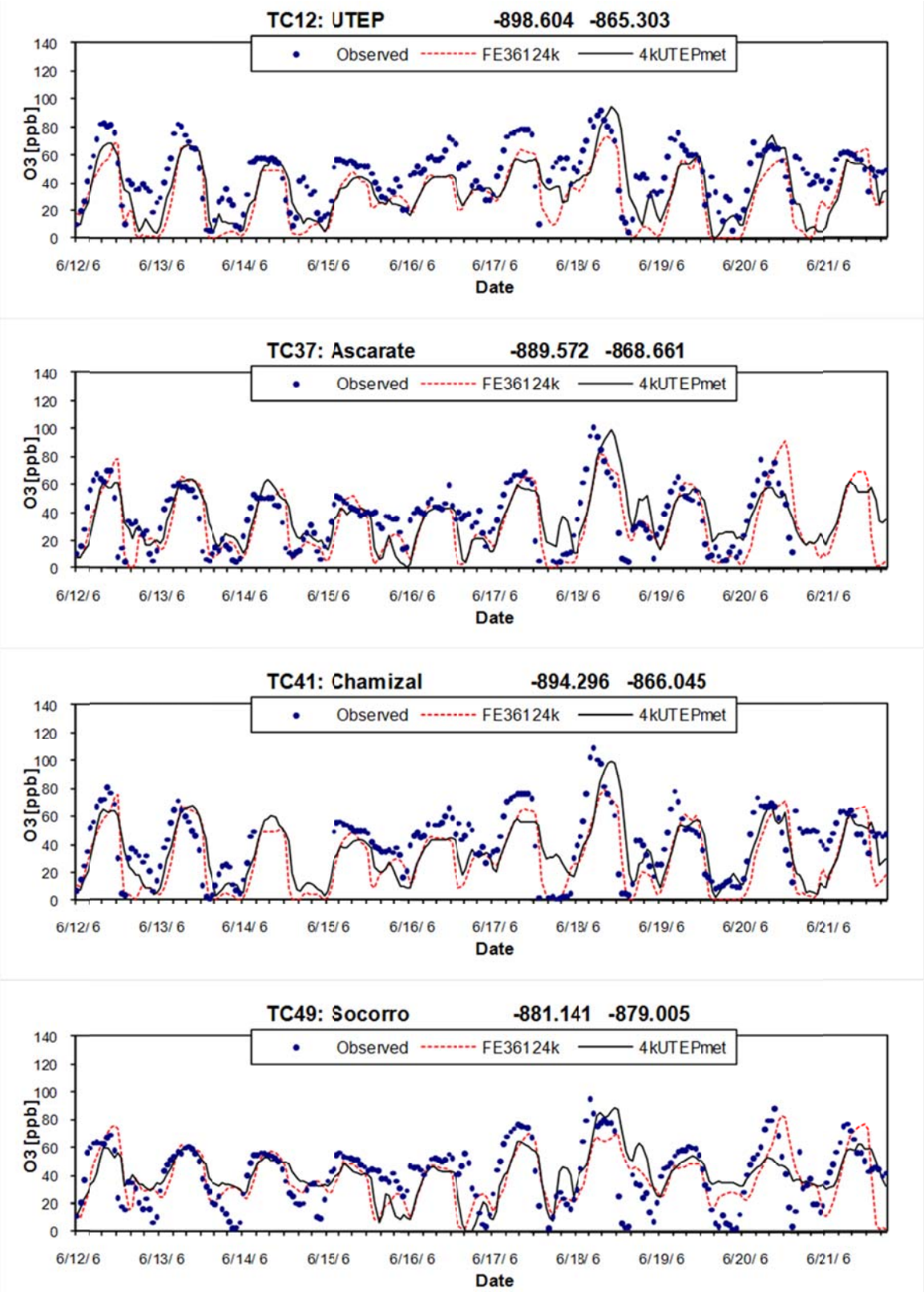

Figure 4-4. Time series of 1-hour ozone comparing two CAMx simulations.

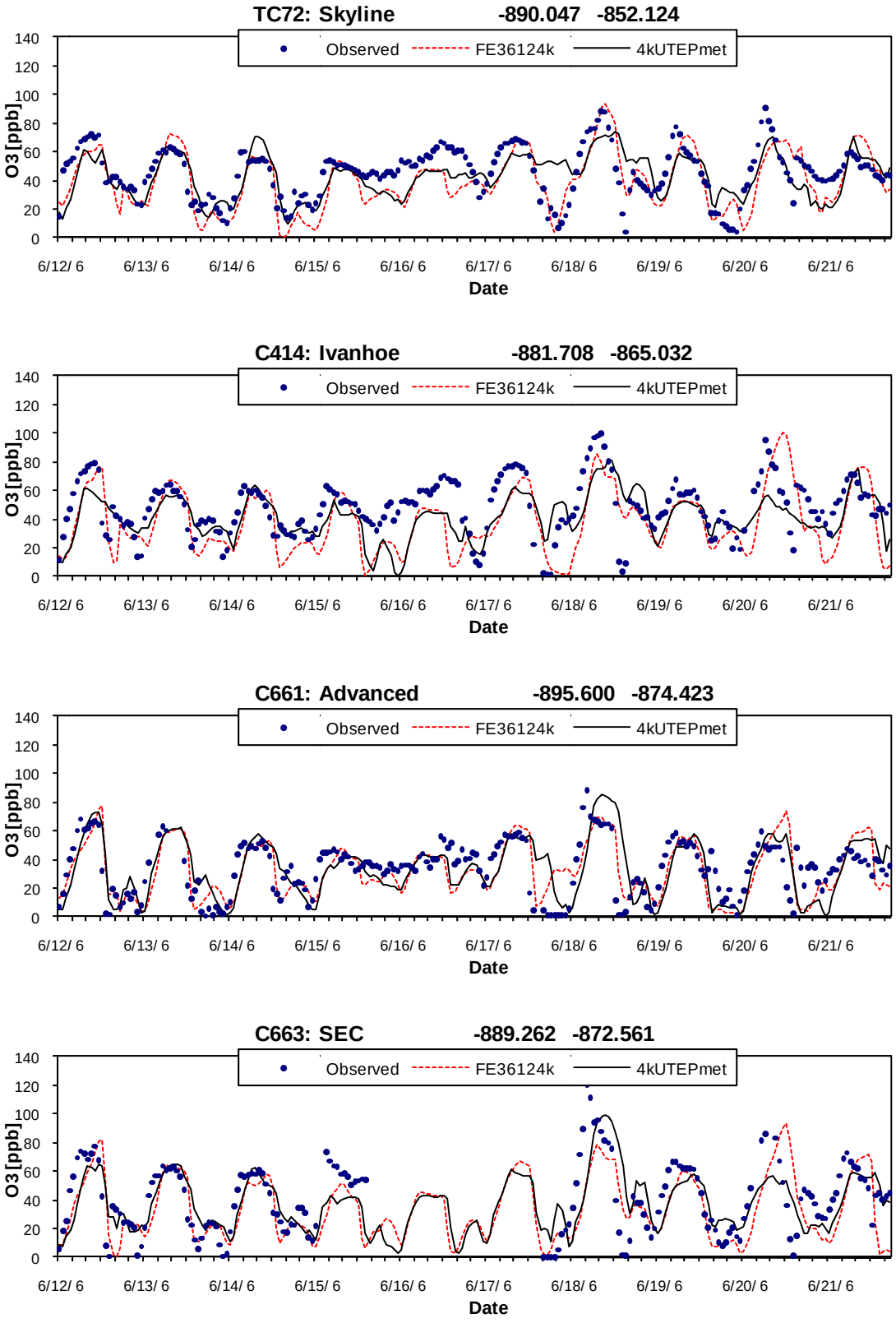

Figure 4-4 (continued). Time series of 1-hour ozone comparing two CAMx simulations.

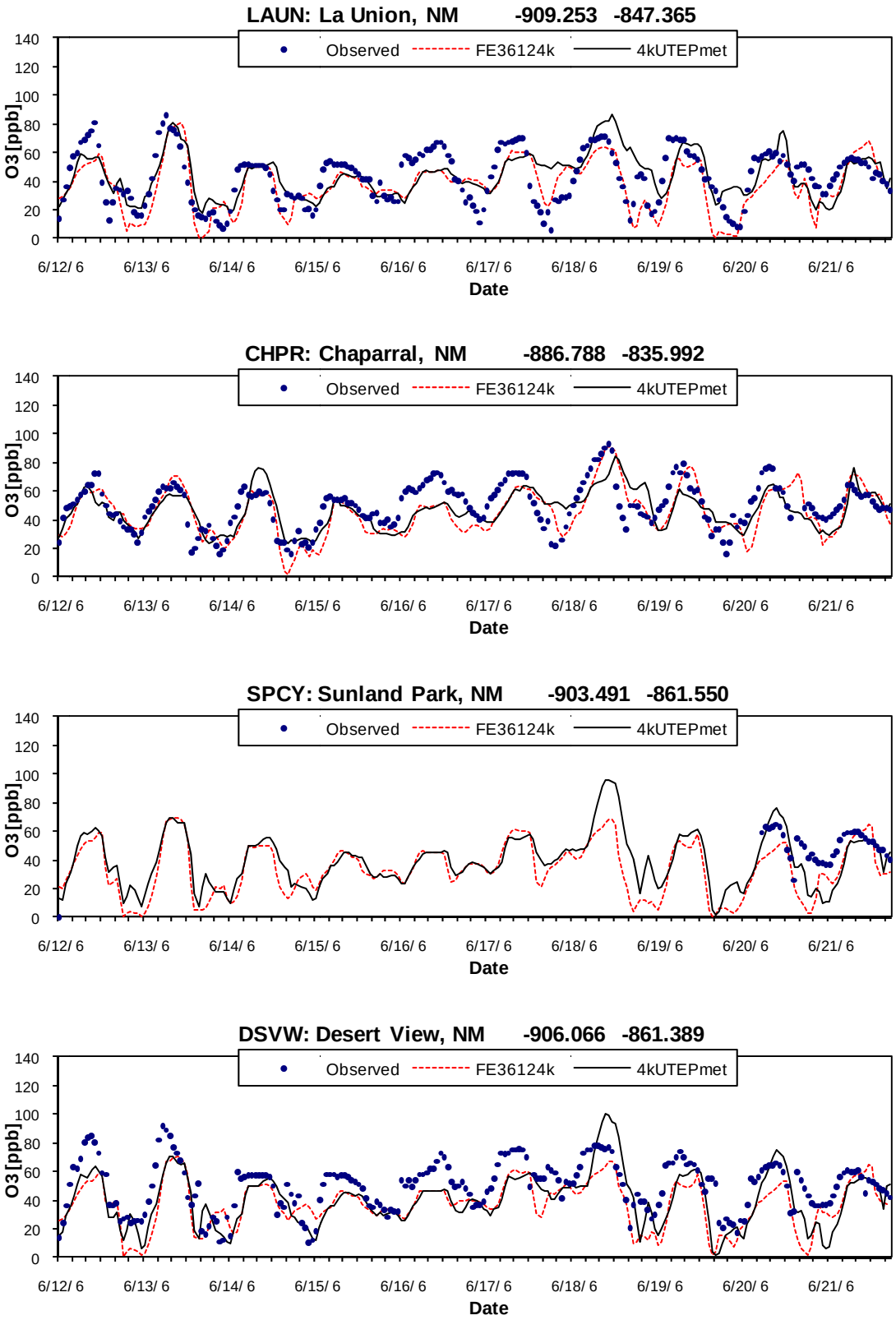

Figure 4-4 (continued). Time series of 1-hour ozone comparing two CAMx simulations.

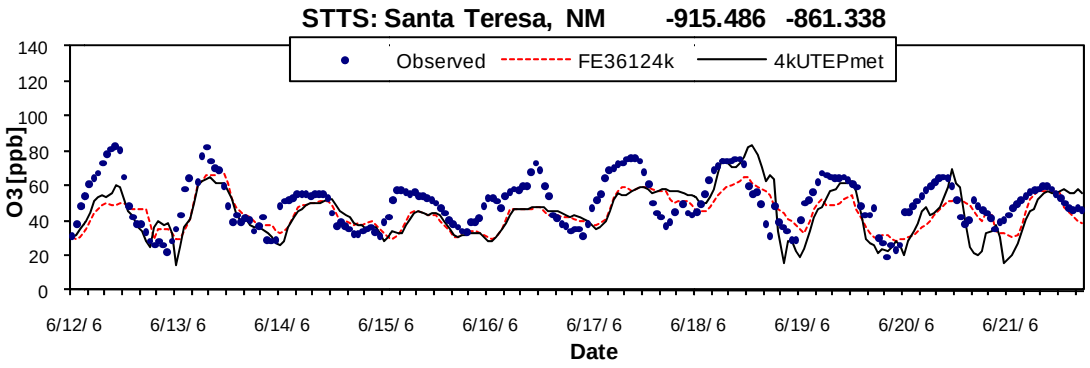

Figure 4-4 (continued). Time series of 1-hour ozone comparing two CAMx simulations.

Time series of observed and predicted 1-hour ozone are shown in Figure 4-4 for each monitor. The diurnal cycle of ozone was reproduced by both simulations although it was offset due to the consistent low bias. The UTEP site in El Paso was well under predicted on all dates, especially in the CAMx flexi-nested simulation.

4.2.2 NOx

Model performance was evaluated for 1-hour NOx at seven monitors throughout the El Paso/Juarez area. Daily statistics are presented in Figure 4-5. Both CAMx simulations under estimated the peak observation on all dates except June 20 in the flexi-nested simulation (Figure 4-5, top). The highest observed NOx was 462 ppb and both simulations failed to capture this extremely high NOx event at Chamizal CAMS 41 during the afternoon (12:00 to 16:00 CST) on June 18 (Figure 4-6). Ozone was titrated to below 20 ppb during this high NOx event and both simulations reproduced the strong ozone titration that was observed (Figure 4-4) even though they under-predicted the observed NOx.

The average paired peak accuracy (Figure 4-5) compares the highest observed 1-hour NOx from each of the seven monitors with their co-located predicted peaks. The NOx average paired peak is less accurate than ozone because NOx is more influenced by local scale features. Days were evenly split between over- and under-prediction of peak NOx for the flexi-nested simulation whereas the 1-way nested simulation under-predicted peak NOx on 7 of 10 days.

The last two statistics compare the normalized bias and error using all hours and sites. Pairings when the observed 1-hour NOx was less than 2 ppb were excluded. There are no model performance goals for NOx. Both simulations over predicted NOx on all dates except June 16 in the flexi-nested simulation. The biases were comparable between the two simulations on high NOx dates (June 17 and 18). Performance was poorest on June 21, the last day of the episode. The CAMx 1-way nested simulation performed better than the flexi-nested simulation on half of the dates modeled. The largest discrepancy between the two simulations occurred on June 20

when the bias of the flexi-nested simulation was four times higher than the 1-way nested simulation.

Time series of NOx (Figure 4-6) reveal an event with very high NOx on the afternoon of June 18. The elevated NOx plume appeared to pass Chamizal and later the Ascarate monitoring sites. Even though both CAMx simulations tended to over-predict NOx on average, they generally could not replicate events with very high NOx that occurred at multiple monitors and on multiple days during the episode. Consequently, it is difficult to reach conclusions about the overall accuracy of the NOx emission inventory used for the CAMx modeling.

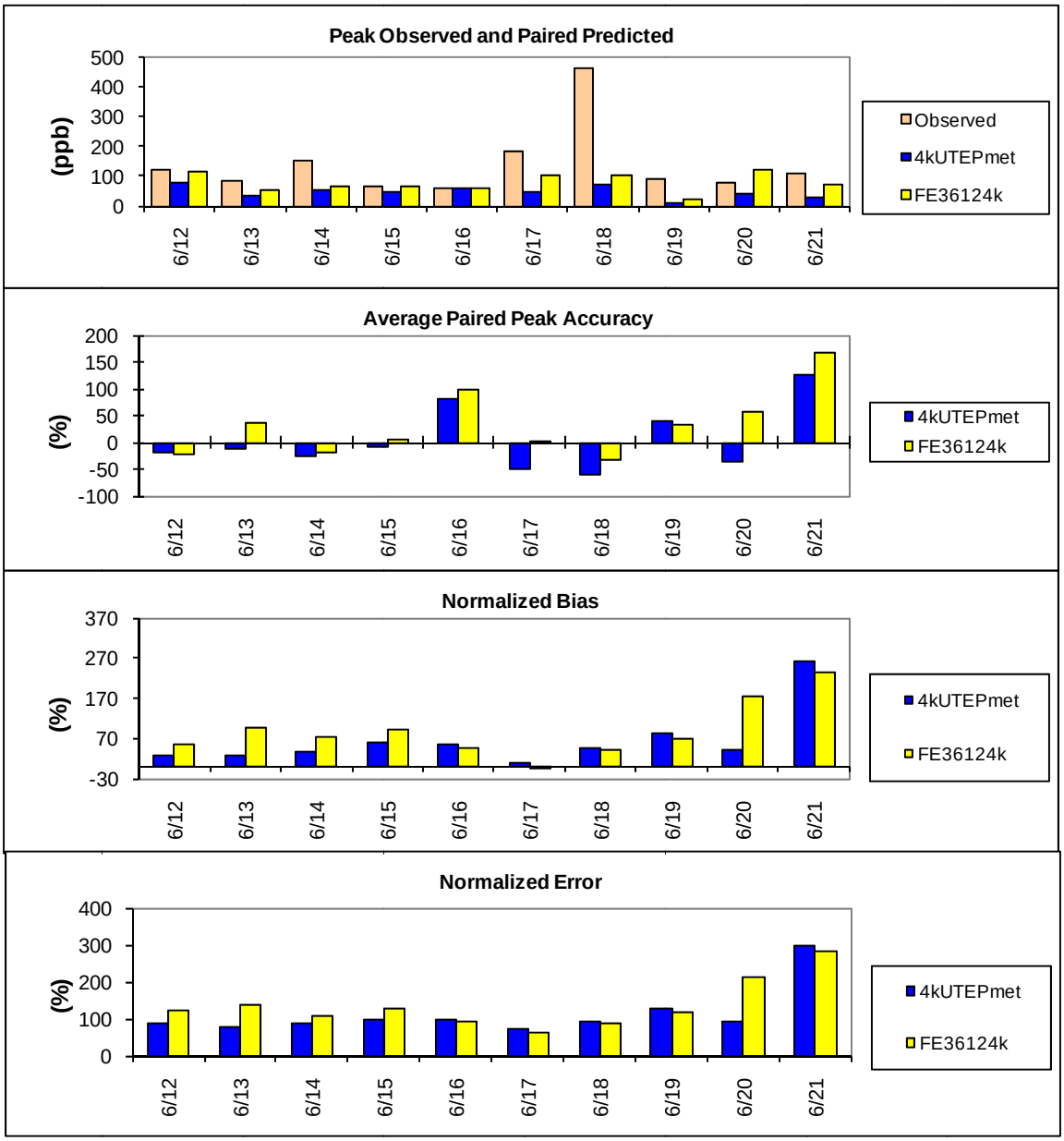

Figure 4-5. Model performance statistics for 1-hour NOx.

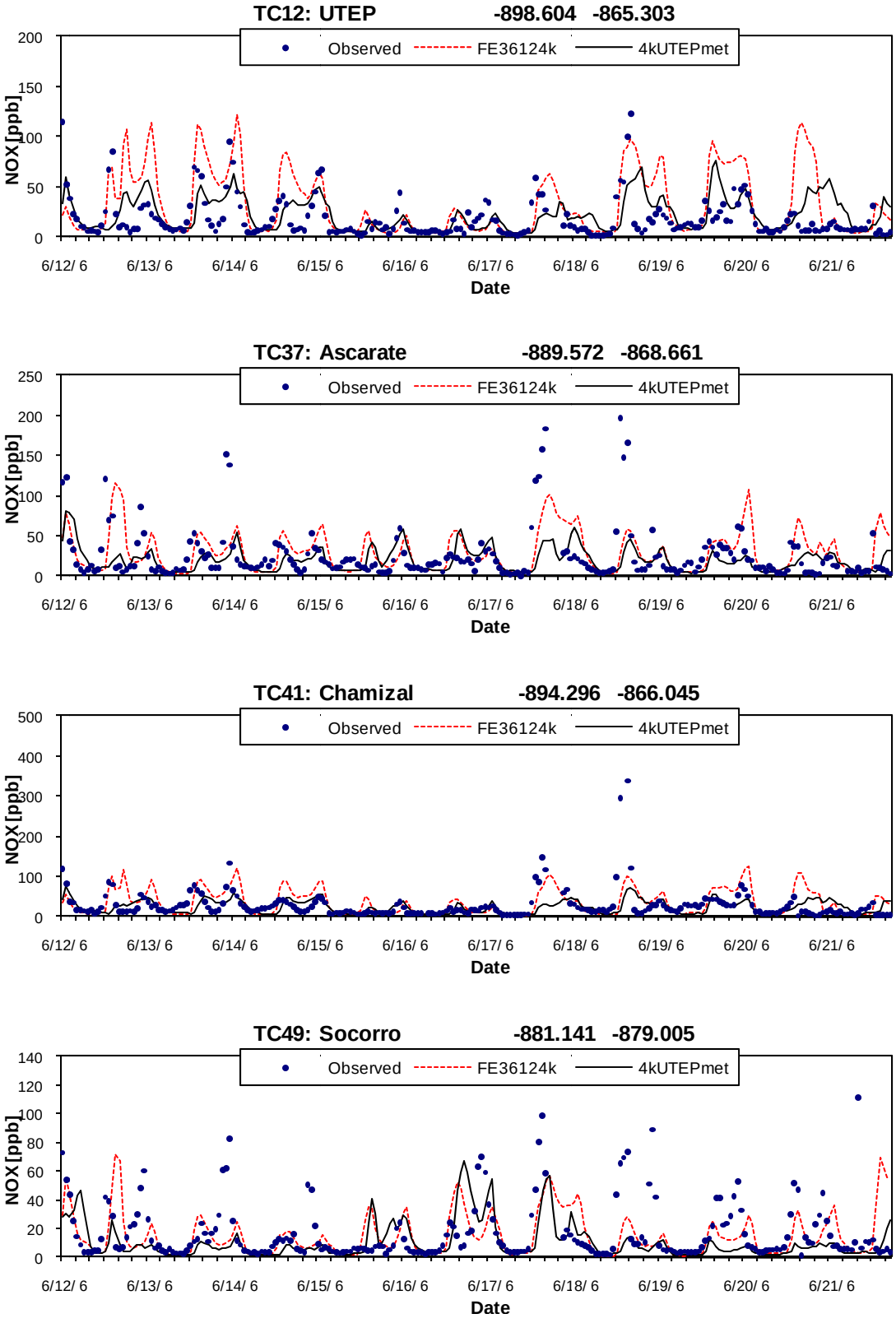

Figure 4-6. Time series of 1-hour NOx comparing two CAMx simulations.

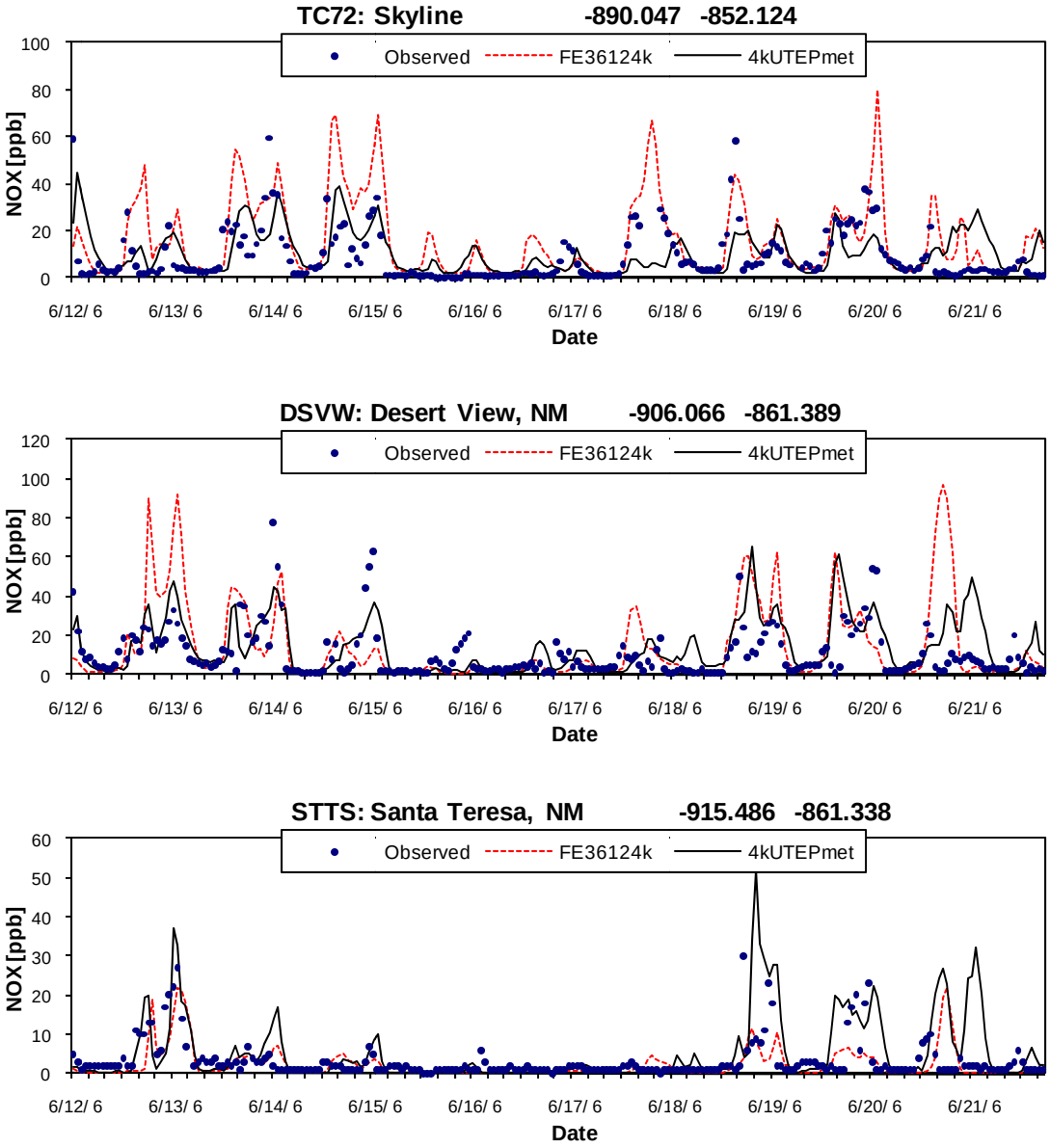

Figure 4-6 (continued). Time series of 1-hour NOx comparing two CAMx simulations.

4.3 Graphical Comparison

4.3.1 Ozone

Spatial plots of the daily maximum 8-hour ozone for each date are shown in Figure 4-7. The 1-way nested simulation is displayed on the left and compared to the flexi-nested simulation in the central panel. The differences (1-way nested minus flexi-nested) are shown on the right. The domain peak location is different on most dates. June 12 and June 18 exemplify this. Animations of hourly ozone and wind vectors for June 12 reveal that the different ozone peak locations result from differences in modeled wind directions. At the UTEP monitoring site, the

observed daily maximum 8-hour ozone was 82 ppb on June18. The 1-way nested run predicted 8-hour ozone in agreement with the observations at UTEP while the flexi-nested run predicted an 8-hour ozone in the 60s (Figure 4-4) with a domain peak of 73 ppb nearby (Figure 4-7).

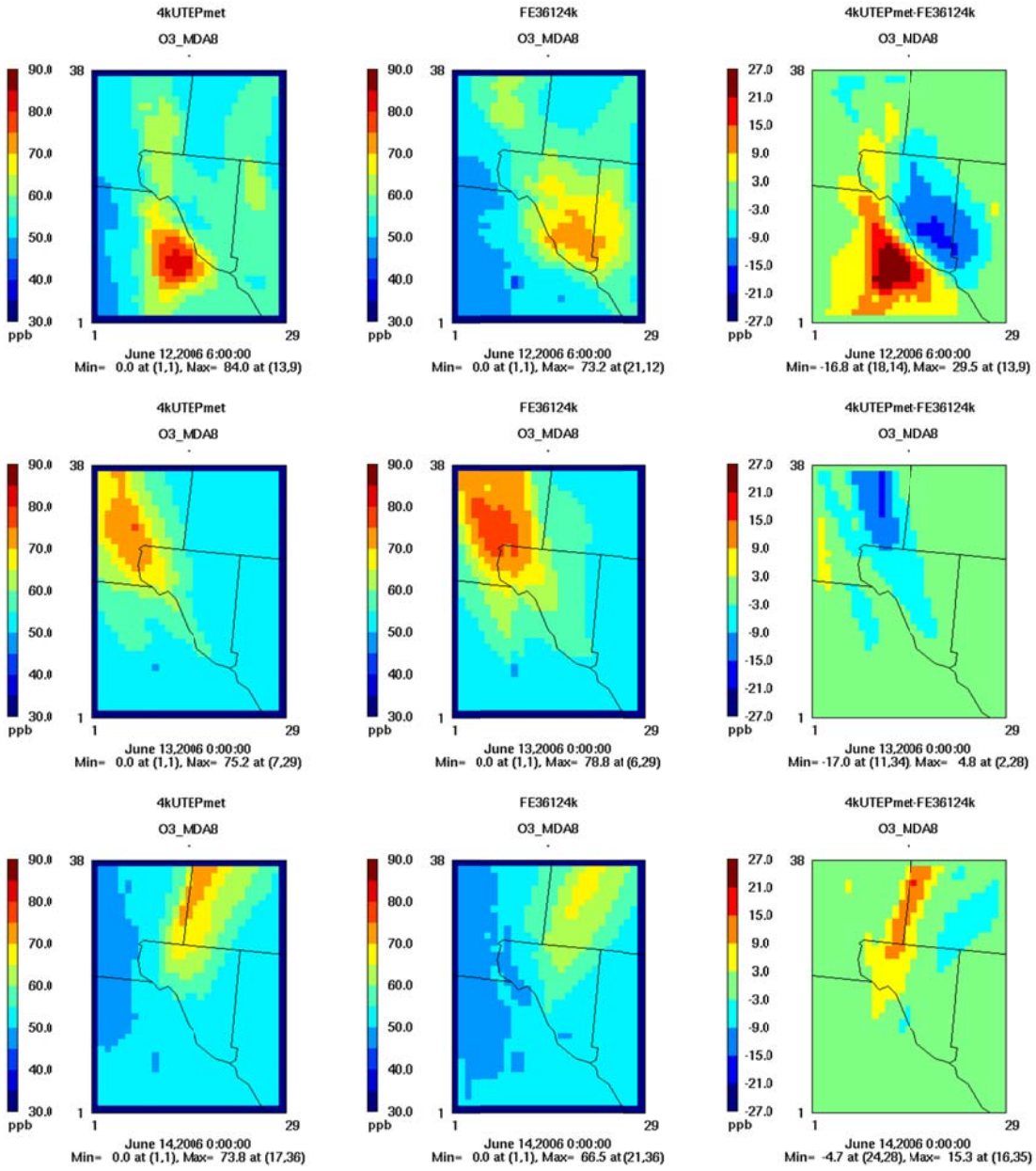

Figure 4-7. Air quality maps showing daily maximum 8-hour ozone concentrations predicted in the 1-way nested CAMx simulation (left panel), the flexi-nested simulation (center panel), and differences between the two simulations (1-way nested minus flexi-nested; right panel) during June 12-21.

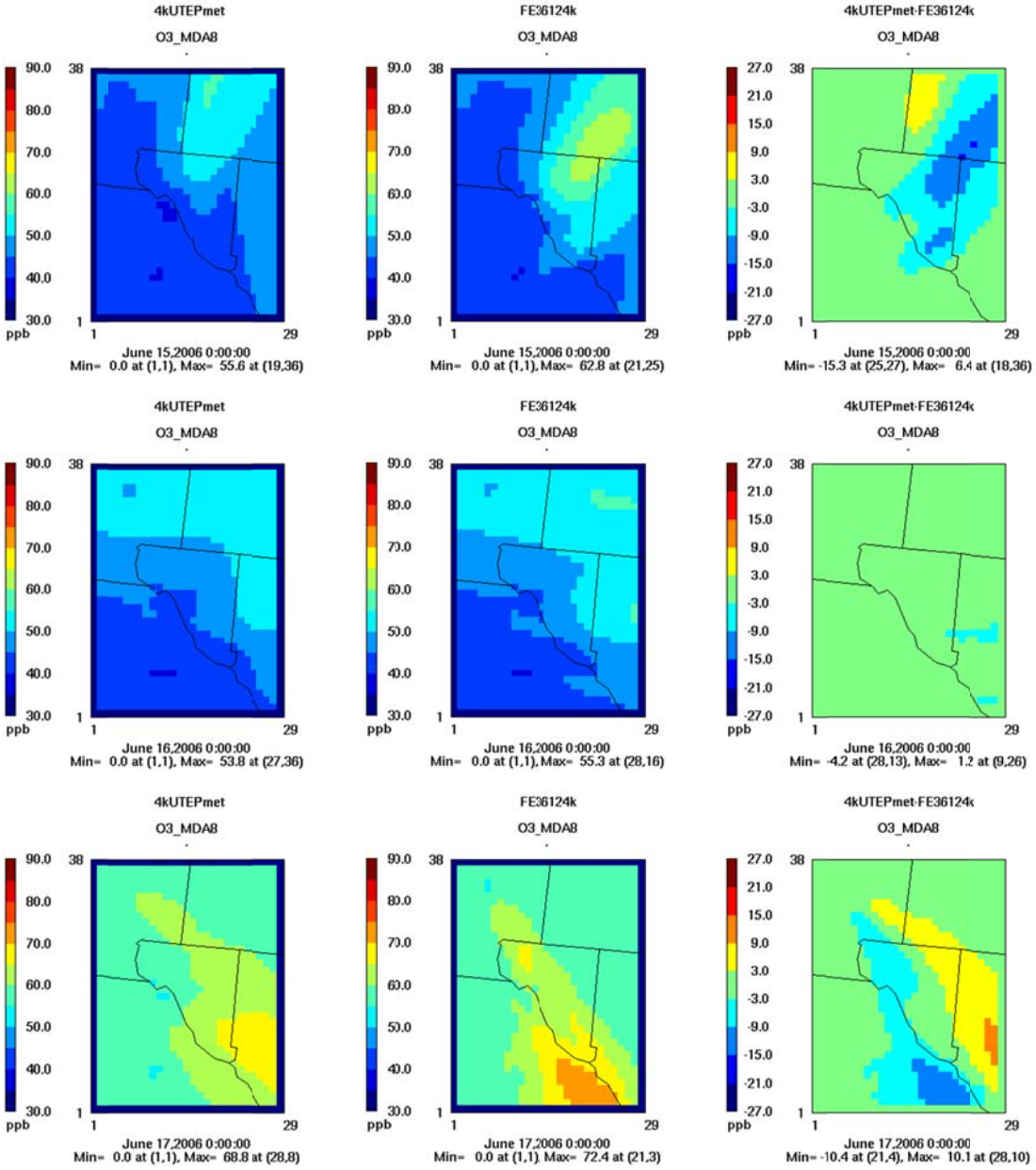

Figure 4-7 (continued). Air quality maps showing daily maximum 8-hour ozone concentrations predicted in the 1-way nested CAMx simulation (left panel), the flexi-nested simulation (center panel), and differences between the two simulations (1-way nested minus Flexi-nested; right panel).

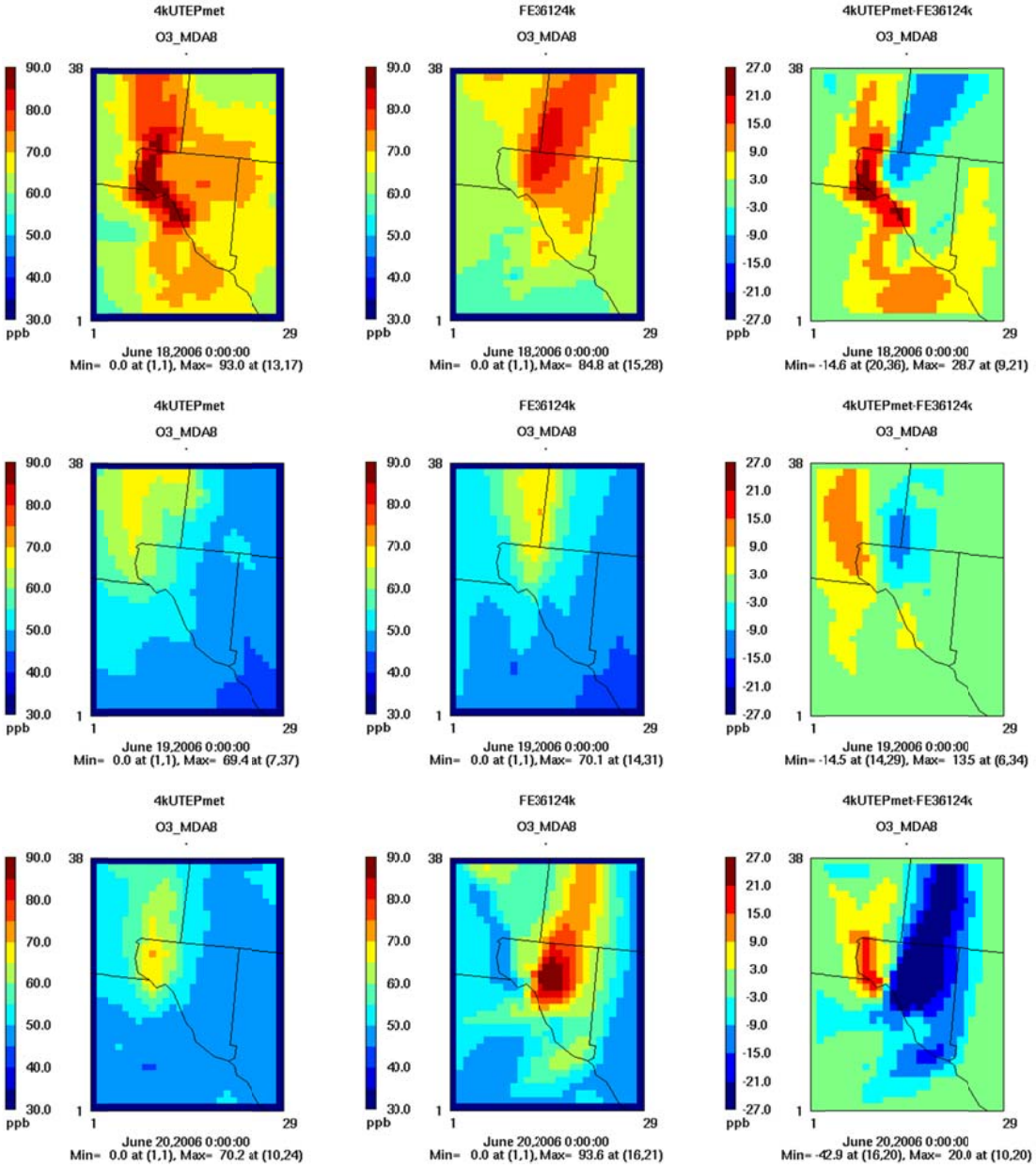

Figure 4-7 (continued). Air quality maps showing daily maximum 8-hour ozone concentrations predicted in the 1-way nested CAMx simulation (left panel), the flexi-nested simulation (center panel), and differences between the two simulations (1-way nested minus Flexi-nested; right panel).

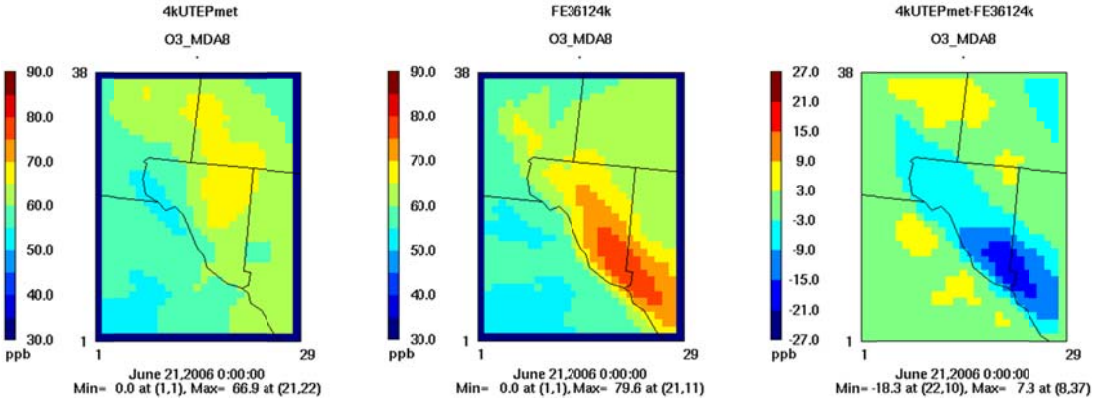

Figure 4-7 (continued). Air quality maps showing daily maximum 8-hour ozone concentrations predicted in the 1-way nested CAMx simulation (left panel), the flexi-nested simulation (center panel), and differences between the two simulations (1-way nested minus Flexi-nested; right panel)

4.3.2 NOx

Spatial plots of the daily maximum 1-hour NOx for each date are shown in Figure 4-8. The 1-way nested simulation is displayed on the left, so they can be compared to the flexi-nested simulation on the right. Overall, the flexi-nested run resulted higher domain peaks and spread out the areas of elevated NOx. The two runs agree well on the domain peak location.

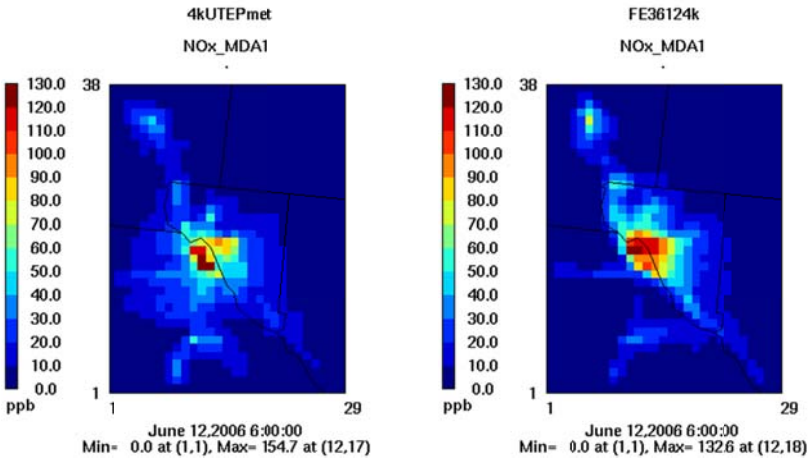

Figure 4-8. Air quality maps showing daily maximum 1-hour NOx concentrations predicted in the 1-way nested CAMx simulation (left panel) and the flexi-nested simulation (right panel).

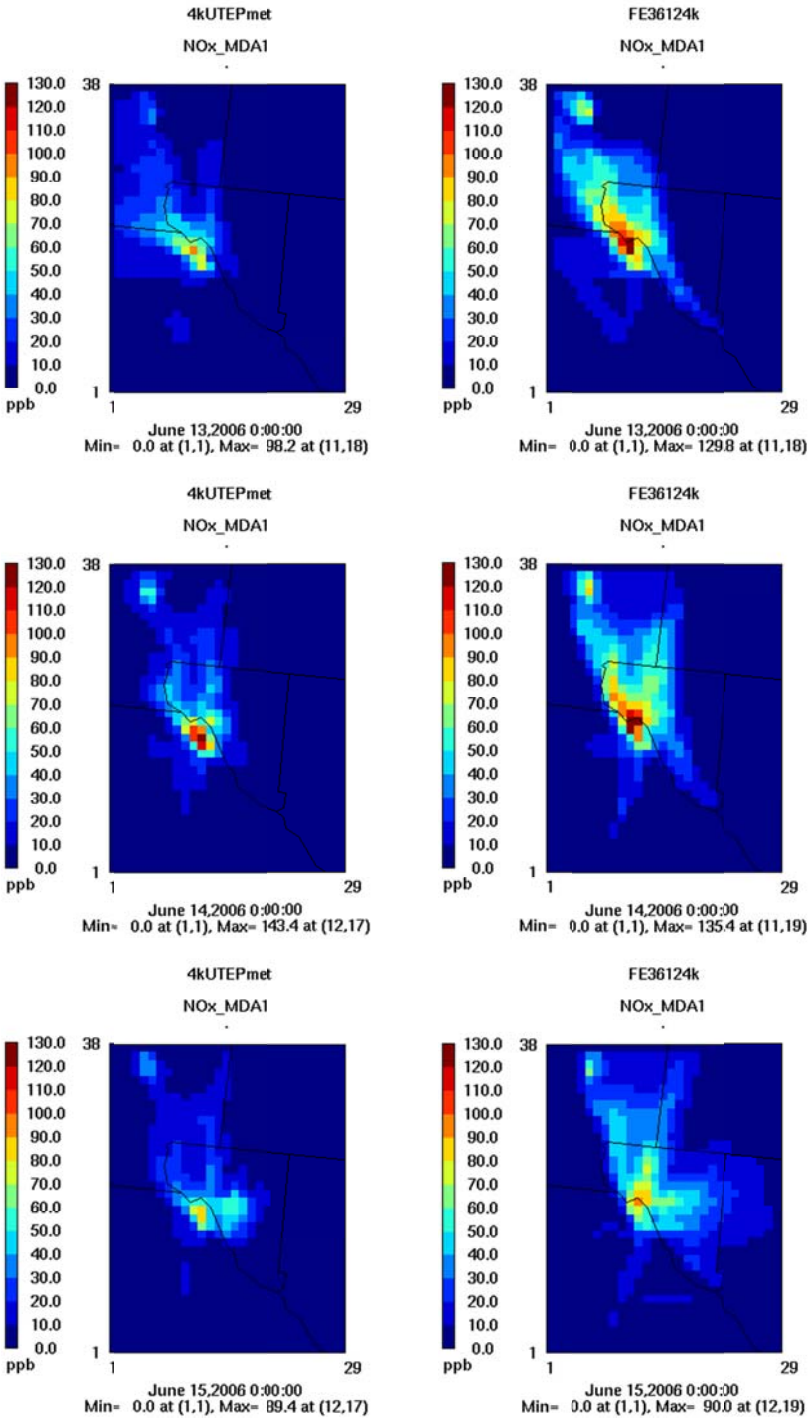

Figure 4-8 (continued). Air quality maps showing daily maximum 1-hour NOx concentrations predicted in the 1-way nested CAMx simulation (left panel) and the flexi-nested simulation (right panel).

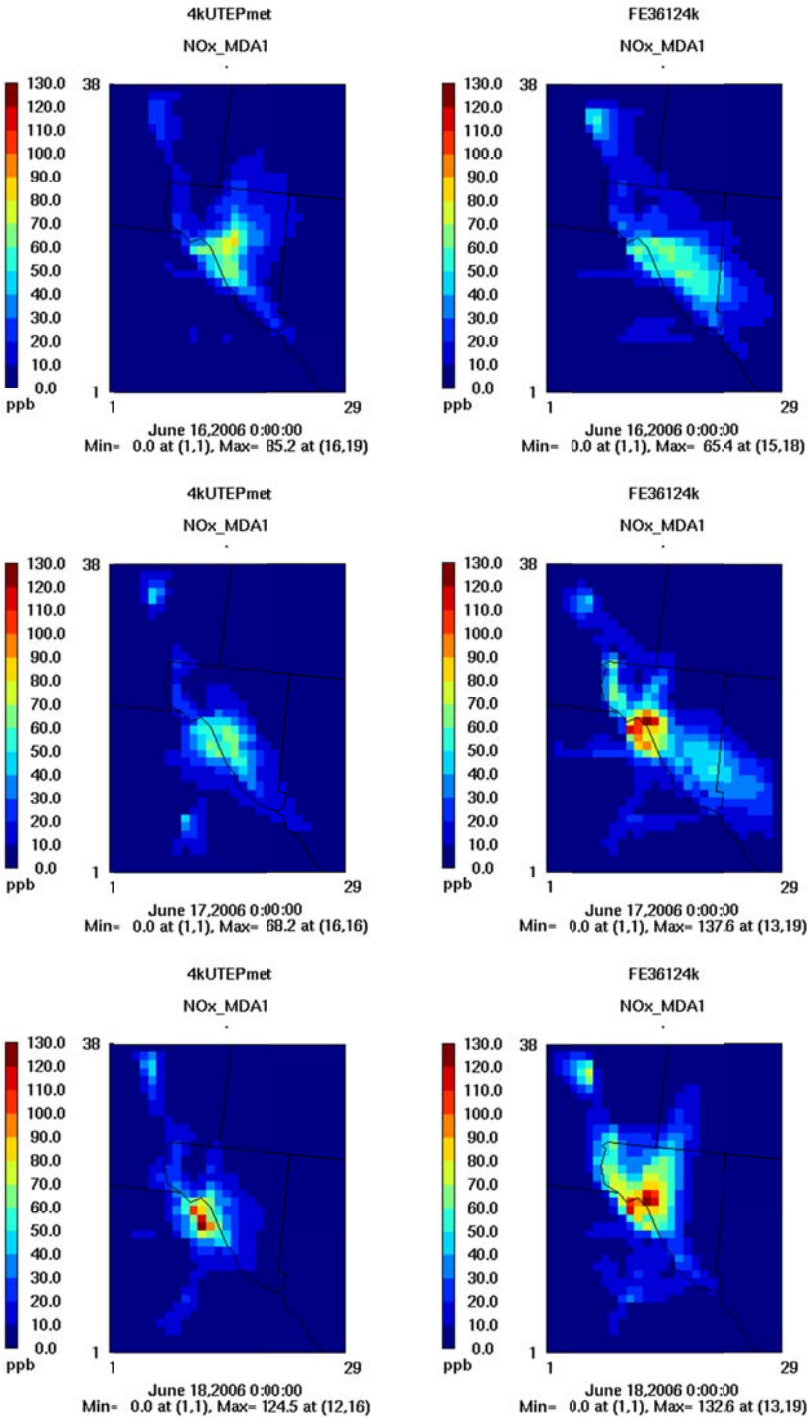

Figure 4-8 (continued). Air quality maps showing daily maximum 1-hour NOx concentrations predicted in the 1-way nested CAMx simulation (left panel) and the flexi-nested simulation (right panel).

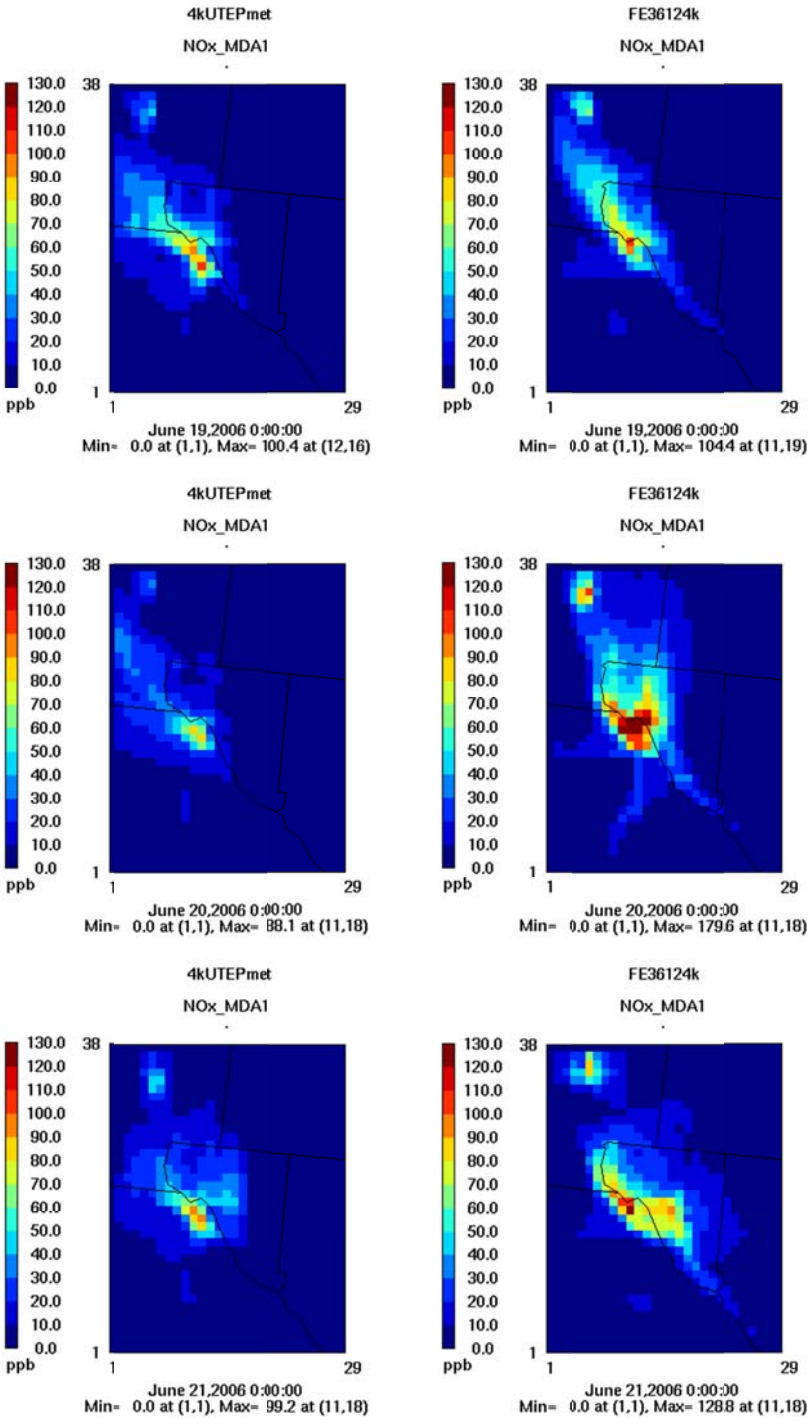

Figure 4-8 (continued). Air quality maps showing daily maximum 1-hour NOx concentrations predicted in the 1-way nested CAMx simulation (left panel) and the flexi-nested simulation (right panel).

5.0 SUMMARY

ENVIRON enhanced the Rider 8 June 2006 CAMx modeling dataset developed by the TCEQ, which consists of a national grid with 36 km resolution and a south-central US grid with 12 km resolution, by adding a 4 km resolution grid specifically covering El Paso/Juarez. ENVIRON developed 4 km modeling inputs including anthropogenic and biogenic emissions, meteorology, initial/boundary conditions, and other CAMx input data.

ENVIRON performed two CAMx base case simulations of June 12-21, 2006 employing alternative approaches in defining 4 km grid meteorology. Both simulations used identical 4 km El Paso/Juarez emission inputs. The first CAMx simulation ran the TCEQ 36/12 km grids together with the 4 km grid in 2-way nested mode, where meteorology on the 4 km grid was internally interpolated by CAMx from the 12 km meteorology (called flexi-nesting). The second CAMx simulation was run for the single 4 km grid alone using meteorological data from UTEP's application of WRF. Boundary conditions for the 4 km grid were extracted from CAMx runs on the 36/12 km grid in a manner referred to as 1-way nesting. This was necessary to most appropriately accommodate the potentially different meteorology and different vertical grid structures between the 4 km (UTEP) and 12 km (TCEQ) meteorological data.

A model performance evaluation for ozone and NOx was carried out for monitoring sites in the El Paso/Juarez area. The model performance evaluation showed:

- CAMx under predicted ozone on all dates for both simulations. The CAMx 1-way nested simulation met the ±15% normalized bias goal on the two ozone exceedance dates and the bias was lower than the flexi-nested simulation on nine out of ten dates modeled.
- Both simulations satisfied the 35% error performance goal for ozone on all dates. The errors are similar in magnitude to bias indicating that underestimation trends are consistent in time and space.
- Both CAMx simulations tended to over-predict NOx on average but under-predicted events with very high NOx that occurred throughout the episode. Consequently, it is difficult to reach conclusions about the overall accuracy of the NOx emission inventory used for the CAMx modeling.

Review of the spatial distributions of ozone and NOx reveals that ozone under prediction is related to the NOx over prediction. Potential causes include over estimated NOx emissions or under estimated dispersion of NOx emissions (e.g., because of under estimated vertical dilution). Under estimated VOC emissions also could be a contributing factor to under estimated peak ozone concentrations. Sensitivity tests with alternative meteorology or modified vertical diffusivity fields (Kv) should be conducted.

Note that the set of observational data utilized in these model performance evaluations should be reviewed. There are many occurrences where observed NOx concentrations are lower than the sum of individual NO and NO_2 concentrations. In addition, zero NOx is reported for multiple consecutive hours.

6.0 REFERENCES

DeFries, R. Hansen, M., Townshend, J.R.G., Janetos, A.C., and Loveland, T.R. 2000. A new global 1km data set of percent tree cover derived from remote sensing, Global Change Biology, 6, 47-254.

ENVIRON, 2011 . User's Guide to the Comprehensive Air Quality Model with Extensions (CAMx). Version 5.4.Available at: http://www.camx.com.

EPA. 2007. Guidance on the Use of Models and Other Analyses for Demonstrating Attainment of Air Quality Goals for Ozone, PM2.5, and Regional Haze. Prepared by the U.S. Environmental Protection Agency, Office of Air Quality Planning and Standards, Air Quality Analysis Division, Air Quality Modeling Group, Research Triangle Park, NC (EPA - 454/B-07-002, April 2007).

Guenther, A., T. Karl, P. Harley, C. Wiedinmyer, P. Palmer, and C. Geron. 2006. Estimates of global terrestrial isoprene emissions using MEGAN (Model of Emissions of Gases and Aerosols from Nature), Atmos. Chem Phys., 6, 3181-3210.

Hansen, M., DeFries, R., Townshend, J. R. G., and Sohlberg, R. 2000. Global land cover classification at 1km resolution using a decision tree classifier, International Journal of Remote Sensing. 21, 1331-1365.

Hansen, M., DeFries, R. S., Townshend, J. R. G., Carroll, M., Dimiceli, C., and Sohlberg. R. A., 2003. Global Percent Tree Cover at a Spatial Resolution of 500 Meters: First Results of the MODIS Vegetation Continuous Fields Algorithm" Earth Interactions, 7 (10), 1–15.

Latifovic, R., Z-L Zhu, J. Cihlar and C. Giri. 2002. Land cover of North America 2000. Natural Resources Canada, Canada Centre for Remote Sensing, US Geological Service EROS Data Center.

Sakulyanontvittaya, T., Duhl, T., Wiedinmyer, C., Helmig, D., Matsunaga, S., Potosnak, M., Milford, J., and Guenther, A. 2008. Monoterpene and Sesquiterpene Emission Estimates for the United States, Environ. Sci. Technol., 42, p. 1623-1629.

Appendix B

Sensitivity Analysis

CAMx simulations were developed for 12 scenarios which modified Cd. Juárez area source VOC and / or NOx emissions. Model performance was evaluated for daily maximum 1-hour and 8-hour ozone. Comparisons were made of the PREDICTED ozone concentrations vs. ozone concentrations OBSERVED at the regional CAMS across the modeled domain. Only 1 CAMS, C662, was not included in this assessment due to the current limitations in the OBSCAT, which is one of the CAMx post-processing tools.

This appendix discusses CAMx simulation results for 18 June, 2006. Photochemical modeling relies on a suite of statistics to determine model performance. Each of the 12 simulations produced a set of results to assess potential air quality improvement strategies based on modifications to NOx or VOC emissions. More importantly, CAMx includes a suite of statistical tools to determine if the emissions modifications fall within acceptable parameters regarding model performance.

On 18 June, C663 observed the highest 8-hour ozone concentration among the 8 CAMS observing an exceedance of the 8-hour ozone NAAQS. C663 also observed the highest 8-hour ozone concentrations in the PdN region during 2006, 0.099 ppm on 26 August, 2006 as indicated in Table 11.5. On the US side of the border, C12 at UTEP tends to observe the highest ozone concentrations and multiple exceedances during the year.

1. Model Performance Goals

Each simulation must generate results that are within acceptable parameters for Normalized Bias (NB) and Normalized Error (NE) as air quality models in order to be acceptable for NAAQS modeling purposes (EPA, 2007). NB and NE are important statistics in assessing the accuracy of the model to predict ambient ozone. Model performance goals for NB and NE are $\pm$15% and $\leq$35% respectively. Positive NB indicates over-prediction of ozone and negative NB indicates under-prediction of ozone. NE and NB are based on all predicted and observed values in the modeling simulation for the entire 4 km domain. Equation 1.1 is applied to calculate NE, and Equation 1.2 is applied to calculate NB.

Acceptable Parameters

$$NME = \frac{\sum_{1}^{N} |Model - Obs|}{\sum_{1}^{N} (Obs)} \cdot 100\%$$

NE $\leq$ 35% Equation 1.1

$$NMB = \frac{\sum_{1}^{N} (Model - Obs)}{\sum_{1}^{N} (Obs)} \cdot 100\%$$ -15% ≤ NB ≥ +15% Equation 1.2

1.1 Model Performance Definitions

Table 1.1 presents model performance results and statistics for 1-hour ozone. PEAK OBSERVED (PeakObs) and PREDICTED PEAK (PredPeak) ozone plus the suite of statistics generated by CAMx are identified. The maximum PeakObs on 6/18 was 120.7 ppb.

Table 1.1 Results and Statistics for 1-Hour Ozone Simulations

RUN ID		1201-0000	1201-0900	1201-1100	1201-1300	1201-2100	1201-2300	1202-1000	1202-1300	1202-1500	1202-1800	1202-2330	1203-0200
RUN ID	BASELINE	1	2	3	4	5	6	7	8	9	10	11	12
Cell	13,18	13,18	13,17	11,26	13,17	13,18	13,18	13,18	13,17	13,17	11,26	13,17	11,26
PredPeak	103.3	102.1	102.4	91.7	102.9	113.0	92.7	100.1	102.3	119.7	86.8	118.8	87.8
PeakObs	120.7	120.7	120.7	120.7	120.7	120.7	120.7	120.7	120.7	120.7	120.7	120.7	120.7
PairPred	99.3	89.1	98.4	86.7	107.8	108.7	96.9	89.1	97.6	112.1	80.1	113.6	83.3
UPPA	-14.4	-23.2	-15.1	-24	-5.6	-6.4	-15.4	-23.2	-15.3	-0.9	-28.1	-1.6	-27.2
APPA	-1.5	-8.7	-2.1	-10	4.8	5.2	-2.6	-8.7	-2.7	7.8	-14.6	8.6	-12.8
EPPA	12.2	14.4	11.9	15.3	13.1	13.2	12.6	14.4	11.9	15.2	17.2	15.2	16
PTB	4	4	3	4	3	4	4	4	3	3	4	4	4
NB	-3.3	-6.7	-2.1	-8.7	1.2	0.1	-5.2	-6.7	-1.8	3.1	-11.5	1.8	-8.7
NE	25.6	23.2	24.2	24.2	27.1	28.1	26.2	23.2	23.3	27.8	23.9	29.5	22.4
PredPeak | BL-PredPeak		-1.1	-0.8	-11.2	-0.4	9.4	-10.3	-3.1	-1.0	15.8	-16.0	15.0	-15.0
PairPred | BL-PairPred		-10.3	-0.9	-12.7	8.6	9.5	-2.4	-10.3	-1.7	12.9	-19.3	14.4	-16.1
PredPeak | Peak Obs		-15.4	-15.1	-24.0	-14.8	-6.4	-23.2	-17.1	-15.3	-0.9	-28.1	-1.6	-27.2
NOx		↑ 50%	↓ 50%			↑ 50%	↓ 50%	↑ 75%	↓ 75%			↑ 75%	↓ 75%
VOC				↓ 50%	↑ 50%	↑ 50%	↓ 50%			↑ 75%	↓ 75%	↑ 75%	↓ 75%

Mid-Table 1.1 presents the difference between RUNS with modified emissions compared to BASELINE results, where BASELINE has the same run configuration as Run 2a in Chapter 5 and Appendix A of this report. Abbreviations in Table 1.1 are explained below:

- PredPeak | BL-PredPeak indicates the difference between the PredPeak for the specific RUN and BASELINE PredPeak.
- PairPred | BL PairPred indicates the difference between the PAIRED PREDICTED PEAK value and the BASELINE PAIRED PREDICTED PEAK. The PairPred Peak represents the peak value predicted by CAMx that is paired to the specific CAMS observed value. CAMx generates a PredPeak value for each grid cell for each time-step and interpolates a predicted ozone concentration at the CAMS within the grid cell taking into consideration

the concurrent time-step ozone values at the adjacent cells for the purposes of interpolating an ozone concentration value at the specific CAMS.

- PredPeak | PeakObs indicates the difference between the PREDICTED PEAK and the PEAK OBSERVED value for each RUN. The PeakObs value does not change given this is the peak 1-hour ozone concentration on 6/18. This variable helps determine the model performance by indicating the variation between predicted and observed peaks and the impact on ozone concentrations due to emissions modifications.

1.2 Model Performance Summary for 1-Hour Ozone

Comparing each RUN to BASELINE data in Table 1.1 indicates that modifying VOC emissions generated the greatest variability in 1-hour ozone. Modifications to NOx generated minimal variability in 1-hour ozone. Comparing PredPeak | BL-PredPeak indicates that increasing only NOx by 50% (RUN 1) or 75% (RUN7) results in reduced 1-hour ozone by 1.1 ppb and 3.1 ppb respectively. Reducing only NOx by 50% (RUN2) or 75% (RUN8) reduced 1-hour ozone 0.8 ppb and 1.1 ppb respectively. NOx tends to titrate ozone albeit minimally as compared to the BASELINE results.

Increasing only VOC by 50% or 75% resulted in improved bias by 2% compared to BASELINE. Increasing or decreasing both VOC and NOx combined did not produce results significantly different from VOC-only modifications. Modifications to NOx emissions, at existing concentrations, are insignificant contributors to improvements or further degradation of air quality. These results indicate that the PdN region ozone formation conditions are VOC-limited as will be discussed for each RUN in the following section.

Figure 1.1 presents the PAIRED PREDICTED PEAK for 1-hour ozone CAMx simulation RUNS. The yellow bar at the base of the graph represents results identified as BASELINE. The PAIRED PREDICTED PEAK for 1-hour compares ozone concentrations observed at the CAMS to a concentration predicted by CAMx.

Figure 1.2 presents the PREDICTED PEAK 1-hour ozone concentrations. This value represents the maximum ozone concentration within any particular grid cell in the modeling domain regardless of location within the cell. As can be observed in either Figure 1.1 or Figure 1.2, the greatest variability in 1-hour ozone concentrations occurs when VOC emissions are modified.

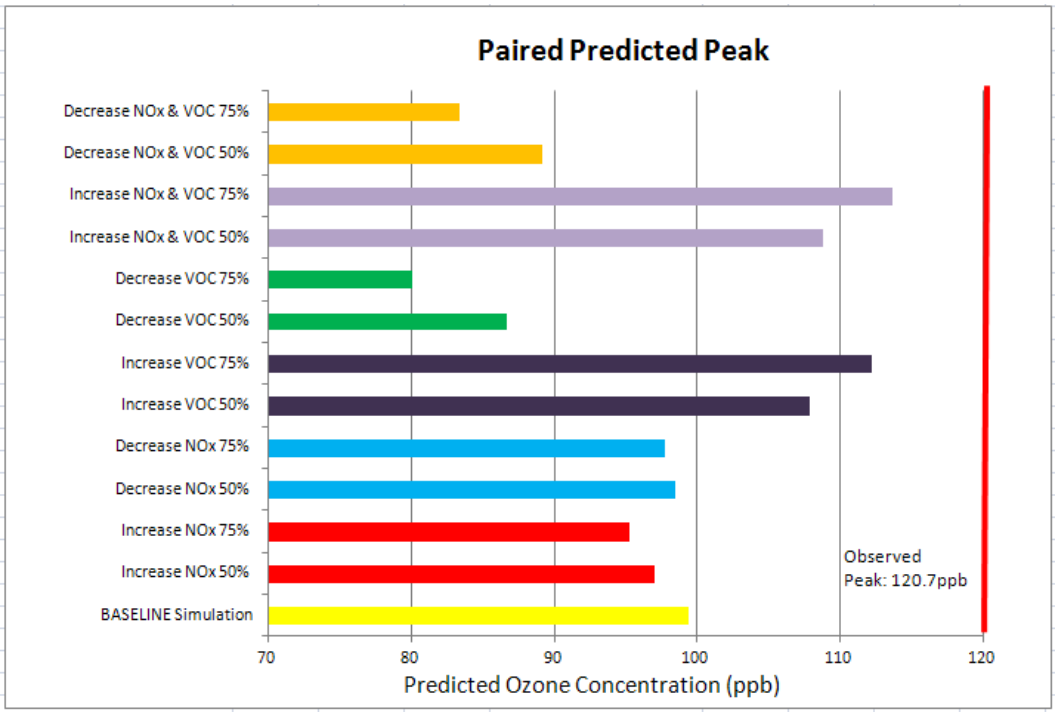

Figure 1.1 Paired Predicted Peak for CAMx Simulations and 1-Ho

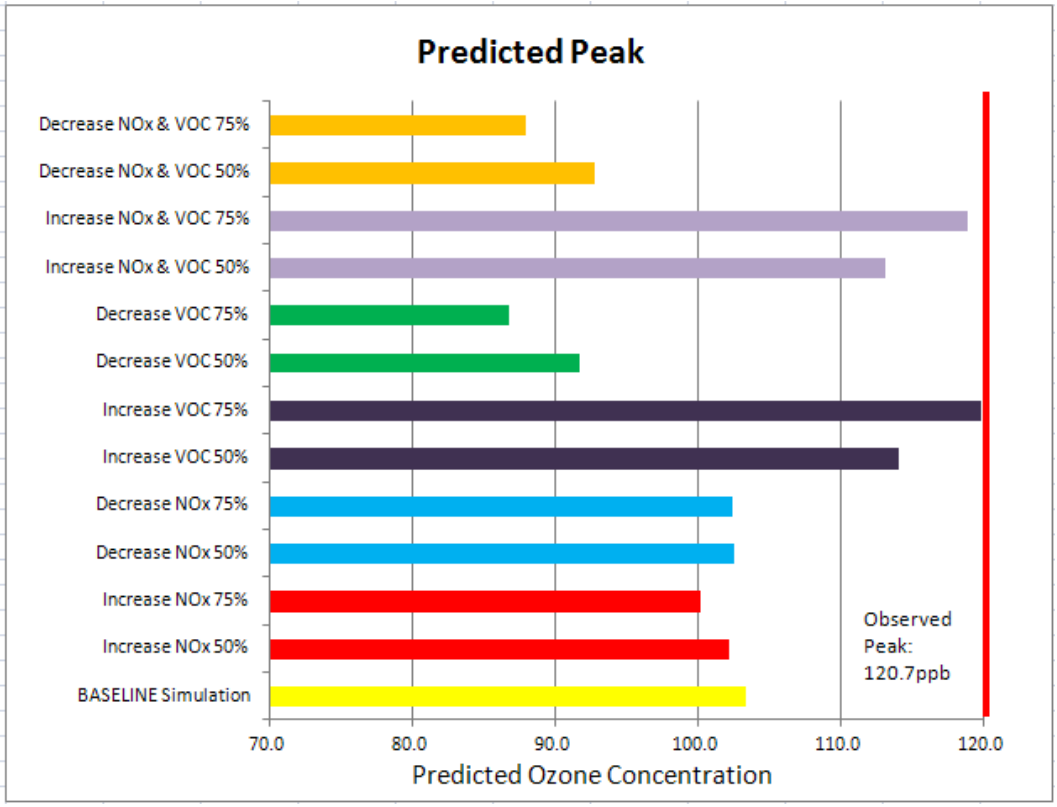

Figure 1.2 PREDICTED PEAK for CAMx Simulations and 1-Hour Ozone

While all simulations consistently under-predict the PEAK OBSERVED 1-hour ozone concentrations, modifying VOC emissions tends to generate predicted 1-hour ozone peaks closer to the PEAK OBSERVED concentration. Increasing or decreasing combined NOx and VOC emissions vary little from modifications to VOC emissions alone.

1.3 Results and Statistics for 8-Hour Ozone

Table 1.2 presents the results and statistics for 8-hour ozone simulations for 18 June. PEAK OBSERVED and PREDICTED PEAK ozone plus the suite of statistics generated by CAMx are also indicated. 8-hour ozone results varied significantly from 1-hour ozone results. The maximum 8-hour PEAK OBSERVATION on 6/18 was 95.1 ppb.

Table 1.2 Results and Statistics for 8-Hour Ozone Simulations

RUN ID		1201-0000	1201-0900	1201-1100	1201-1300	1201-2100	1201-2300	1202-1000	1202-1300	1202-1500	1202-1800	1202-2330	1203-0200
RUN ID	BASELINE	1	2	3	4	5	6	7	8	9	10	11	12
Cell	13,18	13,18	13,17	11,27	13,17	13,18	13,18	14,17	13,17	13,17	11,27	13,17	11,27
PeakObs	95.1	95.1	95.1	95.1	95.1	95.1	95	95.1	95.1	95.1	95.1	95.1	95.1
PredPeak	93	90.11	94.05	83.22	102.85	101.76	84.49	89	93.28	107.08	80.51	106.31	80.71
PairPred	92.1	83.6	92.6	80.3	100.5	100	83.6	88.3	86.9	103.7	73.8	104.1	78.8
UPPA	-2.1	-11.1	-1	-12.4	8.3	7.1	-11.1	-5.2	-7	12.7	-15.3	11.9	-15.1
APPA	2.5	-3.9	3	-5.9	9	8.5	-3.9	0.6	-0.7	11.6	-10.5	11.7	-7.6
EPPA	9	8.3	9.5	8.9	14.3	13.7	8.3	8.5	8.5	16.6	12.1	16.4	9.5
PTB	3	3	3	3	3	3	3	3	3	3	3	3	3
NB	3.9	0.4	5.4	-1.8	8.8	7.4	0.4	1.8	0.6	10.8	-4.8	9.2	-1.6
NE	23.7	22.1	22.4	23	24.4	25.4	22.1	24.3	24.5	24.8	22.8	26.5	21.5
PredPeak | BL-PredPeal		-3.1	1.1	-10.5	10.6	9.4	-9.2	-4.3	0.3	15.1	-13.4	14.3	-13.2
PairPred | BL-PairPred		-9.2	0.5	-12.8	9.1	8.6	-9.2	-4.1	-5.6	12.6	-19.9	13.0	-14.4
PredPeak | Peak Obs		-5.2	-1.1	-12.5	8.1	7.0	-11.1	-6.4	-1.9	12.6	-15.3	11.8	-15.1
NOx		↑ 50%	↓ 50%			↑ 50%	↓ 50%	↑ 75%	↓ 75%			↑ 75%	↓ 75%
VOC				↓ 50%	↑ 50%	↑ 50%	↓ 50%			↑ 75%	↓ 75%	↑ 75%	↓ 75%

Comparing each RUN to the BASELINE data indicate that modifying VOC emissions generates the greatest variability in 8--hour ozone concentrations. Model performance statistics presented in Table 1.2 are generated by comparing 8-hour predicted averages to 8-hour average observed ozone.

Modifications to NOx generated minimal variability in 8-hour ozone. NE and NB improved by 1.6% and 0.7% when NOx emissions increase or decrease by 50% respectively when compared to the BASELINE. The variability in 8-hour ozone was sufficient to quality modifications to NOx emissions as a potential air quality control strategy if only a 1 or 2 ppb reduction in ozone is required to attain a modified 8-hour ozone NAAQS. As reported earlier, El Paso's design value in 2011 was 71 ppb. Reducing the NAAQS to a hypothetical concentration of 70 ppb, for example, would cause El Paso to be designated nonattainment of the new NAAQS. As reported by ENVIRON (Appendix A), elevated NOx concentrations in the PdN ambient air tends to titrate ozone albeit minimally.

Increasing only VOC by 50% or 75% produced results which did not significantly change the NE or NB. Increasing or decreasing both VOC and NOx combined did not produce results which significantly differ from modification on RUNs with only VOC modifications. This indicates that modifications to NOx emissions, at existing concentrations, are insignificant contributors to improvements or further degradation of air quality when coupled with modification to VOC. It should be noted that Cd. Juarez comprises 83.4% of regional area source NOx emissions (20.1 TPD vs. 3.35 TPD for El Paso). Juarez area sources comprise roughly 33% of all Cd. Juarez NOx emissions considering only the modeled emissions inventory. As has been indicated, the regional modeled EI requires substantial modifications insofar as point source NOx emissions are concerned.

It should also be noted that NE for all simulations was $\leq$35% which is within acceptable parameters. NB for all simulations was between $\pm$15% which is also within acceptable parameters. A discussion on the specific runs is provided in the following section. Figure 1.3 presents the PAIRED PREDICTED PEAK for CAMx simulations and 8-hour ozone. The yellow bar at the base of the graph represents BASELINE results. The greatest variability in 8-hour ozone concentrations occurs when VOC emissions increase or decrease.

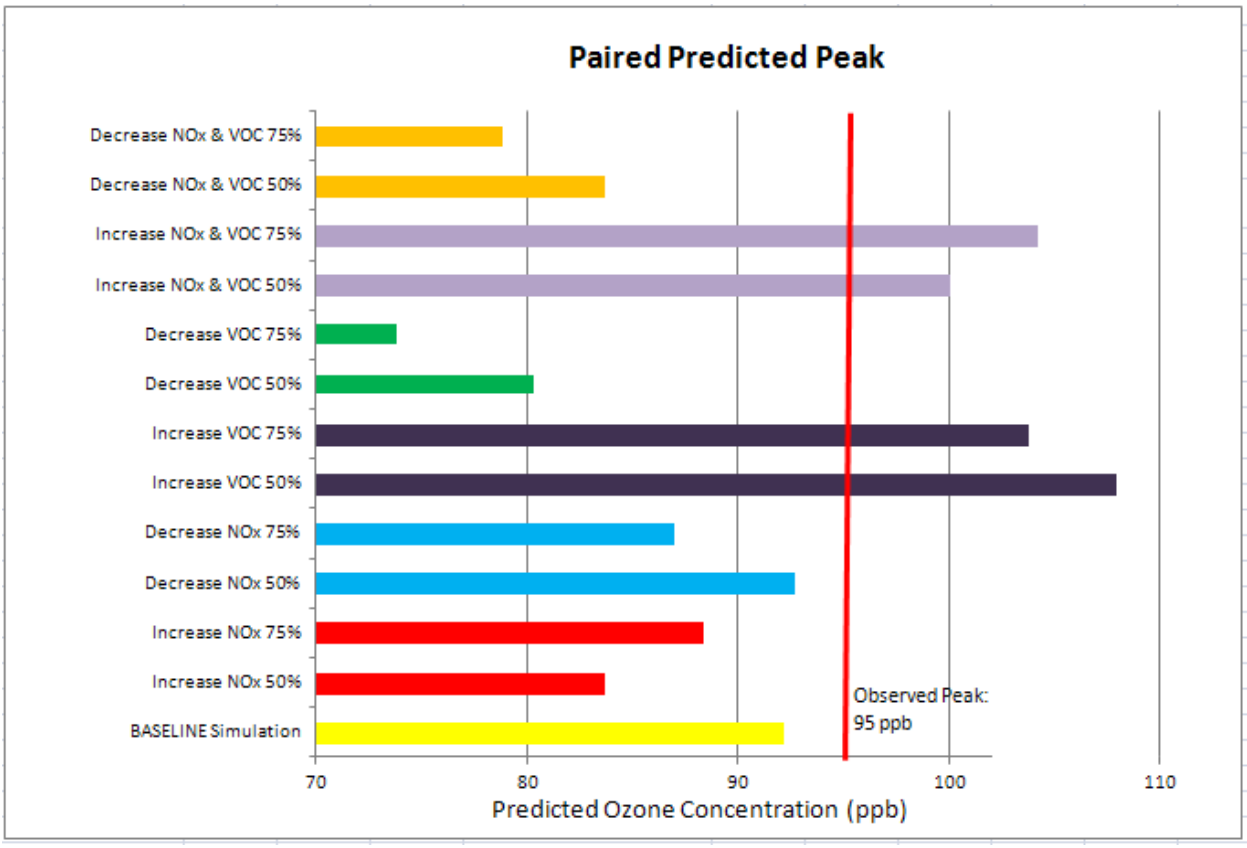

Figure 1.2 Paired Predicted Peak for CAMx Simulations and 8-Hour Ozone

Figure 1.4 illustrates the PEAK PREDICTED 8-hour ozone concentration generated by the CAMx simulations. Most of the simulations under-predict 8-hour ozone. Results indicate the model over-predicts the PEAK OBSERVED 8-hour ozone concentration in simulations where VOC emissions were increased either 50% or 75% either alone or in combination with concurrent increases in NOx.

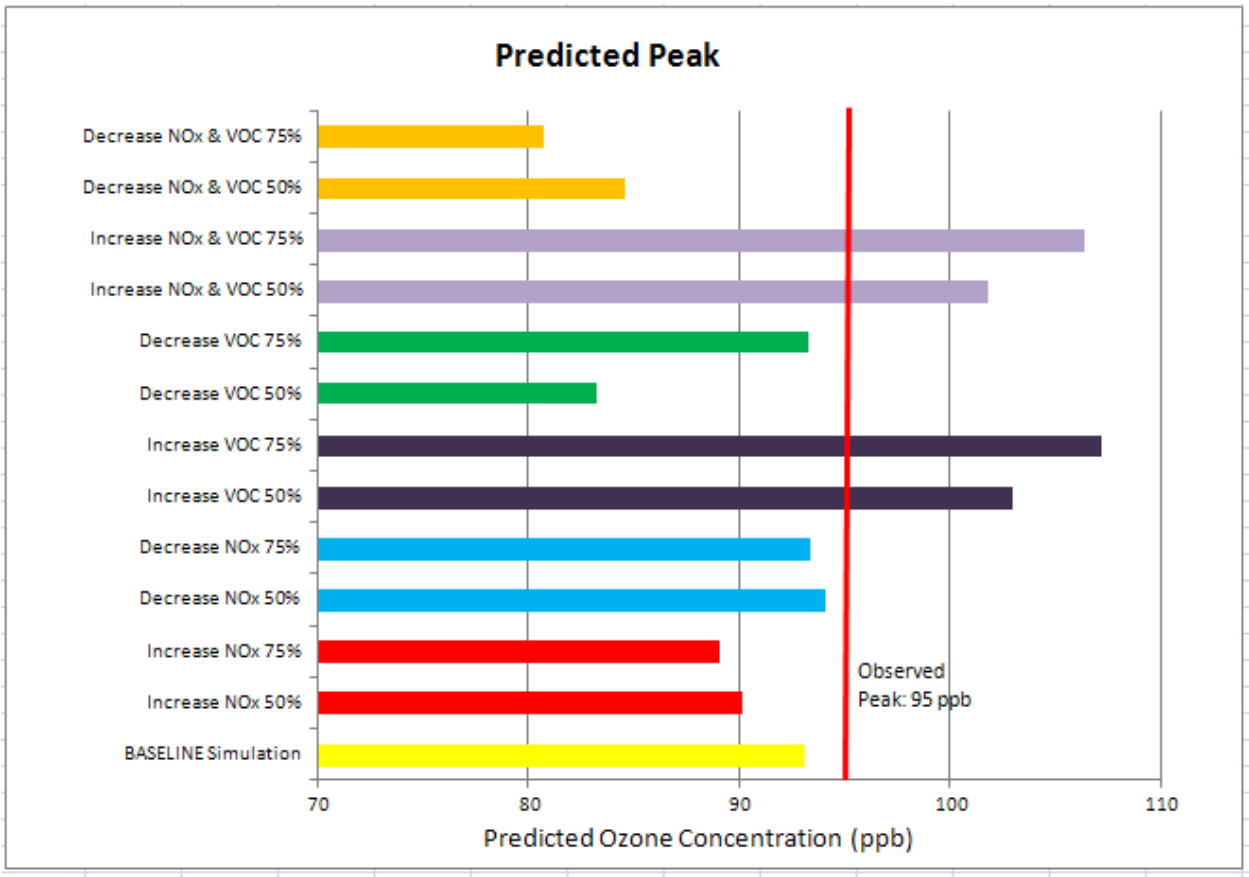

Figure 2.3 PREDICTED PEAK for CAMx Simulations and 1-Hour Ozone

Of note are increases in NOx tend to reduce 8-hour ozone compared to BASELINE results due to the ability of NOx to titrate ozone. Decreases in NOx did very little to change 8-hour ozone concentrations. The greatest decreases in 8-hour ozone occurred when both NOx and VOC were reduced 50% and 75%.

2 Model Performance Evaluations for Each Simulation.

Model performance was evaluated for 1-hour and 8-hour ozone concentrations only at the regional CAMS which were included in the modeling simulation. This section addresses the diurnal formation and destruction of ozone on 6/18 which is the day of the ozone exceedance.

Each RUN including the BASELINE provides model performance data and the model's ability to predict ozone within acceptable parameters. The BASELINE model performance was discussed in Appendix A and will briefly be discussed in this section. Model performance statistics for all RUNs are compared to the BASELINE.

As indicated in the previous section the model should obtain NE $\leq$35% and NB $\pm$15%. Tables 1.1 and 1.3 indicate model performance parameters were achieved for all simulations. Varying NOx and VOC either improved or diminished model performance, but NE and NB were within acceptable modeling performance parameters on all simulations.

This section presents model performance statistics as bar graphs for PEAK OBSERVED and PAIRED PREDICTED ozone concentrations. The maximum observed 1-hour and 8-hour ozone concentrations are plotted along with co-located daily maximum 8-hour and 1-hour ozone among all sites. The following statistics are measures of model performance (ENVIRON, 2011):

- Average paired peak accuracy (APPA).
- Normalized Error (NE)
- Normalized Bias (NB)

APPA compares the PEAK OBSERVED 1-hour or 8-hour ozone concentration from each regional CAMS included in the simulation with the co-located PEAK PREDICTED value. The following formula is applied to calculate APPA:

$$APPA = \frac{Cp\ \ x,t\ - Co(x,t)}{Co(x,t)}\ 100\% \qquad \text{Equation 1.1}$$

APPA quantifies the difference between the magnitude of the peak 1-hour or 8-hour ozone concentrations observed at a monitoring station (C_o) and the PEAK PREDICTED ozone concentrations $C_{p,}$ at the same space and time (x,t). Model estimates and observations are thus "paired in space and time." The paired peak estimation accuracy is a stringent model evaluation measure. It quantifies the model's ability to reproduce, at the same time and location, the highest observed ozone concentrations during the simulation. APPA does not have specifications regarding acceptable limits.

NE observes the scatter of the entire dataset generated by CAMx during the simulation for all sites and observations. The goal is to minimize NE to ≤35%. NB describes the ability of the model to over-predict or under-predict ozone concentrations.

2.1 BASELINE Model Performance

Figure 2.1 depicts daily BASELINE model statistics, the highest 8-hour ozone PEAK OBSERVED among all sites in the PdN region, and the co-located daily PAIRED PREDICTED PEAK. The model under-predicts 1-hour ozone on 9 of 10 simulation-days. Model performance was good on 6/18, the ozone exceedance day. The positive APPA on 6/14 indicates several other CAMS over-predicted maximum 1-hour ozone.

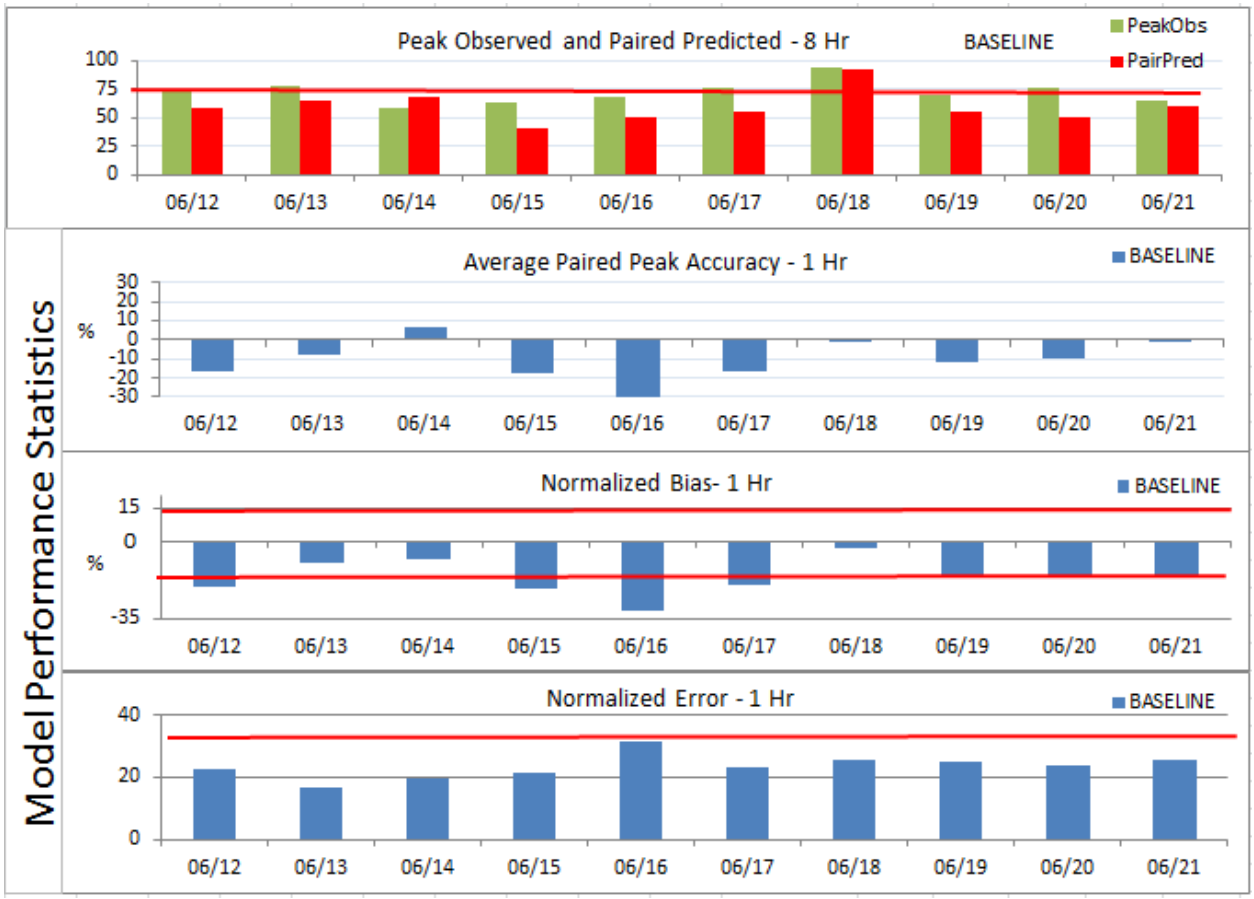

Figure 2.1 Model Performance Statistics – BASELINE

The very low APPA (-29.8%) on 6/16 is validated by the low NB and NE (-31.2% & -31.5% respectively) indicating a very strong under-prediction. On 6/18 the model performed very well regarding NB & NE notwithstanding under-prediction of the maximum peak. The APPA on 6/18 was very good at -1.5% indicating minimal under-prediction of ozone concentrations.

Figure 2.2 illustrates the diurnal variability in 1-hour ozone comparing the OBSERVED and PREDICTED diurnal values.

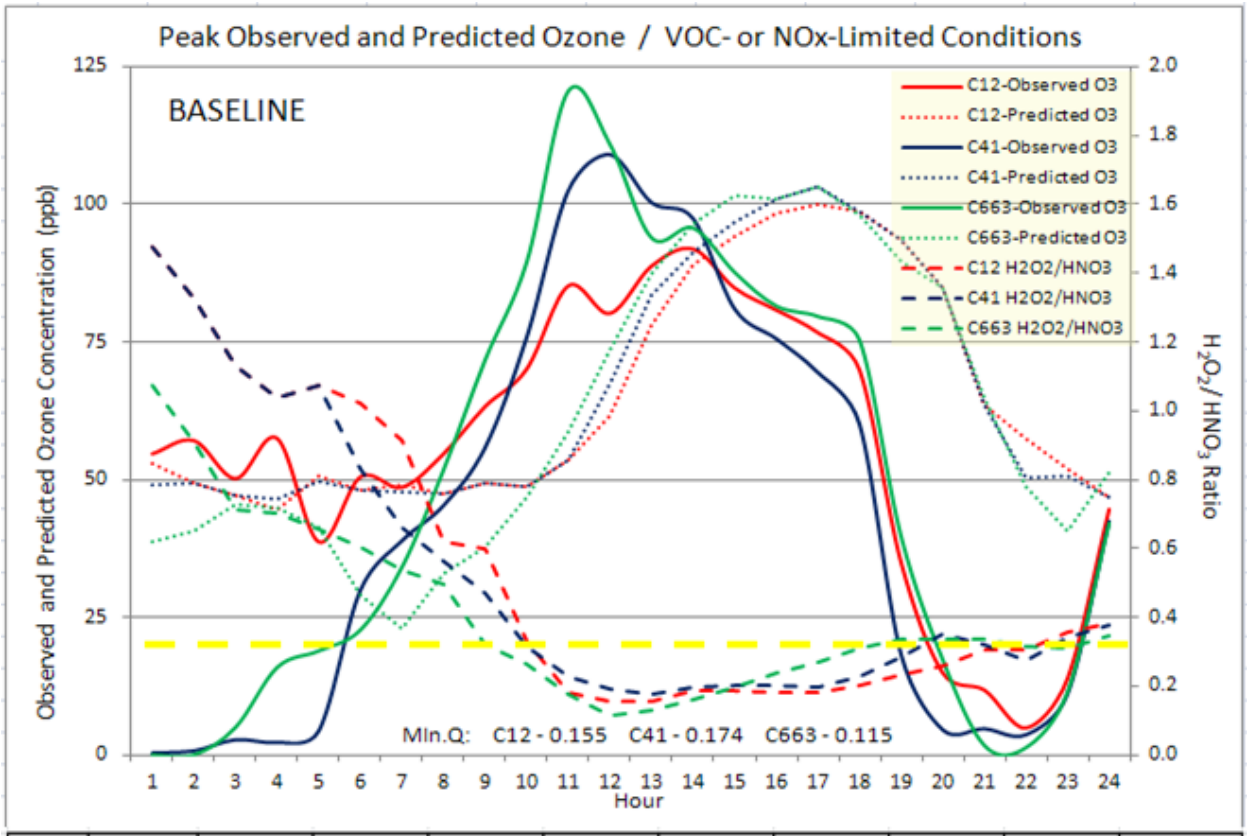

NOx	---	PeakObs	PeakPred	PairPred	UPPA	APPA	EPPA	PTB	NB	NE
VOC	---	120.7	103.3	99.3	-14.4	-1.5	12.2	4	-3.3	25.6

Figure 2.2 Diurnal Predicted and Observed 1-Hour Ozone (ppb) / H_2O_2/HNO_3 Ratios – BASELINE

Predicted hourly ozone is presented as dotted lines, and observed hourly ozone is presented as solid lines. The H_2O_2/HNO_3 ratio is presented as a dashed line. The difference between the occurrence of the PeakObs and PredPeak is indicted as PEAK TIME BIAS (PTB), which for the BASELINE simulation is 4 hours.

Three stations are presented in Figure 2.2. The purpose of the 3 stations (C663, C12, and C41) is C663 is the CAMS observing the daily maximum 1-hour ozone across the PdN region, C12 at UTEP is the site in El Paso observing the most exceedances on the US side of the border, and an Auto-GC is deployed at C41 providing the opportunity to observe hourly TNMHC concentrations and prepare TNMHC/NOx ratios as discussed in Section 4 which includes a discussion on ozone

limiting conditions associated with the model's production of H_2O_2 and HNO_3. The diurnal ozone formation graphic includes the H_2O_2:HNO_3 ratio which helps in determining whether ozone formation conditions are NOx- or VOC-limited. A ratio $\geq$0.35 indicates NOx-limited conditions while a ratio <0.35 indicates VOC-limited conditions (ENVIRON, 2011).

Figure 2.3 illustrates the diurnal variability in 8-hour ozone comparing the OBSERVED and PREDICTED concentrations. PREDICTED 8-hour ozone is presented as dotted lines; observed 8-hour ozone is presented as solid lines. The H_2O_2/HNO_3 ratio is presented as dashed lines and provides a general reference given 8-hour average H_2O_2/HNO_3 ratios are not applicable to this analysis. A red line is set at 75ppb indicating the 8-hour ozone NAAQS.

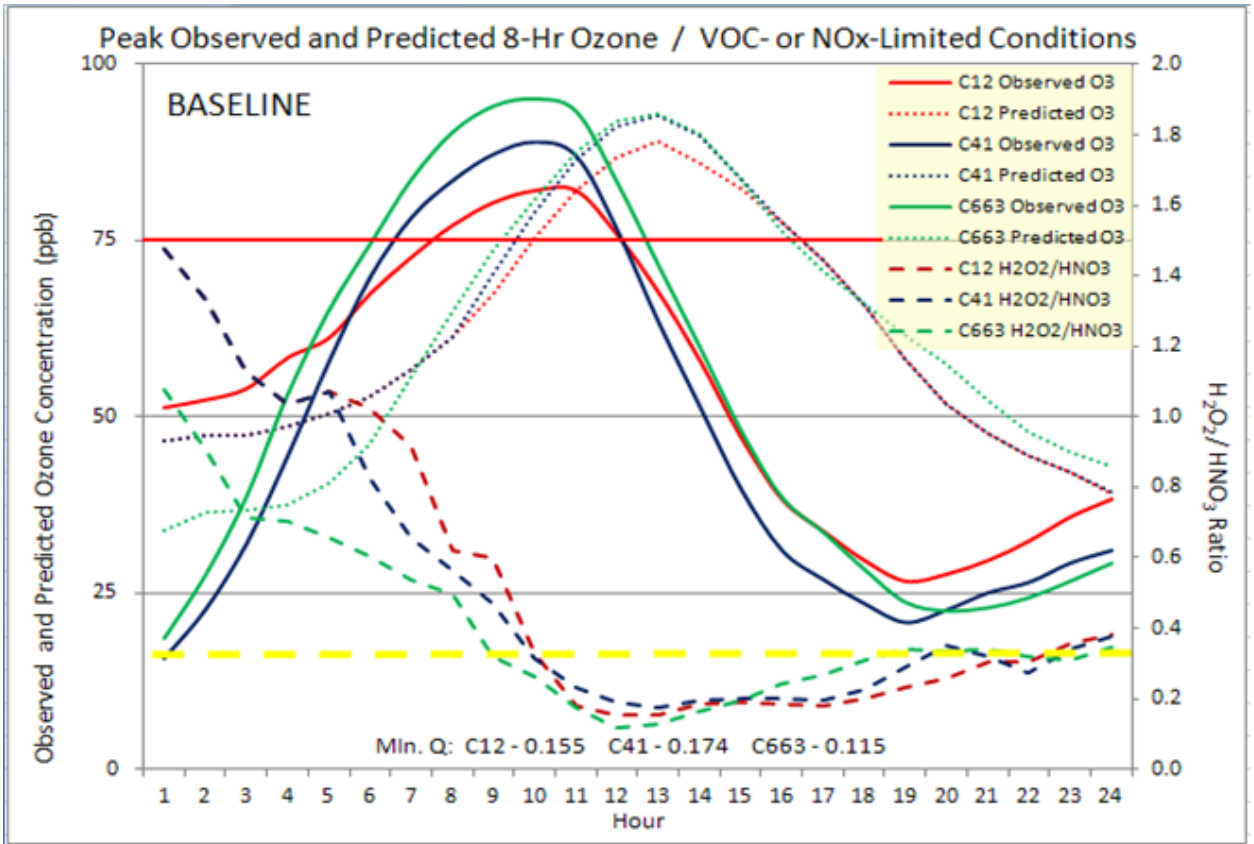

BASELINE	PeakObs	PeakPred	PairPred	UPPA	APPA	EPPA	PTB	NB	NE
	95.1	93	92.1	-2.1	2.5	9	3	3.9	23.7

Figure 2.3 Diurnal Predicted and Observed 8-Hour Ozone (ppb) / H_2O_2/HNO_3 Ratios – BASELINE

8-hour ozone data indicate the PTB is slightly improved to 3 hours compared to 1-hour ozone. CAMx under-predicts the peak ozone (93 ppb) and the PAIRED PREDICTED (92.1 ppb) 8-hour

average ozone concentration. NB (3.9%) and NE (23.7%) are within acceptable model performance parameters.

2.2 RUN 1 Model Performance Evaluation

Figure 2.4 presents performance statistics for RUN 1, 8-hour ozone PEAK OBSERVED, and co-located daily PAIRED PREDICTED PEAK among all sites in the PdN region.

The model under-predicts 8-hour ozone on 9 of 10 simulation-days. On 6/14 the 8-hour PAIR PREDICTED concentration at several CAMS exceeded the OBSERVED 8-hour ozone concentration. The worse under-prediction occurred on 6/16 when APPA was -30.1%, NB was -31.2%, and NE was 32%.

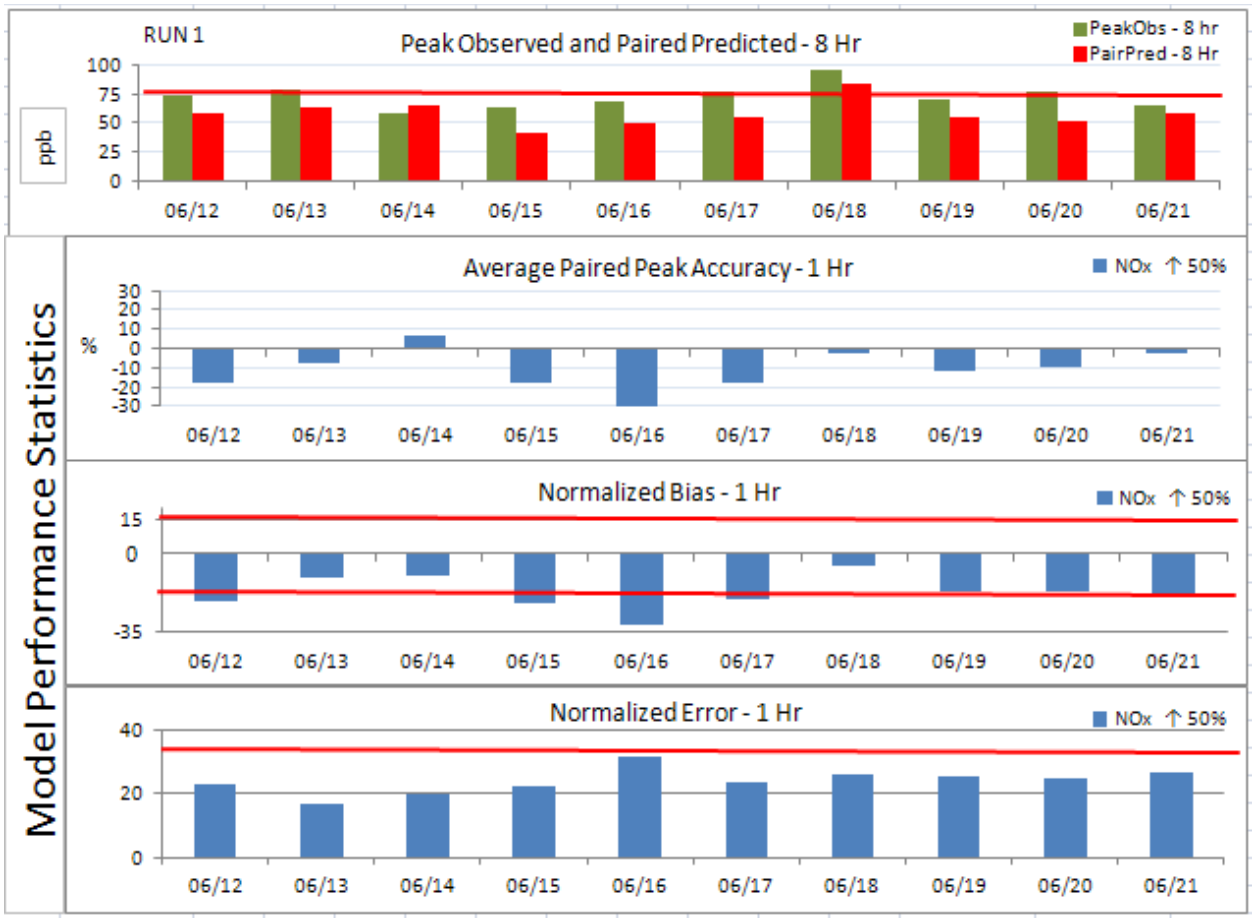

Figure 2.4 Model Performance Statistics – RUN 1

Overall NB exceeded acceptable model performance parameters of ±15% on 7 of 10 days. NE for all 10 simulation days was acceptable and within the ≤35% threshold. On 6/18 the model

performed well regarding NB & NE where both increased compared to BASELINE (1.9% and 0.6% respectively). PTB is comparable to BASELINE, as seen in Figure 2.5. PeakPred 1-hour ozone drops slightly compared to BASELINE. PAIRED PREDICTED 1-hour ozone drops 2.4 ppb.

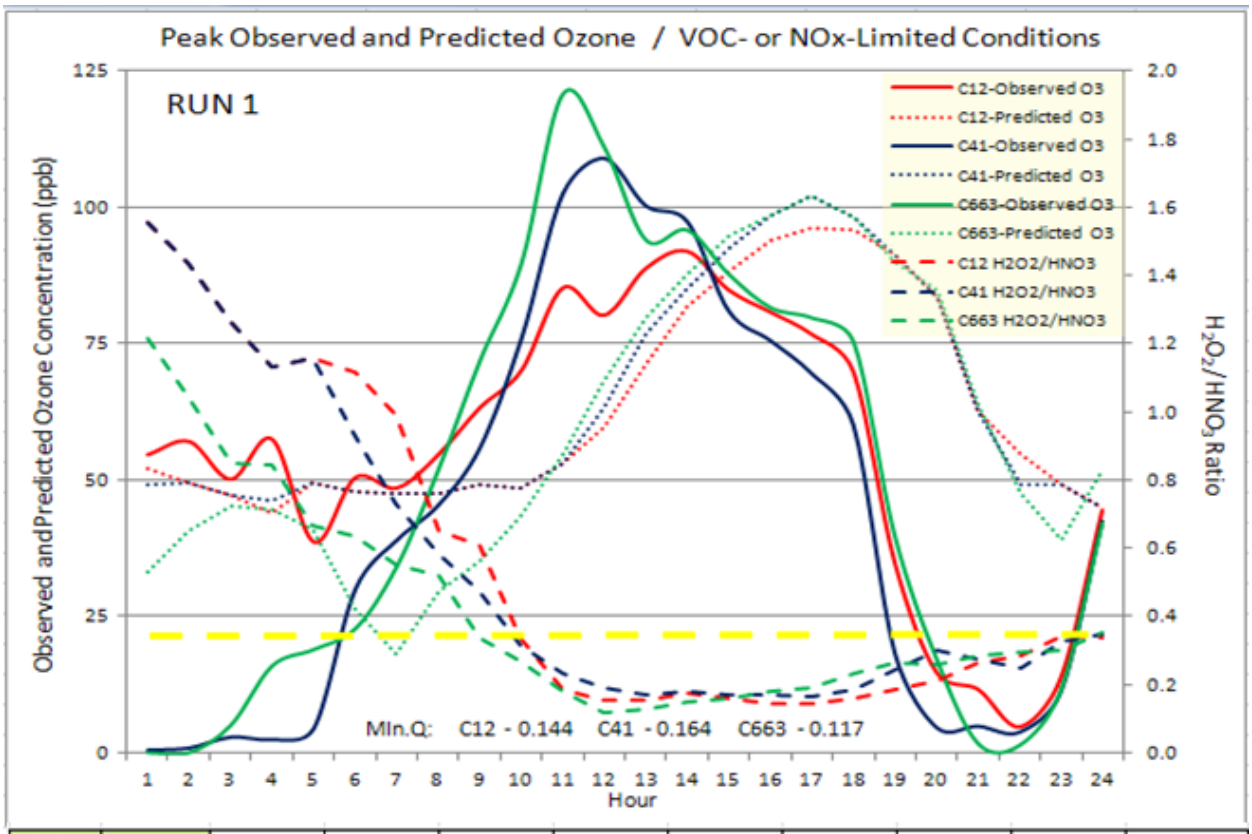

NOx	↑ 50%	PeakObs	PeakPred	PairPred	UPPA	APPA	EPPA	PTB	NB	NE
VOC	---	120.7	102.1	96.9	-15.4	-2.6	12.6	4	-5.2	26.2
BASECASE			103.3	99.3	-14.4	-1.5	12.2	4	-3.3	25.6

Figure 2.5 Diurnal Predicted and Observed 1-Hour Ozone (ppb) / H_2O_2/HNO_3 Ratios–6/18/2006–RUN 1

The diurnal H_2O_2/HNO_3 ratio indicates NOx-limiting conditions exist during the early morning hours. As photochemistry increases and HNO_3 production accelerates a VOC-limiting condition develops for the duration of the elevated ozone event on 6/18. The shift from NOx-limited to VOC-limited conditions occurs at 0900hrs however given the PTB of 4 hours it is possible the VOC-limited condition developed 4-hours earlier.

Figure 2.6 illustrates diurnal OBSERVED and PREDICTED 8-hour average ozone concentrations. H_2O_2/HNO_3 ratios are provided as reference.

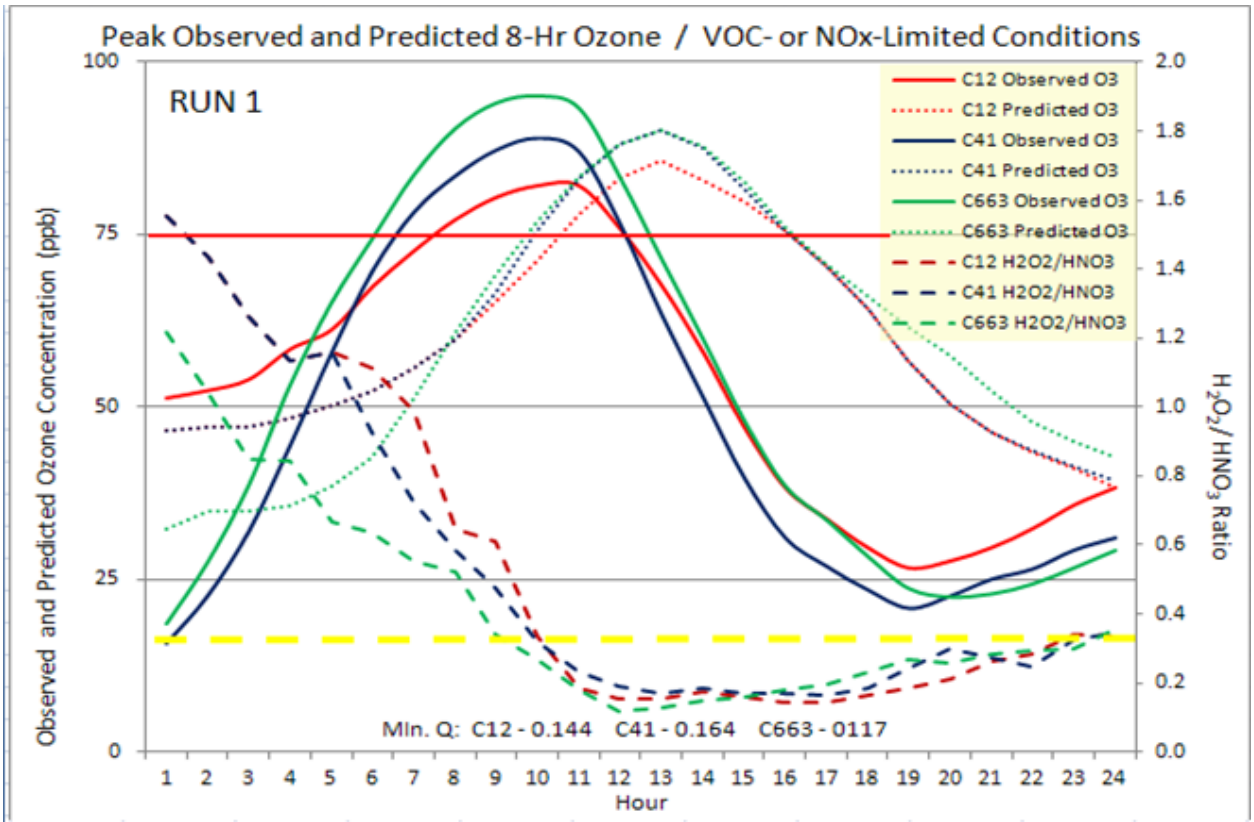

NOx	↑ 50%	PeakObs	PeakPred	PairPred	UPPA	APPA	EPPA	PTB	NB	NE
VOC	---	95.1	90.11	83.6	-11.1	-3.9	8.3	3	0.4	22.1
BASELINE			93	92.1	-2.1	2.5	9	3	3.9	23.7

Figure 2.6 Diurnal Predicted and Observed 8-Hour Ozone (ppb) / H_2O_2/HNO_3 Ratios – RUN 1

PTB between PEAK OBSERVED and PEAK PREDICTED 8-hour averages is 3 hours. PEAK PAIRED PREDICTED 8-hour average ozone is 83.6 ppb. Both OBSERVED and PREDICTED 8-hour ozone exceed the 75 ppb NAAQS for several hours.

Of interest during this simulation is the reduction of ozone compared to the BASELINE simulation with the 50% increase in NOx emissions. This occurs when NOx titrates ozone due to the abundance of this pollutant. However this may be observed, reducing ozone by increasing NOx is not a good air quality improvement planning strategy.

2.3 RUN 2 Model Performance Evaluation

RUN 2 decreases NOx emissions by 50%. Figure 2.7 presents performance statistics for RUN 2, 8-hour ozone PEAK OBSERVED, and co-located daily PAIRED PREDICTED PEAK among all sites in the PdN region.

The model under-predicts 8-hour ozone on 9 of 10 simulation-days. On 6/14 the 8-hour PAIRED PREDICTED PEAK concentration at 6 CAMS exceeds the OBSERVED 8-hour ozone. The worse under-prediction occurred on 6/16 observing APPA (-29.4%), NB(-30.5%), and NE (30.9%). 6/18 simulation results indicate good model performance with minimal bias (-2.1%) for 8-hour ozone.

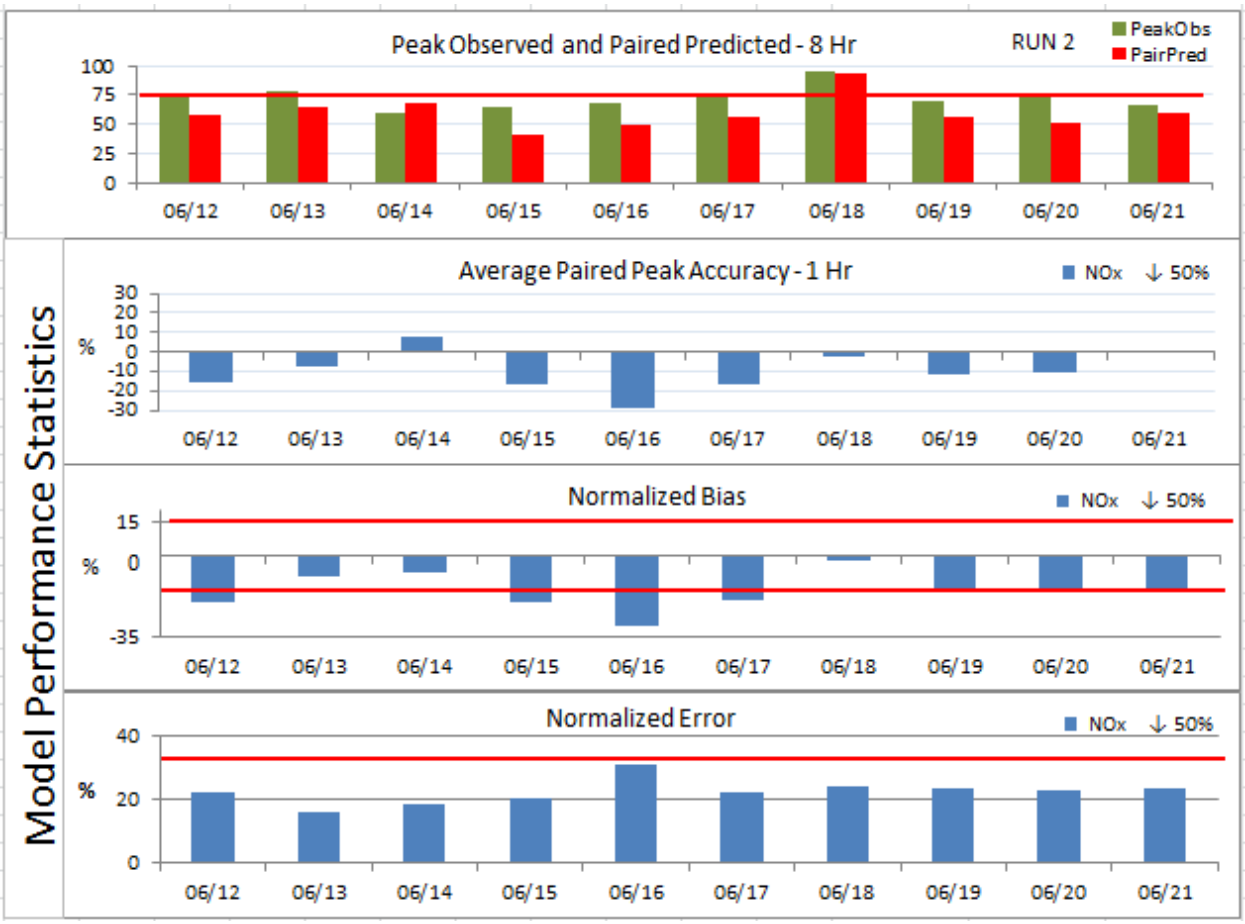

Figure 2.7 Model Performance Statistics – Run 2

The model under-predicts 1-hour ozone on 9 of 10 simulation-days. On 6/14 the PREDICTED PEAK 1-hour ozone was 0.5 ppb below BASELINE. The positive APPA for 6/14 indicates several other CAMS over-predicted maximum 1-hour ozone. PEAK PREDICTED 1-hour ozone (102.4 ppb) on 6/18 is 0.9 ppb less than the BASELINE PEAK PREDICTED. The negative NB for all days indicates the model under-predicts 1-hour ozone across all co-located sites.

APPA on 6/16 (-29.4%) indicates very poor model performance which is confirmed by low NB (-30.5%) and NE (30.9%). On 6/18 the model performed very well regarding NB (-2.1%) & NE (24.2%) where both statistics improved slightly compared to BASELINE (Figure 2.8). The model performed within acceptable NE and NB parameters on RUN 2 for 1-hour ozone.

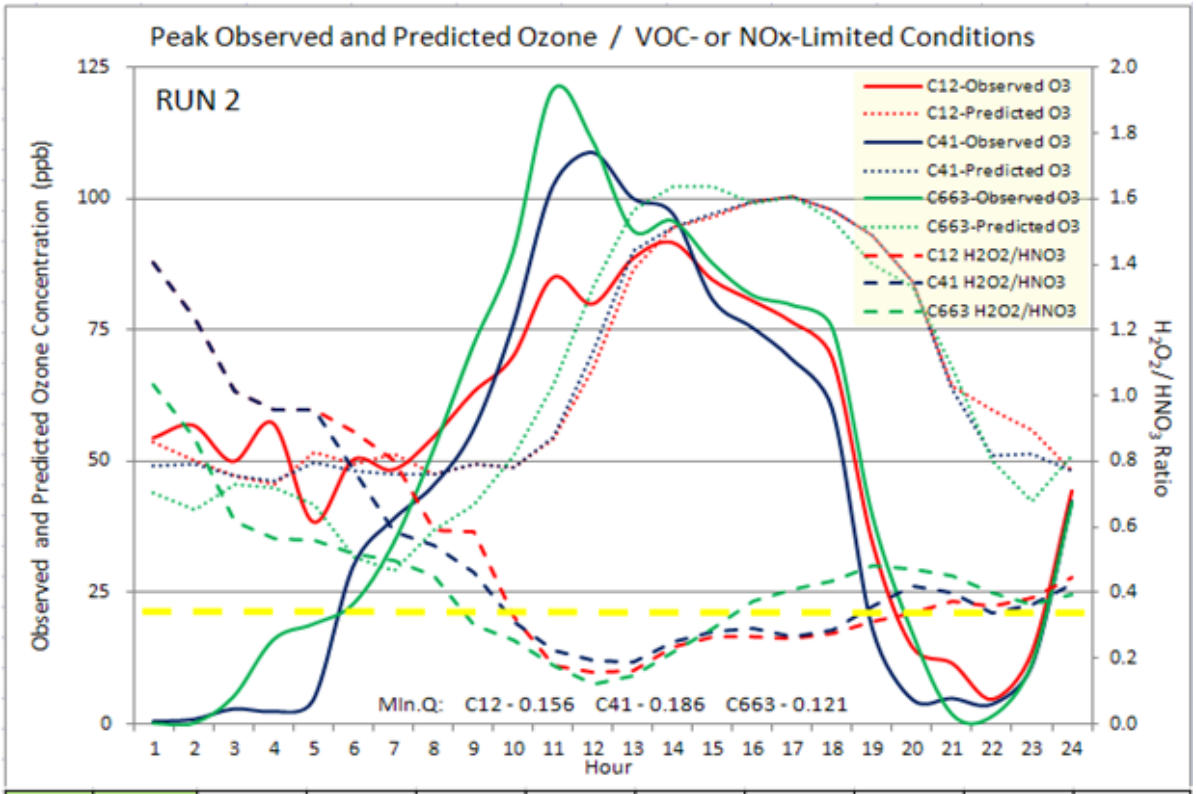

NOx	↓ 50%	PeakObs	PeakPred	PairPred	UPPA	APPA	EPPA	PTB	NB	NE
VOC	---	120.7	102.4	98.4	-15.1	-2.1	11.9	3	-2.1	24.2
BASECASE			103.3	99.3	-14.4	-1.5	12.2	4	-3.3	25.6

Figure 2.8 Diurnal Predicted and Observed 1-Hour Ozone (ppb) / H_2O_2/HNO_3 Ratios – RUN 2

The diurnal variation for 6/18 presented in Figure 14.8 indicates an improved PTB which shifts to 3 hours compared to 4 hours in the BASELINE. H_2O_2/HNO_3 ratios indicate early morning NOx limited conditions becoming VOC-limited at ~9 AM for C663 observations. C663 also generated a predicted minimum H_2O_2/HNO_3 ratio (0.121) compared to C12 and C41 H_2O_2/HNO_3 ratios (0.158 and 0.186 respectively).

Figure 2.9 illustrates diurnal OBSERVED and PREDICTED 8-hour average ozone concentrations. H_2O_2/HNO_3 ratios are provided as reference. The PTB between OBSERVED and PREDICTED 8-hour averages is unchanged (3 hours) compared to BASELINE. PEAK PAIRED PREDICTED 8-hour average ozone is 92.6 ppb.

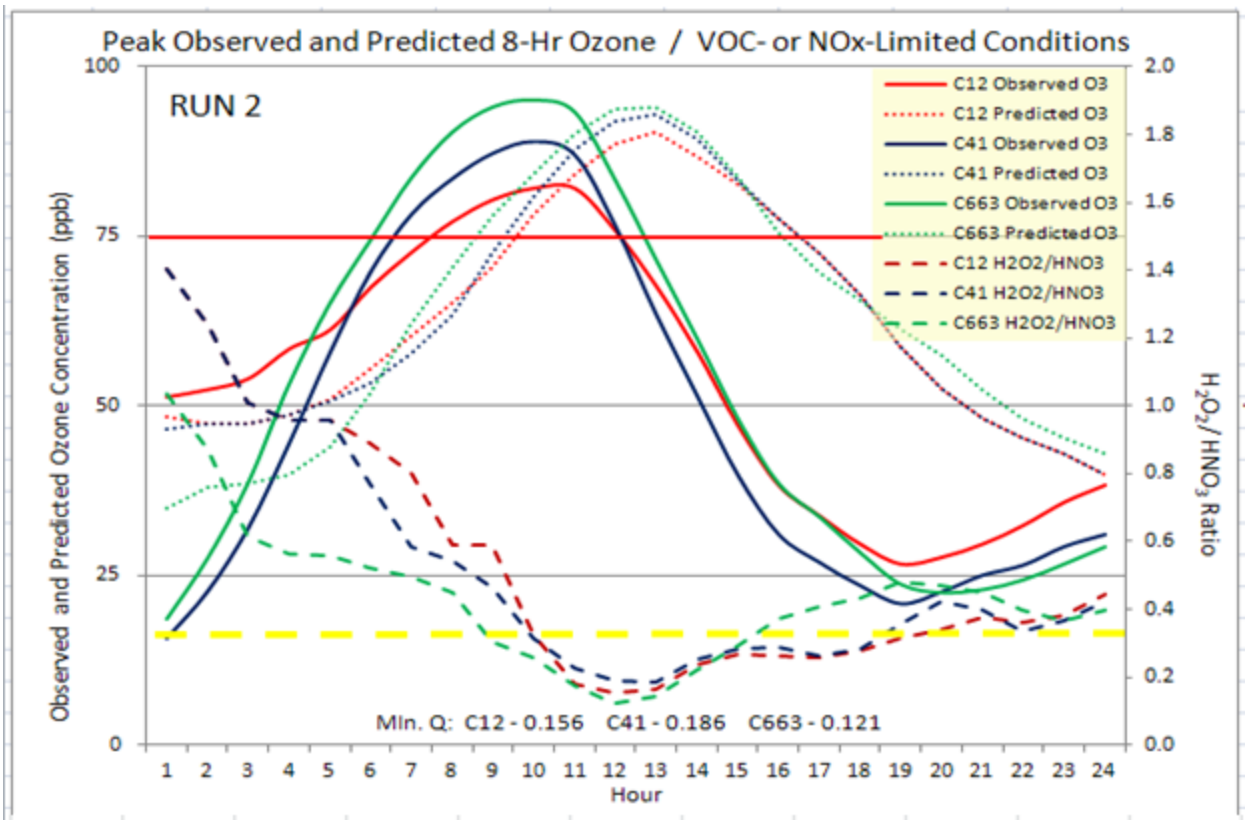

NOx	↓ 50%	PeakObs	PeakPred	PairPred	UPPA	APPA	EPPA	PTB	NB	NE
VOC	---	95.1	94.05	92.6	-1	3	9.5	3	5.4	22.4
BASELINE			93	92.1	-2.1	2.5	9	3	3.9	23.7

Figure 2.9 Diurnal Predicted and Observed 8-Hour Ozone (ppb) / H_2O_2/HNO_3 Ratios – RUN 2

PREDICTED 8-hour ozone exceeds the 75 ppb standard for several hours on 6/18. 8-hour ozone increases 1 ppb compared to BASELINE. Of interest during this simulation is the increase of ozone compared to the BASELINE given the 50% decrease in NOx emissions.

2.4 RUN 3 Model Performance Evaluation

RUN 3 involved reducing area source VOC emissions in Juárez by 50%. Figure 2.10 presents performance statistics for RUN 3, 8-hour ozone PEAK OBSERVED, and co-located daily PAIRED PREDICTED PEAK among all sites in the PdN region.

The model under-predicts 1-hour ozone on all 10 simulation days. The difference between this and previous RUNs is the over-prediction occurs on 6/13. The simulation presented failing NB on 7 of 10 days. The PREDICTED PEAK on 6/18 for 1-hour ozone was 91.7 ppb indicating good model response to modifications in VOC emission.

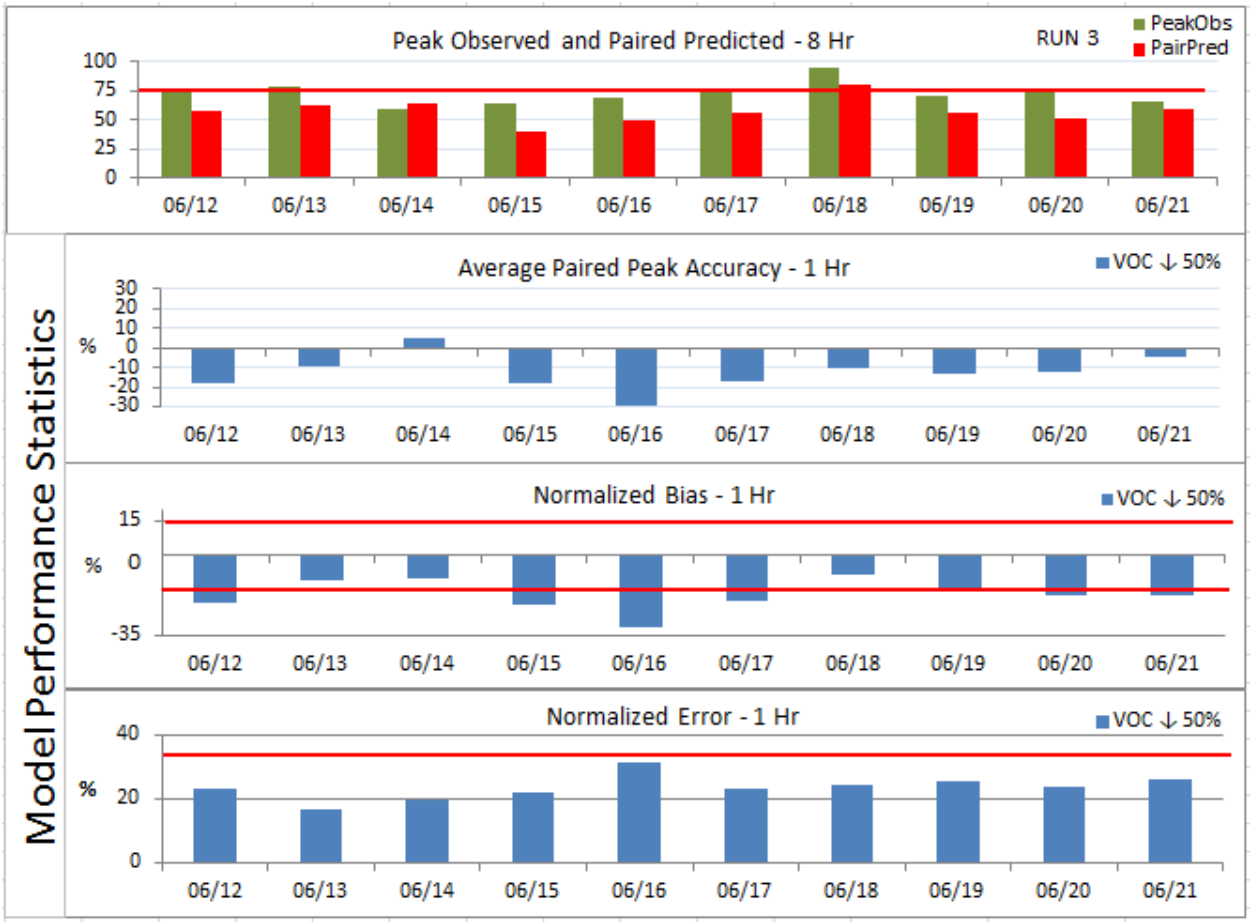

Figure 2.10 Model Performance Statistics – Run3

Figure 2.11 presents diurnal OBSERVED and PREDICTED 1-hour ozone and H_2O_2/HNO_3 ratios . The PAIRED PREDICTED PEAK 1-hour ozone (86.7 ppb) is 12.6 ppb less than BASELINE. The PTB is unchanged from BASELINE at 4 hours. NE improves from 25.6% to 24.2%. NB (-8.7%) decreases from BASELINE. Figure 2.12 presents diurnal PREDICTED and OBSERVED 8-hour ozone and H_2O_2/HNO_3 Ratios . The PAIRED PREDICTED PEAK 8-hour ozone is 80.3 ppb and the PREDICTED PEAK 8-hour is 83.2 ppb. This simulation shows good response to the 50% reduction in VOC emission. NB (-1.8%) indicates minimal under-prediction, and NE (23%) indicates the simulation is relatively unchanged from BASELINE and operating within acceptable parameters for these statistics.

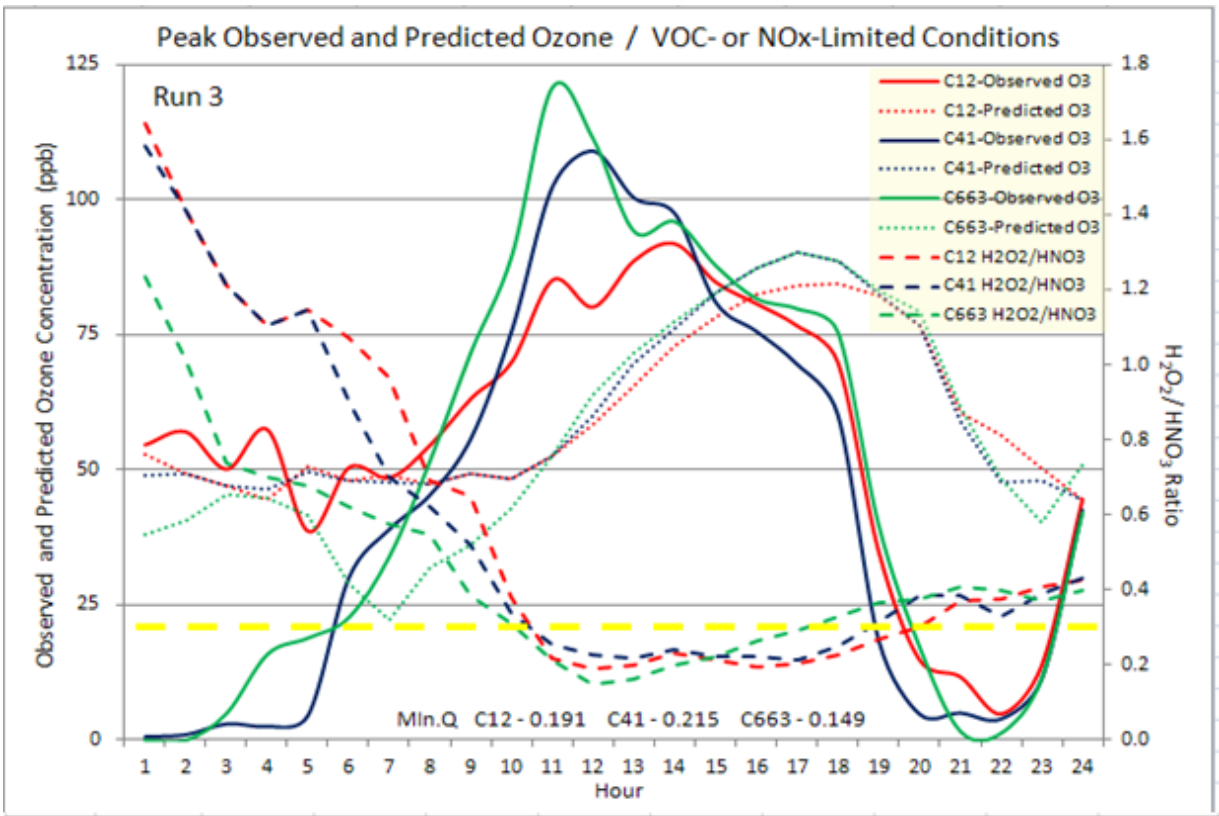

NOx	---	PeakObs	PeakPred	PairPred	UPPA	APPA	EPPA	PTB	NB	NE
VOC	↓ 50%	120.7	91.7	86.7	-24	-10	15.3	4	-8.7	24.2
BASECASE			103.3	99.3	-14.4	-1.5	12.2	4	-3.3	25.6

Figure 2.11 Diurnal Predicted and Observed 1-Hour Ozone (ppb) / H_2O_2/HNO_3 Ratios – RUN 3

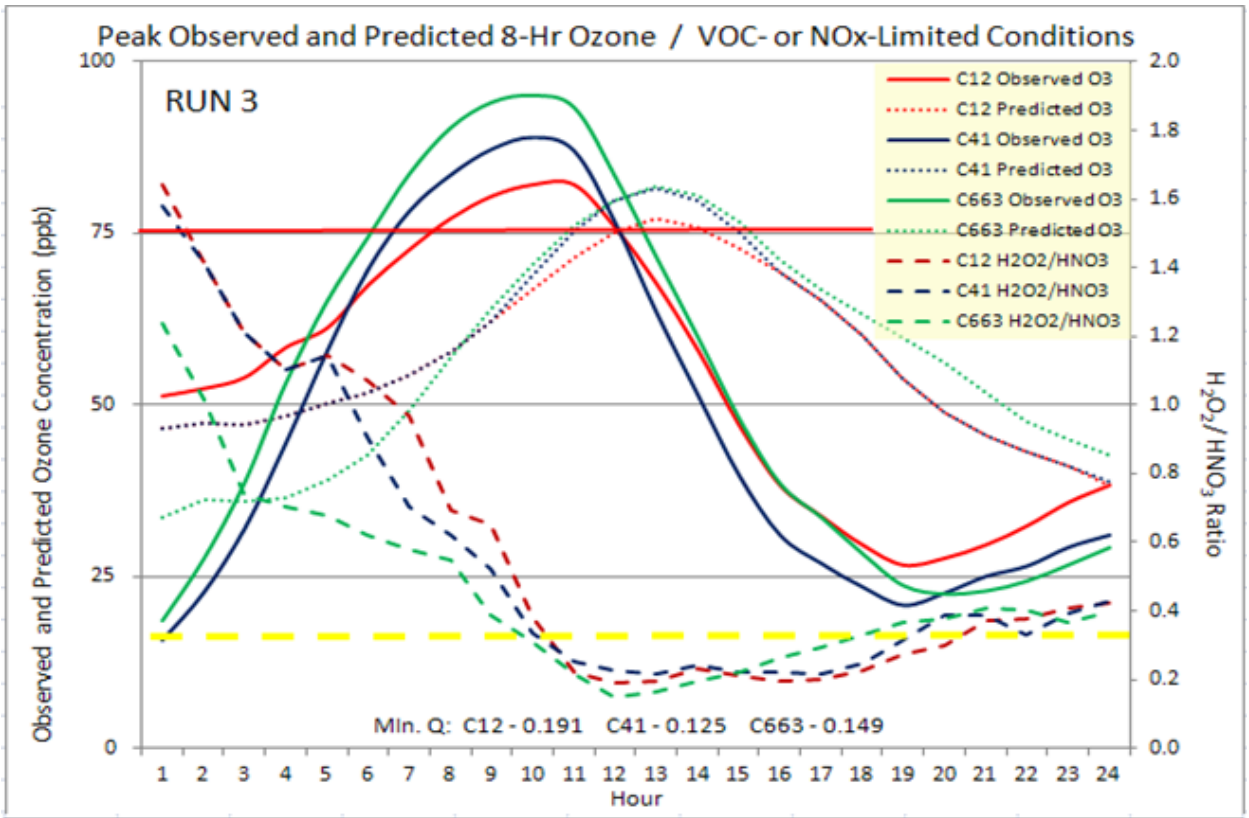

NOx	---	PeakObs	PeakPred	PairPred	UPPA	APPA	EPPA	PTB	NB	NE
VOC	↓ 50%	95.1	83.22	80.3	-12.4	-5.9	8.9	3	-1.8	23
BASELINE			93	92.1	-2.1	2.5	9	3	3.9	23.7

Figure 2.12 Diurnal Predicted and Observed 8-Hour Ozone (ppb) / H_2O_2/HNO_3 Ratios – RUN 3

2.5 RUN 4 Model Performance Evaluation

RUN 4 involved increasing area source VOC emissions in Juárez by 50%. Figure 2.13 presents performance statistics for RUN 4, 8-hour ozone PEAK OBSERVED, and co-located daily PAIRED PREDICTED PEAK among all sites in the PdN region.

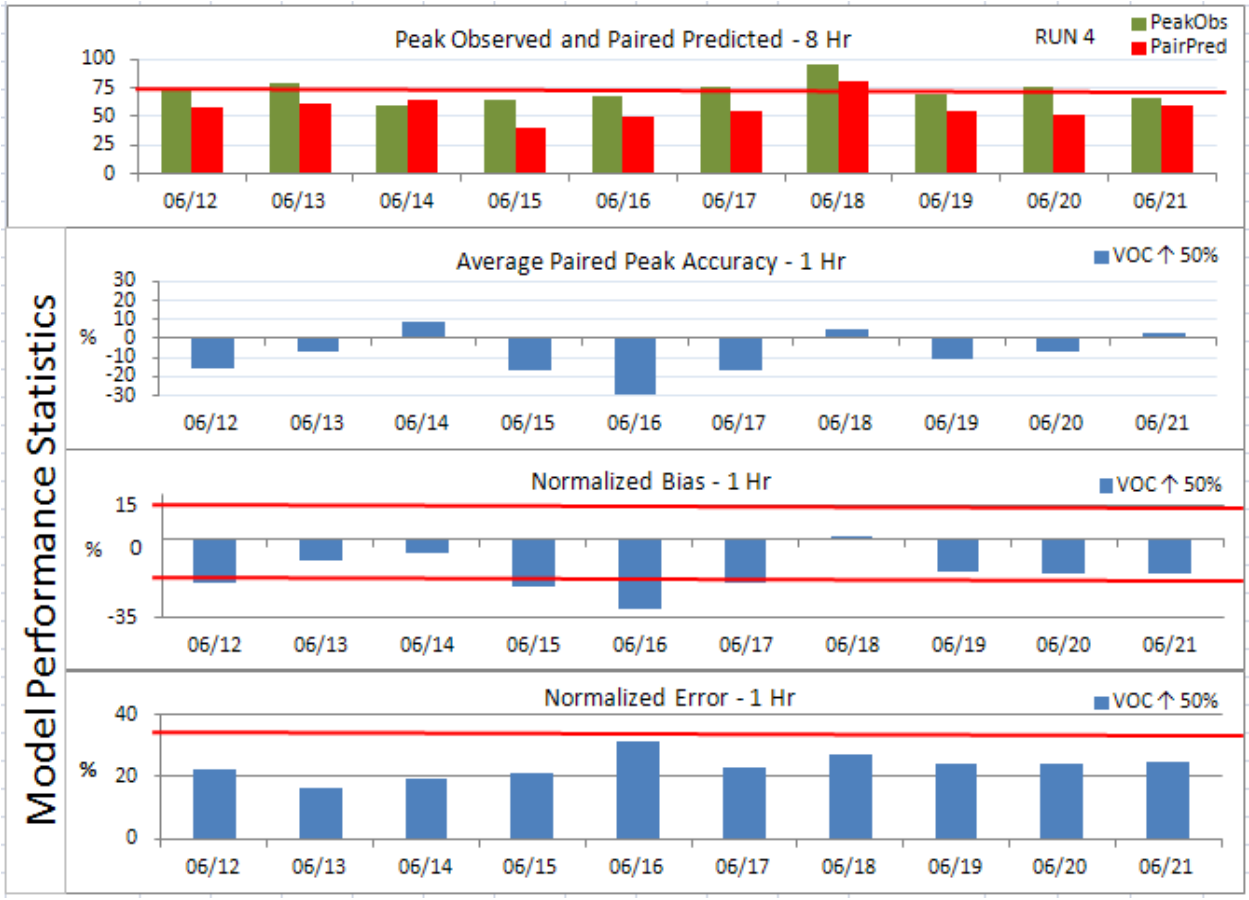

Figure 2.13 Model Performance and Statistics - RUN 4

The model under-predicts 1-hour ozone on 9 of 10 days. On 6/18 the model moderately over-predicts OBSERVED ozone as indicated by NB (1.2%). The simulation failed NB on 4 of 10 days where NB was <-15%. The PREDICTED PEAK on 6/18 for 1-hour ozone was 113.9 ppb indicating good model response to increased VOC emissions. The PAIRED PREDICTED PEAK which occurred at C663 was 107.8 ppb.

Figure 2.14 presents diurnal PREDICTED and OBSERVED 1-hour ozone and H_2O_2/HNO_3 ratios.

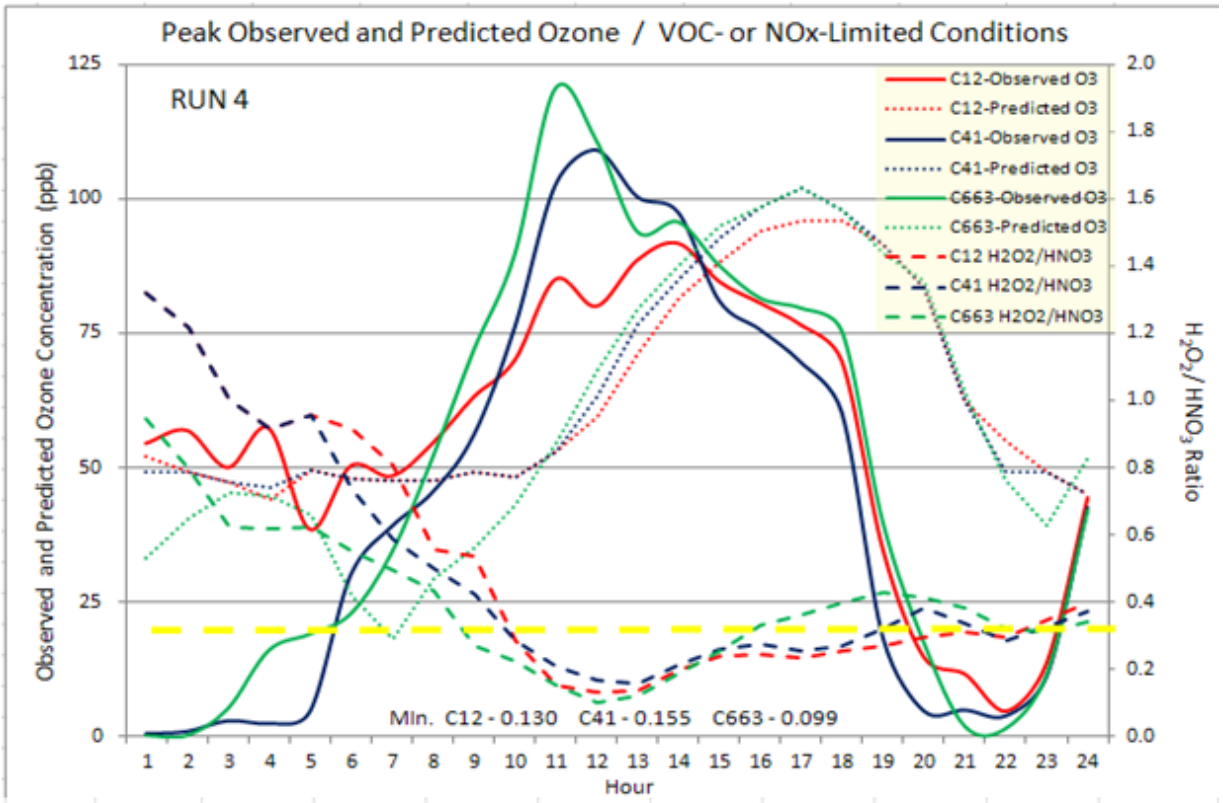

NOx	---	PeakObs	PeakPred	PairPred	UPPA	APPA	EPPA	PTB	NB	NE
VOC	↑ 50%	120.7	113.93	107.8	-5.6	4.8	13.1	3	1.2	27.1
BASECASE			103.3	99.3	-14.4	-1.5	12.2	4	-3.3	25.6

Figure 2.14 Diurnal Predicted and Observed 1-Hour Ozone (ppb) / H_2O_2/HNO_3 Ratios – RUN 4

An increase of 50% in area source VOC emissions increased the PREDICTED PEAK 1-hour ozone ~114 ppb or ~10.6%. The increase in 10 ppb greater than BASELINE continues to be less than 10 ppb below the PEAK OBSERVED. PTB improves (3 hours) compared to the BASELINE (4 hours). NE is reduced by 1.5 percentage points. H_2O_2/HNO_3 ratios indicate a NOx-limited condition exists in the early morning hours and a shift to VOC-limited conditions at ~9 AM remaining VOC-limited for the duration of the ozone event. Figure 2.15 presents diurnal predicted and observed 8-hour ozone and H_2O_2/HNO_3 ratios. 8-hour ozone PAIRED PREDICTED PEAK (100.5 ppb) and 8-hour

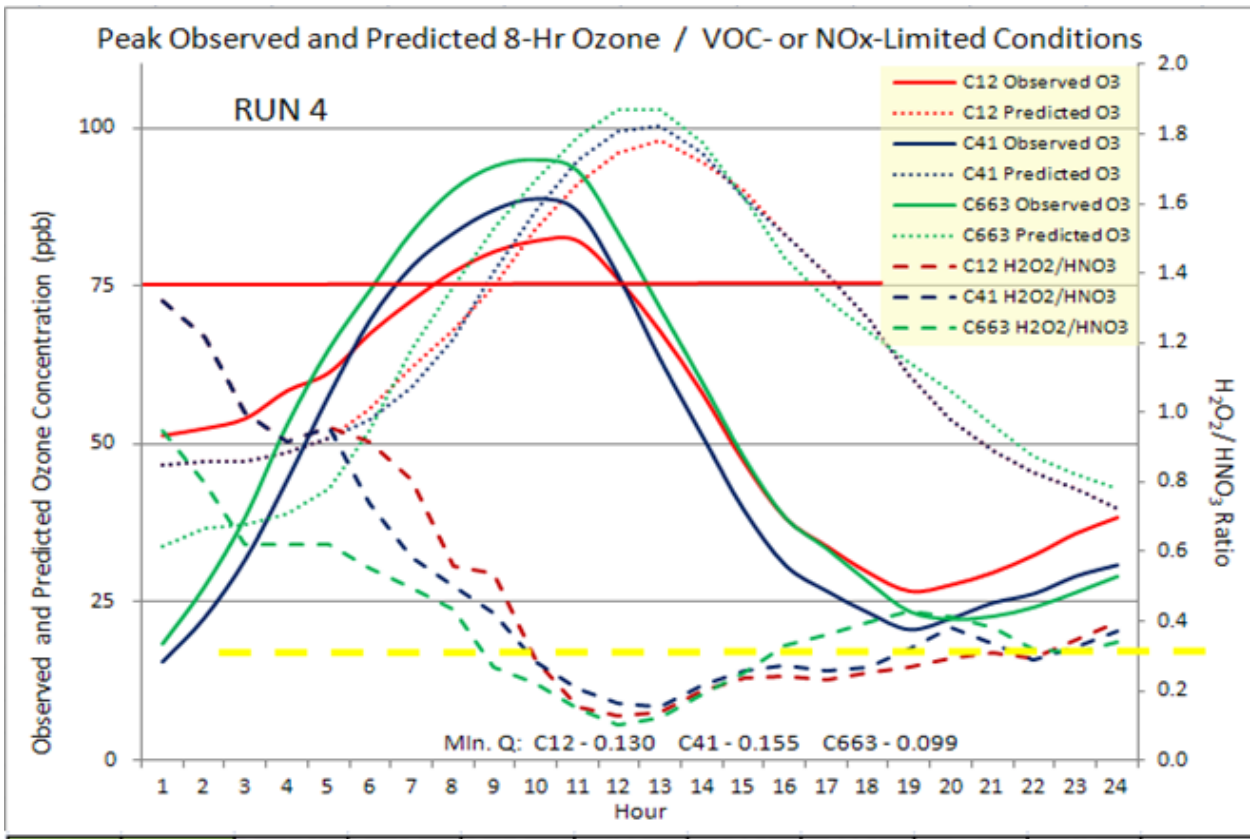

NOx	---	PeakObs	PeakPred	PairPred	UPPA	APPA	EPPA	PTB	NB	NE
VOC	↑ 50%	95.1	102.85	100.5	8.3	9	14.3	3	8.8	24.4
BASELINE			93	92.1	-2.1	2.5	9	3	3.9	23.7

Figure 2.15 Diurnal Predicted and Observed 8-Hour Ozone (ppb) H_2O_2/HNO_3 Ratios – RUN 4

ozone PREDICTED PEAK (102.85 ppb) over-predicts OBSERVED 8-hour ozone and indicate good model response to increased VOC emissions. Positive NB (8.8%) indicating the over-prediction and NE (24.4%) indicate the simulation is operating within acceptable parameters for these statistics.

2.6 RUN 5 Model Performance Evaluation

RUN 5 involved increasing Juárez area source NOx and VOC emissions by 50%. Figure 2.16 presents performance statistics for RUN 5, 8-hour ozone PEAK

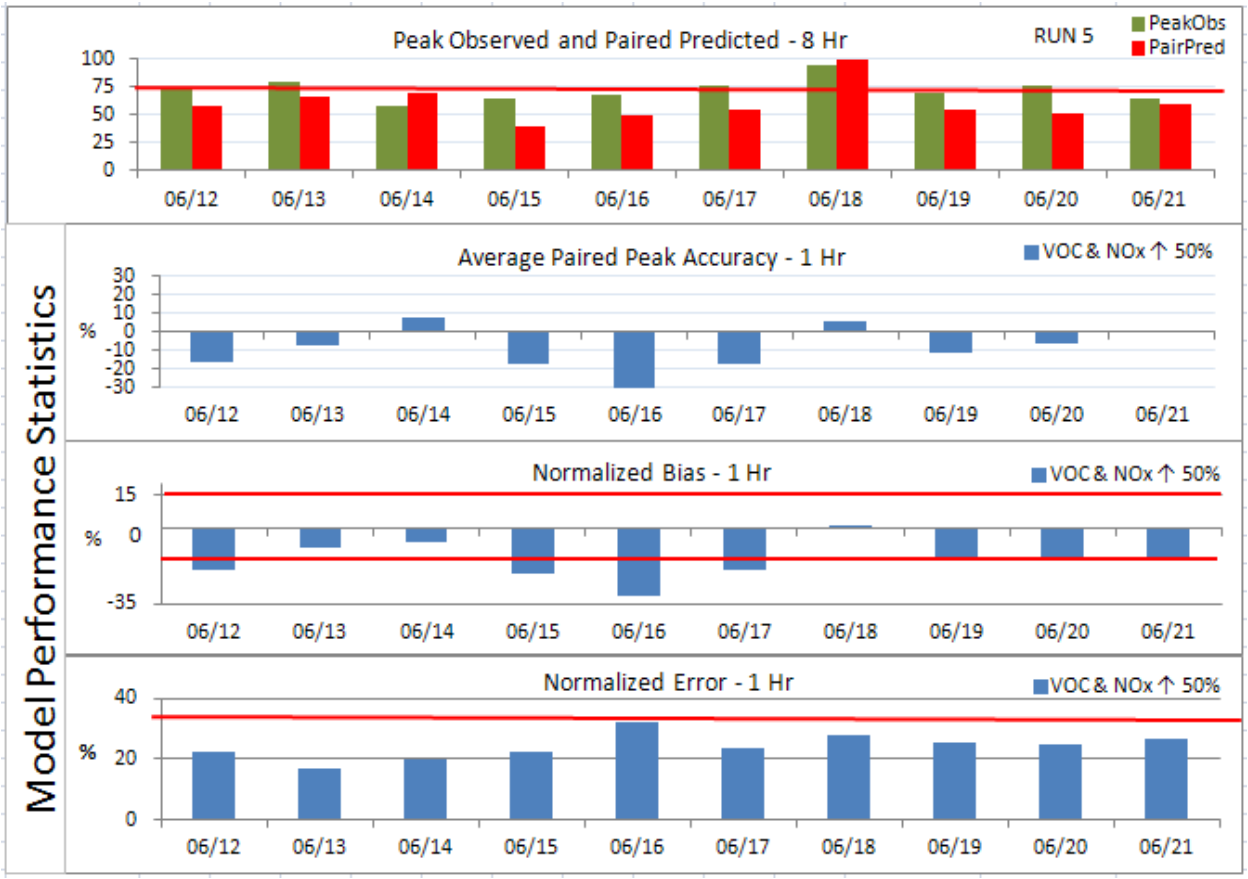

Figure 2.16 Model Performance Statistics – RUN 5

OBSERVED, and co-located daily PAIRED PREDICTED PEAK among all sites in the PdN region.

The model under-predicts 1-hour ozone on 9 of 10 days. The model over-predicts OBSERVED 1-hour ozone on 6/18 as indicated by NB (0.1%). The simulation presented failing NB on 7 of 10 days where NB was <-15%. There was minimal improvement of NB with 2 days (6/19 and 6/20) reaching -15.9%. The 1-hour ozone PREDICTED PEAK on 6/18 (113 ppb) indicates good model response to increased VOC and NOx emissions. The PAIRED PREDICTED PEAK (108.7 ppb) occurred at C663. It should be noted that the increase in both VOC and NOx emissions significantly increased the PEAK PREDICTED 1-hour ozone by 9.7 ppb.

Figure 2.17 presents diurnal PREDICTED and OBSERVED 1-hour ozone and H_2O_2/HNO_3 ratios for RUN 5.

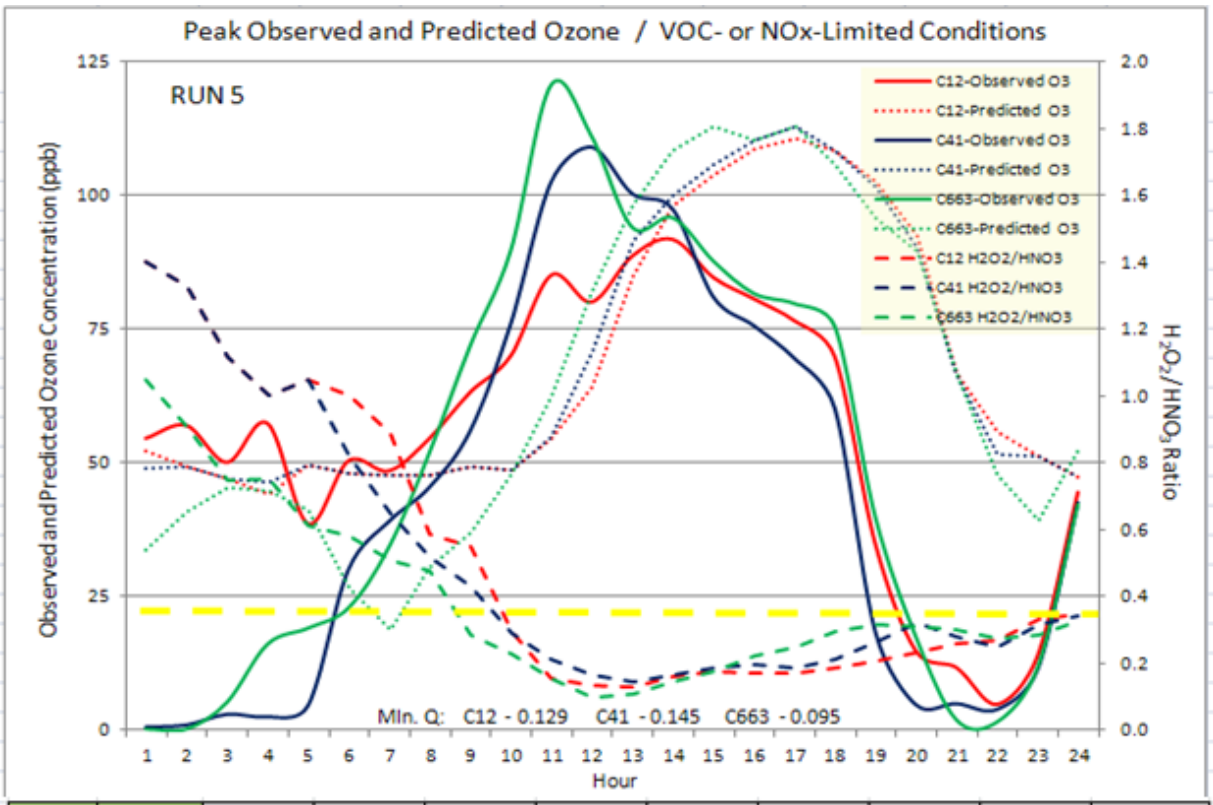

NOx	↑ 50%	PeakObs	PeakPred	PairPred	UPPA	APPA	EPPA	PTB	NB	NE
VOC	↑ 50%	120.7	113.0	108.7	-6.4	5.2	13.2	4	0.1	28.1
BASECASE			103.3	99.3	-14.4	-1.5	12.2	4	-3.3	25.6

Figure 2.17 Diurnal Predicted and Observed 1-Hour Ozone (ppb) / H_2O_2/HNO_3 Ratios – RUN 5

An increase of 50% in Juarez area source VOC emissions increased the PREDICTED PEAK 1-hour ozone (113 ppb or ~9.4%). The increase in 9.7 ppb greater than BASELINE continues to be 6.3 ppb below the OBSERVED PEAK. The PTB (4 hours) remained unchanged compared to BASELINE. NE (28.1%) increased by 2.5 percentage points from BASELINE. The model performed within acceptable NB (0.1%) and NE (28.1%) parameters.

Figure 2.18 presents diurnal PREDICTED and OBSERVED 8-hour ozone and H_2O_2/HNO_3 ratios for RUN 5.

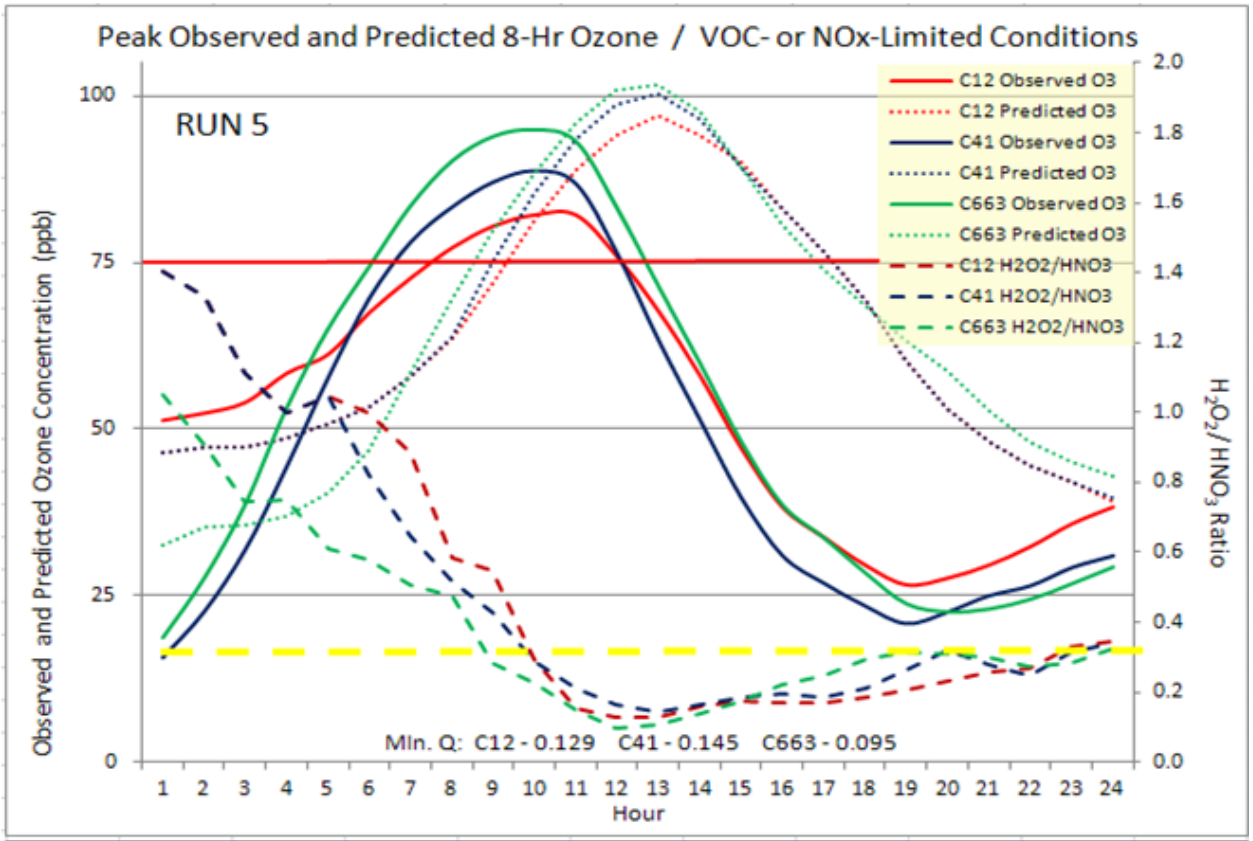

NOx	↑ 50%	PeakObs	PeakPred	PairPred	UPPA	APPA	EPPA	PTB	NB	NE
VOC	↑ 50%	95.1	101.76	100	7.1	8.5	13.7	3	7.4	25.4
BASELINE			93	92.1	-2.1	2.5	9	3	3.9	23.7

Figure 2.18 Diurnal Predicted and Observed 8-Hour Ozone (ppb) / H_2O_2/HNO_3 Ratios – RUN 5

The PAIRED PREDICTED PEAK 8-hour ozone (100 ppb) and the PREDICTED PEAK 8-hour (102.76) ppb indicate good model response to increased emissions. It should be noted that RUN 5 with 50% increase in both VOC and NOx generated an 8-hour ozone PREDICTED PEAK 1 ppb below RUN 4 which increased just VOC area source emissions by 50%. Both PREDICTED PEAK and the PAIRED PREDICTED PEAK over-predict OBSERVED 8-hour ozone and indicate good response to the 50% increase in Juárez area source VOC and NOx emissions. The positive NB (7.4%) substantiating the over-prediction and NE (25.4%) indicates the simulation generated results within acceptable parameters for these statistics.

H_2O_2/HNO_3 ratios indicated early morning NOx-limited conditions converting to VOC-limited conditions at 9 AM as photochemistry and HNO_3 production begins. The H_2O_2/HNO_3 ratio (0.095) is the lowest observed during the series of simulations and is closely associated with PREDICTED PEAK ozone concentrations. The minimum Q is observed at 12 PM. Of note is the lowest Q at 663 coincides with the PREDICTED PEAK.

2.7 RUN 6 Model Performance Evaluation

RUN 6 involved decreasing Juárez area source NOx and VOC emissions by 50%. Figure 2.19 presents performance statistics for RUN 6, 8-hour ozone PEAK OBSERVED, and co-located daily PAIRED PREDICTED PEAK among all sites in the PdN region.

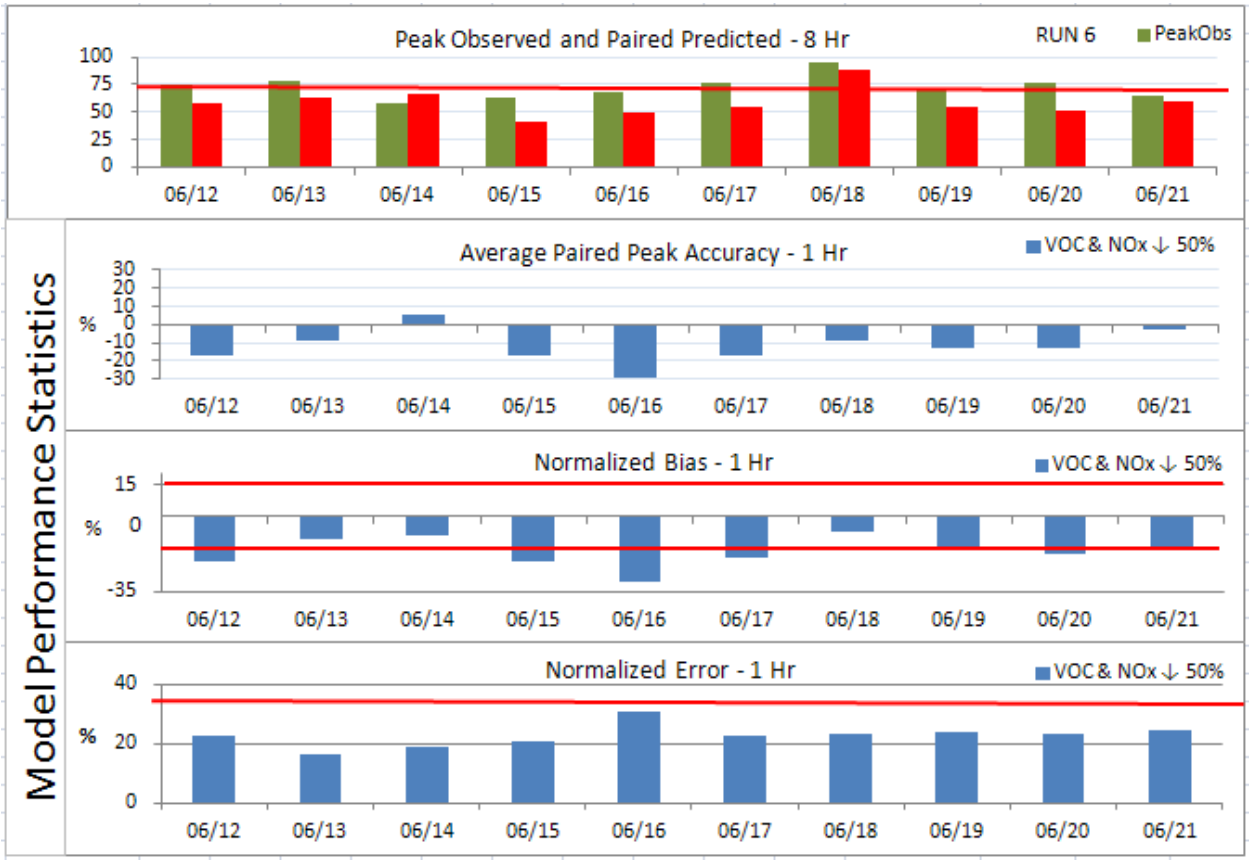

Figure 2.19 Model Performance Statistics - RUN 6

The simulation under-predicts 1-hour ozone on all 10 days as indicated by the negative NB for all simulated days. The simulation passed NB on 4 of 10 days. NB on 6/18 (-6.7%) indicated diminished performance over BASELINE. This simulation presented slightly improved NE (23.2%) for 1-hour ozone. Both NB and NE operated within acceptable parameters.

Figure 2.20 presents diurnal PREDICTED and OBSERVED 1-hour ozone and H_2O_2/HNO_3 ratios for RUN 6. PREDICTED PEAK on 6/18 for 1-hour ozone (92.7 ppb) is 10.6 ppb or ~13% less than BASELINE. The decrease indicates good model response to decreased VOC and NOx emissions. The PAIRED PREDICTED PEAK (89.1 ppb) occurred at C663.

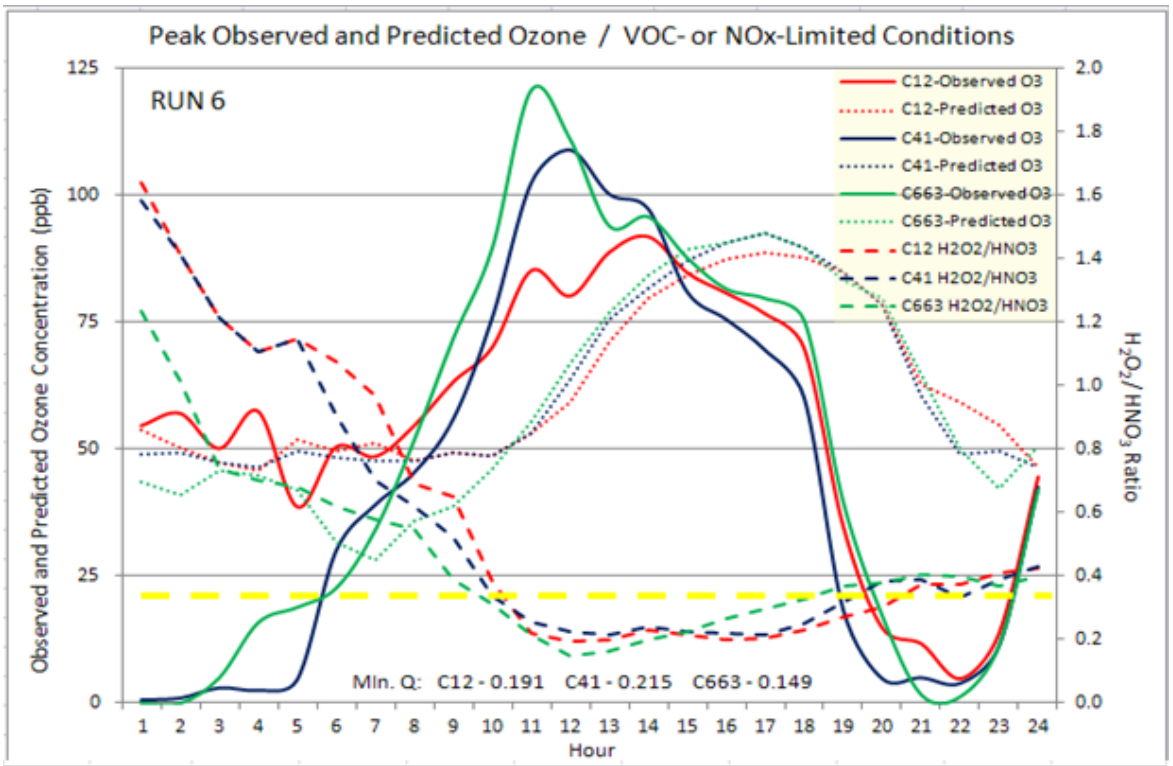

NOx	↓ 50%	PeakObs	PeakPred	PairPred	UPPA	APPA	EPPA	PTB	NB	NE
VOC	↓ 50%	120.7	92.7	89.1	-23.2	-8.7	14.4	4	-6.7	23.2
BASECASE			103.3	99.3	-14.4	-1.5	12.2	4	-3.3	25.6

Figure 2.20 Diurnal Predicted and Observed 1-Hour Ozone (ppb) / H_2O_2/HNO_3 Ratios – RUN 6

The decrease of 10 ppb in the PAIRED PREDICTED PEAK compared to BASELINE is well below the 120 ppb OBSERVED PEAK. PTB remained unchanged (4 hours) compared to BASELINE. NE (23.2%) increased by 1.4 percentage points from BASELINE. The model performed within acceptable parameters for NB and NE.

Figure 2.21 illustrates diurnal variability of PREDICTED and OBSERVED 8-hour ozone and H_2O_2/HNO_3 ratios for RUN 6. The decrease of 50% in Juarez area source VOC and NOx emissions reduced the PREDICTED PEAK 1-hour ozone to 84.5 ppb or ~9.4%.

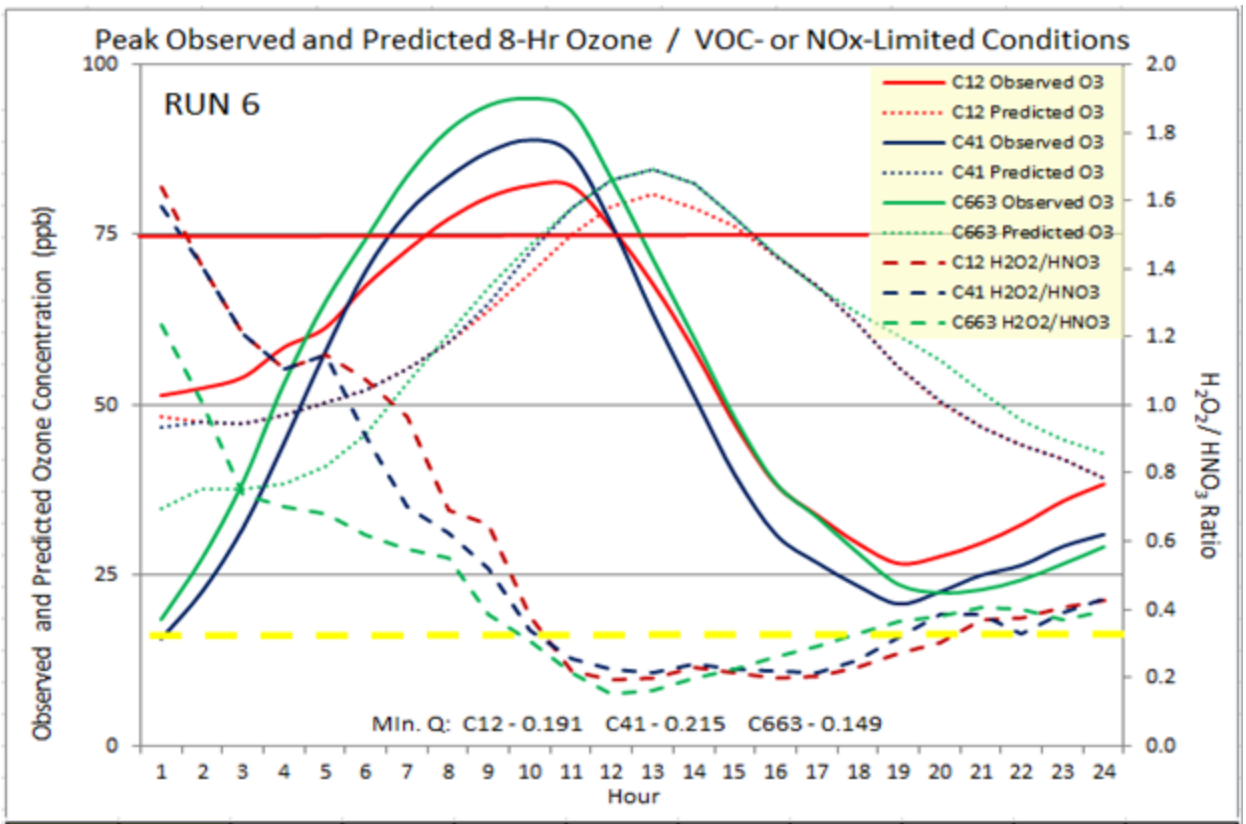

NOx	↓ 50%	PeakObs	PeakPred	PairPred	UPPA	APPA	EPPA	PTB	NB	NE
VOC	↓ 50%	95	84.49	83.6	-11.1	-3.9	8.3	3	0.4	22.1
BASELINE			93	92.1	-2.1	2.5	9	3	3.9	23.7

Figure 2.21 Diurnal Predicted and Observed 8-Hour Ozone (ppb) / H_2O_2/HNO_3 Ratios – RUN 6

PTB remained unchanged (3 hours) compared to BASELINE. NE (22.1%) slightly improved compared to BASELINE. The model performed within acceptable NB and NE parameters for the 8-hour ozone simulation. H_2O_2/HNO_3 ratios indicate a NOx-limited conditon exists during the early morning hours and shifts to VOC-limited at 10 AM due potentially to the decreased emissions applied to this simulation.

2.8 RUN 7 Model Performance Evaluation

RUN 7 involved increasing Juárez area source NOx emissions by 75%. Figure 2.22 presents model performance statistics for RUN 7, 8-hour ozone PEAK OBSERVED, and co-located daily PAIRED PREDICTED PEAK among all sites in the PdN region.

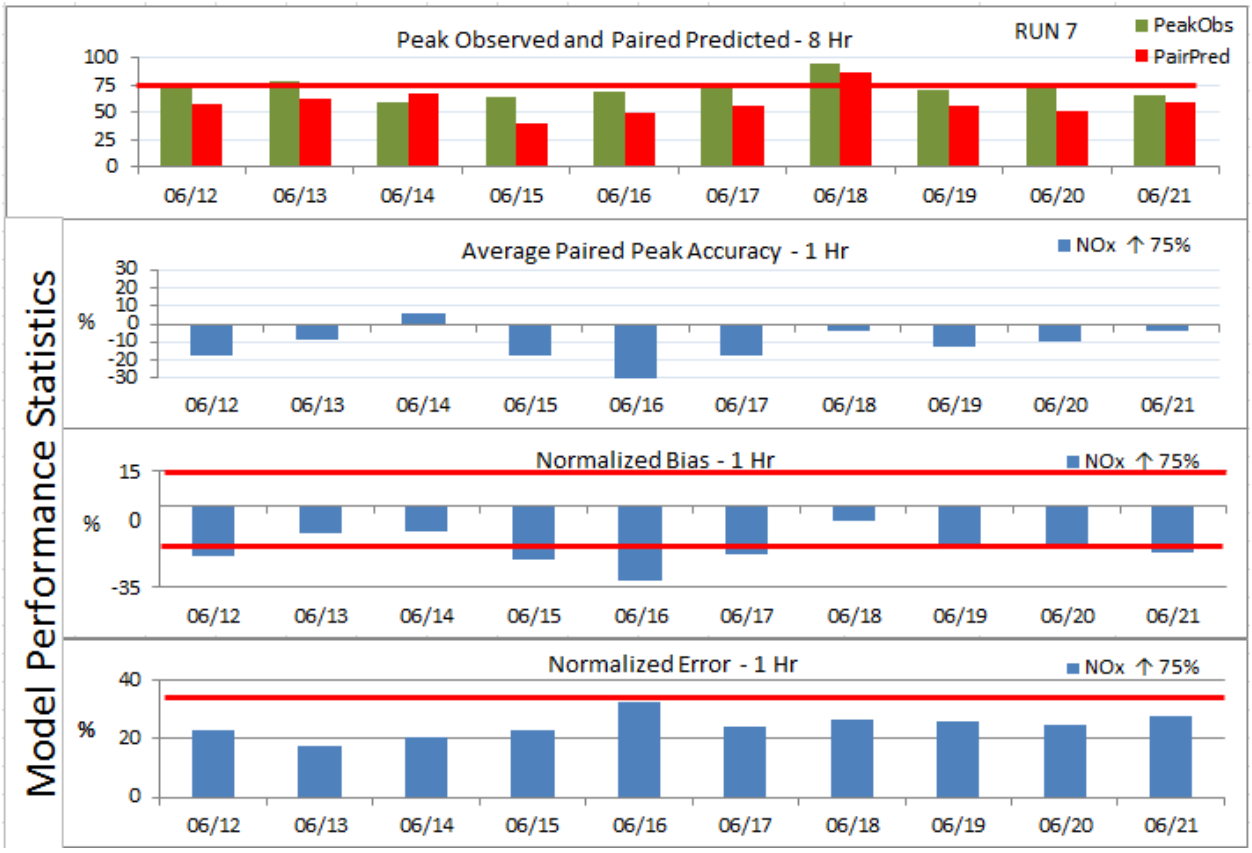

Figure 2.22 Model Performance and Statistics – RUN 7

The simulation under-predicts 1-hour ozone on all 10 days. The simulation passed NB on 3 of 10 days (6/13, 6/14, and 6/18). This simulation presented slightly diminished NE (26.3%) for 1-hour ozone on 6/18. APPA indicates under-prediction of 1-hour PAIRED PEAK ACCURACY during 9 of the 10 simulation days. Both NB (-6.3%) and NE (26.3%) operated within acceptable parameters.

Figure 2.23 presents diurnal PREDICTED and OBSERVED 1-hour ozone and H_2O_2/HNO_3 ratios for RUN 7. The 1-hour ozone PREDICTED PEAK on 6/18 (100.1ppb) was 3.2 ppb less than BASELINE. The model did not strongly respond to the 75% increase in NOx emissions further indicating VOC-limited conditions exist. The PAIRED PREDICTED PEAK which occurred at C663 (95.3 ppb) was 4.1 ppb less than BASELINE. The decrease in 1-hour ozone coinciding with a 75% increase in NOx emissions indicates ozone is titrated by the NOx.

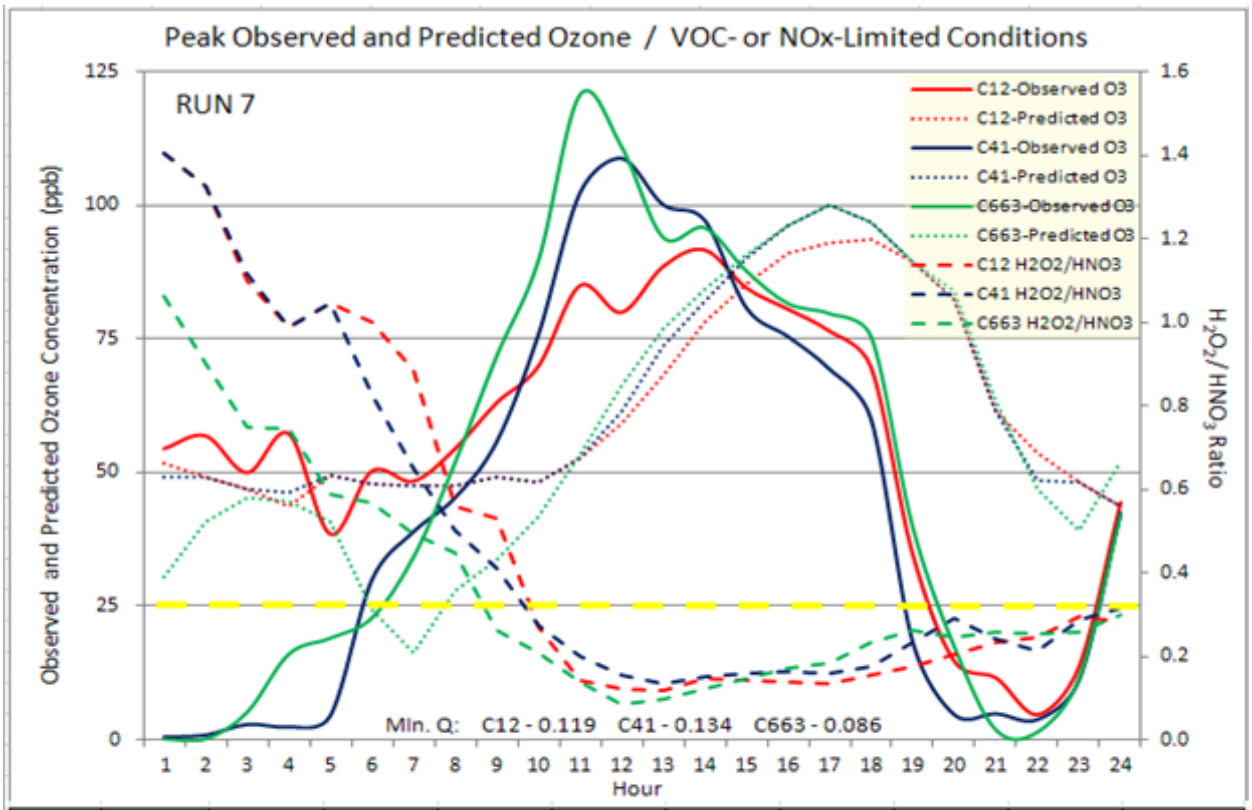

NOx	↑ 75%	PeakObs	PeakPred	PairPred	UPPA	APPA	EPPA	PTB	NB	NE
VOC	---	120.7	100.1	95.2	-17.1	-3.6	13.3	4	-6.3	26.3
BASECASE			103.3	99.3	-14.4	-1.5	12.2	4	-3.3	25.6

Figure 2.23 Diurnal Predicted and Observed 1-Hour Ozone (ppb) / H_2O_2/HNO_3 Ratios – RUN 7

Figure 2.24 illustrates diurnal PREDICTED and OBSERVED 8-hour ozone and H_2O_2/HNO_3 ratios for RUN 7. The 75% increase in Juárez area source NOx emissions reduced the 1-hour ozone PREDICTED PEAK 89 ppb or 14.5%. The PTB remained unchanged (3 hours) compared to BASELINE. NE (24.3%) slightly diminishes compared to BASELINE. The model performed within acceptable NB and NE parameters for the 8-hour ozone simulation. H_2O_2/HNO_3 ratios indicate a NOx-limited conditon exists during the early morning hours and shifts to VOC-limited conditions at 9 AM due potentially to the increase in NOx which will produce greater concentrations of HNO_3. The minimum Q observed (0.086) further confirms VOC-limited conditions control ozone formation.

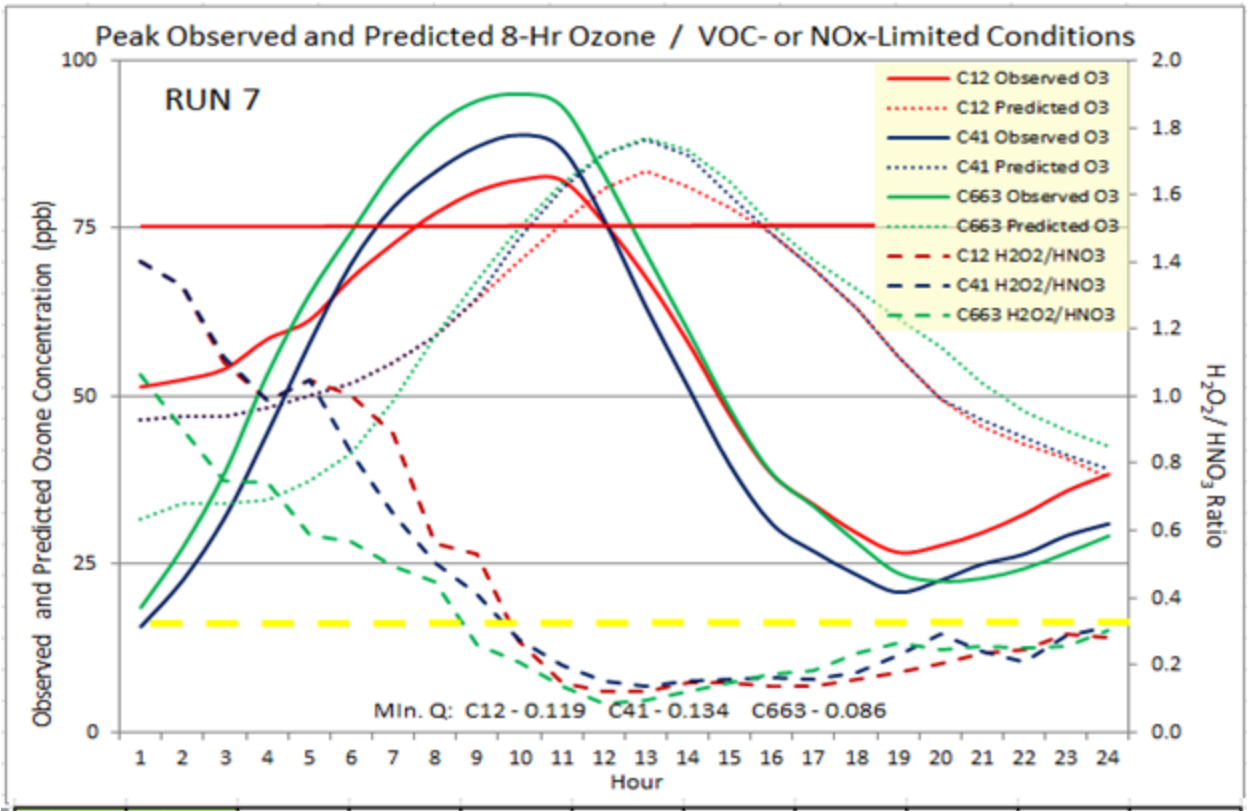

NOx	↑75%	PeakObs	PeakPred	PairPred	UPPA	APPA	EPPA	PTB	NB	NE
VOC	---	95.1	89	88.3	-5.2	0.6	8.5	3	1.8	24.3
BASELINE			93	92.1	-2.1	2.5	9	3	3.9	23.7

Figure 2.24 Diurnal Predicted and Observed 8-Hour Ozone (ppb) / H_2O_2/HNO_3 Ratios – RUN 7

2.9 RUN 8 Model Performance Evaluation

RUN 8 involved a 75% reduction in Juárez area source NOx emissions. Figure 2.25 presents performance statistics for RUN 8, 8-hour ozone PEAK OBSERVED, and co-located daily PAIRED PREDICTED PEAK among all sites in the PdN region.

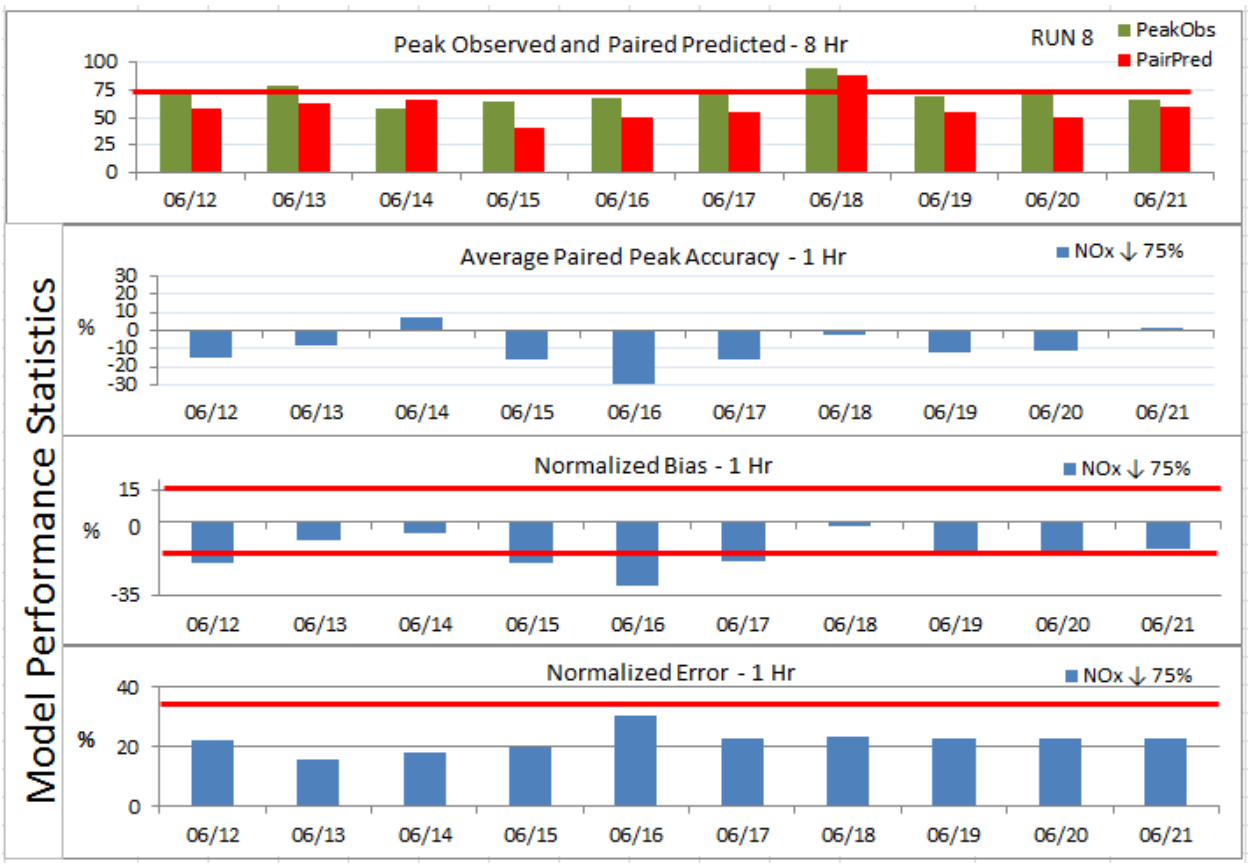

Figure 2.25 Model Performance Statistics – Run 8

The simulation under-predicts 1-hour ozone on all 10 days given. The simulation passed NB on 3 of 10 days. NB was within acceptable parameters on 3 days (6/13, 6/14, and 6/18). This simulation presented slightly improved NB (-1.8%) compared to BASELINE NB (-3.3%) on 6/18. The simulation also presented improved NE (23.3%) compared to BASELINE NE (25.6%) for 1-hour ozone on 6/18. APPA indicates under-prediction of 1-hour ozone during 8 of the 10 simulation days. Figure 2.26 presents diurnal PREDICTED and OBSERVERD 1-hour ozone and H_2O_2/HNO_3 ratios for RUN 8.

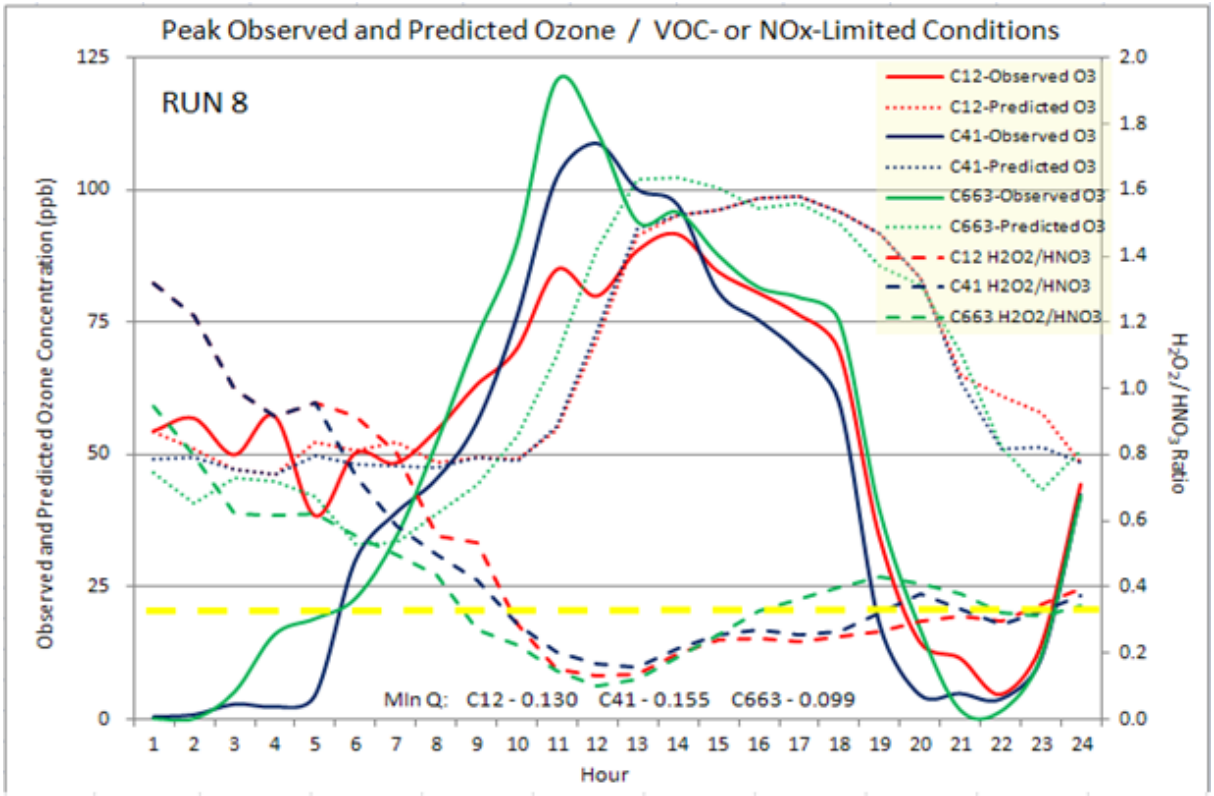

NOx	↓ 75%	PeakObs	PeakPred	PairPred	UPPA	APPA	EPPA	PTB	NB	NE
VOC	---	120.7	102.3	97.6	-15.3	-2.7	11.9	3	-1.8	23.3
BASECASE			103.3	99.3	-14.4	-1.5	12.2	4	-3.3	25.6

Figure 2.26 Diurnal Predicted and Observed 1-Hour Ozone (ppb) / H_2O_2/HNO_3 Ratios – RUN 8

The PREDICTED PEAK on 6/18 for 1-hour ozone (102.3 ppb) was 1 ppb less than BASELINE. PEAK OBSERVED (120.7 ppb) occurred at C663, and PAIRED PREDICTED PEAK (97.6 ppb) is slightly lower than BASELINE (99.3 ppb). There is little difference in 1-hour ozone between BASELINE and modification to NOx emissions continuing to indicate VOC-limited conditions exist in the PdN region.

Figure 2.27 illustrates diurnal PREDICTED and OBSERVED 8-hour ozone and H_2O_2/HNO_3 ratios for RUN 8.

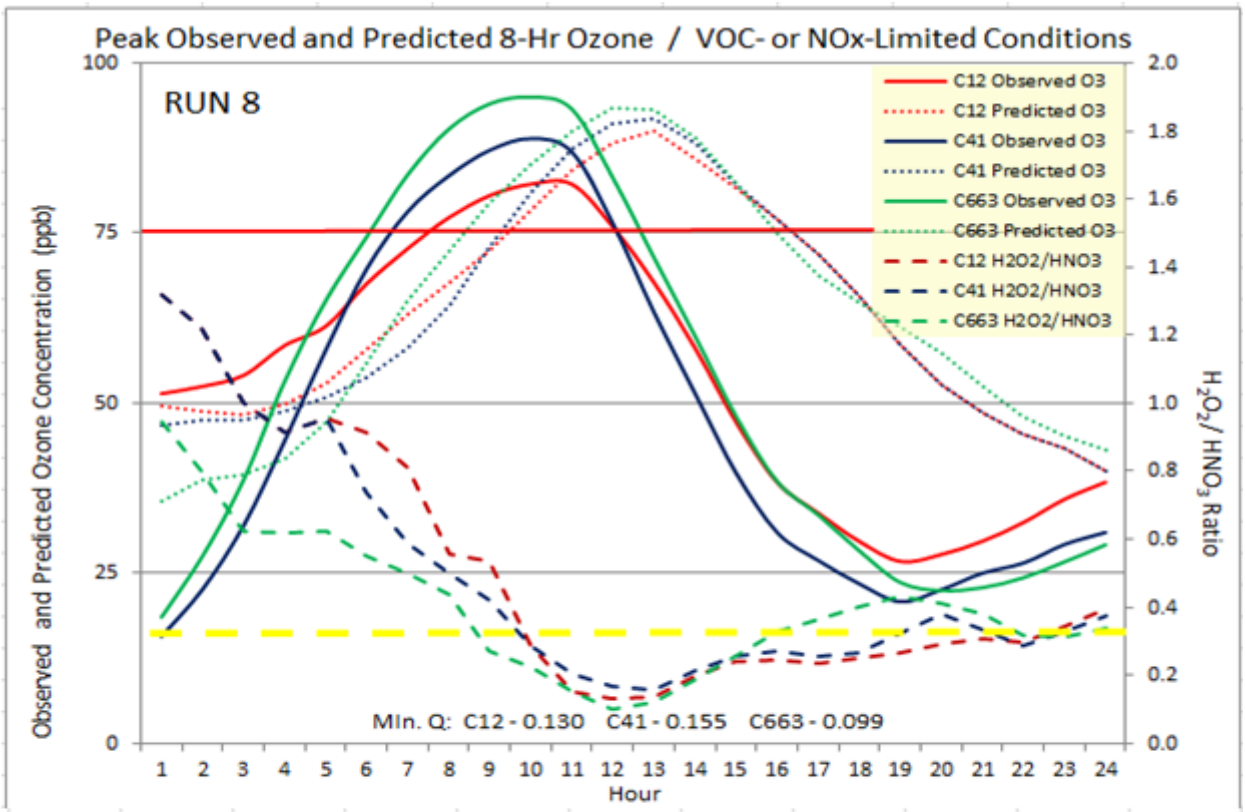

NOx	↓75%	PeakObs	PeakPred	PairPred	UPPA	APPA	EPPA	PTB	NB	NE
VOC	---	95.1	93.28	86.9	-7	-0.7	8.5	3	0.6	24.5
BASELINE			93	92.1	-2.1	2.5	9	3	3.9	23.7

Figure 2.27 Diurnal Predicted and Observed 8-Hour Ozone (ppb) / H_2O_2/HNO_3 Ratios – RUN 8

The 75% decrease in Juárez area source NOx emissions slightly increased the PREDICTED PEAK 8-hour ozone to 93.28 ppb compared to 93 ppb for the BASELINE which for all intents and purposes is an insignificant change in 8-hour ozone. PTB remained unchanged (3 hours) compared to BASELINE. NE (24.5%) slightly diminishes compared to BASELINE (23.7%). The model performed within acceptable NB and NE parameters for the 8-hour ozone simulation. H_2O_2/HNO_3 ratios indicate a NOx-limited condition exists during the early morning hours and shifts to VOC-limited at 9 AM due potentially to sufficient NOx which will titrate ambient ozone. The minimum Q observed (0.099) confirms a VOC-limited conditions control ozone formation.

2.10 RUN 9 Model Performance Evaluation

RUN 9 involved a 75% increase in Juárez area source VOC emissions. Figure 2.28 presents performance statistics for RUN 9, 8-hour ozone PEAK OBSERVED, and co-located daily PAIRED PREDICTED PEAK among all sites in the PdN region.

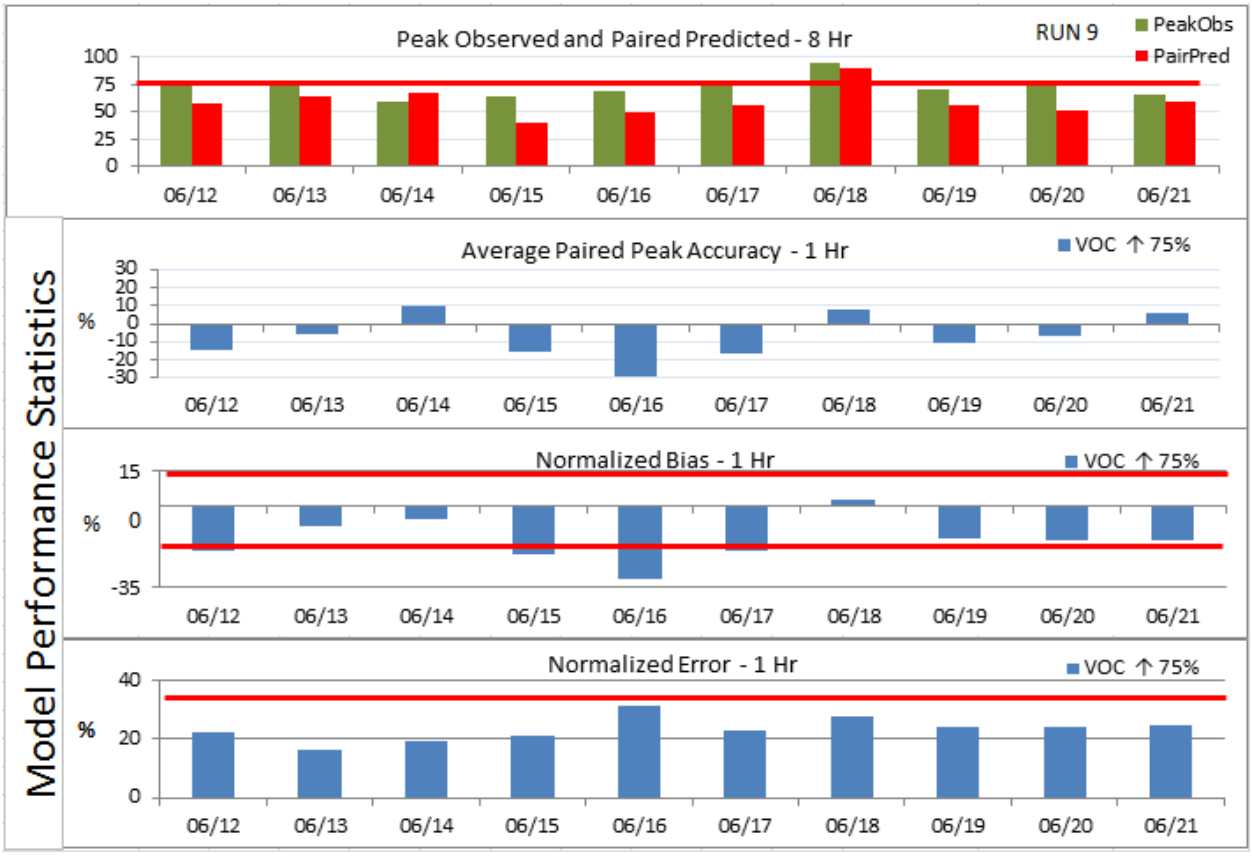

Figure 2.28 Model Performance Statistics – RUN 9

The simulation under-predicts 1-hour ozone on 9 of 10 simulation days. The simulation passed NB on 6 of 10 days. This simulation presented slightly improved NB (3.1%) compared to BASELINE NB (-3.3%) on 6/18 which over-predicts 1-hour ozone in the former and under-predicts 1-hour ozone in the latter. The simulation also presented slightly diminished NE (27.8%) compared to BASELINE NE (25.6%) for 1-hour ozone on 6/18. APPA indicates negative 1-hour prediction accuracy during 7 of the 10 simulation days. APPA was positive on 6/14, 6/18, and 6/21. NE was within acceptable parameters during all 10 simulation days.

Figure 2.29 presents diurnal PREDICTED and OBSERVED 1-hour ozone and H_2O_2/HNO_3 ratios for RUN 9.

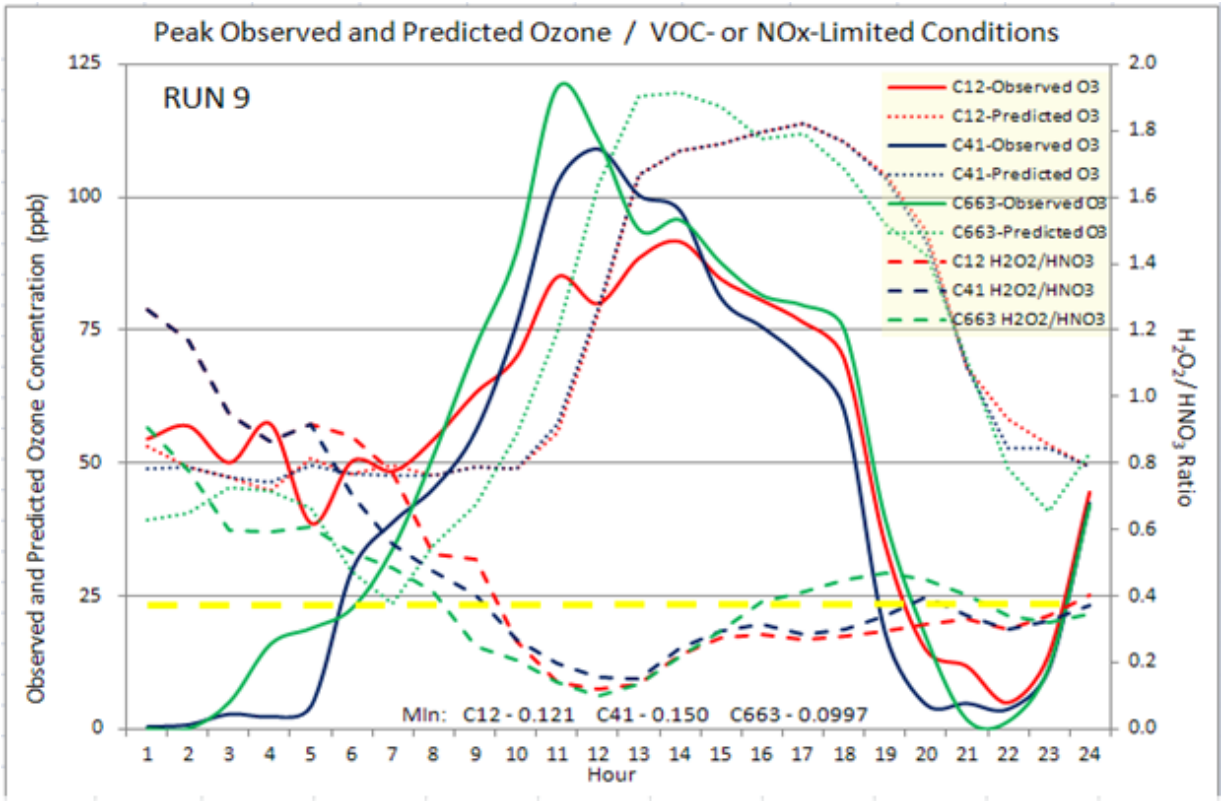

NOx	---	PeakObs	PeakPred	PairPred	UPPA	APPA	EPPA	PTB	NB	NE
VOC	↑ 75%	120.7	119.7	112.1	-0.9	7.8	15.2	3	3.1	27.8
BASECASE			103.3	99.3	-14.4	-1.5	12.2	4	-3.3	25.6

Figure 2.29 Diurnal Predicted and Observed 1-Hour Ozone (ppb) / H_2O_2/HNO_3 Ratios – RUN 9

1-hour PREDICTED PEAK on 6/18 (119.7 ppb) was ~16% greater than BASELINE (103.3 ppb). 1-hour ozone PEAK OBSERVED (120.7 ppb) occurred at C663. PAIRED PREDICTED PEAK (112.1 ppb) was ~13% greater than BASELINE (99.3 ppb). The elevated 1-hour ozone concentration indicates a strong response predicted by the model.

Figure 2.30 illustrates diurnal PREDICTED and OBSERVED 8-hour ozone and H2O2/HNO3 ratios for RUN 9.

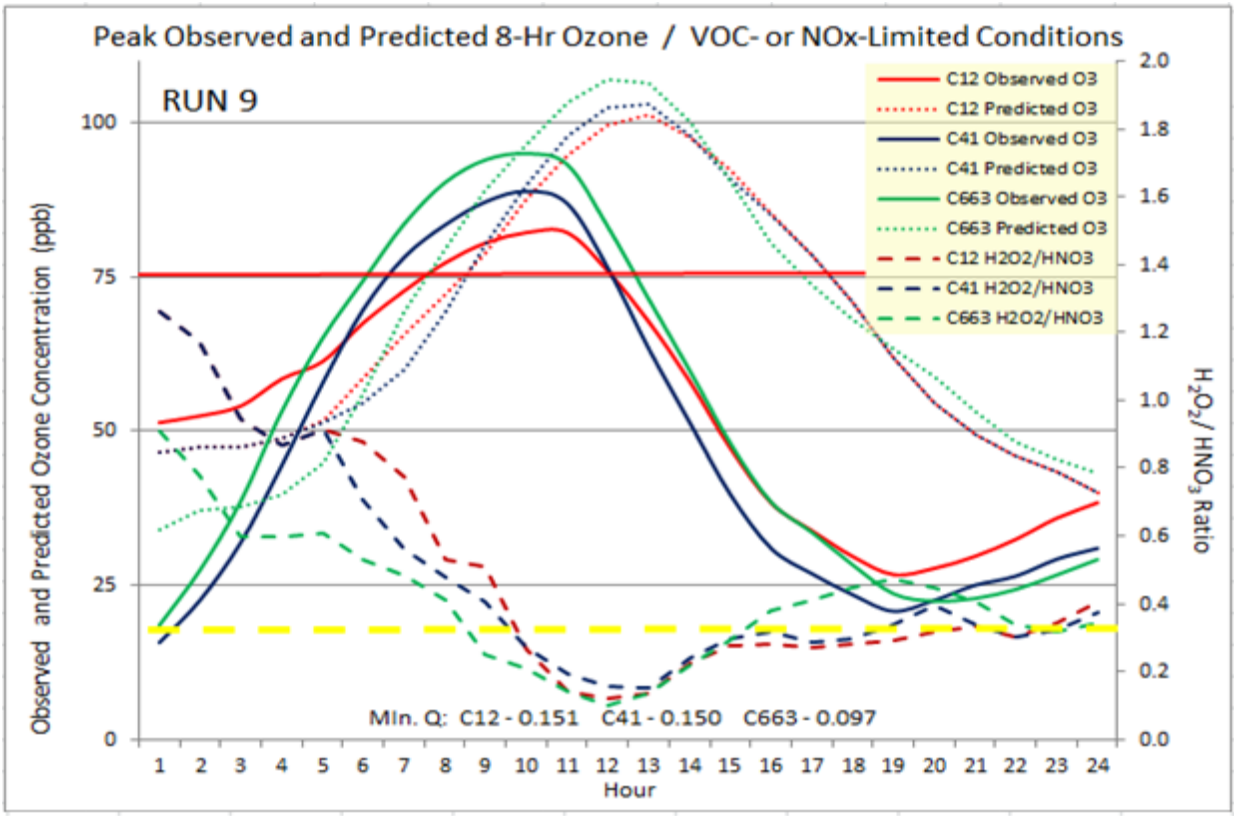

NOx	---	PeakObs	PeakPred	PairPred	UPPA	APPA	EPPA	PTB	NB	NE
VOC	↑ 75%	95.1	107.08	103.7	12.7	11.6	16.6	3	10.8	24.8
BASELINE			93	92.1	-2.1	2.5	9	3	3.9	23.7

Figure 2.30 Diurnal Predicted and Observed 8-Hour Ozone (ppb) / H_2O_2/HNO_3 Ratios – RUN 9

The 75% increase in Juárez area source VOC emissions increased the 8-hour ozone PREDICTED PEAK to 107 ppb compared to 93 ppb for the BASELINE. This indicates strong model response to increases in VOC emissions. PTB remained unchanged (3 hours) compared to BASELINE. NE (24.8%) slightly diminishes compared to BASELINE (23.7%). The model performed within acceptable NB and NE parameters for the 8-hour ozone simulation. H_2O_2/HNO_3 ratios indicate a NOx-limited condition exists during the early morning hours and shifts to VOC-limited at 0800. The minimum Q observed (0.097) confirms VOC-limited conditions control ozone formation.

2.11 RUN 10 Model Performance Evaluation

RUN 10 involved a 75% reduction on Juárez area source VOC emissions. Figure 2.31 presents performance statistics for RUN 10, 8-hour ozone PEAK OBSERVED, and co-located daily PAIRED PREDICTED PEAK among all sites in the PdN region.

The simulation under-predicts 1-hour ozone on all 10 days given. NB was within acceptable parameters during 3 days (6/13, 6/14, and 6/18). This simulation predicts slightly diminished NB (-11.5%) compared to BASELINE NB (-3.3%) on 6/18. Slightly improved NE (23.9%) was observed compared to BASELINE NE (25.6%) for 1-hour ozone on 6/18. APPA indicates under-prediction of 1-hour ozone PAIRED PEAK ACCURACY during 9 of the 10 simulation days. Only 6/14 presented positive APPA. NE was within acceptable limits during all 10 simulation days.

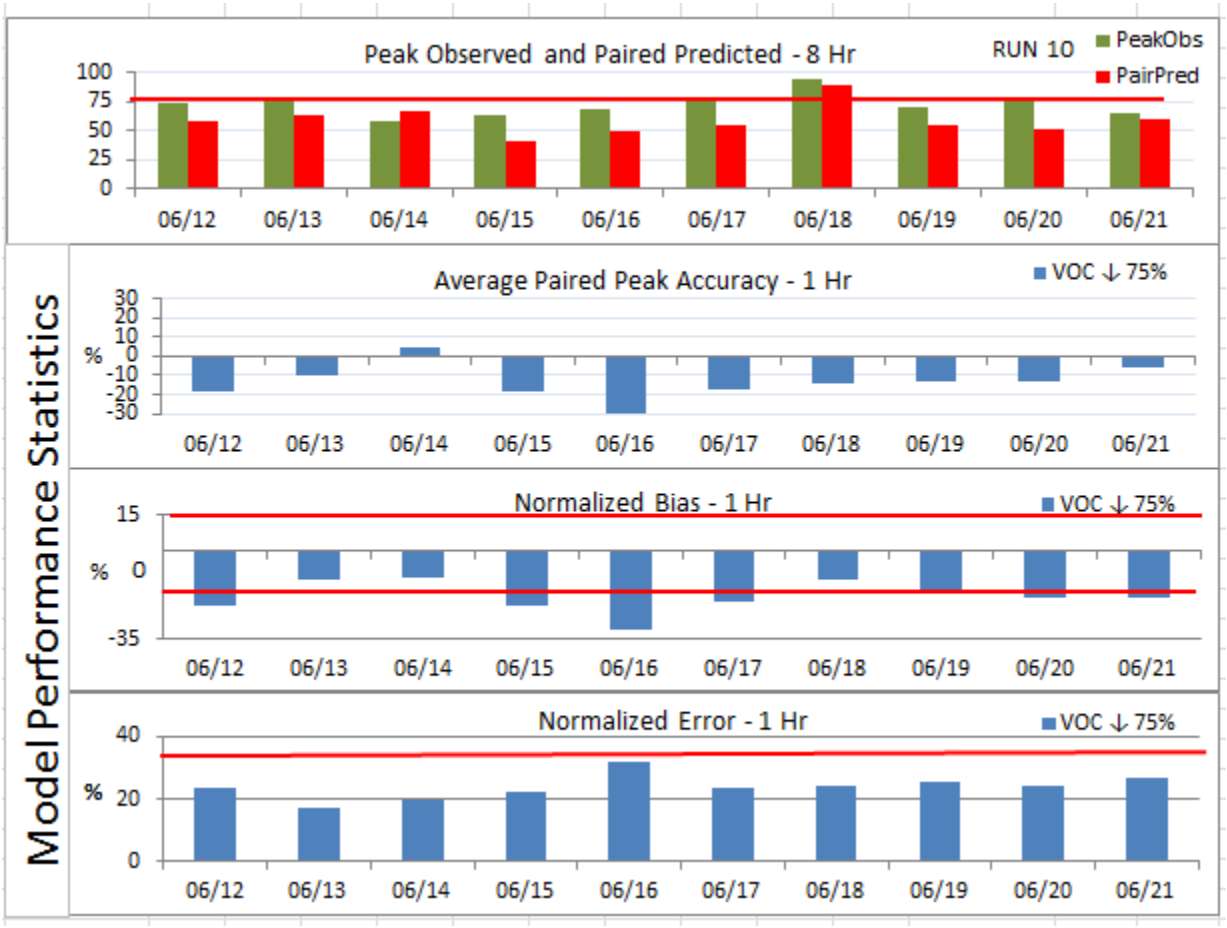

Figure 2.31 Model Performance Statistics - RUN 10

Figure 2.32 presents diurnal predicted and observed 1-hour ozone and H_2O_2/HNO_3 ratios for RUN 10. The PREDICTED PEAK on 6/18 for 1-hour ozone (86.6 ppb) was 16% less than BASELINE (103.3 ppb). PAIRED PREDICTED PEAK (80.1p ppb) is 33% less than PEAK OBSERVED (120.7 ppb). 1-hour PAIRED PREDICTED PEAK (80.1 ppb) is 19% less than BASELINE PAIRED PREDICTED PEAK (99.3 ppb). The model displays strong response to VOC.

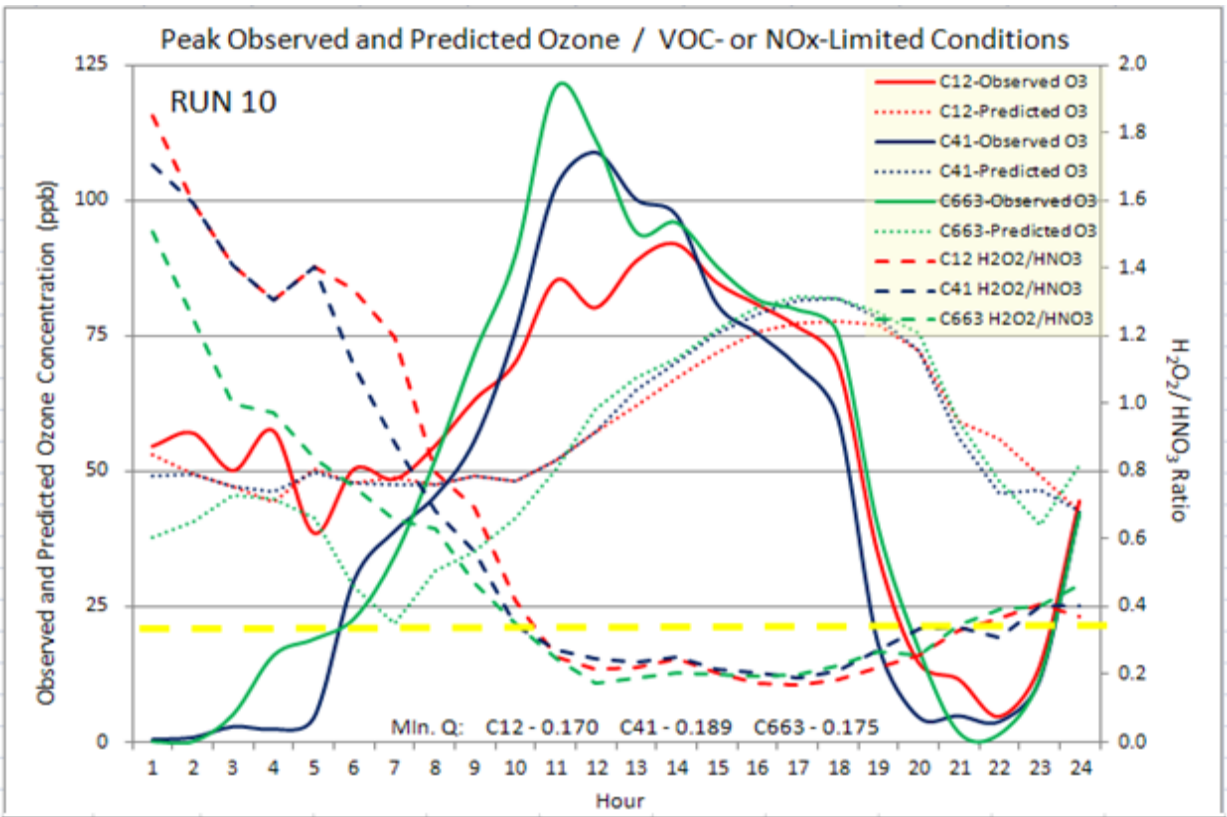

NOx	---	PeakObs	PeakPred	PairPred	UPPA	APPA	EPPA	PTB	NB	NE
VOC	↓ 75%	120.7	86.8	80.1	-28.1	-14.6	17.2	4	-11.5	23.9
BASECASE			103.3	99.3	-14.4	-1.5	12.2	4	-3.3	25.6

Figure 2.32 Diurnal Predicted and Observed 1-Hour Ozone (ppb) / H_2O_2/HNO_3 Ratios – RUN 10

Figure 2.33 illustrates diurnal PREDICTED and OBSERVED 8-hour ozone and H2O2/HNO3 ratios for RUN 10. The 75% decrease in Juárez area source VOC emissions strongly influenced predicted 8-hour ozone concentrations. PREDICTED PEAK 8-hour ozone (80.5 ppb) is 13% less than BASELINE 8-hour ozone PREDICTED PEAK (93 ppb). PTB remained unchanged (3 hours) compared to BASELINE. NE (22.8%) slightly improves compared to BASELINE NE (23.7%).

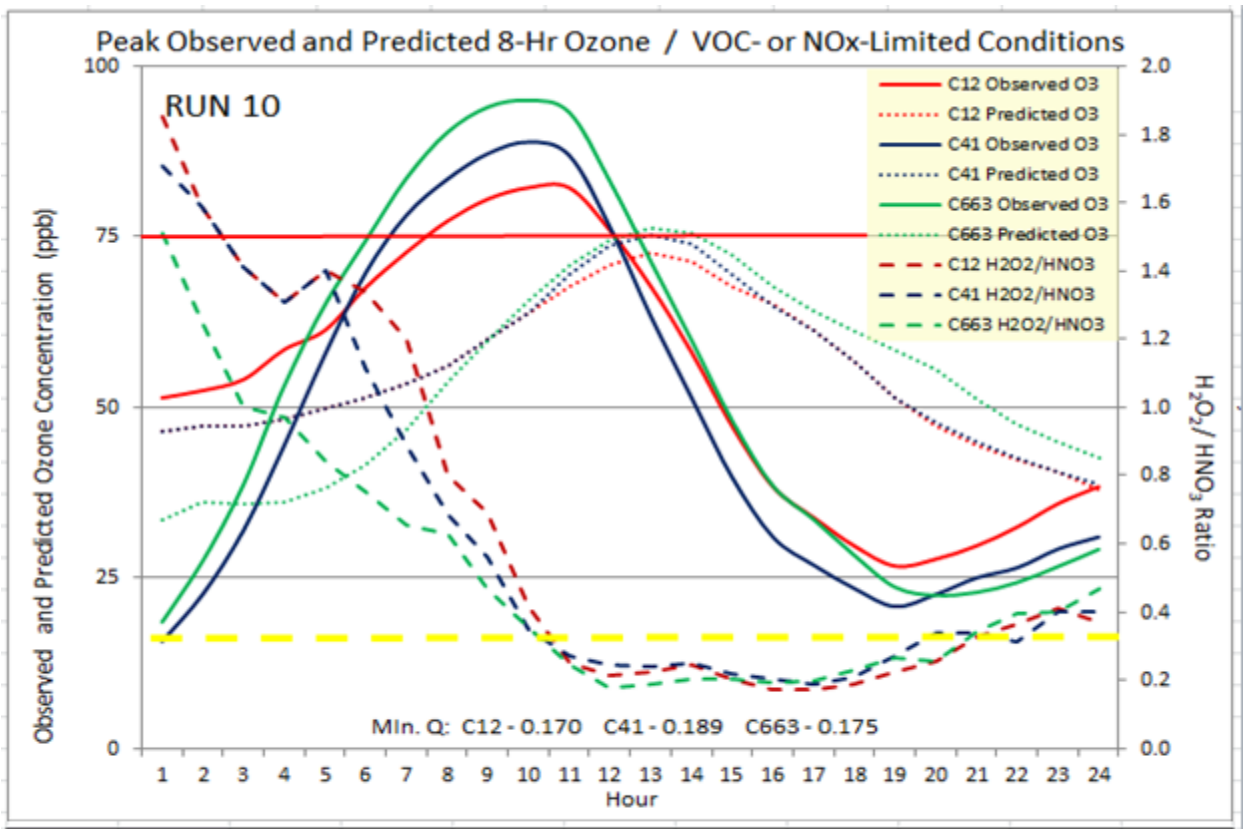

NOx	---	PeakObs	PeakPred	PairPred	UPPA	APPA	EPPA	PTB	NB	NE
VOC	↓75%	95.1	80.51	73.8	-15.3	-10.5	12.1	3	-4.8	22.8
BASELINE			93	92.1	-2.1	2.5	9	3	3.9	23.7

Figure 2.33 Diurnal Predicted and Observed 8-Hour Ozone (ppb) / H_2O_2/HNO_3 Ratios – RUN 10

The model performed within acceptable NB and NE parameters for the 8-hour ozone simulation. H_2O_2/HNO_3 ratios indicate a NOx-limited condition exists during the early morning hours and shifts to VOC-limited at 10 AM. The reduction in initial VOC emissions potentially slowed the photochemical reaction delaying production of HNO_3. The minimum Q observed (0.175) confirms a VOC-limited ENVIRONment controls ozone formation.

2.12 RUN 11 Model Performance Evaluation

RUN 11 involved a 75% increase in Juárez area source NOx and VOC emissions. Figure 2.34 presents performance statistics for RUN 11, 8-hour ozone PEAK OBSERVED, and co-located daily PAIRED PREDICTED PEAK among all sites in the PdN region.

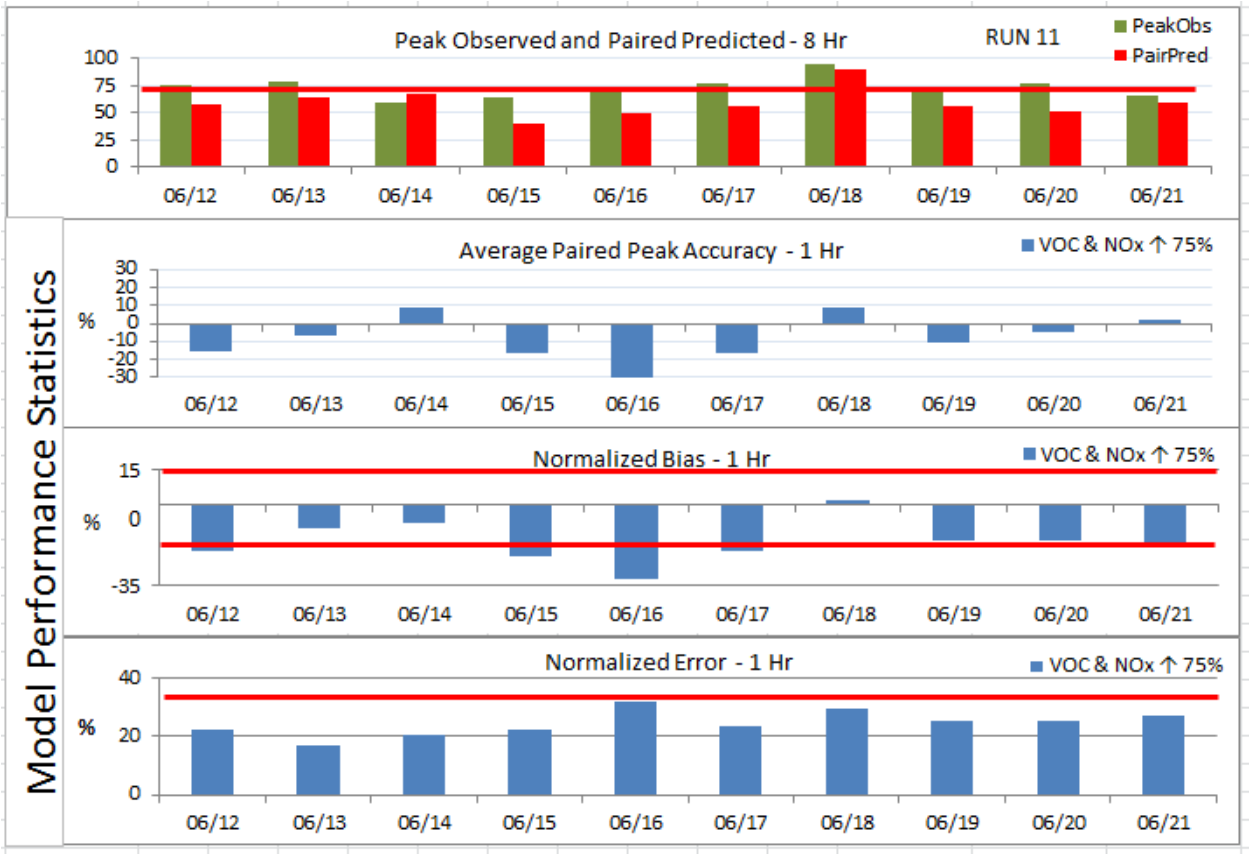

Figure 2.34 Model Performance Statistics - RUN 11

The simulation under-predicts 1-hour ozone on 9 of 10 days. The simulation was within acceptable parameters for NB on 3 of 10 days (6/13, 6/14, and 6/18). Positive APPA on 3 of 10 days indicates the model over—prediction accuracy for 1-hour ozone compared to co-located PAIRED PEAKs. This simulation predicts improved NB (1.8%) compared to BASELINE NB (-3.3%) on 6/18 indicating a slight over-prediction bias during the exceedance day. Diminished 1-hour ozone NE (29.5%) was observed compared to BASELINE NE (25.6%) on 6/18. Both NB and NE operated within acceptable parameters.

Figure 2.35 presents diurnal PREDICTED and OBSERVED 1-hour ozone and H_2O_2/HNO_3 ratios for RUN 11.

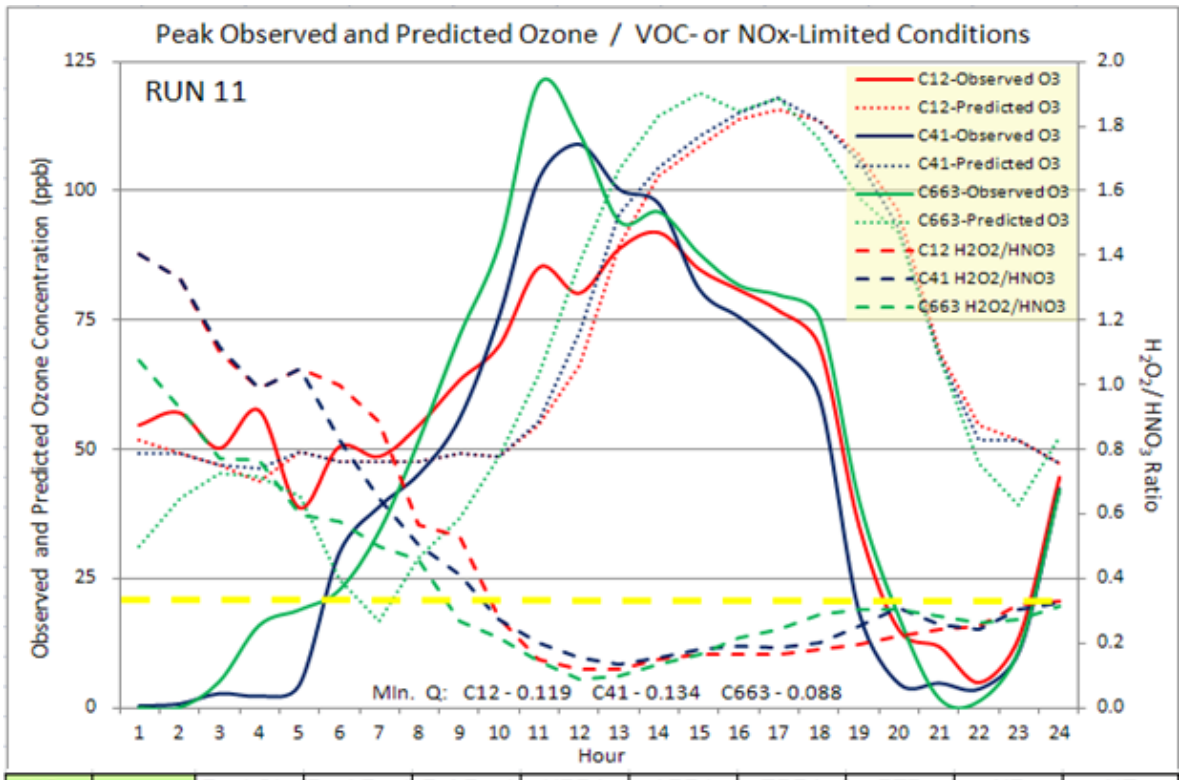

NOx	↑ 75%	PeakObs	PeakPred	PairPred	UPPA	APPA	EPPA	PTB	NB	NE
VOC	↑ 75%	120.7	118.8	113.6	-1.6	8.6	15.2	4	1.8	29.5
BASECASE			103.3	99.3	-14.4	-1.5	12.2	4	-3.3	25.6

Figure 2.35 Diurnal Predicted and Observed 1-Hour Ozone (ppb) / H_2O_2/HNO_3 Ratios – Run 11

1-hour ozone PEAK PREDICTED (118.8 ppb) on 6/18 was ~14% greater than BASELINE PEAK PREDICTED (103.3 ppb). PAIRED PREDICTED PEAK (113.6 ppb) is 5% less than PEAK OBSERVED (120.7 ppb) and exceeds BASELINE (99.3 ppb) by 13%. The model displays strong response to VOC emissions modifications and indicates VOC-limited conditions exist in the PdN region. Figure 2.36 illustrates diurnal PREDICTED and OBSERVED 8-hour ozone and H_2O_2/HNO_3 ratios for RUN 11.

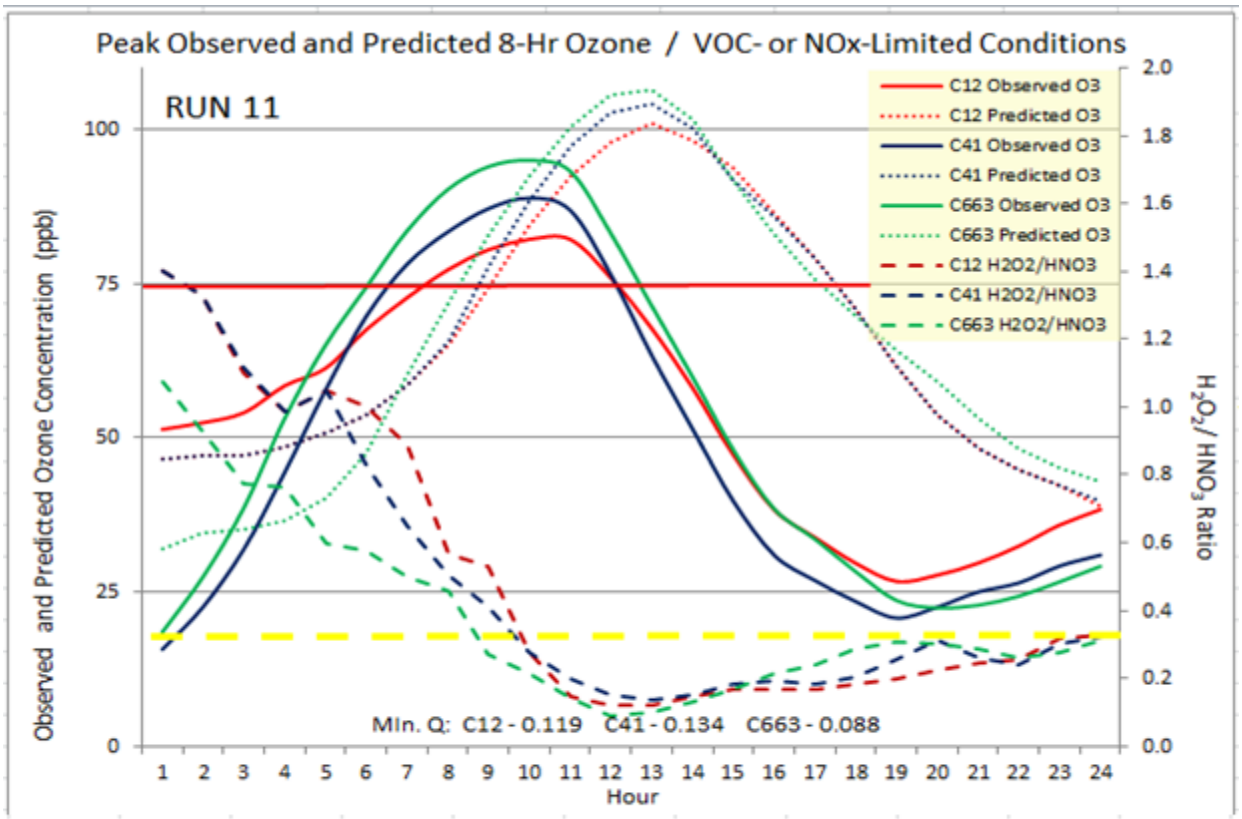

NOx	↑75%	PeakObs	PeakPred	PairPred	UPPA	APPA	EPPA	PTB	NB	NE
VOC	↑75%	95.1	106.31	104.1	11.9	11.7	16.4	3	9.2	26.5
BASELINE			93	92.1	-2.1	2.5	9	3	3.9	23.7

Figure 2.36 Diurnal Predicted and Observed 8-Hour Ozone (ppb) / H_2O_2/HNO_3 Ratios – Run 11

The 75% increase in Juárez area source VOC and NOx emissions strongly influenced predicted 8-hour ozone concentrations. 8-hour ozone PEAK PREDICTED on 6/18 (106.3 ppb) is ~14% greater than BASELINE (93 ppb). PAIRED PREDICTED PEAK (104.1 ppb) exceeds PEAK OBSERVED at C663 (95.1 ppb) by ~9% and exceeds BASELINE (92.1 ppb) by 13%. PTB remained unchanged at 3 hours compared to BASELINE. NE (22.8%) slightly improved compared to BASELINE NE (23.7%).

The model performed within acceptable NB and NE parameters for the 8-hour ozone simulation. H_2O_2/HNO_3 ratios indicate a NOx-limited condition exists during the early morning hours and shifts to VOC-limited at 9 AM. Elevated VOC emissions potentially accelerate the photochemical reactions and promote early HNO_3 production. The minimum Q observed (0.088) confirming a VOC-limited conditions control ozone formation.

2.13 RUN 12 Model Performance Evaluation

RUN 12 involved a 75% reduction in Juárez area source NOx and VOC emissions. Figure 2.37 presents performance statistics for RUN 12, 8-hour ozone PEAK OBSERVED, and co-located daily PAIRED PREDICTED PEAK among all sites in the PdN region.

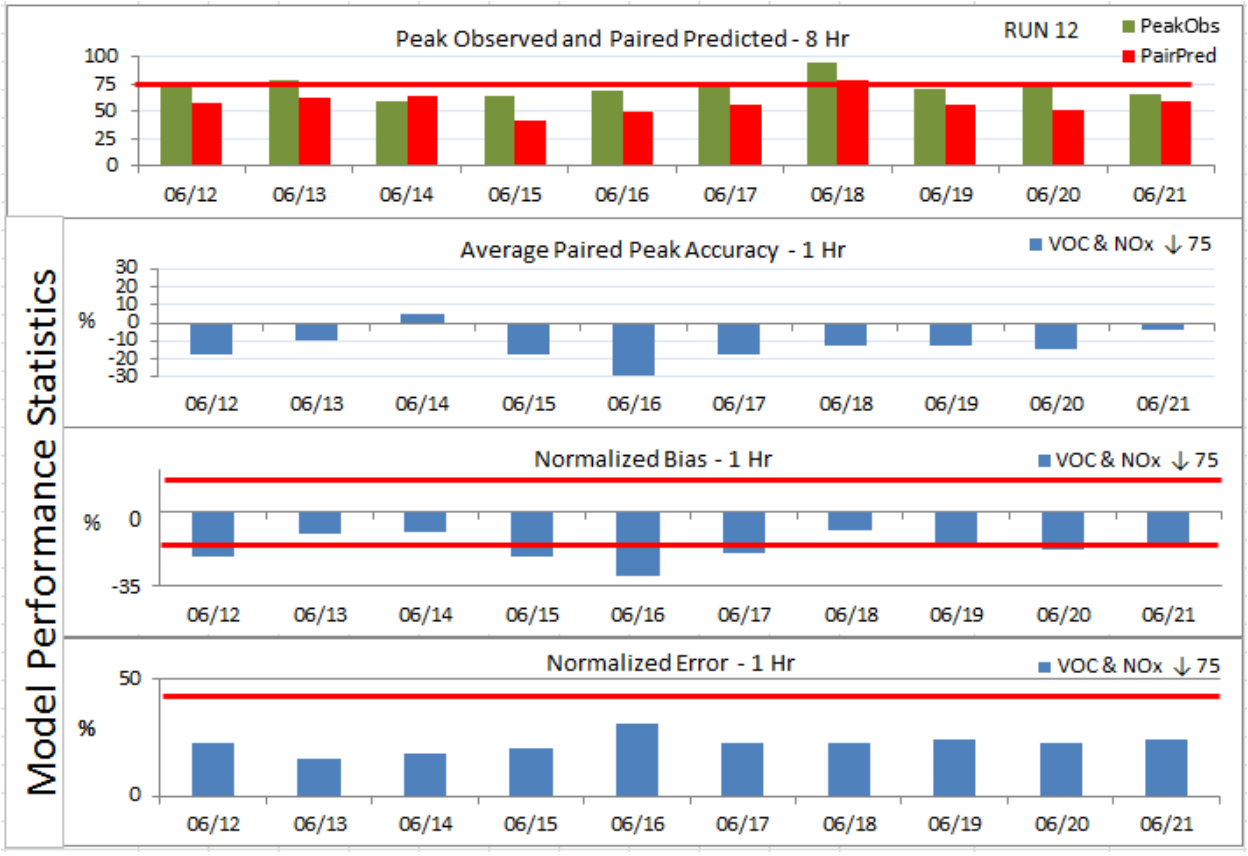

Figure 2.37 Model Performance Statistics – RUN 12

The simulation under-predicts 1-hour ozone on all 10 days given. Negative NB is indicated for each simulation day. 1-hour ozone was predicted within acceptable parameters for NB on 3 of 10 days (6/13, 6/14, and 6/18). This simulation predicts slightly diminished NB (-8.7%) compared to BASELINE NB (-3.3%) on 6/18. Slightly improved NE (22.4%) was observed compared to BASELINE NE (25.6%) for 1-hour ozone on 6/18. APPA indicates under-prediction accuracy for 1-hour ozone during 9 of the 10 simulation days. Only 6/14 presented positive APPA. Both NB and NE operated within acceptable parameters.

Figure 2.38 presents diurnal PREDICTED and OBSERVED 1-hour ozone and H_2O_2/HNO_3 ratios for RUN 12.

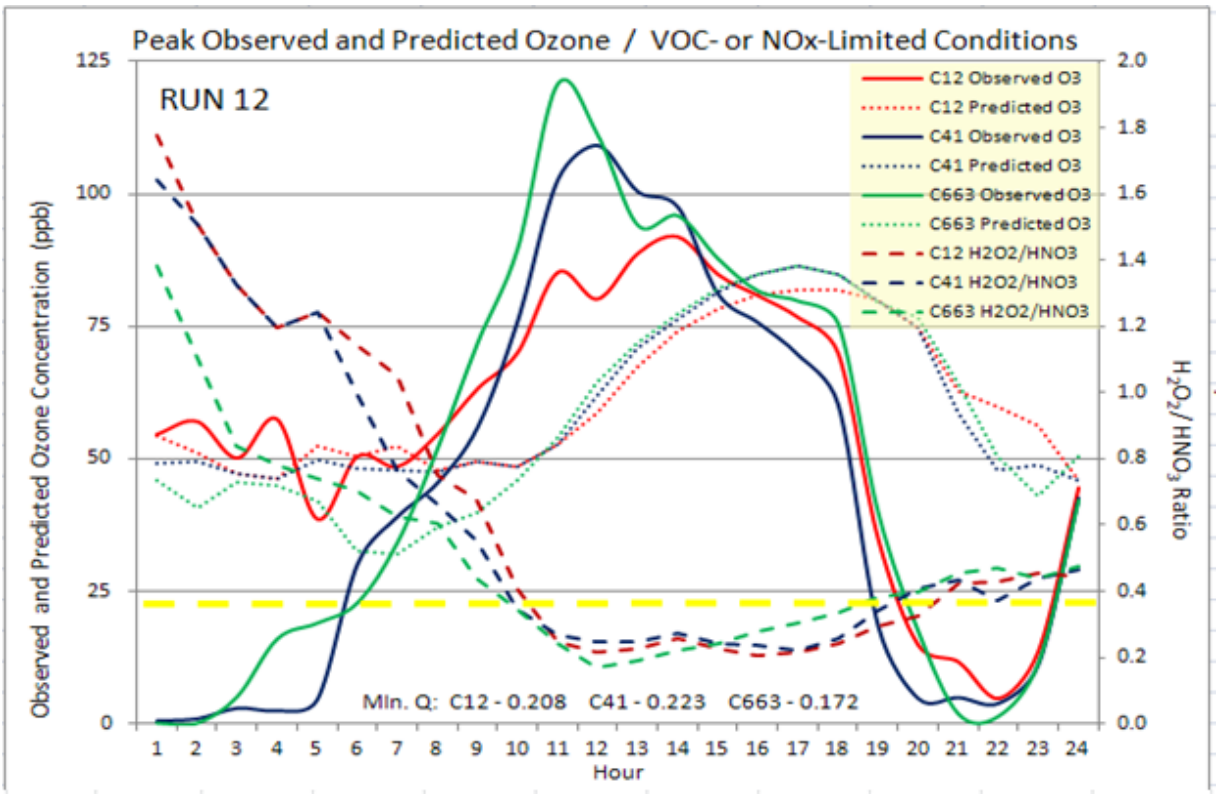

NOx	↓ 75%	PeakObs	PeakPred	PairPred	UPPA	APPA	EPPA	PTB	NB	NE
VOC	↓ 75%	120.7	87.8	83.3	-27.2	-12.8	16	4	-8.7	22.4
BASECASE			103.3	99.3	-14.4	-1.5	12.2	4	-3.3	25.6

Figure 2.38 Diurnal Predicted and Observed 1-Hour Ozone (ppb) / H_2O_2/HNO_3 Ratios – Run 12

1-hour ozone PREDICTED PEAK on 6/18 (87.8 ppb) was 18% less than BASELINE PREDICTED PEAK (103.3 ppb). PAIRED PREDICTED PEAK (83.3 ppb) is 30% less than PEAK OBSERVED (120.7 ppb) and 16% less than the BASELINE PAIRED PREDICTED PEAK (99.3 ppb). The model displays strong response to VOC modifications and indicates VOC-limited conditions exist in the PdN region.

Figure 2.39 illustrates diurnal predicted and observed 8-hour ozone and H_2O_2/HNO_3 ratios for RUN 12.

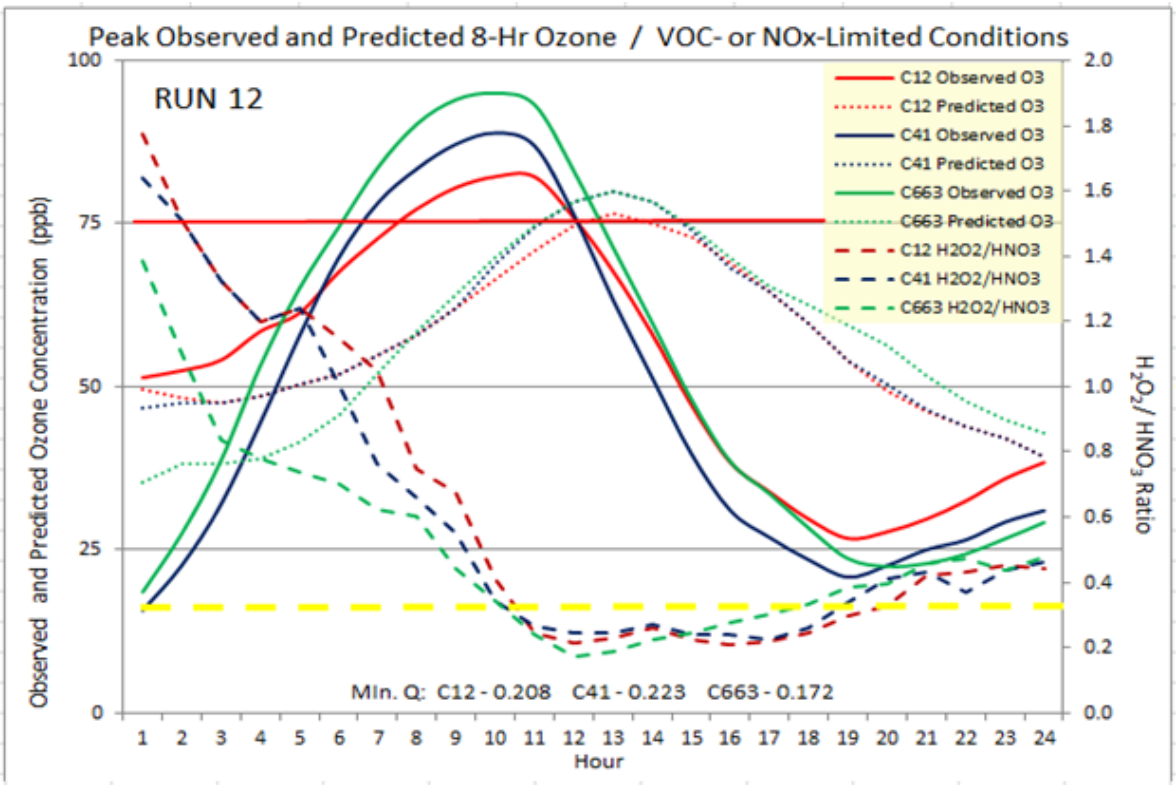

NOx	↓ 75%	PeakObs	PeakPred	PairPred	UPPA	APPA	EPPA	PTB	NB	NE
VOC	↓ 75%	95.1	80.71	78.8	-15.1	-7.6	9.5	3	-1.6	21.5
BASELINE			93	92.1	-2.1	2.5	9	3	3.9	23.7

Figure 2.39 Diurnal Predicted and Observed 8-Hour Ozone (ppb) / H_2O_2/HNO_3 Ratios – Run 12

The 75% decrease in Juárez area source VOC and NOx emissions strongly influenced predicted 8-hour ozone concentrations. PEAK PREDICTED 8-hour ozone on 6/18 (80.7 ppb) is ~13% less than 8-hour BASELINE PEAK PREDICTED (93 ppb). PAIRED PREDICTED PEAK (78.8 ppb) is 17% less than PEAK OBSERVED at C663 (95.1 ppb) and 13% less than BASELINE PAIRED PREDICTED PEAK (92.1 ppb). PTB remained unchanged (3 hours) compared to BASELINE. NE (21.5%) slightly improved compared to BASELINE NE (23.7%).

The model performed within acceptable NB and NE parameters for the 8-hour ozone simulation. H_2O_2/HNO_3 ratios indicate a NOx-limited condition exists during the early morning hours and shifts to VOC-limited at 10 AM. Reduced VOC emissions may have potentially slow the photochemical reactions and HNO_3 production. The minimum Q observed is 0.172 confirming a VOC-limited condtions controls ozone formation.

2.14 Summary

CAMx simulations were RUN to assess model performance after modifications to VOC and NOx emissions. 12 modified emissions scenarios were developed representing an increase or decrease of either 50% or 75% of VOC and / or NOx emissions. All the simulations functioned within acceptable limits for NE and NB on 6/18 which was the date of an ozone event in the PdN region. NB was exceeded (failed) on several days of the modeling simulation on all scenarios including the BASELINE.

The point source modeled EI appears to support substantial improvement given the minimal NOx emissions reported in the source dataset. Notwithstanding the limitations in NOx emissions, emissions increases of this pollutant generate little change in 1-hour or 8-hour ozone.

Appendix C

Time Series Plots for selected CAMS

Time-series (TS) plots of OBERVED and PREDICTED 1-hour ozone are illustrated in this section. TS plots were prepared for the 3 CAMS discussed in the previous section: CAMS 12, 41, and C663. Of note are several days of missing observed 1-hour ozone data at both CAMS 41 and 663. The date is read mm/dd/y. June 12, 2006 is the 1st value in the x-axis. As indicated earlier in this report, the simulation initiates at 0600 Local Standard Time on June 12.

1.1 Time-Series and Pairwise Scatterplots - BASELINE

Figure 1.1 illustrates the TS plot for the BASELINE simulations for CAMS 12, 41, and 663. Missing data for 6/15 – 6/18 is noticeable. OBSERVED data is flagged with a -999 to identify missing data and skipped when applying the CAMxPOST program. Figures 1.2 through 1.4 show the pairwise scatterplot for BASELINE simulation results at CAMS 12, 41, and 663, respectively. Data shows a moderate correlation in each graph (R^2 = 0.4138, 0.3408, 0.3749, respectively).

1.2 Time-Series and Pairwise Scatterplots - RUN 9

Similar graphs for RUN 9, 10, 11, and 12 are displayed in Figures 1.5 through 1.20 below.

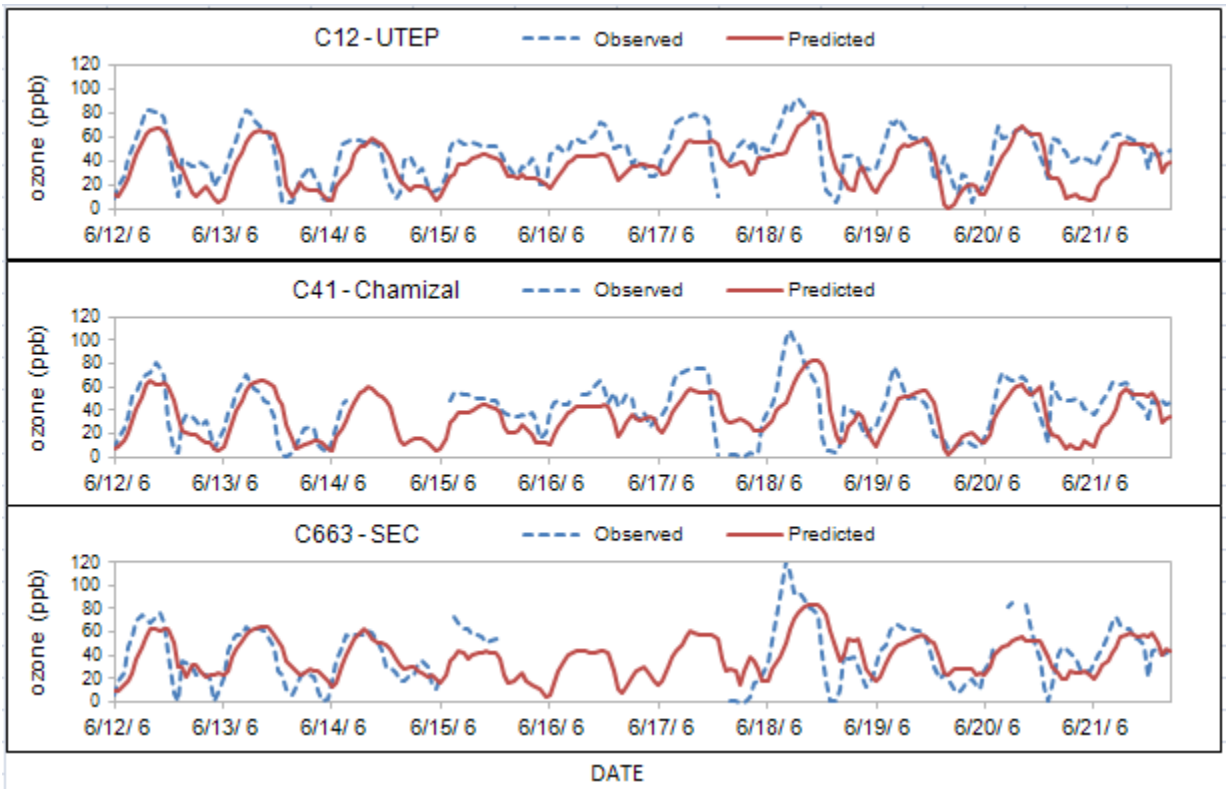

Figure 240 Time-Series Plots for BASELINE Simulation

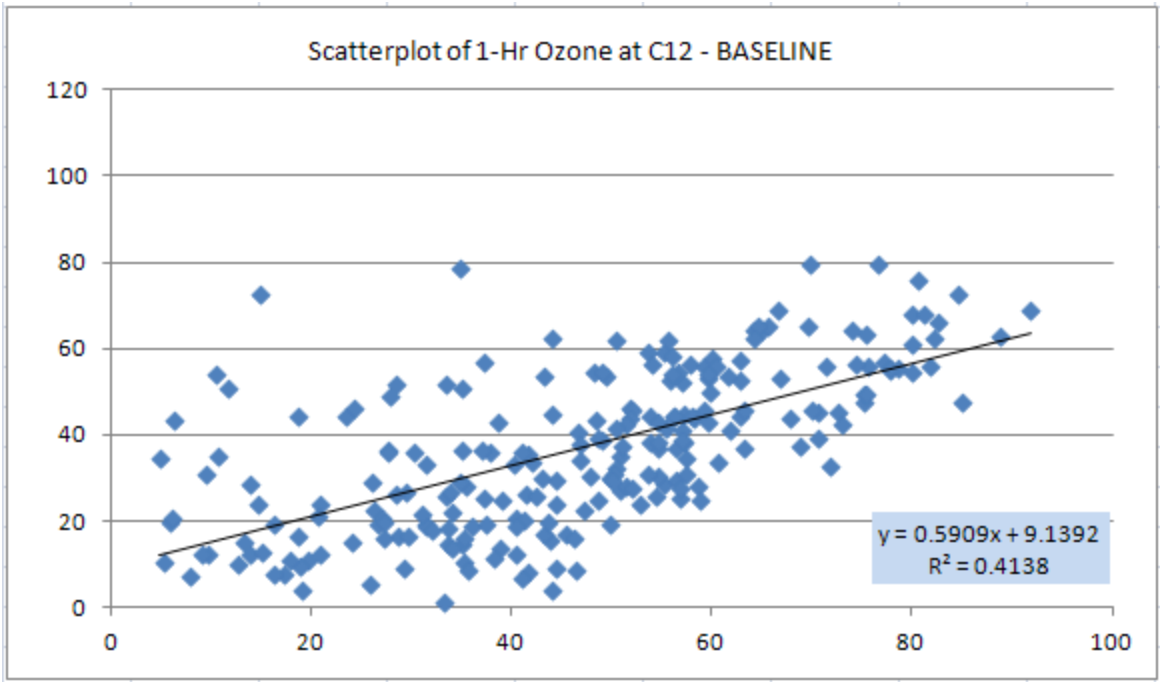

Figure 1.41 Pairwise Scatterplot - BASELINE Simulation – CAMS 12

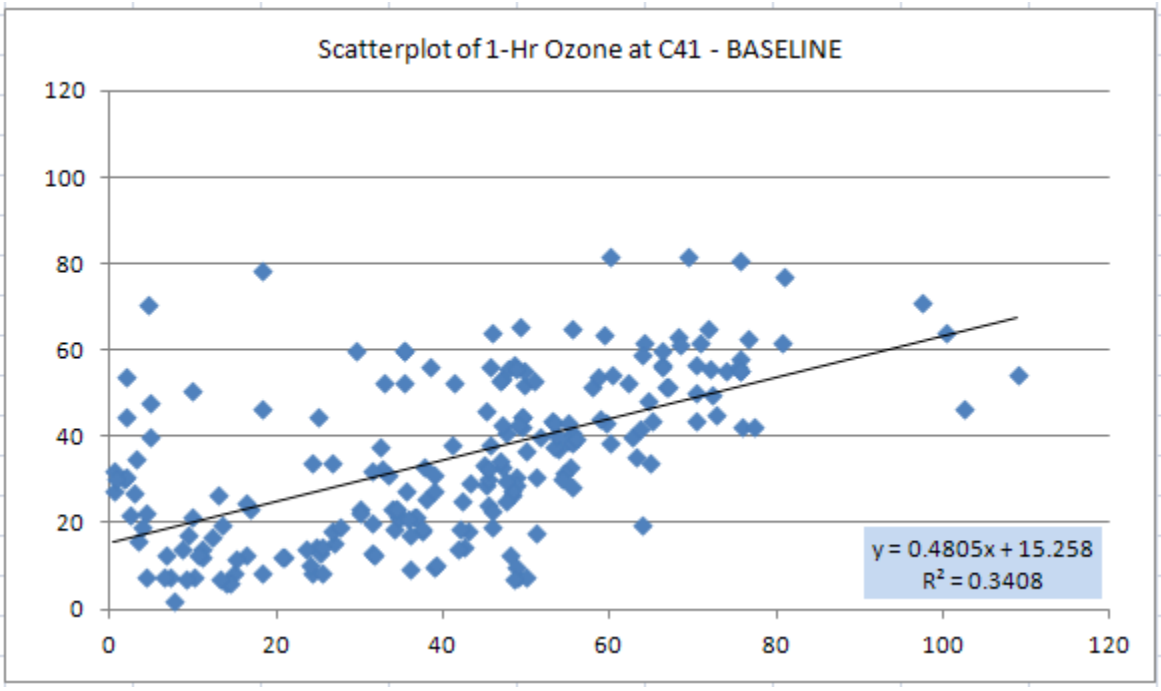

Figure 1.3 Pairwise Scatterplot - BASELINE Simulation – CAMS 41

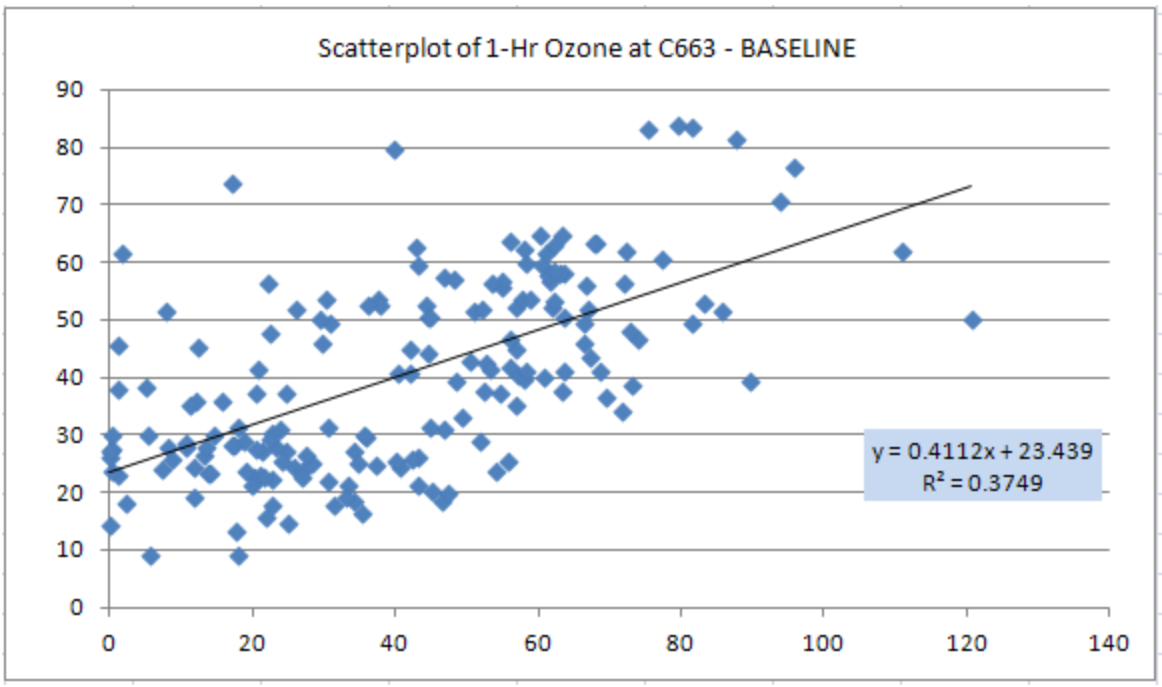

Figure 1.4 Pairwise Scatterplot - BASELINE Simulation – CAMS 663

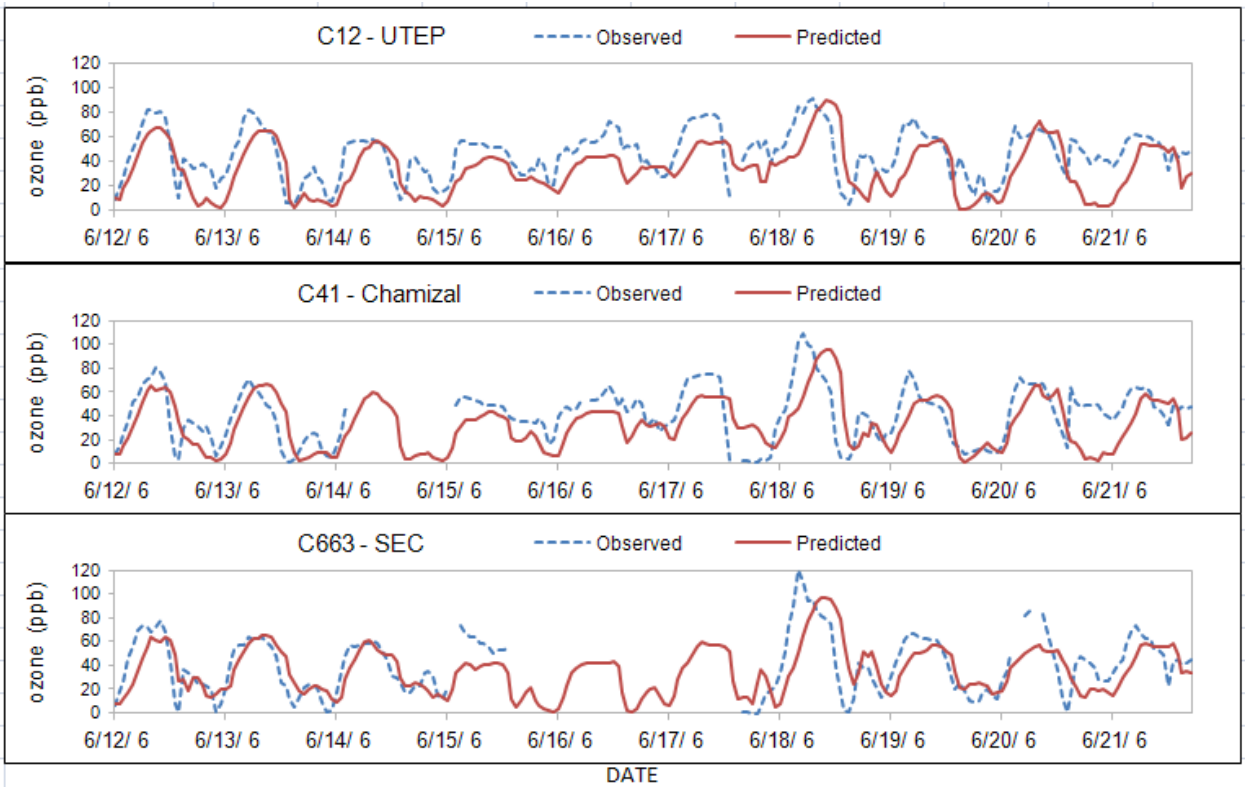

Figure 2.42 Time-Series Plots - RUN 9

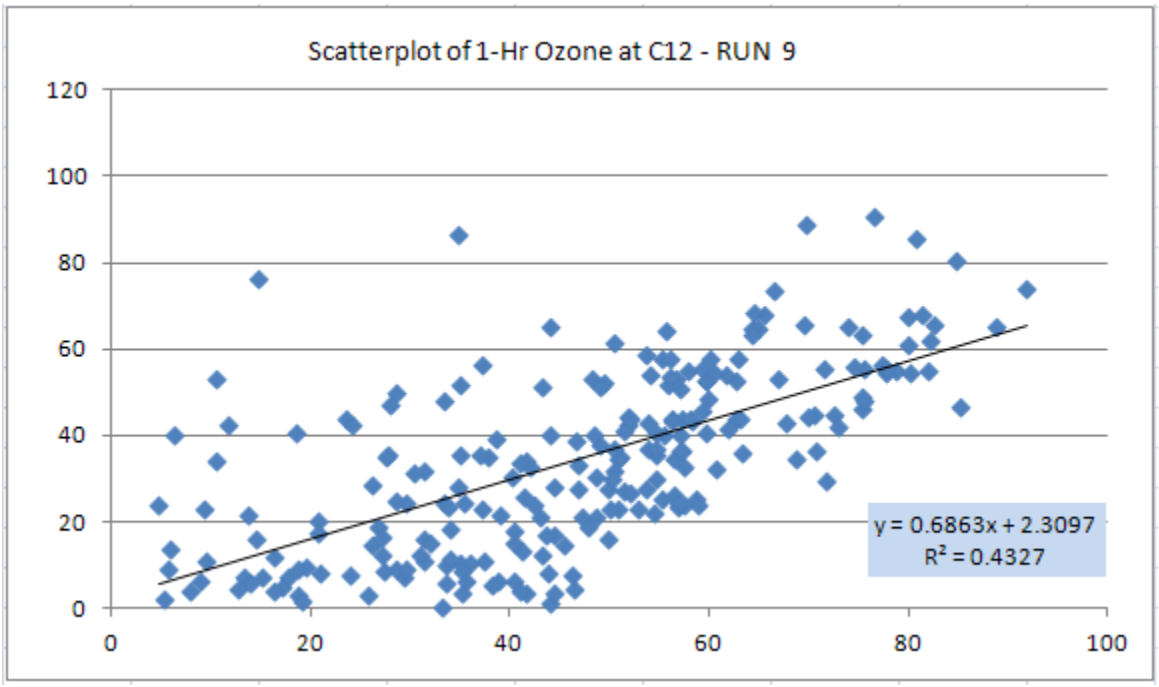

Figure 2.43 Pairwise Scatterplot - RUN 9 – CAMS 12

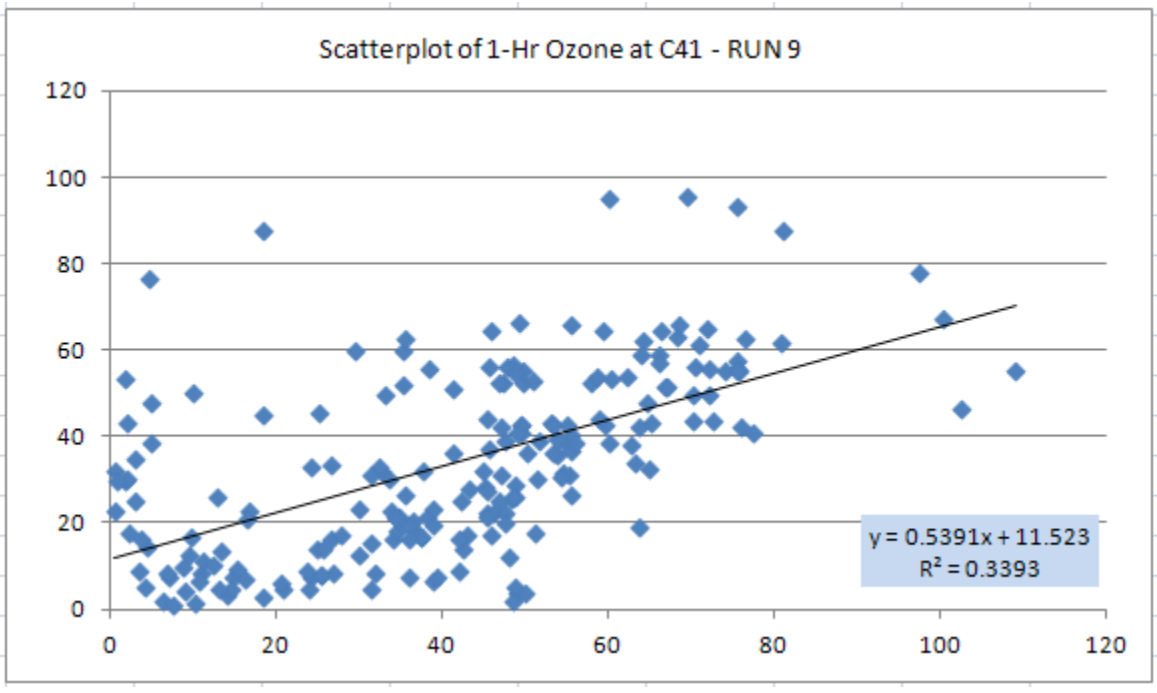

Figure 2.44 Pairwise Scatterplot - RUN 9 – CAMS 41

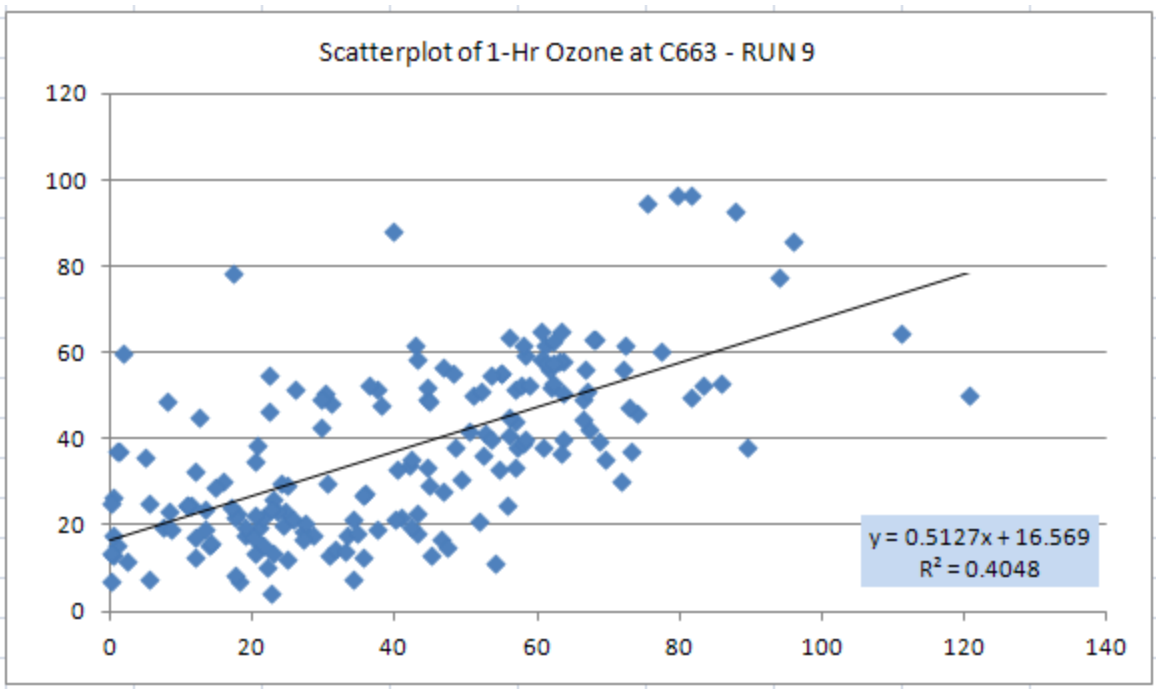

Figure 1.45 Pairwise Scatterplot - RUN 9 – CAMS 663

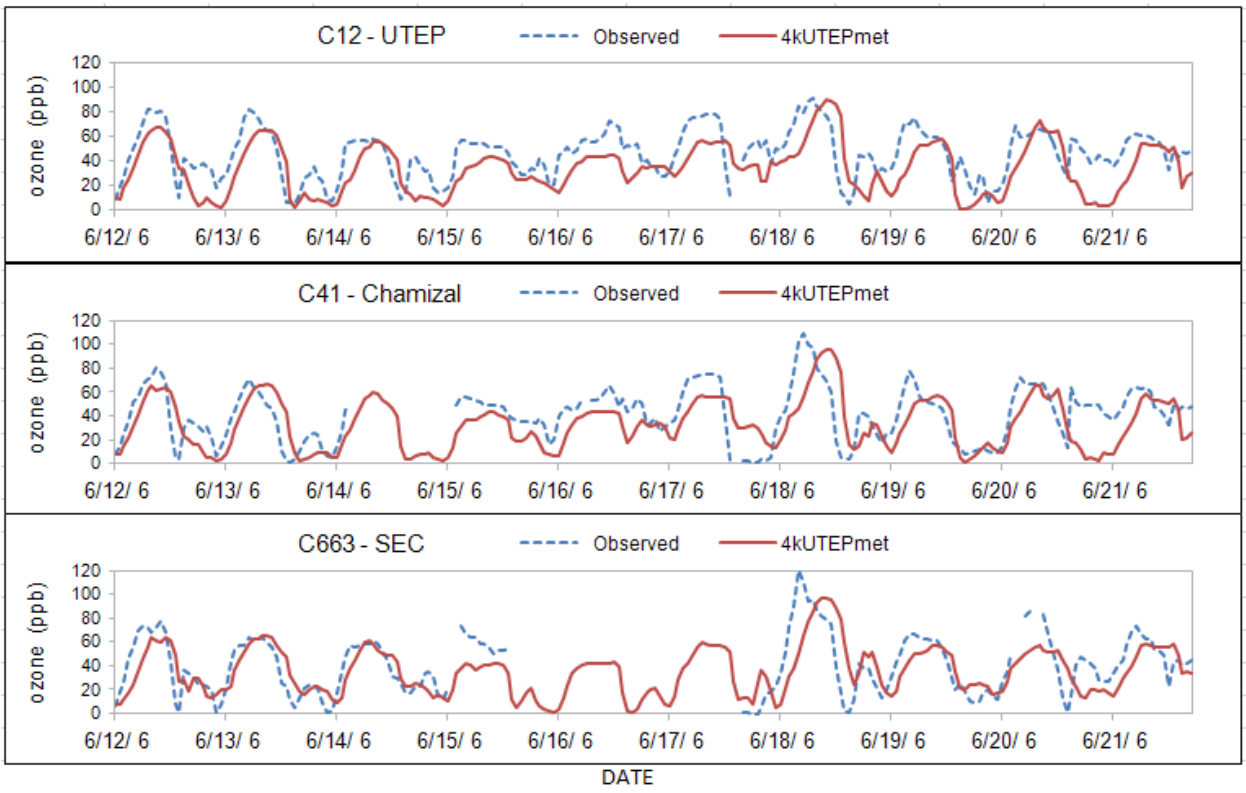

Figure 1.46 Time-Series Plot - RUN 10

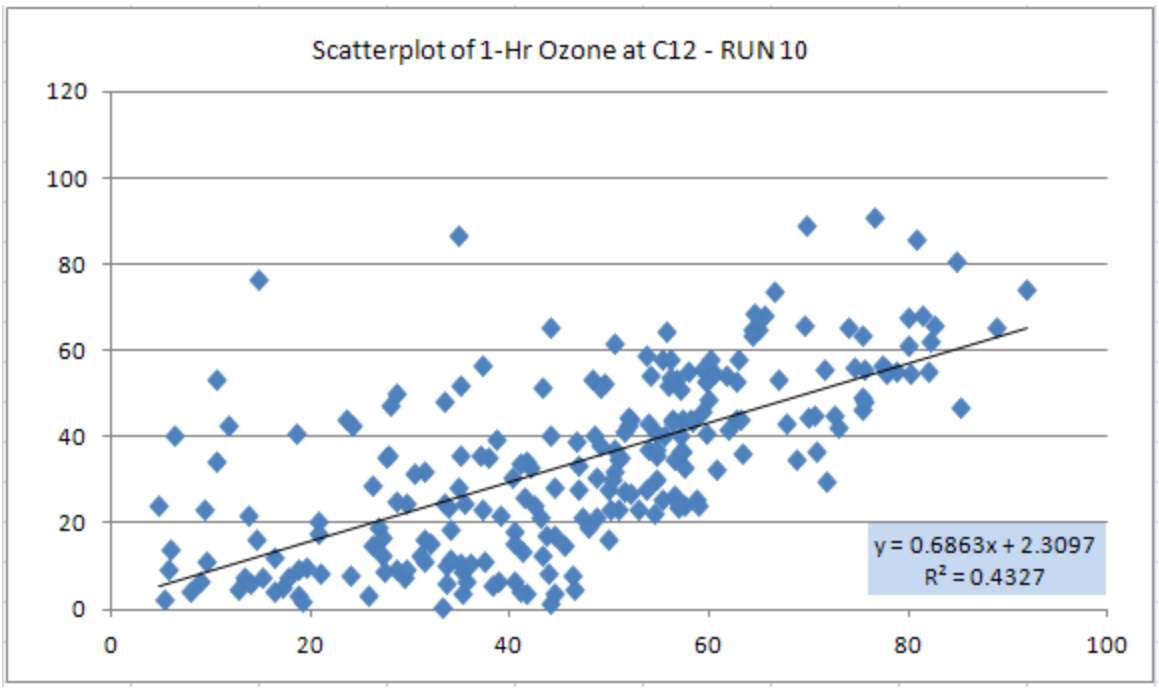

Figure 1.47 Pairwise Scatterplot - RUN 10 – CAMS 12

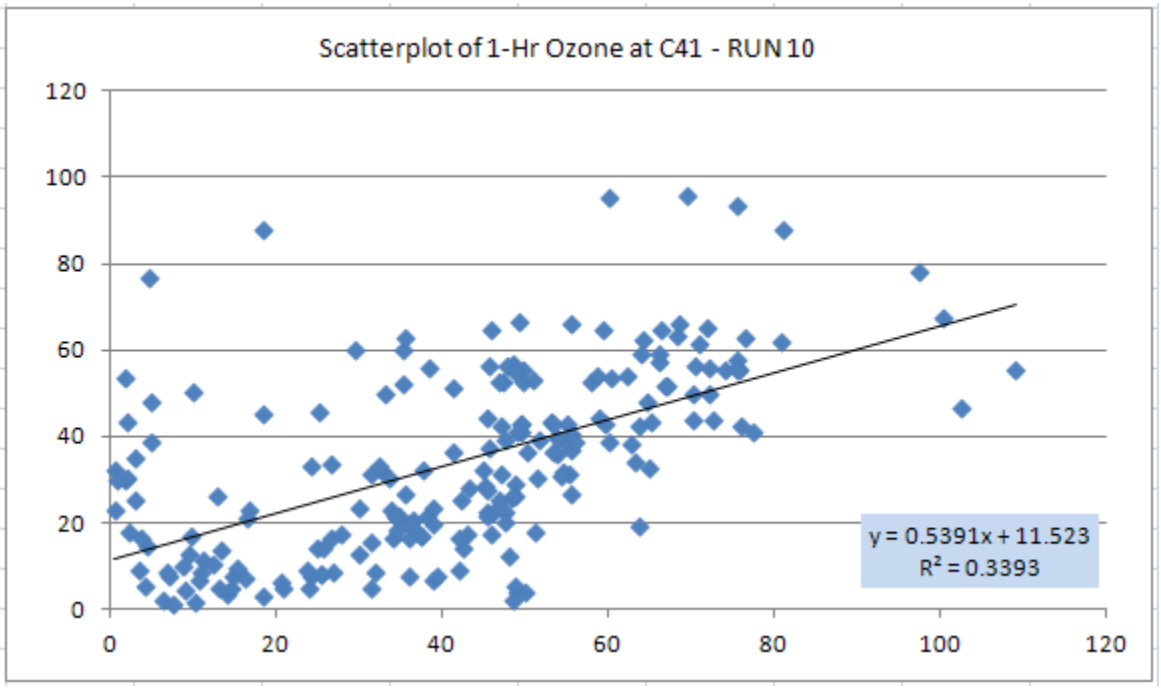

Figure 2.48 Pairwise Scatterplot - RUN 10 – CAMS 41

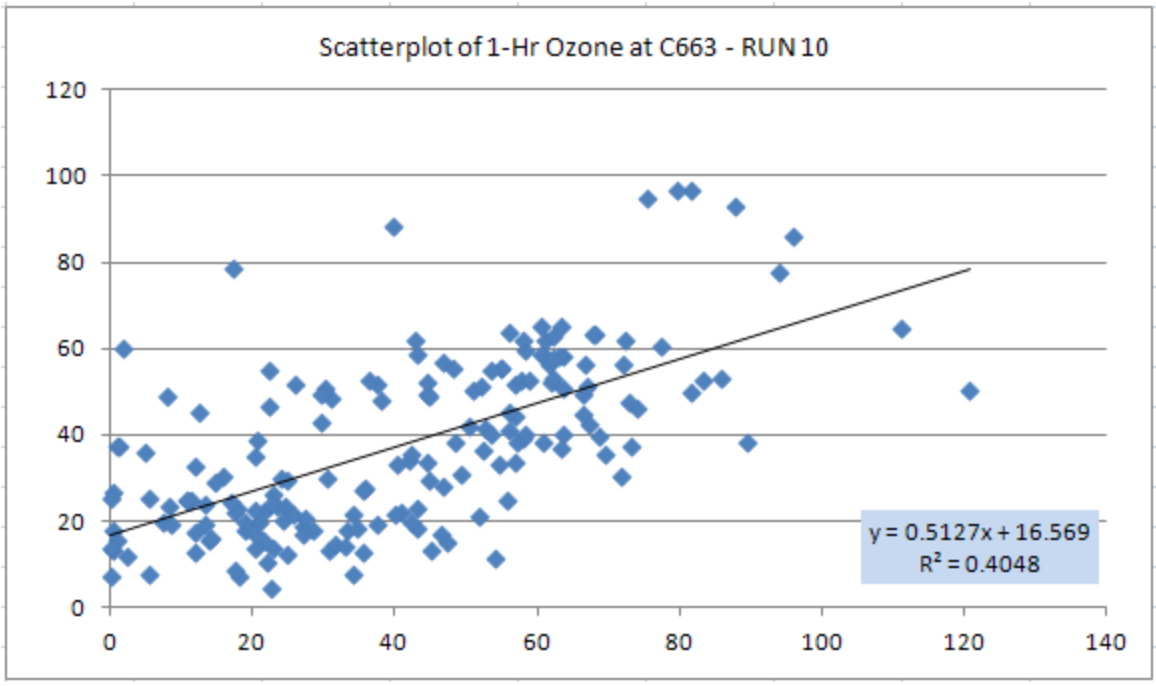

Figure 1.49 Pairwise Scatterplot - RUN 10 – CAMS 663

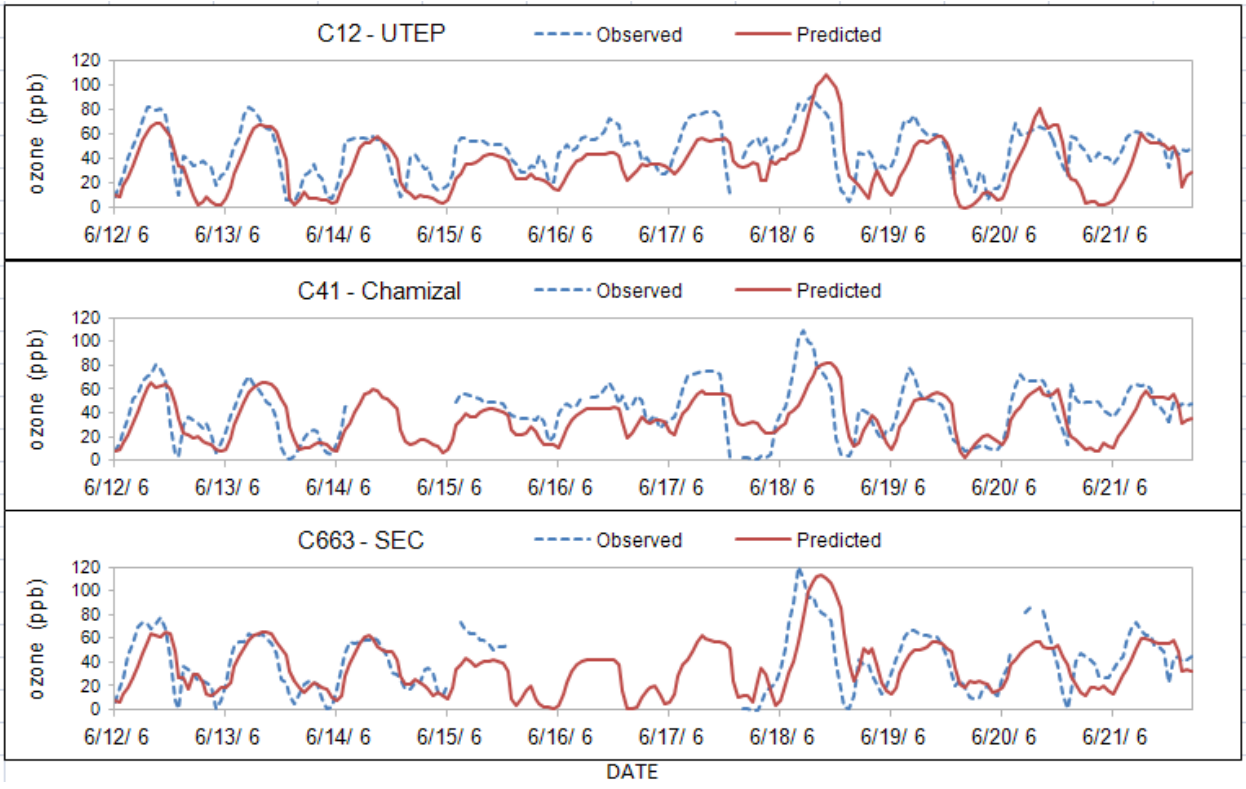

Figure 1.50 Time-Series Plots - RUN 11

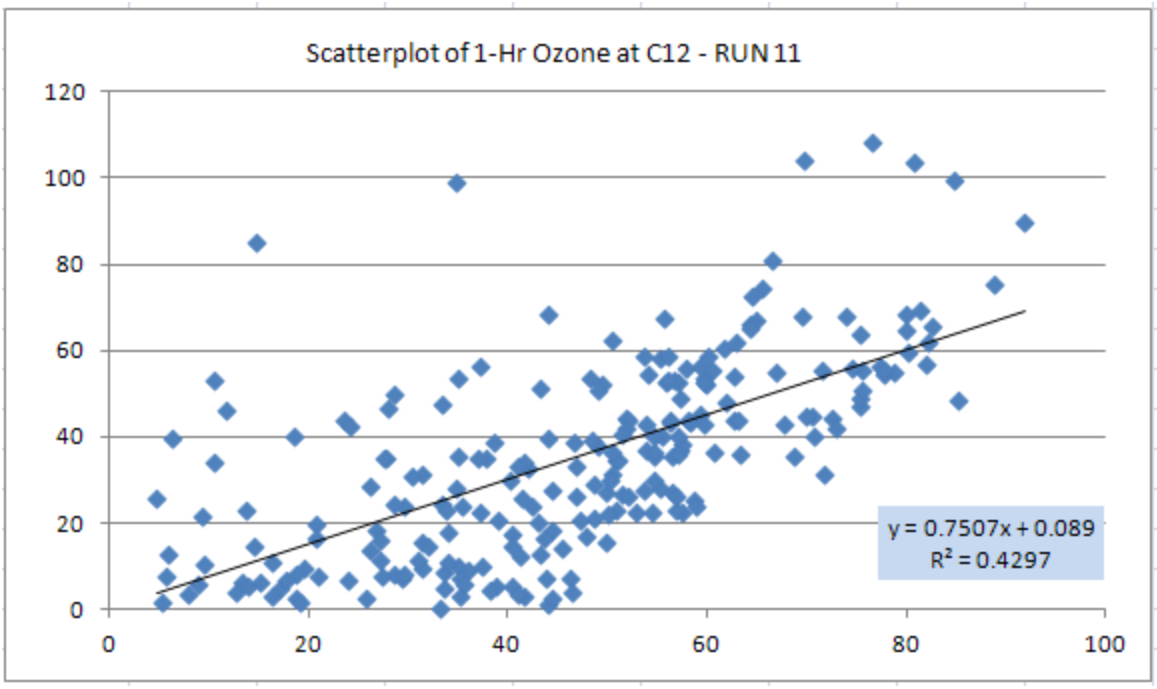

Figure 1.51 Pairwise Scatterplot - RUN 11 – CAMS 12

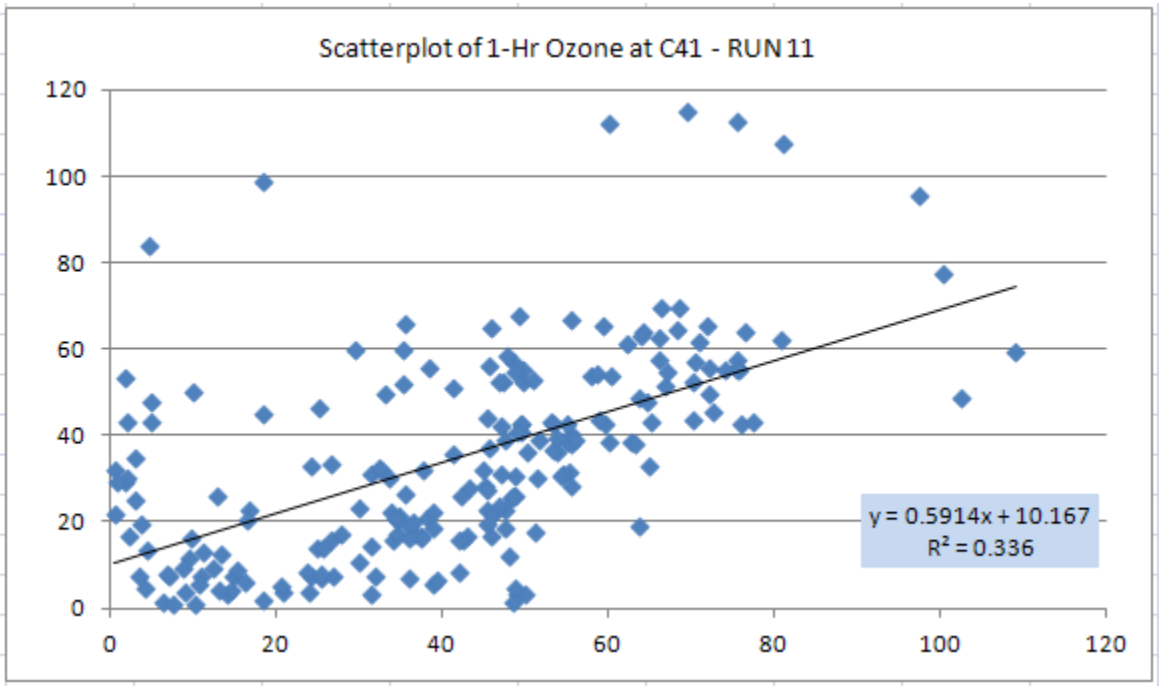

Figure 1.52 Pairwise Scatterplot - RUN 11 – CAMS 41

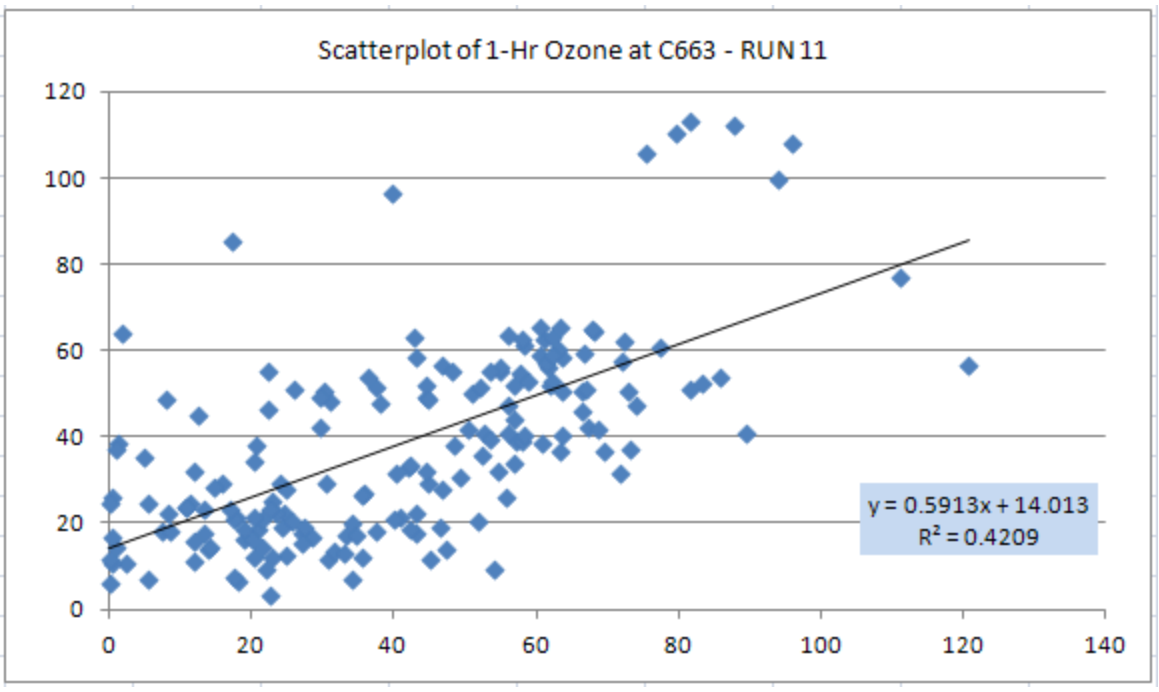

Figure 1.53 Pairwise Scatterplot - RUN 11 – CAMS 663

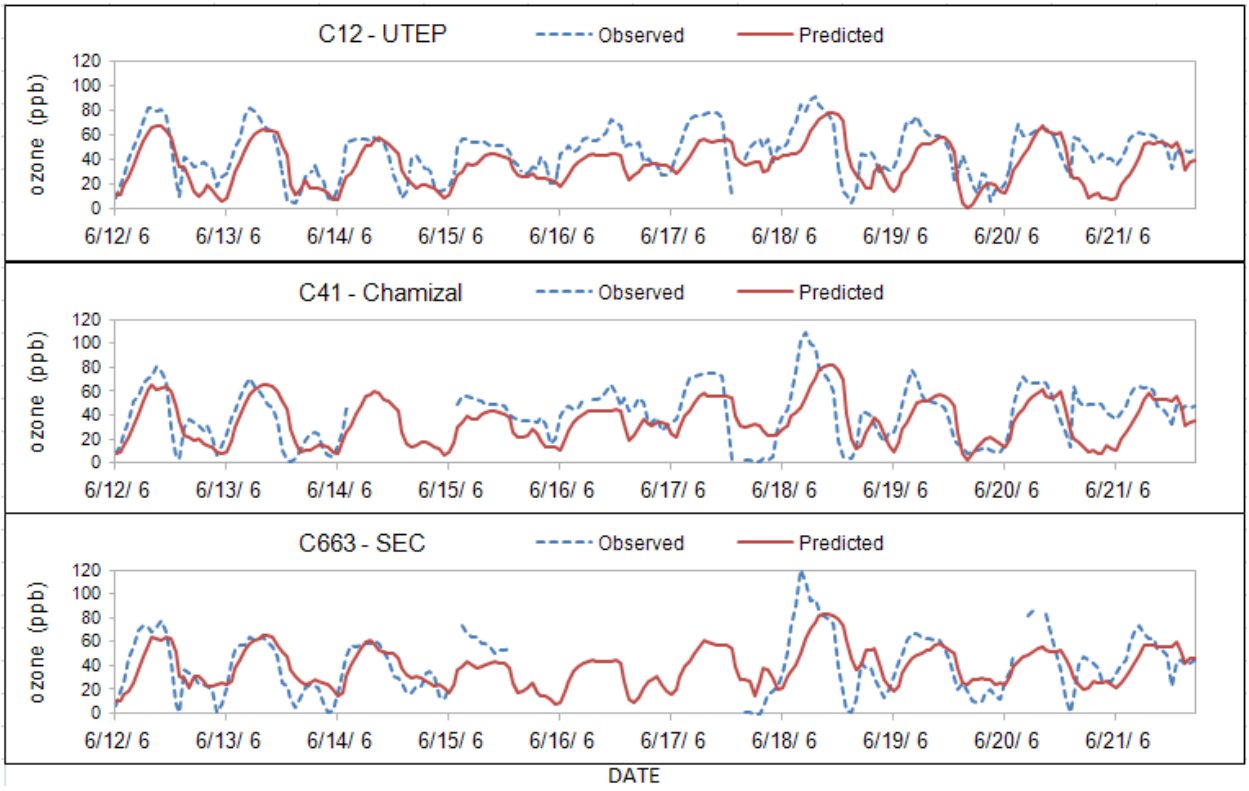

Figure 1.54 Time-Series Plots - RUN 12

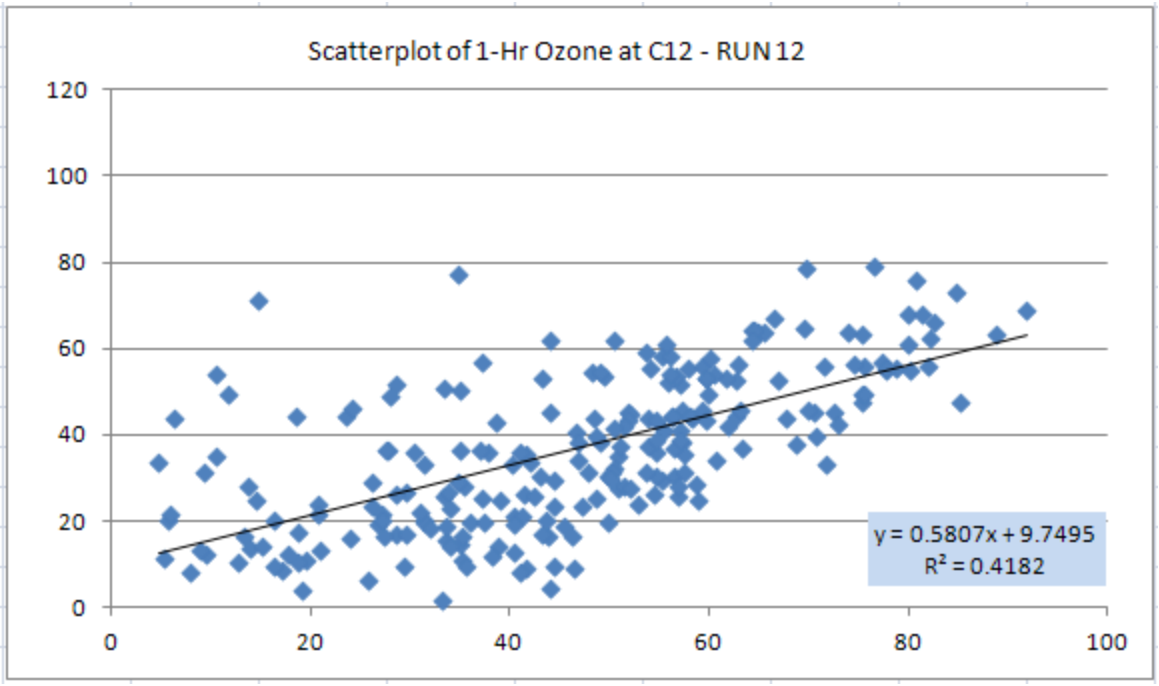

Figure 2.55 Pairwise Scatterplot - RUN 12 – CAMS 12

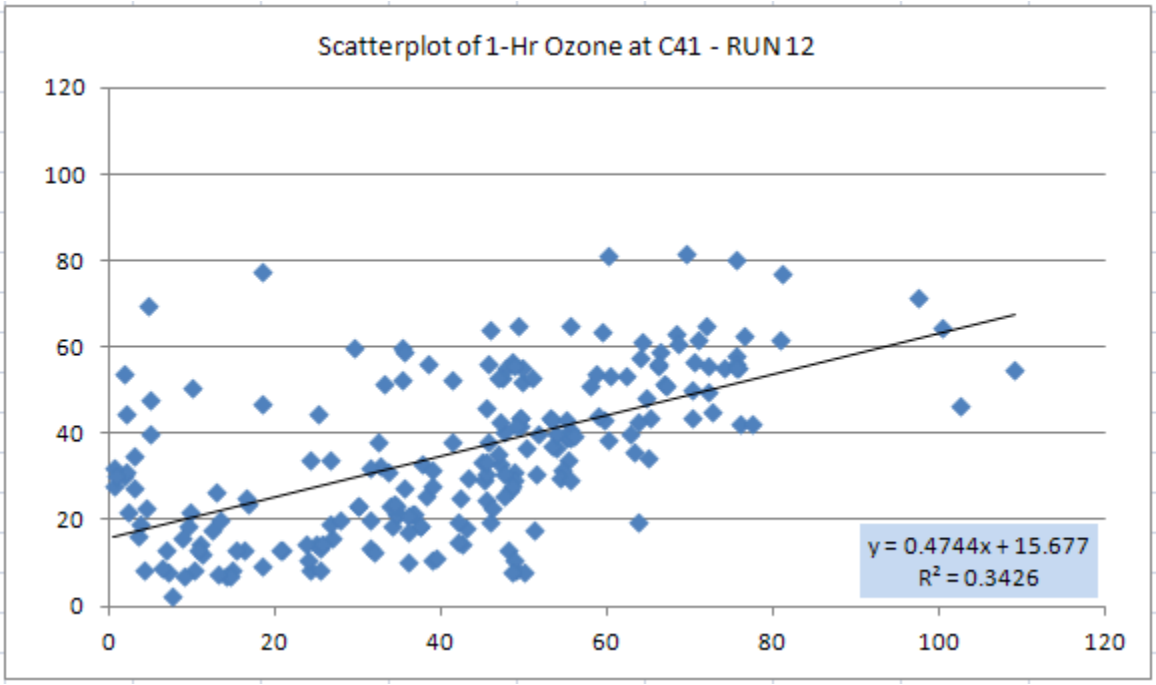

Figure 2.56 Pairwise Scatterplot - RUN 12 – CAMS 41

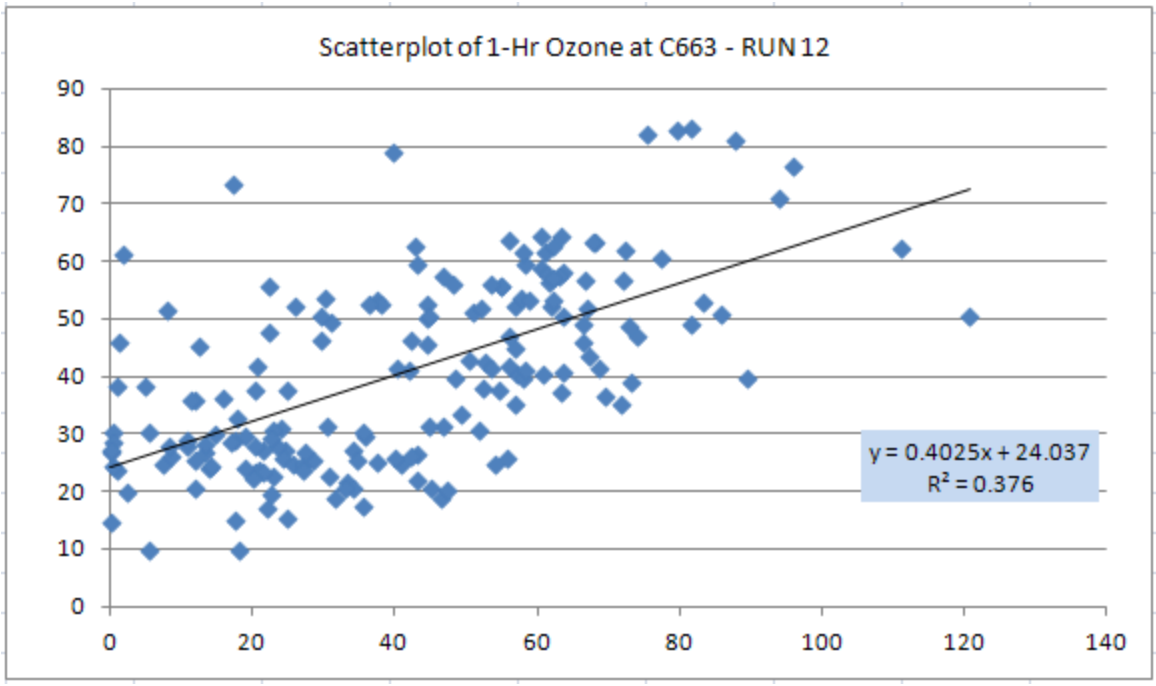

Figure 2.57 Pairwise Scatterplot - RUN 12 – CAMS 663